Safety Reports Series

No. 115

Neutron Monitoring for Radiation Protection

IAEA
International Atomic Energy Agency

IAEA SAFETY STANDARDS AND RELATED PUBLICATIONS

IAEA SAFETY STANDARDS

Under the terms of Article III of its Statute, the IAEA is authorized to establish or adopt standards of safety for protection of health and minimization of danger to life and property, and to provide for the application of these standards.

The publications by means of which the IAEA establishes standards are issued in the **IAEA Safety Standards Series**. This series covers nuclear safety, radiation safety, transport safety and waste safety. The publication categories in the series are **Safety Fundamentals**, **Safety Requirements** and **Safety Guides**.

Information on the IAEA's safety standards programme is available on the IAEA Internet site

https://www.iaea.org/resources/safety-standards

The site provides the texts in English of published and draft safety standards. The texts of safety standards issued in Arabic, Chinese, French, Russian and Spanish, the IAEA Safety Glossary and a status report for safety standards under development are also available. For further information, please contact the IAEA at: Vienna International Centre, PO Box 100, 1400 Vienna, Austria.

All users of IAEA safety standards are invited to inform the IAEA of experience in their use (e.g. as a basis for national regulations, for safety reviews and for training courses) for the purpose of ensuring that they continue to meet users' needs. Information may be provided via the IAEA Internet site or by post, as above, or by email to Official.Mail@iaea.org.

RELATED PUBLICATIONS

The IAEA provides for the application of the standards and, under the terms of Articles III and VIII.C of its Statute, makes available and fosters the exchange of information relating to peaceful nuclear activities and serves as an intermediary among its Member States for this purpose.

Reports on safety in nuclear activities are issued as **Safety Reports**, which provide practical examples and detailed methods that can be used in support of the safety standards.

Other safety related IAEA publications are issued as **Emergency Preparedness and Response** publications, **Radiological Assessment Reports**, the International Nuclear Safety Group's **INSAG Reports**, **Technical Reports** and **TECDOCs**. The IAEA also issues reports on radiological accidents, training manuals and practical manuals, and other special safety related publications.

Security related publications are issued in the **IAEA Nuclear Security Series**.

The **IAEA Nuclear Energy Series** comprises informational publications to encourage and assist research on, and the development and practical application of, nuclear energy for peaceful purposes. It includes reports and guides on the status of and advances in technology, and on experience, good practices and practical examples in the areas of nuclear power, the nuclear fuel cycle, radioactive waste management and decommissioning.

NEUTRON MONITORING
FOR
RADIATION PROTECTION

The following States are Members of the International Atomic Energy Agency:

AFGHANISTAN	GAMBIA	OMAN
ALBANIA	GEORGIA	PAKISTAN
ALGERIA	GERMANY	PALAU
ANGOLA	GHANA	PANAMA
ANTIGUA AND BARBUDA	GREECE	PAPUA NEW GUINEA
ARGENTINA	GRENADA	PARAGUAY
ARMENIA	GUATEMALA	PERU
AUSTRALIA	GUYANA	PHILIPPINES
AUSTRIA	HAITI	POLAND
AZERBAIJAN	HOLY SEE	PORTUGAL
BAHAMAS	HONDURAS	QATAR
BAHRAIN	HUNGARY	REPUBLIC OF MOLDOVA
BANGLADESH	ICELAND	ROMANIA
BARBADOS	INDIA	RUSSIAN FEDERATION
BELARUS	INDONESIA	RWANDA
BELGIUM	IRAN, ISLAMIC REPUBLIC OF	SAINT KITTS AND NEVIS
BELIZE	IRAQ	SAINT LUCIA
BENIN	IRELAND	SAINT VINCENT AND
BOLIVIA, PLURINATIONAL	ISRAEL	THE GRENADINES
STATE OF	ITALY	SAMOA
BOSNIA AND HERZEGOVINA	JAMAICA	SAN MARINO
BOTSWANA	JAPAN	SAUDI ARABIA
BRAZIL	JORDAN	SENEGAL
BRUNEI DARUSSALAM	KAZAKHSTAN	SERBIA
BULGARIA	KENYA	SEYCHELLES
BURKINA FASO	KOREA, REPUBLIC OF	SIERRA LEONE
BURUNDI	KUWAIT	SINGAPORE
CABO VERDE	KYRGYZSTAN	SLOVAKIA
CAMBODIA	LAO PEOPLE'S DEMOCRATIC	SLOVENIA
CAMEROON	REPUBLIC	SOUTH AFRICA
CANADA	LATVIA	SPAIN
CENTRAL AFRICAN	LEBANON	SRI LANKA
REPUBLIC	LESOTHO	SUDAN
CHAD	LIBERIA	SWEDEN
CHILE	LIBYA	SWITZERLAND
CHINA	LIECHTENSTEIN	SYRIAN ARAB REPUBLIC
COLOMBIA	LITHUANIA	TAJIKISTAN
COMOROS	LUXEMBOURG	THAILAND
CONGO	MADAGASCAR	TOGO
COSTA RICA	MALAWI	TONGA
CÔTE D'IVOIRE	MALAYSIA	TRINIDAD AND TOBAGO
CROATIA	MALI	TUNISIA
CUBA	MALTA	TÜRKİYE
CYPRUS	MARSHALL ISLANDS	TURKMENISTAN
CZECH REPUBLIC	MAURITANIA	UGANDA
DEMOCRATIC REPUBLIC	MAURITIUS	UKRAINE
OF THE CONGO	MEXICO	UNITED ARAB EMIRATES
DENMARK	MONACO	UNITED KINGDOM OF
DJIBOUTI	MONGOLIA	GREAT BRITAIN AND
DOMINICA	MONTENEGRO	NORTHERN IRELAND
DOMINICAN REPUBLIC	MOROCCO	UNITED REPUBLIC
ECUADOR	MOZAMBIQUE	OF TANZANIA
EGYPT	MYANMAR	UNITED STATES OF AMERICA
EL SALVADOR	NAMIBIA	URUGUAY
ERITREA	NEPAL	UZBEKISTAN
ESTONIA	NETHERLANDS	VANUATU
ESWATINI	NEW ZEALAND	VENEZUELA, BOLIVARIAN
ETHIOPIA	NICARAGUA	REPUBLIC OF
FIJI	NIGER	VIET NAM
FINLAND	NIGERIA	YEMEN
FRANCE	NORTH MACEDONIA	ZAMBIA
GABON	NORWAY	ZIMBABWE

The Agency's Statute was approved on 23 October 1956 by the Conference on the Statute of the IAEA held at United Nations Headquarters, New York; it entered into force on 29 July 1957. The Headquarters of the Agency are situated in Vienna. Its principal objective is "to accelerate and enlarge the contribution of atomic energy to peace, health and prosperity throughout the world".

IAEA SAFETY REPORTS SERIES No. 115

NEUTRON MONITORING
FOR
RADIATION PROTECTION

INTERNATIONAL ATOMIC ENERGY AGENCY
VIENNA, 2023

COPYRIGHT NOTICE

All IAEA scientific and technical publications are protected by the terms of the Universal Copyright Convention as adopted in 1952 (Berne) and as revised in 1972 (Paris). The copyright has since been extended by the World Intellectual Property Organization (Geneva) to include electronic and virtual intellectual property. Permission to use whole or parts of texts contained in IAEA publications in printed or electronic form must be obtained and is usually subject to royalty agreements. Proposals for non-commercial reproductions and translations are welcomed and considered on a case-by-case basis. Enquiries should be addressed to the IAEA Publishing Section at:

Marketing and Sales Unit, Publishing Section
International Atomic Energy Agency
Vienna International Centre
PO Box 100
1400 Vienna, Austria
fax: +43 1 26007 22529
tel.: +43 1 2600 22417
email: sales.publications@iaea.org
www.iaea.org/publications

FOREWORD

Exposures to neutrons account for a significant fraction of the occupational exposure received by workers at nuclear facilities and at high energy accelerator facilities. The requirements for monitoring and assessment of occupational exposure are established in IAEA Safety Standards Series No. GSR Part 3, Radiation Protection and Safety of Radiation Sources: International Basic Safety Standards. Detailed guidance on the approach to meeting the requirements is provided in IAEA Safety Standards Series No. GSG-7, Occupational Radiation Protection. However, monitoring exposure to neutron radiation can be difficult because of the dramatic variation of neutron spectra among different workplaces and the disparities in energy responses of the personal dosimeters and survey meters used. For accurate monitoring of neutron exposures, it is important to use the appropriate radiological quantities and units and to have information available on the dosimetric features of personal dosimeters and monitoring equipment and on the energy spectral characteristics of neutron radiation fields at workplaces. The selection of the dosimeters and monitoring equipment as well as the optimization of the calibration conditions and correction factors for the differences between the calibration and workplace fluence spectra depend on this information.

This Safety Report describes the neutron monitoring procedures and equipment that may be needed for the nuclear power production industry, medical and industrial applications, nuclear research institutions, operation of nuclear powered vessels and aircrew dosimetry. This report is also expected to be helpful to designers and manufacturers of area survey monitors and personal dosimeters, along with international standards developers. The publication provides guidance on the measurement of the operational dose equivalent quantities for neutron radiation. It is also intended to provide practical information for carrying out neutron radiation protection dosimetry, including methods for establishing traceability of those measurements to national standards. The inaccuracies, or potential inaccuracies, still inherent in neutron dosimetry with present day capabilities are outlined. It is hoped that this report will be of use to a range of individuals, from those with little experience of neutron measurements with the task of setting up and organizing neutron monitoring arrangements through to those with reasonable background knowledge but a need to learn more about this complex topic.

The IAEA is grateful to D.J. Thomas (United Kingdom), the late J.C. McDonald (United States of America) and M. Luszik-Bhadra (Germany). The IAEA officer responsible for this report was J. Ma of the Division of Radiation, Transport and Waste Safety.

CONTENTS

1. INTRODUCTION

1.1. BACKGROUND

Monitoring and assessment of occupational exposure is essential for the protection of workers exposed to ionizing radiation. In IAEA Safety Standards Series No. GSR Part 3, Radiation Protection and Safety of Radiation Sources: International Basic Safety Standards [1.1], jointly sponsored by the IAEA and seven other international organizations, it is indicated that "The regulatory body shall establish and enforce requirements for the monitoring and recording of occupational exposures in planned exposure situations" and "Employers, registrants and licensees shall be responsible for making arrangements for assessment and recording of occupational exposures and for workers' health surveillance". IAEA Safety Standards Series No. GSG-7, Occupational Radiation Protection [1.2], provides guidance on the control of occupational exposure. Specific guidance on the monitoring and assessment of occupational exposure is also given in GSG-7. However, because of the complexity of neutron interactions with matter and the variation of the spectra of neutron radiation fields in different nuclear or radiation facilities, neutron monitoring is still a challenging technical area compared with photon and electron radiation monitoring. Detailed technical guidance on the topic is therefore needed.

A neutron fluence, like a gamma ray fluence, is a type of indirectly ionizing radiation. It is thus of concern for radiation protection purposes in certain specific locations, such as nuclear reactors. Neutrons are not generally considered to be an environmental, and hence a public, radiation protection problem, except possibly in the case of a nuclear accident, at the boundaries of nuclear facilities or during medical treatment with high energy X rays or protons. Naturally occurring sources of neutrons are relatively rare, although there is one important example of this: the cosmic neutron fluence to which aircrew and astronauts are exposed. At the surface of the Earth, the neutron background is not considered to pose a significant risk. However, there are activities in which the exposure of workers to neutrons can pose a risk, and that exposure requires monitoring. Those activities include the production of nuclear fuel, operation of nuclear reactors for the purpose of producing electricity, transport and storage of nuclear waste, reprocessing of nuclear fuel, production and use of radioactive sources, oil well logging, operation of high energy medical accelerators and nuclear physics research.

The neutron was identified and characterized by James Chadwick in 1932 [1.3]. His work was recognized with the award of the Nobel Prize in Physics in 1935. The basic methods used by Chadwick to investigate the rather

penetrating radiation that was produced by the bombardment of light elements by alpha particles are still used today. Since neutrons are an indirectly ionizing radiation, their properties were studied by means of the secondary particles that were produced as neutrons collided with charged particles, such as protons, or as they produced secondary particles in nuclear reactions. In order to do this, Chadwick made use of an ionization chamber with a paraffin block placed between the chamber and the neutron source. Recoiling protons from neutron interactions with the hydrogen-rich paraffin were detected by the ionization chamber. The particles responsible for producing these secondary protons were observed to be quite penetrating, as are high energy gamma rays. However, Chadwick correctly deduced that the new particle responsible for these effects was not a gamma ray, as thought by others, but rather a neutral particle with a mass nearly equal to that of the proton. His work was a confirmation of the existence of a neutron, as had been suggested earlier by Ernest Rutherford.

Neutrons can pose a radiation hazard, but they are also useful as probes of materials whose properties are not amenable to study by other means. X rays or charged particles, for example, may be quickly absorbed by thick samples, whereas neutrons may be able to penetrate to a greater distance. Neutrons are an essential element of the sustained criticality that is maintained in a nuclear reactor. Neutrons have been used in radiation therapy to treat human cancers, and the activation of atoms by neutrons has become a useful tool in identifying the composition of materials. Radionuclide neutron sources and small neutron generators are used in oil well logging and in moisture gauging. The possible use of neutron sources or fissile material by terrorists has meant that neutron detection is now an integral part of counterterrorism activities.

The dosimetry of neutrons is fairly complex as compared with that for photons (gamma rays, X rays and bremsstrahlung), and among the reasons for this complexity are the following. The energy of neutrons encountered in workplaces such as nuclear power reactors and high energy research accelerators can range over more than ten orders of magnitude. A radiation field composed solely of neutrons is extremely rare, as neutrons are nearly always accompanied by photons. Therefore, some method for determining the effects of these two types of radiation is necessary. The interactions of neutrons with materials used as detectors, and in biological tissues, are complex because of the nature of the neutron reaction cross-sections in various elements as functions of neutron energy. The neutron cross-section is basically a measure of the probability that a neutron will interact with the nucleus of an atom. In addition, the elements and materials used to produce neutron detectors and dosimeters are nearly always significantly different from those elements that comprise biological tissues. This complication requires the use of conversion coefficients to determine the dose equivalent in tissue, and it explains why there are no perfect neutron dosimeters. Nevertheless,

there are many useful, practical and reasonably accurate neutron dosimeters that can be used in various situations to measure quantities appropriate for monitoring exposures to neutrons.

1.2. OBJECTIVE

The objective of this Safety Report is to provide guidance on neutron monitoring for radiation protection. The guidance and examples given are intended for radiation protection professionals in the nuclear industry, medicine, research and other areas where neutron monitoring is required. The report will also be useful to regulatory authorities and technical support organizations, as well as organizations responsible for the design and development of nuclear and radiation facilities or radiation protection equipment used during neutron monitoring for radiation protection. Guidance and recommendations provided here in relation to identified good practices represent expert opinion but are not made on the basis of a consensus of all Member States.

1.3. SCOPE

This Safety Report addresses the technical aspects of neutron monitoring for radiation protection. The intention is to provide guidance on the monitoring and assessment of occupational exposure resulting from neutron radiation.

The report reviews the physical and dosimetric properties of neutrons, their interactions with matter and their interactions with human tissues and organs. The conversion coefficients used to evaluate the dose equivalent in different neutron fields are presented, and common sources of neutrons are discussed. Neutron detection principles, the characterization of neutron fields, neutron survey instruments and personal neutron dosimeters are covered, along with the methods for calibrating those devices. Guidance on the choice of an operational monitoring system is also provided.

1.4. STRUCTURE

This Safety Report consists of 14 sections and 2 appendices. Section 1 provides the background, objectives, scope and structure of the publication. Sections 2–4 introduce the quantities and units for radiation measurement and provide fundamental knowledge on the physical properties of neutrons and neutron interactions with matter.

Sections 5–7 present neutron dosimetry, conversion coefficients for operational quantities and neutron sources. Neutron detection principles and characterization of neutron fields are described in Sections 8–9.

Sections 10–14 review neutron survey meters and installed instruments, personal neutron dosimeters and nuclear accident dosimetry, and give guidance on how to choose an operational system and how to perform calibration and type testing of neutron monitoring radiation protection equipment. Appendix I provides definitions, and Appendix II contains a list of acronyms and abbreviations used in the publication.

Each section in this Safety Report is intended to be a largely 'standalone' section of text that the reader can refer to in order to learn about a particular topic without needing to read the whole report. To this end, each section has its own list of references, and where appropriate, definitions, such as those from the quantities and units section, are repeated to avoid the need for cross-referencing.

REFERENCES TO CHAPTER 1

[1.1]   EUROPEAN COMMISSION, FOOD AND AGRICULTURE ORGANIZATION OF THE UNITED NATIONS, INTERNATIONAL ATOMIC ENERGY AGENCY, INTERNATIONAL LABOUR ORGANIZATION, OECD NUCLEAR ENERGY AGENCY, PAN AMERICAN HEALTH ORGANIZATION, UNITED NATIONS ENVIRONMENT PROGRAMME, WORLD HEALTH ORGANIZATION, Radiation Protection and Safety of Radiation Sources: International Basic Safety Standards, IAEA Safety Standards Series No. GSR Part 3, IAEA, Vienna (2014).

[1.2]   INTERNATIONAL ATOMIC ENERGY AGENCY, INTERNATIONAL LABOUR OFFICE, Occupational Radiation Protection, IAEA Safety Standards Series No. GSG-7, IAEA, Vienna (2018).

[1.3]   CHADWICK, J., The existence of a neutron, Proc. R. Soc. A **136** (1932) 692.

2. QUANTITIES AND UNITS

The quantities discussed in this section are those concerned with the determination of absorbed dose or dose equivalent delivered to the human body or to materials of interest.

Dosimetric quantities and dose equivalent quantities can be measured directly, for example by making a calorimetric measurement of absorbed dose, but they can also be determined using the products of radiometric quantities and interaction coefficients. Calculations of these quantities require knowledge of radiometric quantities, such as fluence, and interaction coefficients, such as fluence to dose equivalent conversion coefficients. The basic quantity in dosimetry is the absorbed dose, and the basic quantity in radiation protection dosimetry is the dose equivalent. The aim for protection purposes is to make as accurate as possible a measurement of the operational dose equivalent quantities, which were defined by the International Commission on Radiation Units and Measurements (ICRU) [2.1] for practical measurements and which are intended to act as adequate approximations (avoiding underestimation and too much overestimation) to the limiting quantity. The limiting quantity presently recommended by the International Commission on Radiological Protection (ICRP) for whole body exposure is the effective dose [2.2, 2.3].

The definitions given here for the various quantities are based on ICRU reports [2.4, 2.5] and International Organization for Standardization (ISO) standards [2.6].

In addition to the definitions of quantities, certain concepts associated with measurements, and in particular with calibrations, derived mainly from ISO standards, are presented here.

2.1. RADIOMETRIC QUANTITIES

The **neutron fluence**, Φ, is the quotient of $\mathrm{d}N$ by $\mathrm{d}a$, where $\mathrm{d}N$ is the number of neutrons incident on a sphere of cross-sectional area $\mathrm{d}a$:

$$\Phi = \frac{\mathrm{d}N}{\mathrm{d}a}$$

(2.1)

Note: the unit of the neutron fluence is m^{-2}; a frequently used unit is cm^{-2}.

The **neutron fluence rate; neutron flux density**, $\dot{\Phi}$, is the quotient of $\mathrm{d}\Phi$ by $\mathrm{d}t$, where $\mathrm{d}\Phi$ is the increment of neutron fluence in the time interval $\mathrm{d}t$:

$$\dot{\Phi} = \frac{\mathrm{d}\Phi}{\mathrm{d}t} = \frac{\mathrm{d}^2 N}{\mathrm{d}a\ \mathrm{d}t} \tag{2.2}$$

Note: the unit of the neutron fluence rate is $\mathrm{m}^{-2}{\cdot}\mathrm{s}^{-1}$; a frequently used unit is $\mathrm{cm}^{-2}{\cdot}\mathrm{s}^{-1}$.

The **spectral neutron fluence; energy distribution of the neutron fluence**, Φ_E, is the quotient of $\mathrm{d}\Phi$ by $\mathrm{d}E$, where $\mathrm{d}\Phi$ is the increment of neutron fluence in the energy interval between E and $E+\mathrm{d}E$:

$$\Phi_E = \frac{\mathrm{d}\Phi}{\mathrm{d}E} \tag{2.3}$$

Note: the unit of the spectral neutron fluence is $\mathrm{m}^{-2}{\cdot}\mathrm{J}^{-1}$; a frequently used unit is $\mathrm{cm}^{-2}{\cdot}\mathrm{eV}^{-1}$.

The **spectral neutron fluence rate; spectral neutron flux density**, $\dot{\Phi}_E$, is the quotient of $\mathrm{d}\Phi_E$ by $\mathrm{d}t$, where $\mathrm{d}\Phi_E$ is the increment of spectral neutron fluence in the time interval $\mathrm{d}t$:

$$\dot{\Phi}_E = \frac{\mathrm{d}\Phi_E}{\mathrm{d}t} = \frac{\mathrm{d}^2\Phi}{\mathrm{d}E\mathrm{d}t} \tag{2.4}$$

Note: the unit for the spectral neutron fluence rate is $\mathrm{m}^{-2}{\cdot}\mathrm{s}^{-1}{\cdot}\mathrm{J}^{-1}$; a frequently used unit is $\mathrm{cm}^{-2}{\cdot}\mathrm{s}^{-1}{\cdot}\mathrm{eV}^{-1}$.

The **neutron emission rate (sometimes called source strength) of a neutron source at a given time,** B, is the quotient of $\mathrm{d}N^*$ by $\mathrm{d}t$, where $\mathrm{d}N^*$ is the expectation value of the number of neutrons emitted by the source in the time interval $\mathrm{d}t$:

$$B = \frac{\mathrm{d}N^*}{\mathrm{d}t} \tag{2.5}$$

Note: the unit of the source emission rate is s^{-1}.

The **angular source emission rate,** B_Ω, is the quotient of dB by dΩ, where dB is the number of neutrons per unit time propagating in a specified direction within the solid angle dΩ:

$$B_\Omega = \frac{\mathrm{d}B}{\mathrm{d}\Omega} \qquad (2.6)$$

Note: the unit of the angular source emission rate is $\mathrm{s}^{-1}\cdot\mathrm{sr}^{-1}$.

The **spectral source emission rate, or energy distribution of the neutron source emission rate,** B_E, is the quotient of dB by dE, where dB is the increment of neutron source strength in the energy interval between E and E + dE:

$$B_E = \frac{\mathrm{d}B}{\mathrm{d}E} \qquad (2.7)$$

Note: the unit of the spectral source emission rate is $\mathrm{s}^{-1}\cdot\mathrm{J}^{-1}$; a frequently used unit is $\mathrm{s}^{-1}\cdot\mathrm{eV}^{-1}$.

The source emission rate B is derived from B_E as follows:

$$B = \int_0^\infty B_E \mathrm{d}E \qquad (2.8)$$

At a distance l from a point source, the spectral neutron fluence rate $\dot\Phi_E$, resulting from neutrons emitted isotropically from the point source with a spectral neutron source emission rate B_E (neglecting the influence of surrounding material), is given by

$$\dot\Phi_E = \frac{B_E}{4\pi\, l^2} \qquad (2.9)$$

The **fluence average neutron energy,** $\bar{E}$, is the neutron energy averaged over the spectral neutron fluence. It is calculated from the product of E and $\Phi_E(E)$, the spectral neutron fluence at neutron energy E:

$$\bar{E} = \frac{1}{\Phi}\int_0^\infty E\cdot\Phi_E(E)\mathrm{d}E \qquad (2.10)$$

The **dose equivalent average neutron energy,** $\tilde{E}$, is the neutron energy averaged over the dose equivalent spectrum. The dose equivalent spectrum is

given by the product of Φ_E and $h_\Phi(E)$, where Φ_E is the spectral neutron fluence at neutron energy E, and $h_\Phi(E)$ is the neutron fluence to dose equivalent conversion coefficient at this energy:

$$\tilde{E} = \frac{1}{H}\int_0^\infty E \cdot h_\Phi(E)\Phi_E \mathrm{d}E \tag{2.11}$$

where

$$H = \int_0^\infty h_\Phi(E)\Phi_E \mathrm{d}E \tag{2.12}$$

2.2. INTERACTION COEFFICIENTS AND RELATED QUANTITIES

The **cross-section**, σ, of a target entity, for a particular interaction produced by incident charged or uncharged particles, is the quotient of P by Φ, where P is the probability of that interaction for a single target entity when subjected to the particle fluence, Φ, thus

$$\sigma = \frac{P}{\Phi} \tag{2.13}$$

The unit of σ is m^2, although it is often expressed in cm^2. A special unit often used for the cross-section is the barn, b, which is defined by $1\mathrm{b} = 10^{-28}$ m^2 = 10^{-24} cm^2.

The **linear energy transfer** or **linear collision stopping power**, L, of a material for a charged particle is the quotient of $\mathrm{d}E$ by $\mathrm{d}l$, where $\mathrm{d}E$ is the mean energy lost by the particle in collisions with electrons in traversing a distance $\mathrm{d}l$:

$$L = \frac{\mathrm{d}E}{\mathrm{d}l} \tag{2.14}$$

The unit of L is J·m^{-1}, and the quantity may also be expressed in keV·μm^{-1}.

The **lineal energy**, y, is the quotient of ε by $\bar{l}$, where ε is the energy imparted to the matter in a volume of interest by an energy deposition event, and $\bar{l}$ is the mean chord length in that volume:

$$y = \frac{\varepsilon}{\bar{l}} \qquad (2.15)$$

The unit of y is J·m^{-1}, and the quantity may also be expressed in keV·μm^{-1}.

2.3. DOSIMETRIC QUANTITIES

The kinetic energy released per unit mass, **kerma**, K, is the quotient of dE_{tr} by dm, where dE_{tr} is the sum of the initial kinetic energies of all the charged particles liberated by uncharged particles in a mass dm of material, thus

$$K = \frac{dE_{tr}}{dm} \qquad (2.16)$$

Note: the unit of kerma is the J·kg^{-1} with the special name gray (Gy).

The **absorbed dose, D,** is the quotient of $d\bar{\varepsilon}$ by dm, where $d\bar{\varepsilon}$ is the mean energy imparted by ionizing radiation to matter of mass dm:

$$D = \frac{d\bar{\varepsilon}}{dm} \qquad (2.17)$$

Note: the unit of the absorbed dose is J·kg^{-1} with the special name gray (Gy).

2.4. DOSE EQUIVALENT QUANTITIES

The **quality factor**, Q, weights the absorbed dose for the biological effectiveness of the charged particles (generated by neutrons) producing the absorbed dose. A functional dependence of Q on linear energy transfer, L, in water has been given by the ICRP. The quality factor, Q, at a point in tissue is given by

$$Q = \frac{1}{D} \int_{L=0}^{\infty} Q(L) D_L \, dL \qquad (2.18)$$

where D is the absorbed dose at that point, D_L is the distribution of D in linear energy transfer L, and $Q(L)$ is the corresponding quality factor at the point of interest. The integration is to be performed over the distribution D_L, which results from all charged particles excluding their secondary electrons.

The **dose equivalent, H,** is the product of Q and D at a point in tissue, where D is the absorbed dose and Q is the quality factor at that point:

$$H = Q \cdot D \tag{2.19}$$

Note: the unit for the dose equivalent is $J \cdot kg^{-1}$ with the special name sievert (Sv).

The **dose equivalent rate, $\dot{H}$,** is the quotient of dH by dt, where dH is the increment of dose equivalent in the time interval dt:

$$\dot{H} = \frac{dH}{dt} \tag{2.20}$$

Note: the unit for the dose equivalent rate is $J \cdot kg^{-1} \cdot s^{-1}$ with the special name sievert per second ($Sv \cdot s^{-1}$).

2.5. OPERATIONAL QUANTITIES

The **ambient dose equivalent, $H^*(d)$,** is the dose equivalent at a point in a radiation field that would be produced by the corresponding expanded and aligned field in the ICRU sphere at a depth of d mm on the radius opposing the direction of the aligned field.

Note 1: the unit of ambient dose equivalent is $J \cdot kg^{-1}$ with the special name sievert (Sv).

Note 2: for strongly penetrating radiation (e.g. neutrons), a depth of 10 mm is currently recommended. The ambient dose equivalent for this depth is then denoted by $H^*(10)$.

The **personal dose equivalent, $H_p(d)$,** is the dose equivalent in soft tissue at a depth of d mm below a specified point on the human body.

Note 1: the unit of personal dose equivalent is $J \cdot kg^{-1}$ with the special name sievert (Sv).

Note 2: for strongly penetrating radiation (e.g. neutrons), a depth of 10 mm is currently recommended. The personal dose equivalent for this depth is then denoted by $H_p(10)$.

Note 3: in ICRU Report 47 [2.5], the ICRU has considered the definition of the personal dose equivalent to include the dose equivalent at a depth, d, in a phantom having the composition of ICRU tissue. Then, $H_p(10)$, for the calibration of personal dosimeters, is the dose equivalent at a depth of 10 mm in a phantom composed of ICRU tissue, but of the size and shape of the phantom used for calibration (a 30 cm × 30 cm × 15 cm parallelepiped), and the conversion coefficients, $h_{p,slab}(10)$, are calculated for this configuration.

2.6. PROTECTION QUANTITIES

The **equivalent dose**, H_T, in a tissue or organ is given by

$$H_T = \sum_R w_R D_{T,R} \tag{2.21}$$

where $D_{T,R}$ is the mean absorbed dose in the tissue or organ, T, caused by radiation R, and w_R is the corresponding radiation weighting factor.

Note: the unit of equivalent dose is $J \cdot kg^{-1}$ with the special name sievert (Sv).

The **effective dose**, E, in a tissue or organ is given by

$$E = \sum_T w_T H_T \tag{2.22}$$

where H_T is the equivalent dose in the tissue or organ, T, and w_T is the corresponding tissue weighting factor.

Note: the unit of effective dose is $J \cdot kg^{-1}$ with the special name sievert (Sv).

2.7. CONVERSION COEFFICIENTS

The **neutron fluence to dose equivalent conversion coefficient**, h_Φ, is the quotient of the neutron dose equivalent, H, and the neutron fluence, Φ, at a point in the radiation field undisturbed by the irradiated object:

$$h_\Phi = \frac{H}{\Phi} \tag{2.23}$$

Note 1: any statement of a fluence to dose equivalent conversion coefficient requires the statement of the type of dose equivalent, such as ambient dose equivalent, or personal dose equivalent.

Note 2: values for the conversion coefficients for point energies are given in a joint ICRP/ICRU report [2.7, 2.8]. Spectrum averaged values for several radionuclide source spectra are given by ISO [2.6].

2.8. CALIBRATION AND RESPONSE RELATED QUANTITIES

The **indication or reading**, M, is the value indicated by an instrument.

The **conventional value of a quantity** is the value attributed by formal agreement to a quantity for a given purpose; usually, it is the best estimate of the value.

Note 1: The conventional value is sometimes called the assigned value, best estimate, conventional true value or reference value.

Note 2: A conventional value is, in general, regarded as being sufficiently close to the true value for the difference to be insignificant for the given purpose.

The **response**, R, is the indication divided by the conventional true value of the quantity causing it. The type of response should be specified, for example 'fluence response',

$$R_\Phi = \frac{M}{\Phi} \tag{2.24}$$

or 'dose equivalent response',

$$R_H = \frac{M}{H} \qquad (2.25)$$

If M is a measurement of a rate, then the quantities fluence, Φ, and dose equivalent, H, are replaced by fluence rate, $\dot{\Phi}$, and dose equivalent rate, $\dot{H}$, respectively.

The **energy dependence of response** or **the energy response function**, $R_\Phi(E)$ or $R_H(E)$, is the response, R, with respect to fluence, Φ, or dose equivalent, H, as a function of neutron energy E.

The **calibration factor,** N, is the multiplying factor that relates a device indication under reference exposure conditions to the quantity of interest. It is the reciprocal of the response when the response is determined under reference conditions.

2.9. RADIOACTIVITY

The **activity of an amount of radioactive nuclide in a particular energy state at a given time,** A, is the quotient of dN^+ by dt, where dN^+ is the expectation value of the number of spontaneous nuclear transitions from that energy state in the time interval dt:

$$A = \frac{dN^+}{dt} \qquad (2.26)$$

Note: the unit of the activity is s^{-1} with the special name becquerel (Bq).

REFERENCES TO CHAPTER 2

[2.1] INTERNATIONAL COMMISSION ON RADIATION UNITS AND MEASUREMENTS, Determination of Dose Equivalents Resulting from External Radiation Sources, Report 39, ICRU, Bethesda, MD (1985).

[2.2] INTERNATIONAL COMMISSION ON RADIOLOGICAL PROTECTION, ICRP Publication 60, Pergamon Press, Oxford and New York (1991).

[2.3] INTERNATIONAL COMMISSION ON RADIOLOGICAL PROTECTION, ICRP Publication 103, Elsevier, Amsterdam (2007).

[2.4] INTERNATIONAL COMMISSION ON RADIATION UNITS AND MEASUREMENTS, Fundamental Quantities and Units for Ionizing Radiation, Report 60, ICRU, Bethesda, MD (1998).

[2.5] INTERNATIONAL COMMISSION ON RADIATION UNITS AND MEASUREMENTS, Measurement of Dose Equivalents from External Photon and Electron Radiations, Report 47, ICRU, Bethesda, MD (1992).

[2.6] INTERNATIONAL ORGANIZATION FOR STANDARDIZATION, Reference neutron radiations — Part 3: Calibration of area and personal dosimeters and determination of their response as a function of neutron energy and angle of incidence, International Standard 8529-3, ISO, Geneva (1998).

[2.7] INTERNATIONAL COMMISSION ON RADIOLOGICAL PROTECTION, Conversion Coefficients for Use in Radiological Protection Against External Radiation, ICRP Publication 74, Pergamon Press, Oxford and New York (1996).

[2.8] INTERNATIONAL COMMISSION ON RADIATION UNITS AND MEASUREMENTS, Conversion Coefficients for Use in Radiological Protection Against External Radiation, Report 57, ICRU, Bethesda, MD (1998).

3. PHYSICAL PROPERTIES OF NEUTRONS

Neutrons are one of the fundamental building blocks of matter, making up roughly 50% by weight of all material. Only when they are released from atomic nuclei do they constitute a hazardous form of radiation, and there are only two processes that can achieve this separation and produce 'free' neutrons: a nuclear reaction and spontaneous fission.

Free neutrons are unstable and have a lifetime of 886 s, decaying by emitting an electron and an antineutrino to become a proton. Neutrons have a magnetic moment, and although quite small, it has a value. Represented by the symbol μ_n, its value is $-0.96623640 \times 10^{-26}$ J·T^{-1}, which is approximately 1/1000th of the electron magnetic moment. So, although the neutron is usually thought of as a particle without charge that interacts as though it were a billiard ball, it can be seen that neutrons are more complex entities.

The neutron has a spin of 1/2, and the mass of the neutron is 1.675×10^{-27} kg, which is slightly larger than that of the proton. Neutrons are present in every atomic nucleus with the exception of hydrogen (^{1}H). Neutrons can interact by means of the four common forces: strong nuclear, weak nuclear, electromagnetic (because of their magnetic moment) and gravitational.

Neutrons may be generated by a number of processes, including photoneutron reactions, wherein a high energy gamma ray incident on a high Z target generates neutrons; charged particle interactions, such as a proton impinging on a tritium target; or spontaneous fission in heavy elements. Generally, neutrons are produced with high energies at least above 10 keV, and potentially above 10 MeV, and these fast neutrons are slowed by collisions in matter. These collisions may be elastic, inelastic or non-elastic, and only a small amount of energy may be lost in each collision, and so it will take many collisions to reduce the neutron energy to a low value. Eventually the neutrons will slow to the point where they come to be in thermal equilibrium with the medium through which they are passing, and their distribution of velocities will have a most probable value at 20°C of 2200 m·s^{-1}, which corresponds to a neutron energy of 0.0253 eV. Generally, neutrons whose energies are below the sharp drop in the absorption cross-section in cadmium at ~0.4 eV are referred to as thermal neutrons.

When neutrons interact with matter, they undergo a number of collisions with atoms and may be considered to be acting like gas molecules that eventually come into thermal equilibrium with their surroundings. In order to evaluate the most probable distribution of neutron velocities after they have come to equilibrium, a Maxwellian distribution can be assumed.
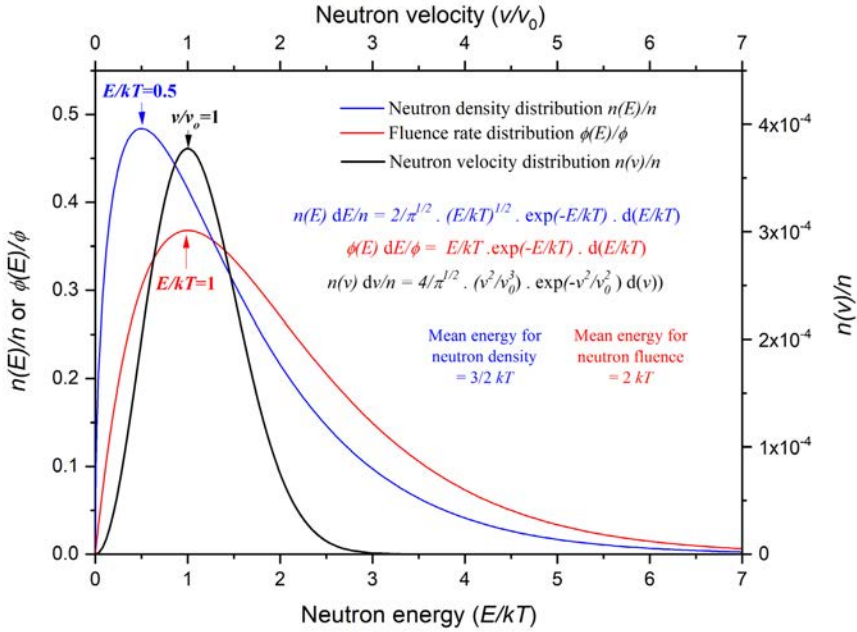
FIG. 3.1. The thermal Maxwell–Boltzmann distributions in energy, fluence and velocity.

The kinetic energy distribution of neutrons in thermal equilibrium with their surroundings at temperature T (K) may be written [3.1] as

$$\frac{n(E)\mathrm{d}E}{n} = \frac{2}{\sqrt{\pi}}\sqrt{\frac{E}{kT}}\exp\left(\frac{E}{kT}\right)\mathrm{d}\left(\frac{E}{kT}\right) \tag{3.1}$$

where n is the total number of neutrons in the system, $n(E)$ is the number of neutrons of energy E per unit energy interval in the range from E to $E + \mathrm{d}E$ and k is the Boltzmann constant.

Thermal neutron distributions approximate to a Maxwell–Boltzmann function and can be represented in several different ways. Figure 3.1 shows thermal distributions in terms of neutron density, $n(E)$, fluence rate, $\Phi(E)$, and velocity, $n(v)$. The reference speed, v_0, in this case is 2200 m·s^{-1}, and the reference energy, kT, is 0.0253 eV.

Relationships among neutron velocity, temperature and energy can be given by

$$T = 1.159 \times 10^4 E \tag{3.2}$$

$$v = 13.83 \cdot \sqrt{E} \tag{3.3}$$

where E is in eV, v is in km·s^{-1} and T is in K [3.2].

Because neutron energies span such a large range, a historical precedent has been established to refer to various energy regions with descriptive terms. There is no general agreement as to the exact energies specified by the following neutron energy classification that is generally used, but the approximate values shown in Table 3.1 for each region can be assumed.

TABLE 3.1. NAMES OF NEUTRON ENERGY REGIONS

Name of neutron energy region	Approximate energy range
High energy (or relativistic)	> 10 MeV
Fast	10 keV to 10 MeV
Intermediate	100 eV to 10 keV
Slow	< 1 eV
Epithermal[a]	0.025 to 1 eV
Thermal[b]	0.025 eV
Cold	5×10^{-5} eV to 0.025 eV

Courtesy of National Physical Laboratory.

[a] The epithermal region is sometimes considered to be above the cadmium cut-off energy at 0.4–0.5 eV, corresponding to the energy at which a sharp decrease in the cadmium cross-section occurs.

[b] At 20°C, the peak of the thermal neutron fluence distribution occurs at an energy of 0.0253 eV. The upper bound of the energy of thermal neutrons is sometimes given the cadmium cut-off energy.

3.1. MODERATION

The process of moderation is the reduction of neutron energy to the level of thermal energy by means of scattering interactions in the material used as a moderator. Materials that are effective moderators are those with a high percentage of protons including hydrogenous compounds. The materials used for the purpose of moderation should have a large neutron scattering cross-section and a small absorption cross-section and should produce a large energy loss per collision. Table 3.2 shows some properties of materials, and it can be seen that water and heavy water, D_2O, are effective since they require only approximately 20–30 collisions on average to thermalize fission neutrons of approximately 2 MeV [3.3].

TABLE 3.2. AVERAGE NUMBER OF COLLISIONS, $\bar{n}$, REQUIRED TO REDUCE APPROXIMATELY 2 MeV NEUTRONS TO 0.025 eV BY ELASTIC SCATTERING FOR VARIOUS MATERIALS AT A TEMPERATURE OF 20°C

Material	Density (10^3 kg·m^{-3})	$\bar{n}$
H_2O	1.00	20
D_2O	1.10	33
Be	1.85	90
C	1.67	119
Concrete	2.3	30
Al	2.70	262
Fe	7.86	540
Pb	11.35	1960
Bi	9.75	1990
U	18.9	2250

Courtesy of National Physical Laboratory (adapted from Ref. [3.3]).

3.2. NEUTRON SHIELDING MATERIALS

Both photons and neutrons are uncharged and are attenuated approximately exponentially in matter. Therefore, rather large thicknesses of shielding materials are necessary to reduce the dose equivalent rate to required levels. Examples of neutron dose equivalent transmission through some common shielding materials are shown in Fig. 3.2.

The data shown in Fig. 3.2 indicate the relative dose equivalent rates behind various thicknesses of shielding materials. The source in each case was a broad beam of ^{252}Cf neutrons. The figure highlights the importance of light element-containing materials like polyethylene in reducing neutron transmission. In construction, concrete is the most important shielding material, with the water content being significant. In actual construction concrete, iron reinforcing bars would be used, and guidance on the addition of the iron is given in Ref. [3.5].
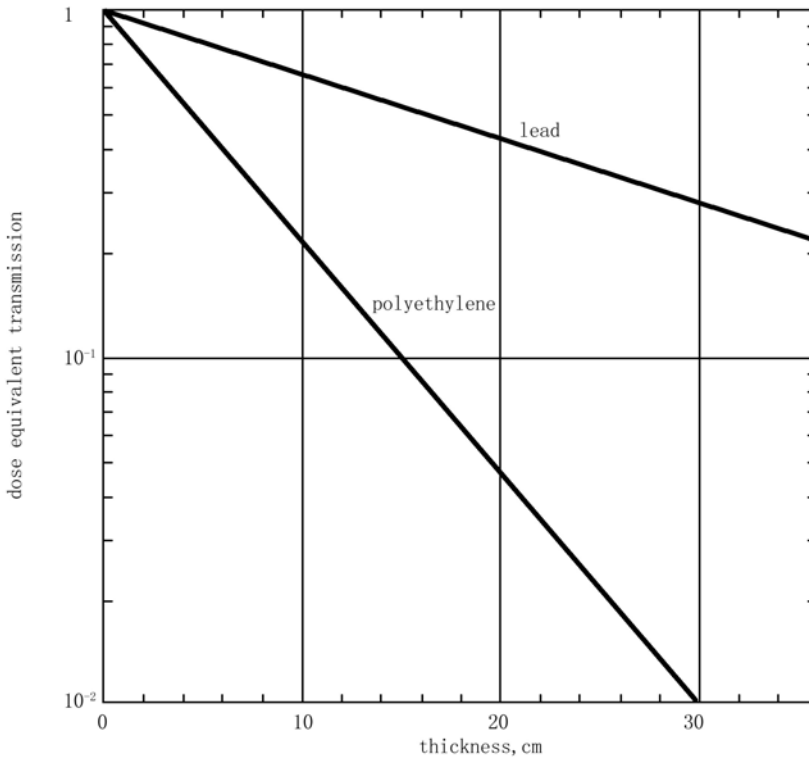
FIG. 3.2. Broad beam dose equivalent transmission of ^{252}Cf neutrons through lead (11.35 g·cm^{-3}) and polyethylene (0.96 g·cm^{-3}). (Reproduced from Ref. [3.4] with permission from ICRP.)

Higher energy neutrons may require the use of laminated shields in order to reduce the neutron energy to the point where moderation and capture are more efficient. A material such as iron (or steel) should be placed nearest the neutron source, since it has a relatively high inelastic cross-section, so interactions with iron will reduce the energy of the neutrons. If polyethylene is placed after the iron, it will provide a large hydrogen elastic scattering cross-section that further attenuates slower neutrons. This is illustrated in Fig. 3.3. When these neutrons have been moderated by the polyethylene, they will be captured by a thermal neutron absorber, such as boron, that can be mixed with the polyethylene. The 0.43 MeV gamma rays from the $^{10}B(n,\alpha)^{7}Li$ interaction can then be absorbed by using a final layer of lead [3.6].
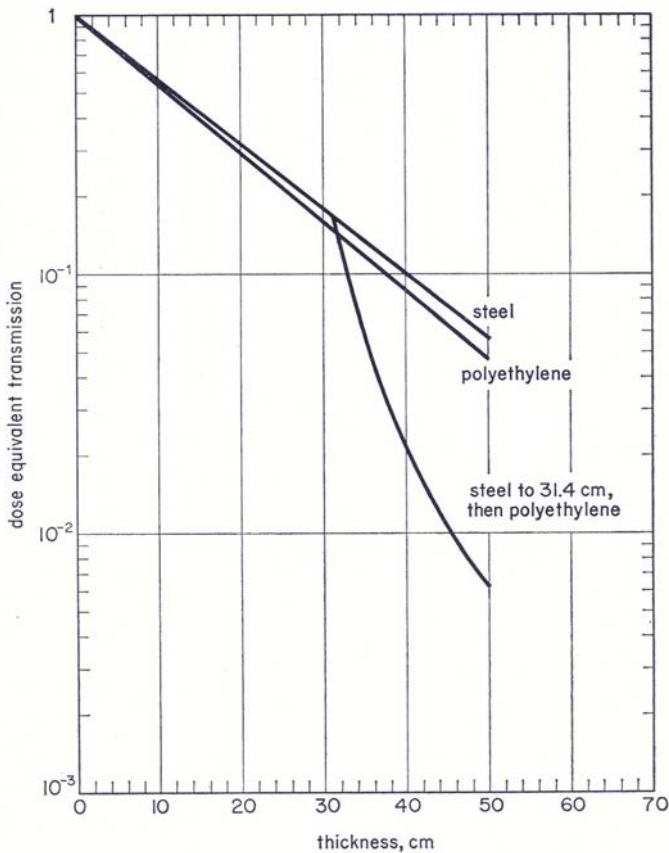
FIG. 3.3. Dose equivalent transmission for a broad beam of approximately 14 MeV neutrons through slabs of steel, polyethylene, and a combination of steel and polyethylene. (Reproduced from Ref. [3.4] with permission from ICRP.)

3.3. GENERAL CHARACTERISTICS OF COMMON NEUTRON FIELDS

Many neutron sources encountered in the workplace exhibit a neutron fluence spectrum that is composed of three basic parts. These are, in order of increasing energy, a thermal neutron peak, followed by a part of the distribution where the fluence follows an approximately $1/E$ behaviour, and a fast neutron peak.

Schematically, this is shown in Fig. 3.4 for a number of sources. The neutrons giving rise to the high energy peaks are from a fission source, a fusion source, a 14 MeV source and a spallation (nuclear fragmentation producing neutrons) source. The spectra are plotted in terms of lethargy, u, defined by

$$\mathrm{d}u = \mathrm{d}\left(\ln(E_0 / E)\right) = -\mathrm{d}E / E \tag{3.4}$$

Additional discussion of lethargy can be found in Section 9.

Figure 3.4 shows the wide range of neutron energies encountered and the distinct regions where different interactions occur. The fact that neutron spectra are complex and that their energies span a wide range adds to the difficulty of detector design and the determination of neutron dose equivalent in general. There is no perfect neutron dosimeter; therefore, multiple detectors are almost always needed for personal and area dosimetry.
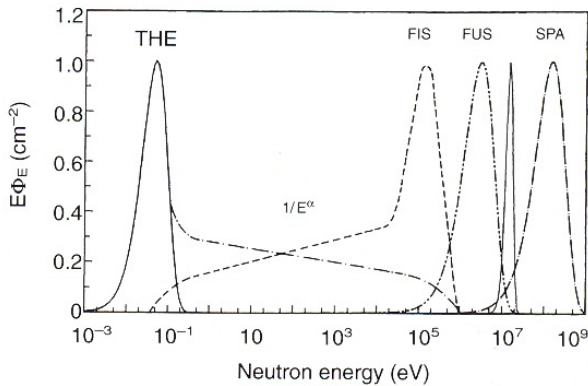
FIG. 3.4. *Normalized spectral neutron fluence of primary neutron sources behind shielding found in nuclear power plants (denoted FIS), plasma fusion experiments (denoted FUS), a 14 MeV source and spallation at high energy accelerators (denoted SPA), along with $1/E\alpha$ where $0.5 < \alpha < 1.5$ and a thermal neutron peak denoted THE. (Reproduced from Ref. [3.7] with permission from Oxford University Press.)*

REFERENCES TO CHAPTER 3

[3.1] INTERNATIONAL ATOMIC ENERGY AGENCY, Neutron Fluence Measurements, Technical Reports Series No. 107, IAEA, Vienna (1970).

[3.2] LAPP, R.E., ANDREWS, H.L., Nuclear Radiation Physics, 4th edn, Prentice Hall, Hoboken, NJ (1972).

[3.3] KAYE, G.W.C., LABY, T.H., Tables of Physical and Chemical Constants, Atomic and Nuclear Physics, 16th edn, National Physical Laboratory, Teddington, UK (1995).

[3.4] INTERNATIONAL COMMISSION ON RADIOLOGICAL PROTECTION, Data for Protection against Ionizing Radiation from External Sources: Supplement to ICRP Publication 15, ICRP Publication 21, Pergamon Press, Oxford (1973).

[3.5] AMERICAN NUCLEAR SOCIETY, Nuclear Analysis and Design of Concrete Radiation Shielding for Nuclear Power Plants, ANSI/ANS Standard 6.4-2006, American Nuclear Society, LaGrange Park, IL (2006).

[3.6] INTERNATIONAL COMMISSION ON RADIATION UNITS AND MEASUREMENTS, Clinical Neutron Dosimetry Part 1: Determination of Absorbed Dose in a Patient Treated by External Beams of Fast Neutrons, Report 45, ICRU, Bethesda, MD (1989).

[3.7] KLEIN, H., Workplace radiation field analysis, Radiat. Prot. Dosim. **70** (1997) 225–234.

4. NEUTRON INTERACTIONS WITH MATTER

As with all types of ionizing radiation, neutrons can cause atoms to gain or lose electrons and thus become ionized. However, neutrons are an indirectly ionizing radiation because they deposit energy by means of secondary charged particles that they produce during interactions with matter. When ionizing radiation is incident on matter, the result may be that the radiation is transmitted, reflected (scattered) or absorbed. The probability that the radiation will interact with matter can be given by an interaction coefficient known as a cross-section, and this term suggests a physical area in which the interactions can take place. In its most basic form, the cross-section, σ, can be defined as the probability, P, of an interaction per unit fluence, Φ (see also Section 2.2):

$$\sigma = \frac{P}{\Phi} \tag{4.1}$$

Photons are also indirectly ionizing and interact with the atomic electrons of matter through a number of processes that are dependent upon the energy of the photon and atomic number of the target material. The shapes of the photon interaction coefficients as a function of energy are generally smooth. On the other hand, the interactions of neutrons with matter are somewhat more complex and involve scattering or absorption by nuclei. Since neutrons are neutral particles, they interact with nuclei more easily than charged particles such as protons or alpha particles. Charged particles experience an electrostatic repulsion from like charges in the nucleus and will need a large amount of energy to enter the nucleus. The following subsections describe the most common types of neutron interactions in matter. There are basically two types of interactions: scattering from, or absorption by, atomic nuclei. The scattering interactions may be either elastic or inelastic. Elastic scattering is usually thought of as being a nuclear analogue of classic billiard ball collisions, in which the incoming particle is a neutron and the outgoing particle is a neutron with a lower energy, leaving the target nucleus unaltered. Inelastic scattering occurs when a neutron is briefly captured by the nucleus and a neutron is subsequently emitted. The incident neutron excites the nucleus to an energy that is the difference between the energies of the incident and emitted neutrons, and the nucleus is left in an excited state that decays with the emission of a gamma ray. Absorption interactions involve the incoming neutron becoming part of the target nucleus, resulting in the emission of gamma rays, charged particles such as protons or alpha particles, secondary neutrons or a fission of the target nucleus with the emission of gamma rays, charged particles, nuclear fragments and neutrons [4.1].

4.1. ENERGY MODERATION/ELASTIC SCATTERING

Neutrons can interact with atomic nuclei by means of elastic scattering, in which the energy transferred by the neutron to the nucleus, E_{tr}, is given by the following non-relativistic expression:

$$E_{tr} = E_n \frac{4Mm}{(M+m)^2} \cos^2 \theta \qquad (4.2)$$

where E_n and m are the neutron's energy and mass, respectively, M is the target nucleus mass and θ is the angle of the recoiling nucleus in the laboratory coordinate system.

The energy transfer is greatest when the neutron hits the nucleus head-on and is least for a glancing incidence. The energy transfer is also at a maximum when the mass of the nucleus is closest to that of the neutron, so that $M \cong m$. For example, the nucleus of the hydrogen atom is a proton whose mass is nearly equal to that of the neutron, and a neutron–proton collision would result in nearly maximum energy transfer. If the neutron is scattered from a nitrogen or oxygen nucleus, the neutron would not lose as much energy because of the heavier masses
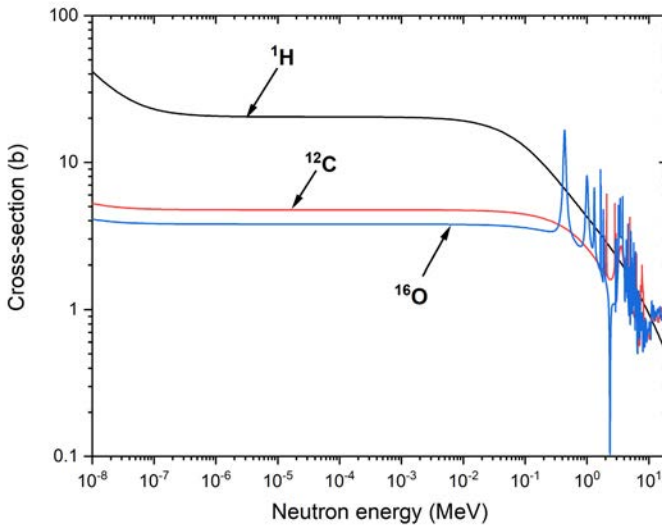
FIG. 4.1. Neutron elastic scattering cross-sections from the Korea Atomic Energy Research Institute (KAERI) evaluated data library [4.3]. Above a neutron energy of approximately 0.3 MeV, the ^{16}O cross-section exhibits sharp increases or decreases (resonances), as does the ^{12}C cross-section above approximately 2 MeV.

of these nuclei. Therefore, materials with a large hydrogen content, and hence more protons, are most efficient in slowing down neutrons through the process of elastic scattering [4.2]. Figure 4.1 shows some examples of elastic scattering cross-sections as a function of neutron energy for three common elements.

4.2. INELASTIC SCATTERING

Inelastic scattering interactions of a neutron and a target nucleus result in a change in the kinetic energy of the target nucleus. This is indicated by an asterisk, as shown in the example below. The emitted neutron will have less kinetic energy than the incoming particle, as indicated by a superscript prime. The compound nucleus will be in an excited state and can return to the ground state by emitting one or more gamma rays and a neutron of lower energy than the incoming neutron (n,n'). A threshold energy is required for inelastic scattering in order to raise the target nucleus to an excited state from which it can emit gamma rays. An example of an inelastic scattering interaction is $^{16}O(n,n')^{16}O^*$, wherein the oxygen nucleus is left in an excited state at 6.1 MeV (indicated by the asterisk), and it subsequently decays with the emission of a 6.1 MeV gamma ray [4.4–4.6]. This interaction can occur in the cooling water of a reactor or accelerator and can pose a significant radiation hazard because of the high energy of the gamma rays.

4.3. NON-ELASTIC COLLISION OR REACTION

These types of absorption interactions occur when the incoming neutron forms a compound nucleus in an excited state that decays with the emission of particles [4.7]. An example of such an interaction is the neutron bombardment of ^{16}O, resulting in the formation of the stable nucleus ^{13}C:

$$n + {}^{16}O \rightarrow {}^{13}C + {}^{4}He$$
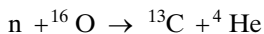
The interaction can also be written in the form, $^{16}O(n,\alpha)^{13}C$. Non-elastic interactions can produce a variety of charged particles such as protons, alpha particles, deuterons or tritons. Prompt gamma ray emissions can also result from this type of interaction. Some non-elastic cross-sections have energy thresholds ranging from a few MeV to approximately 10 MeV, and some exhibit resonance peaks in this region.

4.4. RADIATIVE CAPTURE

After neutrons have undergone a number of scattering interactions, their energies may be degraded to the point where the spectrum contains numerous thermal neutrons. These low energy neutrons have a high probability of entering the nucleus and forming a compound nucleus that is in an excited state and loses all its excitation energy by emitting one or more gamma rays. This absorption process can result in the production of an isotope with one more neutron than the original nucleus. In the case of hydrogen, the neutron can be captured by the nucleus (a proton), forming a deuteron and releasing a 2.2 MeV gamma ray. The isotope produced by a radiative capture interaction can be radioactive, in which case additional gamma rays will subsequently be emitted.

4.5. FISSION

The fission process can occur in heavy elements including Th, U, Np and Pu when neutrons interact with these nuclei. A compound nucleus is formed, which splits into two roughly equal parts with the emission of additional neutrons and gamma rays. Isotopes such as ^{235}U, ^{238}U and ^{239}Pu can undergo fission when hit with neutrons of any energy. The interaction results in the release of
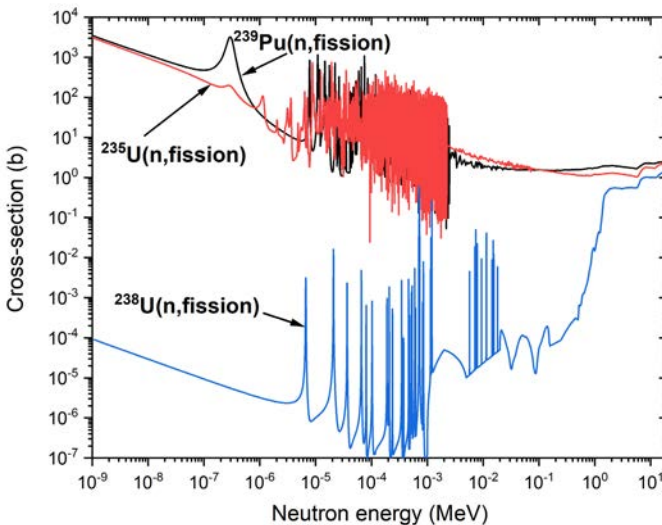
FIG. 4.2. Fission cross-sections for two uranium isotopes and a plutonium isotope [4.3]. These cross-sections are large for most neutron energies and are nearly maximal for thermal neutrons.

the binding energy of the nuclide along with additional neutrons. This process can produce a self-sustaining chain reaction. Naturally occurring uranium can also undergo spontaneous fission, which does not require neutron bombardment, and which produces kinetic energy that is eventually shared by the complete material as thermal energy. The branching ratio for decay by spontaneous fission is, however, extremely small at 7×10^9%.

The cross-sections for neutron induced fission display numerous peaks (resonances) corresponding to energies at which the probability of interaction goes through a maximum. Examples of fission cross-sections are shown in Fig. 4.2. It can be seen that for ^{235}U and ^{239}Pu, the fission cross-sections for thermal neutrons are quite large.

4.6. TRANSMUTATION

An incident neutron may remain in the target nucleus. If the excited nucleus then de-excites by emitting a proton or an alpha particle, its atomic weight will change. It becomes a different element; therefore, the process is called transmutation. In the following example, a ^{7}Li nucleus is formed:

$$^{10}B(n,\alpha)^7Li$$
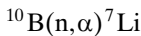
This reaction can be used in a neutron detector. Because the neutron has imparted energy to the alpha particle and the ^{7}Li nucleus, these particles can be detected by the ionization they produce in a BF_3 gas filled counter.

4.7. NEUTRON ACTIVATION

As mentioned earlier, non-elastic neutron interactions can occur, resulting in n,γ or n,α events. The result can be that the nucleus de-excites by emitting one or more prompt gamma rays or alpha particles. The interaction can also result in the production of a radioactive nucleus. Radioactive isotopes of metals such as aluminium, copper and steel result from neutron bombardment, and these radionuclides may have half-lives of minutes to hours, decaying by emitting electrons, neutrinos and gamma rays [4.5]. Two examples of neutron activation interactions are the following:

$$^{27}\text{Al}(n,\alpha)^{24}\text{Na and }^{63}\text{Cu}(n,\alpha)^{60}\text{Co}$$
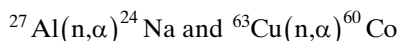
These interactions may occur in the structural materials found in a nuclear installation and thus may represent a radiation protection hazard that persists after the source of radiation ceases. Activation cross-sections generally show thresholds in energy that may be used for detection purposes and for simple few-channel spectral analysis. See Section 12 for examples.

4.8. HIGH ENERGY INTERACTIONS

As the neutron energy increases above 15–20 MeV, more complex interactions are possible, resulting in multiple neutron production: (n,2n), (n,3n) and (n,xn). In addition, fission interactions can be induced at high energies, such as ^{209}Bi(n,f). This interaction has been used for high energy neutron measurements at accelerator laboratories and in space [4.8].

REFERENCES TO CHAPTER 4

[4.1] EVANS, R.D., The Atomic Nucleus, McGraw Hill, New York (1955).

[4.2] MARION, J.B., FOWLER, J.L., Fast Neutron Physics, Vol. 2, Interscience Publishers, New York (1963).

[4.3] KOREA ATOMIC ENERGY RESEARCH INSTITUTE, Table of Nuclides, KAERI, Taejon, South Korea (2005), www.atom.kaeri.re.kr; data also obtained from the National Nuclear Data Center, Brookhaven, NY at www.nndc.bnl.gov

[4.4] INTERNATIONAL ATOMIC ENERGY AGENCY, Neutron Monitoring for Radiological Protection, Technical Reports Series No. 252, IAEA, Vienna (1985).

[4.5] DENNIS, J.A., Neutron flux and energy measurements, Phys. Med. Biol. **11** (1966) 1–14.

[4.6] US DEPARTMENT OF ENERGY, DOE Fundamentals Handbook, Nuclear Physics and Reactor Theory, Volume 1 of 2, DOE-HDBK-1019/1-93, Department of Energy, Washington, DC (1993).

[4.7] RINARD, P., Chapter 12, Neutron Interactions with Matter, Passive Nondestructive Assay of Nuclear Materials, Los Alamos National Laboratory Report LA-UR-90-732, NUREG/CR-5550, LANL, Los Alamos, NM (1991).

[4.8] CROSS, W.G., TOMMASINO, L., Dosimetry of high energy neutrons and protons by ^{209}Bi fission, Radiat. Prot. Dosim. **70** (1997) 419–424.

5. NEUTRON DOSIMETRY

Neutron irradiation of materials results in the production of physical, chemical and biological effects related to the quantity of energy deposited in the material. For neutrons, as well as all other types of ionizing radiation, the fundamental quantity for specifying the effects of that radiation is the energy transfer to the material as given by the absorbed dose. In addition to the absorbed dose deposited in a material, the nature of the effects produced by irradiation is dependent upon the physical characteristics of the incident radiation field. The effects produced by neutrons are generally different from those produced by electrons and photons, and this is especially true for the biological effects of neutron irradiation.

Dosimetric quantities, such as absorbed dose, and dose equivalent quantities, such as ambient dose equivalent, can be thought of as being products of radiometric quantities and interaction coefficients. Radiometric quantities include particle number and fluence, the number of particles incident on a spherical surface. Interaction coefficients include the kerma coefficient and the fluence to dose equivalent conversion coefficient.

5.1. ABSORBED DOSE AND KERMA

The dosimetric quantities are defined by the ICRU, and the definitions for the kinetic energy released in matter, kerma and absorbed dose, D, are given by Eqs (2.16) and (2.17) in Section 2.3.

For a fluence of neutrons, Φ, of energy, E, according to Eq. (2.16), the kerma in a specified material can be expressed as

$$K = \Phi E \frac{\mu_{tr}}{\rho} \tag{5.1}$$

where μ_{tr}/ρ is the mass energy transfer coefficient of the material for neutrons. The kerma per unit fluence, K/Φ, is called the kerma coefficient and it has a physical dimension (J kg^{-}1·m^{-2}).

Tables of kerma coefficients for various materials and neutron energies are available [5.1, 5.2], and the kerma coefficient for a distribution of neutron energies can be calculated using

$$K = \int \Phi_E E \frac{\mu_{tr}}{\rho} dE \qquad (5.2)$$

Knowing a value for the neutron fluence, one can relate the value of kerma for two materials such as tissue and bone. For dosimetric calculations, an assumption can be made that the values of absorbed dose and kerma for neutrons are approximately equal at the point of charged particle equilibrium in matter, where the same number of secondary charged particles of the same type and energy are entering a volume as have left it.

Further information about these quantities can be found in reports on quantities and units (e.g. ICRU Report 51 [5.3]), and a discussion of their relationships and of the basic stochastic quantity, energy imparted, $\bar{\varepsilon}$, can be found in ICRU Report 26 [5.4].

In the case of ICRU four element tissue, neutron interactions with H, O, C and N produce the secondary charged particles that give rise to kerma or absorbed dose. Figure 5.1 shows the relative contributions to kerma from neutron interactions with the major tissue elements [5.5]. Although hydrogen comprises only approximately 10% of tissue by weight, the n,p scattering cross-section is large for lower energy neutrons. Therefore, hydrogen interactions are the largest
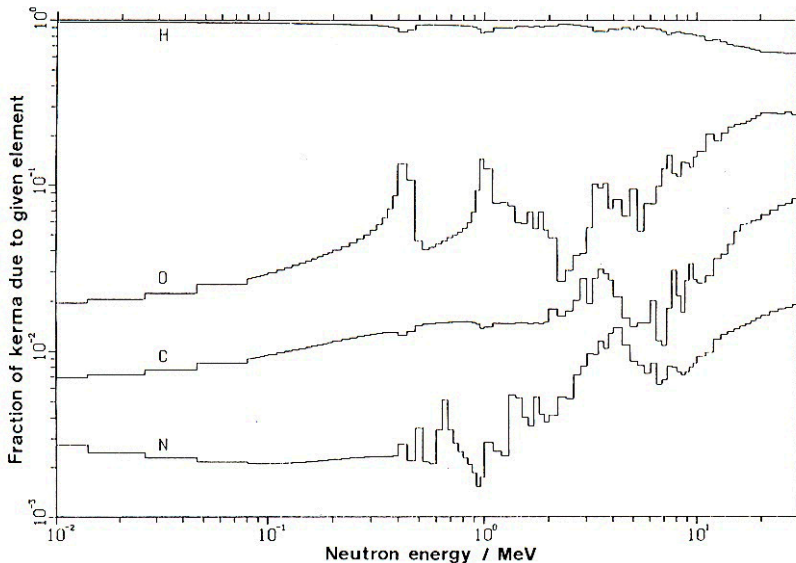
FIG. 5.1. Relative contributions to kerma for ICRU tissue from interactions with the elements H, O, C and N. (Reproduced from Ref. [5.5] with permission from ICRU).

contributor to tissue kerma, representing approximately 90% of the kerma. However, as the neutron energy increases above about 10 MeV, contributions from interactions in the other elements become more important. At a neutron energy of 14 MeV, the contribution to kerma from hydrogen interactions drops to approximately 70%.

The initial energy of neutrons strongly affects the energy spectra of the secondary charged particles produced in the irradiated material. This can be seen in the two plots of Fig. 5.2, depicting the calculated neutron induced secondary charged particle spectra in ICRU tissue [5.6]. The left hand plot shows the spectra of several charged particles such as oxygen, carbon and nitrogen nuclei, along with protons, all generated by 1 MeV neutrons incident on ICRU tissue. The right hand plot shows the same set of spectra for incident 14 MeV neutrons, where it can be seen that there are additional particle types and higher energies extending approximately to the maximum energy of the incident neutrons. The protons appearing above the energy of the incoming neutrons in both plots arise from the exoergic n,p reaction in nitrogen, $^{14}N(n,p)^{14}C$.

Table 5.1 lists the percentage mass compositions of human tissues and reference materials. It can be seen that most of the tissues are composed primarily of H, C, O and N. Cortical bone is a slight exception in terms of composition, having only a small percentage of hydrogen. Therefore, it is expected that
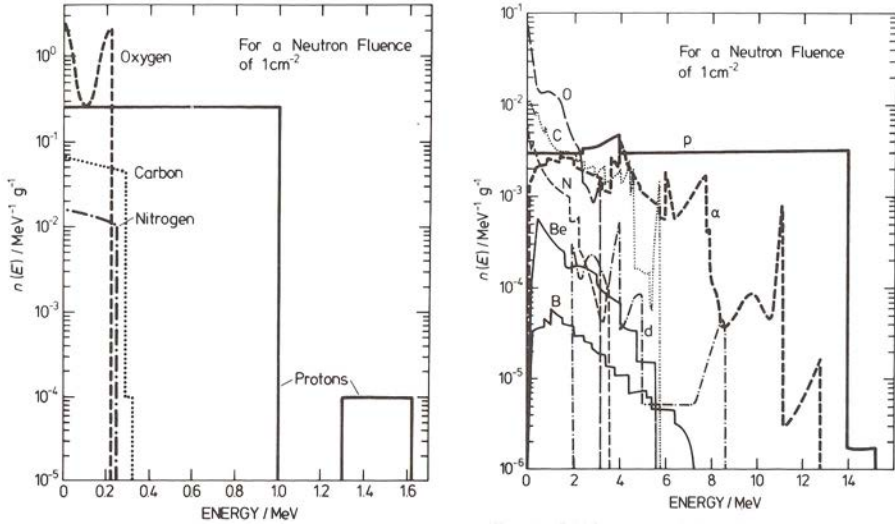
FIG. 5.2. *Initial spectra of charged particles for a 1 cm^{-2} neutron fluence of 1 MeV (left panel) and 14 MeV (right panel) neutrons in ICRU tissue. The symbols p, d and α refer to recoil protons, deuterons and alpha particles (helium nuclei), respectively. (Reproduced from Ref. [5.6] with permission from ICRU.)*

TABLE 5.1. PERCENTAGE MASS COMPOSITION OF HUMAN TISSUES
AND REFERENCE MATERIALS

Tissue or organ	H	C	N	O	Na	Mg	P	S	Cl	K	Ca
Muscle (ICRU)	10.2	12.3	3.5	72.9	0.1	—	0.2	0.5	—	0.3	—
Skin	10.0	22.7	4.6	61.5	—	—	—	0.2	0.3	0.1	—
Blood	10.0	9.8	2.9	74.5	0.2	—	—	0.2	0.3	0.2	—
Brain (cerebrum)	10.8	13.3	1.3	72.5	0.2	—	0.4	0.2	0.2	0.3	—
Soft tissue (ICRU)	10.1	11.1	2.6	76.2	—	—	—	—	—	—	—
Fat (adipose)	11.6	64.0	0.8	22.7	0.1	—	—	0.1	0.1	—	—
Yellow marrow	11.3	63.3	0.6	22.7	0.4	—	—	0.1	0.1	—	—
Red marrow	10.0	41.3	3.2	41.3	—	—	—	—	—	—	—
Intestine	10.0	9.4	2.1	77.0	0.1	—	0.1	0.1	0.1	0.1	—
Kidneys	10.3	12.9	2.7	74.2	0.2	—	0.2	—	0.2	0.2	—
Liver	10.0	14.4	2.8	66.7	0.1	—	0.3	0.3	0.2	0.3	—
Pancreas	9.7	13.0	2.1	67.0	0.1	—	0.2	—	0.2	0.2	—
Lung	9.9	10.0	2.8	74.0	0.2	—	0.1	0.2	0.3	0.2	—
Bone (cortical)	3.4	15.5	4.0	44.1	0.1	0.2	10.2	0.2	—	—	22.2

Reproduced from Ref. [5.5] with permission from ICRU.
—: no significant amount of the element in the tissue.

n,p scattering interactions with hydrogen nuclei will be much less important
in this tissue.

Photons and electrons deposit energy predominantly via secondary
electrons produced by interactions with atomic electrons. The neutron interacts
predominantly with the atomic nucleus, and the energy deposition is by recoiling

charged particles extending from protons to higher Z particles. The energy deposition density is thus rather different. For this reason, the biological effects of equal dose deposition by photons and neutrons are not the same, and there is a requirement in radiation protection to introduce a parameter that makes allowance for the different energy deposition densities; in other words, there is a need for a measure of the *quality* of the radiation.

5.2. SECONDARY CHARGED PARTICLE SPECTRA

Since neutrons are indirectly ionizing and can generate secondary charged particles that deposit energy, it is necessary to consider the details of this energy deposition process. The mass stopping power, S/ρ, for charged particles, such as electrons, protons or alpha particles, is dependent upon the energy lost per differential element of distance that the particles traverse in the material, thus

$$\frac{S}{\rho} = \frac{1}{\rho}\frac{\mathrm{d}E}{\mathrm{d}l} \tag{5.3}$$

where dE is the energy lost by charged particles traversing a distance dl in a material of density ρ.

In order to consider the charged particle interactions that actually contribute to energy deposition, it is necessary to define another related quantity, the linear energy transfer, L. The linear energy transfer, or linear collision stopping power, of a material is the quotient of dE by dl for a charged particle, where dE is the mean energy lost by the particle in collisions while traversing a distance dl (see also Section 2.2):

$$L = \frac{\mathrm{d}E}{\mathrm{d}l} \tag{5.4}$$

In this case, dE is the total energy lost by a charged particle due to collisions in traversing a distance dl. E may be expressed in terms of eV, and L, the unrestricted linear energy transfer, may be expressed in eV·μm^{-1} or a convenient multiple such as keV·μm^{-1} [5.6].

The linear energy transfer cannot be directly measured, but there is another quantity, lineal energy, that can be directly measured in a radiation monitoring situation. Rather than dealing with the energy lost along a distance traversed, the lineal energy quantifies the energy imparted within a volume of interest. For radiation protection purposes, that volume might be considered as the volume of a biological cell.
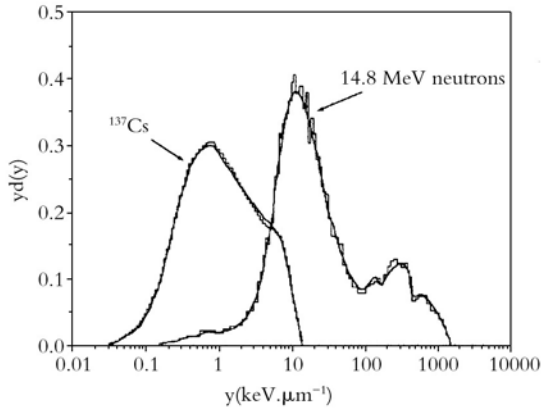
FIG. 5.3. Distribution of dose in lineal energy, y, measured with a tissue equivalent proportional counter (TEPC) having an effective diameter of 2 μm. Photons from ^{137}Cs have lower lineal energy, whereas 14.8 MeV neutrons have a lineal energy distribution extending above 1000 keV μm^{-1}. (Reproduced from Ref. [5.7] with permission from Oxford University Press.)

The lineal energy, y, is the quotient of ε by $\bar{l}$, where ε is the energy imparted to the matter in a volume of interest by an energy deposition event and $\bar{l}$ is the mean chord length in that volume (see also Section 2.2):

$$y = \frac{\varepsilon}{\bar{l}} \tag{5.5}$$

Lineal energy is a statistical or stochastic quantity, since the charged particle energy depositions in a volume such as a biological cell are random. An example of a measured distribution of absorbed dose in lineal energy for both photons and neutrons is shown in Fig. 5.3.

5.3. QUALITY FACTORS AND RADIATION WEIGHTING FACTORS

The quality factor, Q, is used to account for the different biological effects of charged particles produced by neutrons. Q weights the absorbed dose for the biological effectiveness of the charged particles depositing the absorbed dose. It is a quantity that is used only at the low doses encountered in radiation protection. In its simplest form, the dose equivalent is expressed as a product of the absorbed dose and the quality factor. ICRP has provided a relationship between the linear

energy transfer, L, and the mean quality factor, $\bar{Q}$ [5.8]. The mean quality factor at a point in tissue is given by

$$\bar{Q} = \frac{1}{D}\int_{L} Q(L)D_L \ \mathrm{d}L \qquad\qquad (5.6)$$

where D is the absorbed dose at the point, D_L is the distribution of dose in L, and $Q(L)$ is the quality factor at the point of interest. The integration is performed over the D_L that results from all charged particles excluding their secondary electrons.

As mentioned above, the quantity lineal energy can be directly measured, and for radiation protection purposes the ICRU recommends specifying radiation quality in terms of lineal energy in a 1 μm diameter sphere of ICRU muscle tissue [5.6].

Several forms have been adopted over the years for the dependence of Q on L; see, for example, Ref. [5.9]. The currently recommended dependence, and the one used to calculate the fluence to dose equivalent conversion coefficients for the operational quantities used for measurements in radiation protection, is that published in ICRP 60 [5.10], and is given by

$$Q(L) \begin{cases} 1 & \text{for} \quad L \le 10 \\ 0.32L - 2.2 & \text{for} \quad 10 < L < 100 \\ 300/\sqrt{L} & \text{for} \quad L \ge 100 \end{cases} \qquad\qquad (5.7)$$

where L is the unrestricted linear energy transfer value in water at the point of interest.

Figure 5.4 shows the $Q(L)$ relationship presently recommended by the ICRP in Ref. [5.11] and compares it with an earlier form, given in ICRP 26 [5.10], which was in use for some years. The figure also displays the approximate range of L values over which electrons, protons and alpha particles deposit their dose. These ranges show the very different quality factors to be expected for photons, which deposit their energy mainly via electrons, and neutrons, which deposit their energy in tissue predominantly via recoil protons.

The human body is a complex structure with tissues of different densities, compositions and radiosensitivities. Therefore, the distribution of neutron dose as a function of position in the body, as well as the radiosensitivity of the individual tissues or organs, all contribute to the biological effects of neutrons. As neutrons penetrate the body, two important phenomena occur. First, the neutron fluence as a function of depth in the body will generally decrease because of absorption and scattering. Second, there is an energy dependent effect because the rate of decrease with depth in the body is greater for low energy neutrons and less
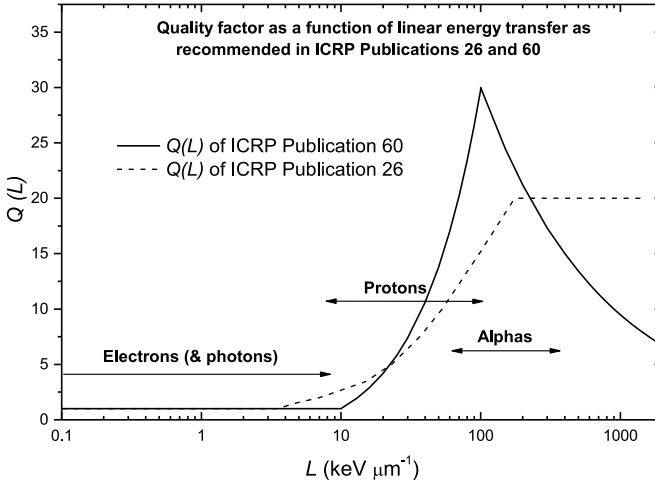
FIG. 5.4. Q(L) *relationships of ICRP 26 and 60. Also shown is the range of* L *values over which electrons, protons and alpha particles tend to deposit dose.*

for higher energy neutrons. This results in a change in the neutron energy distribution. At greater depths, there will be more neutrons of higher energy present in the distribution.

Neutron interactions with tissue include the elastic scattering with protons in hydrogen and nitrogen atoms, and neutrons can be captured via the ^{1}H(n,γ)^{2}H or ^{14}N(n,p)^{14}C interactions. The former interaction results in the production of 2.2 MeV photons. Thus, the fraction of photons as a function of depth in the body increases as more photons are produced and more neutrons are scattered and absorbed; this is illustrated in Fig. 5.5. Since photons have a Q of 1, and quality factors for neutrons can range from approximately 5 to 20 or more, the biological effects of the mixed radiation field will change with position in the body [5.11].

5.4. OPERATIONAL DOSE EQUIVALENT QUANTITIES

The dosimetric quantities used in radiation protection are the ambient dose equivalent, $H^*(d)$, and the personal dose equivalent, $H_p(d)$, where d refers to the depth of interest. The ambient dose equivalent refers to the dose equivalent that would be obtained when no individual is necessarily present in the radiation field. The dose equivalent is assumed to result from a hypothetical radiation field known as an expanded radiation field. This field has the same values for fluence, direction and energy distributions throughout the volume being surveyed as the actual workplace or environmental field at the point of interest. The ambient dose
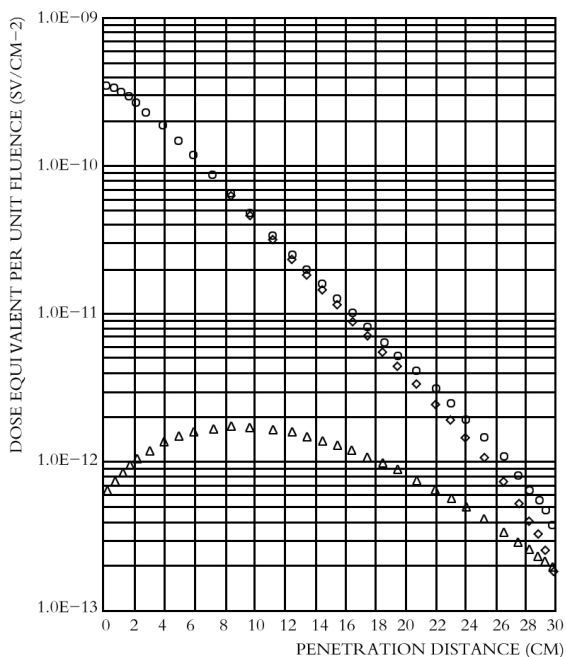
FIG. 5.5. The dose equivalent from 1 MeV neutrons as a function of position within the ICRU phantom (0.3 m diameter sphere). Symbols: ◊ indicates neutron dose equivalent, △ indicates the secondary gamma ray dose produced by the $^1H(n,\gamma)^2H$ reaction and ○ indicates the total (neutron + gamma) dose equivalent. (Reproduced from GSF Report S-1072 [5.12] with permission from Helmholtz Zentrum, Germany.)

equivalent refers to the dose equivalent that would be produced at a depth in the ICRU sphere, and therefore it is often written as $H^*(10)$, where 10 refers to a depth of 10 mm. It is important to note that the quantity is calculated for the ICRU sphere, but the sphere (or receptor) is not actually present at the time of measurement. It can be considered as merely a mathematical tool for calculating the value of the fluence to dose equivalent conversion coefficients.

The quantity personal dose equivalent requires the presence of a receptor, which is the individual who is present in the workplace or environment where he or she may be subject to irradiation by neutrons. The personal dose equivalent at a depth of 10 mm in the individual is written as $H_p(10)$. For neutron dosimetry purposes, it is assumed that $H_p(10)$ is defined in ICRU tissue at a depth of 10 mm below a specified point on the body. This point is usually 10 mm deep, immediately beneath the personal dosimeter that is worn by the individual. It should also be noted that the personal dose equivalent can be specified at depths other than 10 mm. For example, the dose equivalent to the lens of

the eye would be determined at a 3 mm depth and written as $H_p(3)$. The dose equivalent to the skin would be determined at a 0.07 mm depth and would be written as $H_p(0.07)$. Personal dosimeters should be calibrated while mounted on a phantom recommended by ISO [5.13] or ICRU [5.14] while being exposed to ISO recommended reference radiations (see Section 14). Fluence to ambient or personal dose equivalent conversion coefficients recommended by a joint ICRP/ICRU task group can be found in Refs [5.9, 5.15].

5.5. QUANTITIES USED FOR LIMITATION PURPOSES

The quantities used for limitation of dose equivalent are the effective dose, E, and the equivalent dose, H_T. The equivalent dose is the summation of average tissue or organ doses, $D_{T,R}$, for a radiation type, R, weighted by the radiation weighting factor, w_R. The radiation weighting factor roughly corresponds to the quality factor Q, since it takes into account the variation in biological effects caused by different radiations. The equivalent dose is defined by

$$H_T = \sum_R w_R \, D_{T,R} \tag{5.8}$$

Values given in ICRP 60, which first introduced the radiation weighting factors, are shown in Table 5.2.

The effective dose is computed from the sum of the tissue weighted contributions of equivalent doses to tissues or organs:

$$E = \sum_T w_T \sum_R w_R \, D_{T,R} \tag{5.9}$$

Tissue weighting factors given in ICRP 60 [5.11] are shown in Table 5.3. They have been derived from a reference population of equal numbers of both sexes and a wide range of ages. In the definition of effective dose they apply to workers, to the whole population and to either sex.

If the neutron fluence distribution is known, the equivalent dose can be calculated using the fluence to effective dose conversion coefficients recommended by the ICRP. These conversion coefficients are dependent on the direction of radiation incidence upon the body. They are calculated using a mathematical model of the human body for radiation incident from the directions shown in Fig. 5.6. Figure 5.7 shows the fluence to effective dose conversion coefficients for neutron radiation for various irradiation directions.

TABLE 5.2. RADIATION WEIGHTING FACTORS AS GIVEN IN ICRP 60 [5.11]

Radiation type and energy range		Radiation weighting factor, w_R
Photons, all energies		1
Electrons or muons, all energies		1
Neutrons of	$E < 10$ keV	5
	10 keV $< E < 100$ keV	10
	100 keV $< E < 2$ MeV	20
	$2 < E < 20$ MeV	10
	$E > 20$ MeV	5
Protons $E > 2$ MeV		5
Alpha particles, heavy ions		20

Reproduced with permission from ICRP.

TABLE 5.3. TISSUE WEIGHTING FACTORS AS GIVEN IN ICRP 60 [5.11]

Tissue or organ	Tissue weighting factor, w_T
Gonads	0.20
Bone marrow (red)	0.12
Colon	0.12
Lung	0.12
Stomach	0.12
Bladder	0.05
Breast	0.05
Liver	0.05
Oesophagus	0.05
Thyroid	0.05
Skin	0.01
Bone surface	0.01
Remainder	0.05

Reproduced with permission from ICRP.
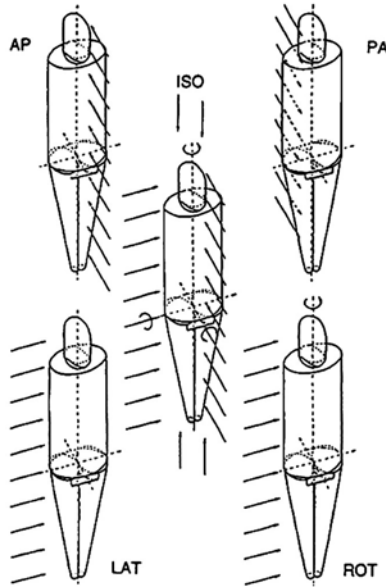
FIG. 5.6. The direction of the incident radiation is indicated by the arrows. Labels denote anterior–posterior (AP), posterior–anterior (PA), lateral (LAT), rotational (ROT) and isotropic (ISO) incidence. (Reproduced from Refs [5.9, 5.16] with permission from ICRP and ICRU.)
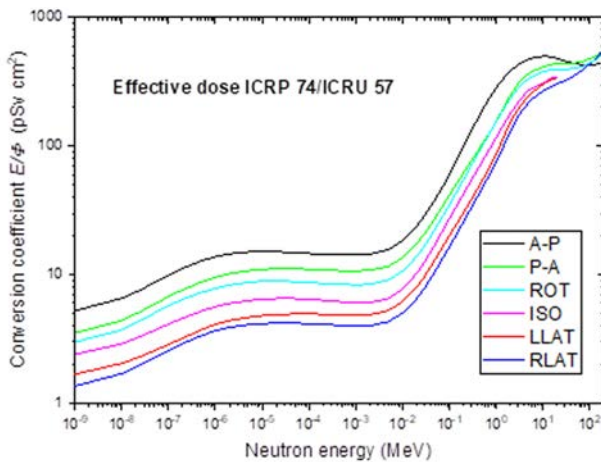
FIG. 5.7. Conversion coefficients for effective dose, E, as a function of neutron energy for various irradiation directions for an anthropomorphic mathematical model of the body [5.9, 5.16]. Directions of incidence on the body are anterior–posterior (A–P), posterior–anterior (P–A), right side (RLAT), left side (LLAT), rotational (ROT) and isotropic (ISO) directions.

5.6. ICRP 2007 RECOMMENDATIONS

Following a review of the parameters used in ICRP 60 [5.11] to calculate the quantity effective dose, in 2007 the ICRP issued revised recommendations in ICRP 103 [5.16] that replaced the previous ones. In ICRP 60, the radiation weighting factor w_R for neutrons was defined by a step function. ICRP 103 recommends that the radiation weighting factor for neutrons be defined by a continuous function (see w_R in Fig. 5.8). It should be noted that the use of a continuous function is based on the practical consideration that most neutron exposures involve a range of energies. The recommendation of a function does not imply a higher precision of basic data. The most significant changes compared with the data in ICRP 60 were the decrease of w_R in the low energy range, which takes account of the large contribution of secondary photons to the absorbed dose in the human body, and the decrease of w_R at neutron energies above 100 MeV. The following continuous function in neutron energy, E_n (MeV), is recommended for the calculation of radiation weighting factors for neutrons:

$$w_R = \begin{cases} 2.5 + 18.2e^{-[\ln(E_n)]^2/6}, & E_n < 1\,\text{MeV} \\ 5.0 + 17.0e^{-[\ln(2E_n)]^2/6}, & 1\,\text{MeV} \le E_n \le 50\,\text{MeV} \\ 2.5 + 3.25e^{-[\ln(0.04E_n)]^2/6}, & E_n > 50\,\text{MeV} \end{cases} \tag{5.10}$$
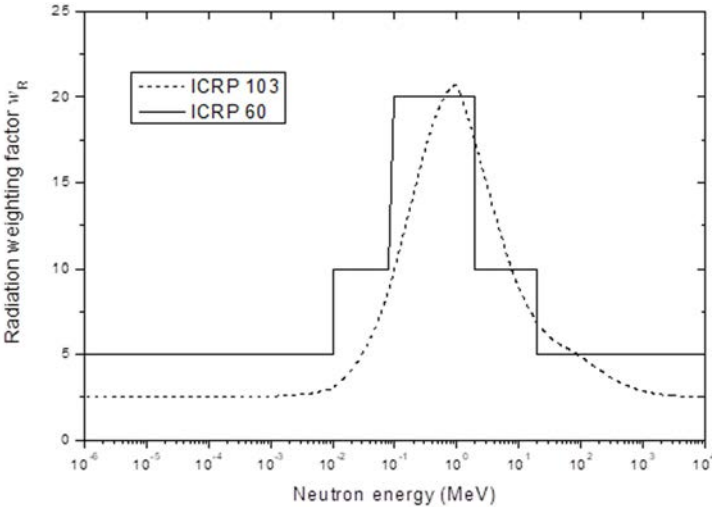
FIG. 5.8. The new radiation weighting factor, w_R, as proposed by the ICRP in Publication 103 [5.17], compared to the values recommended in ICRP 60 [5.11].

This function has been derived empirically and is consistent with existing biological and physical knowledge.

A new w_R value has also been recommended for protons. The value for protons and charged pions (introduced in addition) is now 2 (see Table 5.4.).

In addition, the recommended tissue weighting factors have changed (see Table 5.5).

TABLE 5.4. RECOMMENDED RADIATION WEIGHTING FACTORS [5.17]

Radiation type	Radiation weighting factor
Photons	1
Electrons and muons	1
Protons and charged pions	2
Alpha particles, fission fragments, heavy ions	20
Neutrons	A continuous function (see Eq. (5.12))

Reproduced with permission from ICRP.

TABLE 5.5. RECOMMENDED TISSUE WEIGHTING FACTORS [5.17]

Tissue	w_T	$\sum w_T$
Bone marrow (red), colon, lung, stomach, breast, remainder tissues[a]	0.12	0.72
Gonads	0.08	0.08
Bladder, oesophagus, liver, thyroid	0.04	0.16
Bone surface, brain, salivary glands, skin	0.01	0.04

Reproduced with permission from ICRP.

[a] Remainder tissues: adrenals, extrathoracic region, gall bladder, heart, kidneys, lymphatic nodes, muscle, oral mucosa, pancreas, prostate, small intestine, spleen, thymus, uterus/cervix.

The definitions and values of the operational quantities did not change. This was especially important, since it meant that no change of instrumentation for radiation protection purposes was likely to be necessary.

In 2010, conversion coefficients were published by the ICRP for effective dose as calculated with the revised w_R and w_T values [5.17]. They are illustrated in Fig. 5.9. Some of the considerations involved in calculating these coefficients can be found in Ref. [5.18]. The large variations with energy and angular dependence of the fluence that were present in the ICRP 60 coefficients are again evident.

The most noticeable effect of the change in w_R is that the conversion coefficients for effective dose are lower at neutron energies below approximately 500 keV. This is illustrated in Fig. 5.10, where the new conversion coefficients are compared with the old ones and also with conversion coefficients for the operational quantities. The most noticeable effect is that effective dose is no longer larger than the operational quantities in the intermediate energy region between approximately 1 eV and 50 keV.

Some discussion of the implications of these changes can be found in Ref. [5.19].

The present approach to radiation protection involves equating risk to a product of the absorbed dose and an empirical radiation specific modifying factor. This has distinct advantages in terms of providing calibration fields. Conversion coefficients between neutron fluence and dose equivalent quantities can be
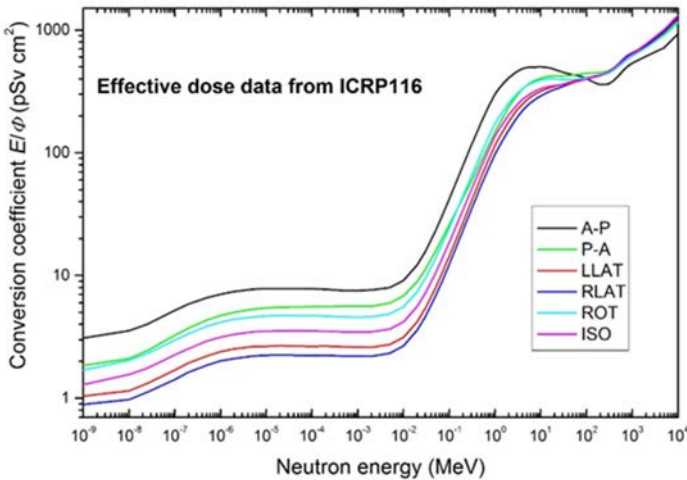
FIG. 5.9. Variation of ICRP 116 conversion coefficients from neutron fluence to effective dose with energy for various angular incidences on the body (for labels see Fig. 5.7).
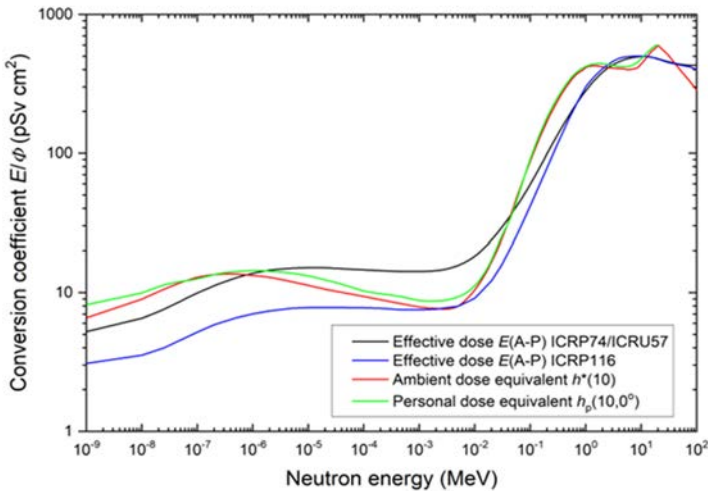
FIG. 5.10. Comparison of ICRP 116 conversion coefficients for E*(A–P) with the older coefficients from ICRP 74 and with coefficients for the operational quantities ambient and personal dose equivalent.*

calculated and calibration standards realized, since they are based on neutron fluence, which is the quantity standardized at standards labs and calibration labs.

However, this approach to specifying the risk quantity has its limitations and in all probability does not reflect the true complexity of radiation effects in humans at low doses. The empirical factors are based somewhat subjectively on a variety of sources, such as animal studies (which may differ from the human case in unrecognized ways) and epidemiological studies with large uncertainties. They were not derived from direct consideration of cell biology. Future studies might favour different values, or even a completely different approach.

Over recent years, techniques to study the interaction of radiation with matter on nanometre scales have improved, as has the understanding of DNA and cell processes. This raises the possibility of defining new risk quantities that are much more directly related to observable and measurable processes in cells in terms of new concepts such as ionization cluster sizes [5.20]. If these efforts are successful, it is possible that dose standards may become more biology related than at present.

REFERENCES TO CHAPTER 5

[5.1] INTERNATIONAL COMMISSION ON RADIATION UNITS AND MEASUREMENTS, Nuclear Data for Neutron and Proton Radiotherapy and for Radiation Protection, Report 63, ICRU, Bethesda, MD (2000).

[5.2] INTERNATIONAL COMMISSION ON RADIATION UNITS AND MEASUREMENTS, Photon, Electron, Proton and Neutron Interaction Data for Body Tissues, Report 46, ICRU, Bethesda, MD (1992).

[5.3] INTERNATIONAL COMMISSION ON RADIATION UNITS AND MEASUREMENTS, Quantities and Units in Radiation Protection Dosimetry, Report 51, ICRU, Bethesda, MD (1993).

[5.4] INTERNATIONAL COMMISSION ON RADIATION UNITS AND MEASUREMENTS, Neutron Dosimetry for Biology and Medicine, Report 26, ICRU, Bethesda, MD (1984).

[5.5] INTERNATIONAL COMMISSION ON RADIATION UNITS AND MEASUREMENTS, Clinical Neutron Dosimetry Part I: Determination of Absorbed Dose in a Patient Treated by External Beams of Fast Neutrons, Report 45, ICRU, Bethesda, MD (1989).

[5.6] INTERNATIONAL COMMISSION ON RADIATION UNITS AND MEASUREMENTS, Microdosimetry, Report 36, ICRU, Bethesda, MD (1983).

[5.7] MARTÍN, G., GERDUNG, S., RAABE, M., AREND, E., A practical design of a cylindrical tissue-equivalent proportional counter for microdosimetry, Radiat. Prot. Dosim. **99** (2002) 379–380.

[5.8] INTERNATIONAL COMMISSION ON RADIOLOGICAL PROTECTION, Conversion Coefficients for Use in Radiological Protection against External Radiation, ICRP Publication 74, Pergamon Press, Oxford and New York (1997).

[5.9] INTERNATIONAL COMMISSION ON RADIOLOGICAL PROTECTION, ICRP Publication 26, Pergamon Press, Oxford and New York (1977).

[5.10] INTERNATIONAL COMMISSION ON RADIOLOGICAL PROTECTION, ICRP Publication 60, Pergamon Press, Oxford and New York (1991).

[5.11] INTERNATIONAL COMMISSION ON RADIOLOGICAL PROTECTION, Relative Biological Effectiveness (RBE), Quality Factor (Q), and Radiation Weighting Factor (w_R), ICRP Publication 92, Pergamon Press, Oxford and New York (2003).

[5.12] MORHART, A., BURGER, G., Axial Kerma and Dose Equivalent for Neutrons in the ICRU-Sphere, GSF Bericht S-1072, Gesellschaft für Strahlen-und Umweltforschung mbH, München (1984).

[5.13] INTERNATIONAL ORGANIZATION FOR STANDARDIZATION, Reference neutron radiations — Part 3: Calibration of area and personal dosimeters and determination of their response as a function of neutron energy and angle of incidence, International Standard 8529-3, ISO, Geneva (1998).

[5.14] INTERNATIONAL COMMISSION ON RADIATION UNITS AND MEASUREMENTS, Determination of Operational Dose Equivalent Quantities for Neutrons, Report 66, ICRU, Bethesda, MD (2001).

[5.15] INTERNATIONAL COMMISSION ON RADIATION UNITS AND MEASUREMENTS, Conversion Coefficients for Use in Radiological Protection against External Radiation, Report 57, ICRU, Bethesda, MD (1998).

[5.16] INTERNATIONAL COMMISSION ON RADIOLOGICAL PROTECTION, ICRP Publication 103, Elsevier, Amsterdam (2007).

[5.17] INTERNATIONAL COMMISSION ON RADIOLOGICAL PROTECTION, Conversion Coefficients for Radiological Protection Quantities for External Radiation Exposures, ICRP Publication 116, Elsevier, Amsterdam (2010).

[5.18] ENDO, A. et al., Overview of the ICRP/ICRU adult reference computational phantoms and dose conversion coefficients for external idealised exposures, Radiat. Prot. Dosim. **161** (2014) 11–16.

[5.19] THOMAS, D.J., The system of radiation protection for neutrons: Does it fit the purpose? Radiat. Prot. Dosim. **161** (2014) 3–10.

[5.20] GROSSWENDT, B., PSZONA, S., BANTSAR, A., New descriptors of radiation quality based on nanodosimetry, a first approach, Radiat. Prot. Dosim. **126** (2007) 432–444.

6. CONVERSION COEFFICIENTS FOR THE OPERATIONAL QUANTITIES

Although the legal quantity for limiting radiation exposure is the effective dose, E, this quantity is deemed to be unmeasurable, and so the ICRU operational quantities were introduced [6.1]. For area monitoring, the quantity to be measured is the ambient dose equivalent, $H^*(d)$, and for individual monitoring, the quantity is the personal dose equivalent, $H_p(d)$. The relationship between the dose equivalent, H, where H stands here for either $H^*(d)$ or $H_p(d)$, and the neutron fluence spectrum, $\Phi_E(E)$, is given by the following equation:

$$H = \int_{E_{min}}^{E_{max}} h_\Phi(E) \cdot \Phi_E(E) \, \mathrm{d}E \qquad (6.1)$$

where $h_\Phi(E)$ is the fluence to dose equivalent conversion coefficient for ambient or personal dose equivalent, and for neutrons d is 10 mm. For individual monitoring, information is also needed on the directional properties of the radiation field when deriving the personal dose equivalent.

The value indicated by a dosimetric instrument, defined as M, is obtained from the fluence response of the instrument, $R_\Phi(E)$, as follows:

$$M = \int_{E_{min}}^{E_{max}} R_\Phi(E) \cdot \Phi_E(E) \, \mathrm{d}E \qquad (6.2)$$

The calibration factor, N, is defined by $N = H_{cal}/M_{cal}$, where the suffix 'cal' indicates calibration conditions. To obtain a dose equivalent value, the indication M is multiplied by N, and, if necessary, a field specific correction factor, K, to make allowance for the differences between the spectra of the calibration and the workplace fields [6.2]:

$$H = M \cdot N \cdot K \qquad (6.3)$$

In order to provide a direct indication of the ambient dose equivalent, $H^*(10)$, survey meters are designed to have a fluence response as a function of neutron energy that matches as closely as possible the energy variation of the fluence to ambient dose equivalent conversion coefficient, $h_\Phi^*(E)$. The most commonly used type of survey meter is based on a thermal neutron sensor inside a moderating sphere or cylinder with some additional absorbing material, usually cadmium or boron, to modify the response. However, no combination of moderator and absorber provides a fluence response that matches

exactly the $h_{\Phi}^{*}(E)$ curve, so survey instrument response functions are far from perfect [6.3]. More recent designs have incorporated lead inserts to extend the response to higher energies and various voids or channels to try to improve the response function.

Personal dosimeters worn by individuals to measure $H_{p}(d)$ suffer with similar problems of imperfect response functions. Two detection methods dominate the measurement technology: the detection of albedo neutrons backscattered from the body and the detection of recoiling protons released from a hydrogenous layer by fast neutrons. Examples of the former in passive dosimeters are thermoluminescent (TL) albedo devices, and examples of the latter are etched track plastics such as polyallyl diglycol carbonate (PADC). For active devices, the corresponding detection techniques involve a thermally sensitive layer, such as a lithium compound, and a hydrogenous layer on a diode. Both detection techniques can provide reasonable response functions over a limited energy region, but neutron workplace fields tend to cover energies ranging from thermal to a few MeV and often contain significant numbers of low energy neutrons [6.4]. The reference radiations used for calibrating the dosimeters may be either unmoderated ^{252}Cf or ^{241}Am–Be, so, the fluence distributions of the reference radiations and those of the workplace often differ significantly.

To overcome the difficulty introduced by the differences between the spectral distributions of the workplace radiation field and the reference radiation, the indication of a dosimeter or a survey instrument may be adjusted using the correction factor, K, to allow for the difference.

An alternative approach is the use of reference neutron fields designed to simulate commonly encountered workplace fields. Guidance on ways of producing simulated workplace fields that mimic those workplaces can be found in ISO Standard 12789 Part 1 [6.5] and on the methods of characterizing such fields in Part 2 [6.6].

6.1. CONVERSION COEFFICIENTS FOR MONOENERGETIC NEUTRONS

Table 6.1 contains the neutron fluence to dose equivalent conversion coefficients for the operational quantities, as given by a joint ICRP/ICRU task group, for specific neutron energies [6.7, 6.8]. For ambient dose equivalent, $H^{*}(10)$, coefficients are tabulated for energies from 1.0×10^{-9} to 200 MeV. For personal dose equivalent, $H_{p}(10)$, defined in the ICRU four element tissue slab phantom, values are for energies between 1.0×10^{-9} and 20 MeV.

The angle, denoted by α in Table 6.1, is the angle of incidence with respect to the normal to the face of the slab phantom on which the dosimeters are attached.

TABLE 6.1. AMBIENT AND PERSONAL DOSE EQUIVALENT PER UNIT NEUTRON FLUENCE, $h^*_\Phi = H^*(10)/\Phi$ AND $h_{p,\Phi} = H_p(10)/\Phi$, IN pSv·cm^2, FOR A PARALLEL, MONOENERGETIC FIELD INCIDENT AT VARIOUS ANGLES ON THE ICRU SPHERE (AMBIENT) AND ICRU SLAB PHANTOMS (PERSONAL). α IS THE ANGLE OF INCIDENCE RELATIVE TO THE NORMAL TO THE PHANTOM FRONT [6.7, 6.8]

Energy (MeV)	h^*_Φ	$h_{p,\Phi}$ $\alpha = 0°$	$h_{p,\Phi}$ $\alpha = 15°$	$h_{p,\Phi}$ $\alpha = 30°$	$h_{p,\Phi}$ $\alpha = 45°$	$h_{p,\Phi}$ $\alpha = 60°$	$h_{p,\Phi}$ $\alpha = 75°$
1.00×10^{-9}	6.60	8.19	7.64	6.57	4.23	2.61	1.13
1.00×10^{-8}	9.00	9.97	9.35	7.90	5.38	3.37	1.50
2.53×10^{-8}	10.6	11.4	10.6	9.11	6.61	4.04	1.73
1.00×10^{-7}	12.9	12.6	11.7	10.3	7.84	4.7	1.94
2.00×10^{-7}	3.5	13.5	12.6	11.1	8.73	5.21	2.12
5.00×10^{-7}	13.6	14.2	13.5	11.8	9.40	5.65	2.31
1.00×10^{-6}	13.3	14.4	13.9	12.0	9.56	5.82	2.40
2.00×10^{-6}	12.9	14.3	14.0	11.9	9.49	5.85	2.46
5.00×10^{-6}	12.0	13.8	13.9	11.5	9.11	5.71	2.48
1.00×10^{-5}	11.3	13.2	13.4	11.0	8.65	5.47	2.44
2.00×10^{-5}	10.6	12.4	12.6	10.4	8.10	5.14	2.35
5.00×10^{-5}	9.90	11.2	11.2	9.49	7.32	4.57	2.16
1.00×10^{-4}	9.40	10.3	9.85	8.64	6.74	4.10	1.99
2.00×10^{-4}	8.90	9.84	9.41	8.22	6.21	3.91	1.83
5.00×10^{-4}	8.30	9.34	8.66	7.66	5.67	3.58	1.68
1.00×10^{-3}	7.90	8.78	8.20	7.29	5.43	3.46	1.66
2.00×10^{-3}	7.70	8.72	8.22	7.27	5.43	3.46	1.67

TABLE 6.1. AMBIENT AND PERSONAL DOSE EQUIVALENT PER UNIT NEUTRON FLUENCE, $h_\Phi^* = H^*(10)/\Phi$ AND $h_{p,\Phi} = H_p(10)/\Phi$, IN pSv·cm^2, FOR A PARALLEL, MONOENERGETIC FIELD INCIDENT AT VARIOUS ANGLES ON THE ICRU SPHERE (AMBIENT) AND ICRU SLAB PHANTOMS (PERSONAL). α IS THE ANGLE OF INCIDENCE RELATIVE TO THE NORMAL TO THE PHANTOM FRONT [6.7, 6.8] (cont.)

Energy (MeV)	h_Φ^*	$h_{p,\Phi}$ $\alpha = 0°$	$h_{p,\Phi}$ $\alpha = 15°$	$h_{p,\Phi}$ $\alpha = 30°$	$h_{p,\Phi}$ $\alpha = 45°$	$h_{p,\Phi}$ $\alpha = 60°$	$h_{p,\Phi}$ $\alpha = 75°$
5.00×10^{-3}	8.00	9.36	8.79	7.46	5.71	3.59	1.69
1.00×10^{-2}	10.5	11.2	10.8	9.18	7.09	4.32	1.71
2.00×10^{-2}	16.6	17.1	17.0	14.6	11.6	6.64	2.11
3.00×10^{-2}	23.7	24.9	24.1	21.3	16.7	9.81	2.85
5.00×10^{-2}	41.1	39.0	36.0	34.4	27.5	16.7	4.78
7.00×10^{-2}	60.0	59.0	55.8	52.6	42.9	27.3	8.10
1.00×10^{-1}	88.0	90.6	87.8	81.3	67.1	44.6	13.7
1.50×10^{-1}	132	139	137	126	106	73.3	24.2
2.00×10^{-1}	170	180	179	166	141	100	35.5
3.00×10^{-1}	233	246	244	232	201	149	58.5
5.00×10^{-1}	322	335	330	326	291	226	102
7.00×10^{-1}	375	386	379	382	348	279	139
9.00×10^{-1}	400	414	407	415	383	317	171
1.00×10^{0}	416	422	416	426	395	332	180
1.20×10^{0}	425	433	427	440	412	335	210
2.00×10^{0}	420	442	438	457	439	402	274
3.00×10^{0}	412	431	429	449	440	412	306

TABLE 6.1. AMBIENT AND PERSONAL DOSE EQUIVALENT PER UNIT NEUTRON FLUENCE, $h_\Phi^* = H^*(10)/\Phi$ AND $h_{p,\Phi} = H_p(10)/\Phi$, IN pSv·cm^2, FOR A PARALLEL, MONOENERGETIC FIELD INCIDENT AT VARIOUS ANGLES ON THE ICRU SPHERE (AMBIENT) AND ICRU SLAB PHANTOMS (PERSONAL). α IS THE ANGLE OF INCIDENCE RELATIVE TO THE NORMAL TO THE PHANTOM FRONT [6.7, 6.8] (cont.)

Energy (MeV)	h_Φ^*	$h_{p,\Phi}$ $\alpha = 0°$	$h_{p,\Phi}$ $\alpha = 15°$	$h_{p,\Phi}$ $\alpha = 30°$	$h_{p,\Phi}$ $\alpha = 45°$	$h_{p,\Phi}$ $\alpha = 60°$	$h_{p,\Phi}$ $\alpha = 75°$
4.00×10^0	408	422	421	440	435	409	320
5.00×10^0	405	420	418	437	435	409	331
6.00×10^0	400	423	422	440	439	414	345
7.00×10^0	405	432	432	449	448	425	361
8.00×10^0	409	445	445	462	460	440	379
9.00×10^0	420	461	462	478	476	458	399
1.00×10^1	440	480	481	497	493	480	421
1.20×10^1	480	517	519	536	599	523	464
1.40×10^1	520	550	552	570	561	562	503
1.50×10^1	540	564	565	584	575	579	520
1.60×10^1	555	576	577	597	588	593	535
1.80×10^1	570	595	593	617	609	615	561
2.00×10^1	600	600	595	619	615	619	570
3.00×10^1	515	—	—	—	—	—	—
5.00×10^1	400	—	—	—	—	—	—
7.50×10^1	330	—	—	—	—	—	—
1.00×10^2	285	—	—	—	—	—	—

TABLE 6.1. AMBIENT AND PERSONAL DOSE EQUIVALENT PER UNIT NEUTRON FLUENCE, $h_\Phi^* = H^*(10)/\Phi$ AND $h_{p,\Phi} = H_p(10)/\Phi$, IN pSv·cm^2, FOR A PARALLEL, MONOENERGETIC FIELD INCIDENT AT VARIOUS ANGLES ON THE ICRU SPHERE (AMBIENT) AND ICRU SLAB PHANTOMS (PERSONAL). α IS THE ANGLE OF INCIDENCE RELATIVE TO THE NORMAL TO THE PHANTOM FRONT [6.7, 6.8] (cont.)

Energy (MeV)	h_Φ^*	$h_{p,\Phi}$ $\alpha = 0°$	$h_{p,\Phi}$ $\alpha = 15°$	$h_{p,\Phi}$ $\alpha = 30°$	$h_{p,\Phi}$ $\alpha = 45°$	$h_{p,\Phi}$ $\alpha = 60°$	$h_{p,\Phi}$ $\alpha = 75°$
1.25×10^2	260	—	—	—	—	—	—
1.50×10^2	245	—	—	—	—	—	—
1.75×10^2	250	—	—	—	—	—	—
2.01×10^2	260	—	—	—	—	—	—

Reproduced with permission from ICRP and ICRU.
—: no data are tabulated in the ICRU report for these neutron energies.

The joint task group recommended that data at energies other than those tabulated should be obtained by interpolation using a four point (cubic) Lagrangian interpolation formula on a log-log scale [6.7, 6.8]. No recommendation is given for a formula to interpolate $h_{p,\Phi}(10,\alpha)$ between angles. At lower energies the conversion coefficient decreases with angle, but at higher energies it can initially increase as α increases. Plotting the data can provide a guide on the best approach to use.

6.2. CONVERSION COEFFICIENTS FOR CONTINUOUS NEUTRON SPECTRA

The fluence to dose equivalent conversion coefficient for a neutron spectrum can be evaluated [6.9] using the equation below:

$$h_\Phi = \frac{\int h_\Phi(E) \cdot \Phi_E(E)\, dE}{\int \Phi_E(E)\, dE} \tag{6.4}$$

The spectrum-averaged fluence to ambient dose equivalent conversion coefficients, $h_\Phi^*(10)$, and fluence to personal dose equivalent conversion

coefficients, $h_{p,\Phi}$ (10), for the reference radionuclide sources recommended by ISO have been calculated and presented by ISO [6.10] (see also Section 14).

6.3. CONVERSION COEFFICIENTS FOR HIGH ENERGY NEUTRONS

As noted, the coefficients provided by the joint ICRP/ICRU task group extend only up to 200 MeV for H^*(10) and 20 MeV for H_p(10). For ambient dose equivalent, the range has been extended by Sannikov and Savitskaya [6.11] and Ferrari and Pelliccioni [6.12]; Fig. 6.1 compares these new data. Sannikov and Savitskaya performed their calculations for the $Q(L)$ values of both ICRP 21 and ICRP 60, but the differences were small. The values plotted are for the ICRP 60 values. In addition to a calculation of the ambient dose equivalent (i.e. the dose equivalent at 10 mm in the ICRU sphere), Ferrari and Pelliccioni also calculated the dose equivalent, H_{Max}, at the location of the maximum dose equivalent in this sphere. Both sets of values are shown in Fig. 6.1. The plot also shows the ambient ICRP 74 dose equivalent, H^*(10), up to 200 MeV, and the older quantity maximum dose equivalent, H_{MADE}, defined in a semi-infinite slab. For comparison, the value of effective dose, E, from ICRP 116 is also shown.

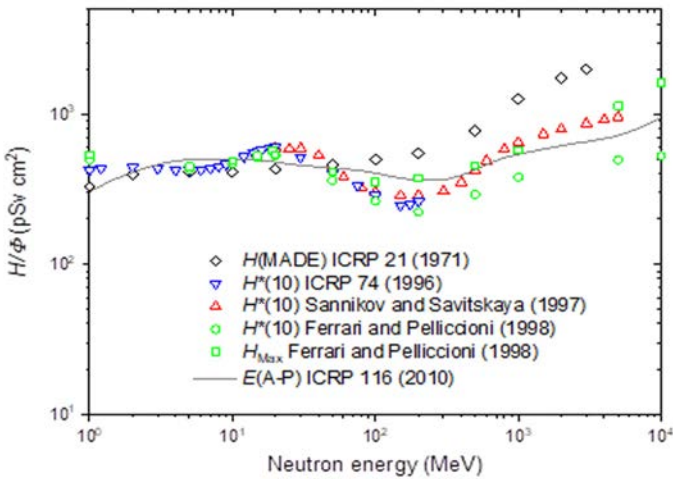*FIG. 6.1. Neutron fluence to dose equivalent conversion coefficients for neutron energies between 1 MeV and 10 GeV. These have been derived from ICRP 74 [6.7] (identical to ICRU Report 57 [6.8]), Sannikov and Savitskaya [6.11], Ferrari and Pelliccioni [6.12] and ICRP 15/21 [6.13]. For comparison with the most recent data for effective dose, E(A–P) from ICRP 116 [6.14], these data are shown as a continuous line.*

Data above 1 GeV are of lesser practical importance for radiation protection in the nuclear industry, but are relevant for protection around high energy accelerators, for passengers and crew at aircraft flight altitudes and in space.

REFERENCES TO CHAPTER 6

[6.1] INTERNATIONAL COMMISSION ON RADIATION UNITS AND MEASUREMENTS, Determination of Dose Equivalents Resulting from External Radiation Sources, Report 39, ICRU, Bethesda, MD (1985).

[6.2] McDONALD, J.C., SIEBERT, B.R.L, ALBERTS W.G., Neutron spectrometry for radiation protection purposes, Nucl. Instrum. Methods Phys. Res. A **476** (2002) 347–352.

[6.3] TANNER, R.J., et al., Practical Implications of Neutron Survey Instrument Performance, Radiation Protection Division Report HPA-RPD-016, Health Protection Agency, Chilton, UK (2006).

[6.4] INTERNATIONAL ATOMIC ENERGY AGENCY, Compendium of Neutron Spectra and Detector Responses for Radiation Protection Purposes, Technical Reports Series No. 318, IAEA, Vienna (1990).

[6.5] INTERNATIONAL ORGANIZATION FOR STANDARDIZATION, Reference neutron radiations — Characteristics and methods of production of simulated workplace neutron fields, International Standard 12789-1, ISO, Geneva (2008).

[6.6] INTERNATIONAL ORGANIZATION FOR STANDARDIZATION, Reference neutron radiations — Calibration fundamentals related to the basic quantities, International Standard 12789-2, ISO, Geneva (2008).

[6.7] INTERNATIONAL COMMISSION ON RADIOLOGICAL PROTECTION, Conversion Coefficients for Use in Radiological Protection Against External Radiation, ICRP Publication 74, Pergamon Press, Oxford and New York (1996).

[6.8] INTERNATIONAL COMMISSION ON RADIATION UNITS AND MEASUREMENTS, Conversion Coefficients for use in Radiological Protection Against External Radiation, Report 57, ICRU, Bethesda, MD (1998).

[6.9] INTERNATIONAL COMMISSION ON RADIATION UNITS AND MEASUREMENTS, Determination of Operational Dose Equivalent Quantities for Neutrons, Report 66, ICRU, Bethesda, MD (2001).

[6.10] INTERNATIONAL ORGANIZATION FOR STANDARDIZATION, Reference neutron radiations — Part 3: Calibration of area and personal dosimeters and determination of their response as a function of neutron energy and angle of incidence, International Standard 8529-3, ISO, Geneva (1998).

[6.11] SANNIKOV, A.V., SAVITSKAYA, E.N., Ambient dose equivalent conversion factors for high energy neutrons based on the ICRP 60 Recommendations, Radiat. Prot. Dosim. **70** (1997) 383–386.

[6.12] FERRARI, A., PELLICCIONI, M., Fluence to dose equivalent conversion data and effective quality factors for high energy neutrons, Radiat. Prot. Dosim. **76** (1998) 215–224.

[6.13] INTERNATIONAL COMMISSION ON RADIOLOGICAL PROTECTION, Data for Protection against Ionizing Radiation from External Sources, and Data for Protection against Ionizing Radiation from External Source, ICRP Publications 15 and 21, Pergamon Press, Oxford and New York *(*1976).

[6.14] INTERNATIONAL COMMISSION ON RADIOLOGICAL PROTECTION, Conversion Coefficients for Radiological Protection Quantities for External Radiation Exposures, ICRP Publication 116, Elsevier, Amsterdam (2010).

7. SOURCES OF NEUTRONS

7.1. INTRODUCTION

Neutron radiation fields can be found in many places in the modern world, but in all cases these 'free' unbound neutrons are produced either by a nuclear reaction or by spontaneous fission. Spontaneous fission occurs in only a very few isotopes, and the majority of neutron sources are thus based on nuclear reactions.[1] Nuclear reactions can be induced by a range of bombarding particles, which themselves can be produced by a variety of mechanisms.

7.2. RADIONUCLIDE NEUTRON SOURCES

Radionuclide neutron sources consist of neutron emitting material encapsulated — usually doubly encapsulated — in metal containers. Several typical source encapsulations are shown in Fig. 7.1. They have a number of uses, for example in oil well logging, in moisture gauging, in medicine, for quality

FIG. 7.1. Typical radionuclide source capsules: from left to right, X14 (60 mm long by 30 mm diameter), X4, X3, X224, X2 and X1 (10 mm long by 7.8 mm diameter). The small capsules are used for ^{252}Cf sources and the larger ones for ^{241}Am(α,n) sources. (Courtesy of National Physical Laboratory.)

---

[1] An argument can even be made that neutrons from commonly used spontaneous fission radionuclide sources such as ^{252}Cf arise from nuclear reactions. The isotopes used are artificial and have been made by a nuclear reaction. The eventual fission of these unstable isotopes can be thought of as delayed emission long after the nuclear reaction.

control of fuel rods, for reactor startup and — of particular relevance for radiation protection — for calibrating survey instruments and personal dosimeters.

The neutron producing material consists of either a high Z nucleus, which decays by spontaneous fission, or a mixture of a radioisotope and a low Z nucleus, where radiation from the radioisotope produces neutrons by a nuclear reaction in the low Z material. The best known spontaneous fission source is [252]Cf. The reaction type radionuclide sources use either alpha particle emitters or high energy gamma emitters, and neutrons are produced by the (α,n) and the (γ,n) reactions, respectively. The various types of radionuclide sources are discussed briefly below. Further details can be found in Refs [7.1–7.3].

7.2.1. Spontaneous fission sources

By far the most commonly used spontaneous fission neutron source is [252]Cf, which is an artificial element produced in high flux reactors. With a relatively short half-life of 2.645 a, a spontaneous fission branching ratio of approximately 3% (the other 97% being by alpha decay) and an average number of neutrons emitted per spontaneous fission, $\bar{v}$, of 3.77, sources with very high neutron emission rates can be fabricated. The neutron emission rate is roughly 2.3×10^9 s^{-1}·mg^{-1}, and because of the small mass involved, [252]Cf sources can be contained in rather small capsules, typically cylinders with dimensions of the order of 1 cm. The [252]Cf fission spectrum is an international reference standard included in the ENDF/B-6 decay data library under MAT 9861, but the representation most commonly used in dosimetric applications is that given in ISO Standard 8529-1 [7.4] and shown in Fig. 7.2. In the energy range from 100 keV to 10 MeV, it is based on the Maxwellian expression:

$$B_E = \frac{2}{\sqrt{\pi}T^{3/2}} \cdot \sqrt{E} \cdot e^{-E/T} \tag{7.1}$$

where

B_E is the neutron emission at energy E;
T is the spectrum parameter, which has a value of 1.42 MeV.

The isotopic purity of californium sources can vary, and the amount of [250]Cf, which has a much longer half-life of 13.08 a, may need to be taken into consideration if the source is kept and used for many years [7.5]. [252]Cf decays to [248]Cm, which also decays by spontaneous fission, but the neutron output from this isotope, which has a half-life of 3.5×10^5 a, remains negligible for a very long time.
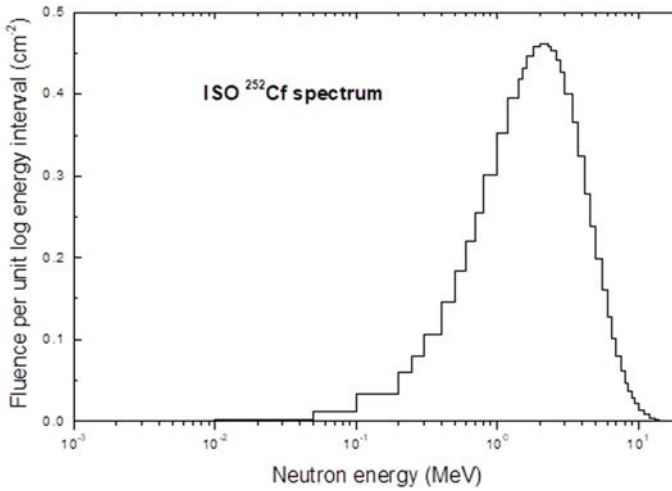
FIG. 7.2. *^{252}Cf neutron spectrum from ISO Standard 8529-1 [7.4].*

7.2.2. Radioisotope (α,n) sources

Radionuclide (α,n) sources can be fabricated using a range of α emitting isotopes, including [7.3] ^{289}Pu, ^{210}Po, ^{238}Pu, ^{244}Cm, ^{242}Cm, ^{226}Ra and ^{227}Ac, but the most commonly used isotope at present is ^{241}Am. Several low Z elements can be used as the target for α-bombardment, and a range of sources based on ^{241}Am have been made available, including ^{241}Am-Be, ^{241}Am-B, ^{241}Am-F and ^{241}Am-Li. Over recent years, however, the ^{241}Am-Be source, with a mean energy of 4.2 MeV, has become by far the most readily available and frequently used, and other ^{241}Am(α,n) sources have become much less common. One reason for the popularity of ^{241}Am-Be sources is the high yield from the ^{9}Be(α,n) reaction for the alpha energies from ^{241}Am, which produce a neutron yield of roughly 6×10^4 s^{-1}·GBq^{-1}. If they are available, the other sources can, nevertheless, be useful for instrument type testing, especially ^{241}Am-F and ^{241}Am-Li, which have lower mean neutron energies of approximately 1.5 MeV and 0.5 MeV, respectively. As was the case for ^{252}Cf sources, (α,n) sources are commonly doubly encapsulated cylinders, although, because relatively large amounts of α emitting and target material are required, they are usually physically larger than ^{252}Cf sources, with dimensions of several cm. The arrangement that makes best use of the α particles available is a 'dilute' concentration of ^{241}Am evenly distributed in the low Z material.
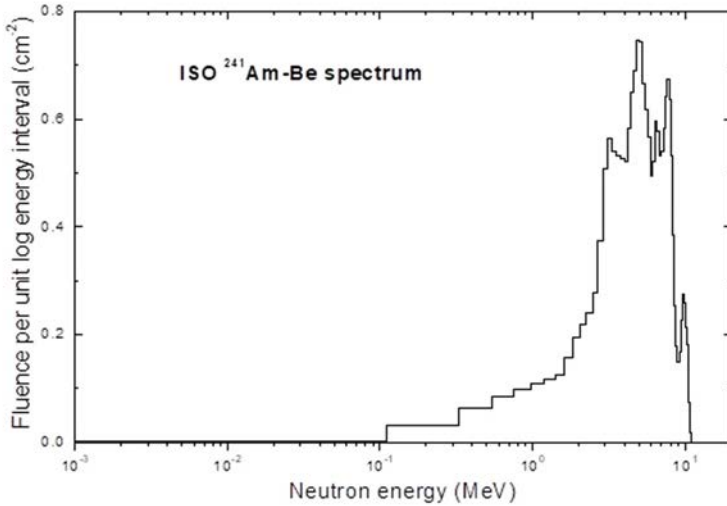
FIG. 7.3. [241]Am-Be spectrum from ISO Standard 8529-1 [7.4].

The [241]Am-Be spectrum is shown in Fig. 7.3. It is derived from ISO 8529-1, and numerical data for spectral fluence can be found in that standard. Because radionuclide sources are contained in finite size cylindrical capsules, the intensity of the emission rate is somewhat anisotropic. In addition, the spectrum may change slightly with angle relative to the axis of the capsule. No information is presently available about spectral variations, and the same spectrum is usually used for all angles of emission. Spectra for the other [241]Am based sources can be found in Refs [7.4] ([241]Am-B), [7.6] (various sources), [7.7] ([241]Am-F) and [7.8] ([241]Am-Li). Because of possible problems from the buildup of helium within source capsules, there is usually a recommended working life for radionuclide sources, which will depend on the source construction and the environment in which it is used.

7.2.3. Radioisotope (γ,n) sources

Radioisotope (γ,n) sources are rarely used nowadays because higher neutron yields can be obtained from (α,n) sources. In addition, (γ,n) sources suffer from having very high photon dose rates, making them a severe radiological hazard to use. However, they have been used extensively in the past [7.1–7.3], and specific sources are still sometimes employed because of particular properties, such as nearly monoenergetic low energy neutrons from the [124]Sb(γ,n) source.

7.2.4. Moderated sources

Radionuclide neutron sources tend to have spectra with much higher mean energies than the spectra in which personal dosimeters and area survey instruments are used and, because of this, attempts have been made over the years to produce calibration fields with lower mean energies by using moderating material around a radionuclide source.

The most well known and frequently used of these is the heavy water (D_2O) moderated ^{252}Cf source [7.9]. The standard design for this source has a physically small ^{252}Cf capsule at the centre of a steel sphere of 300 mm diameter, which is filled with D_2O. A cadmium shell of approximately 1 mm thickness is included on the outside of the steel shell to absorb thermal neutrons. Because D_2O provides good moderation with minimal neutron capture, the fraction of the original ^{252}Cf neutrons that emerges from the assembly is high; only 11.5% of them are lost, most of which are thermal neutrons captured in the cadmium.

Although a number of calculations of the D_2O moderated ^{252}Cf source spectrum have been performed (see, for example, Ref. [7.10]), the spectrum that is usually assumed is the one shown in Fig. 7.4 and given in Ref. [7.4], which derives from an early calculation by Ing and Cross [7.11]. A number of sources of this type are available in calibration laboratories worldwide, but their large size raises problems that are not present for conventional radionuclide sources. For example, the source is heavy, it is difficult to use a shadow cone to estimate
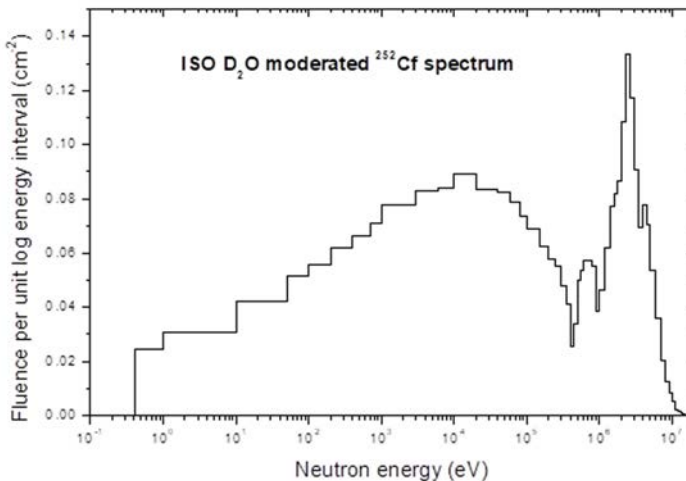

FIG. 7.4. D_2O moderated ^{252}Cf neutron spectrum from ISO Standard 8529-1 [7.4].

the effects of scattered neutrons, and the neutrons do not impinge on any device being irradiated from a single point, or a small volume that approximates a point source but can originate from any point within the 30 cm diameter sphere.

One other type of moderated source that is important in the context of neutron radiation protection is one where very large quantities of moderating material are used in order to create a thermal neutron field, which can be used for instrument calibration or testing (see Section 14.2.6). The moderator is usually polyethylene or graphite, and the neutrons can be produced from conventional radionuclide sources [7.12, 7.13] or by using an accelerator and one or more neutron producing targets [7.14].

7.2.5. General issues for radionuclide neutron sources

The main characteristics of the radionuclide sources recommended by ISO [7.4] for neutron device calibrations are given in Table 7.1. Tabulated spectra for these sources can be found in Ref. [7.4]. Their physical form makes them easy to use.

The emission rates of source capsules into 4π steradians can be measured using the manganese sulphate bath technique [7.15]. This approach involves mounting the neutron source at the centre of a large bath of an aqueous solution of manganese sulphate (see Fig. 7.5).

The neutrons are moderated in the liquid, and a fraction (roughly half) of the thermalized neutrons are captured by the ^{55}Mn producing ^{56}Mn, which decays with a half-life of approximately 2.6 h. By measuring the ^{56}Mn activity, the neutron emission rate can be determined. In fact, if all the neutrons from the source were captured in the manganese, the saturated ^{56}Mn activity would be equal to the neutron source emission rate. However, thermal neutrons are also captured in other materials, the most significant being hydrogen, and neutrons can also be lost by other mechanisms, including fast reactions and leakage from the boundary of the bath. Nevertheless, corrections can be made for these effects, and source emission rates can be measured to an accuracy of better than 1%.

Since fluence to dose equivalent conversion coefficients are reasonably well known for radionuclide source spectra, these sources can be used to provide accurate dose equivalent calibrations. They are, however, always limited by the fact that the spectrum from a particular source is fixed and cannot be altered. Some variety can be obtained by using different source types, but the flexibility is limited. For type testing, the availability of accelerator produced monoenergetic neutrons is a big advantage. There is a further problem with using radionuclide sources for calibrations, and that is the fact that most of the fields in which individuals are exposed are very different to those of unmoderated radionuclide

TABLE 7.1. CHARACTERISTICS OF RADIONUCLIDE SOURCES
RECOMMENDED BY ISO FOR CALIBRATING NEUTRON MEASURING
DEVICES [7.4]

Source	Half-life (years)	Fluence averaged energy (MeV)	Emission rate into 4π sr [a] ($s^{-1} \cdot kg^{-1}$)	Photon dose rate as a % of the neutron dose equivalent rate [b]	Spectrum averaged fluence to dose equivalent conversion coefficients (pSv·cm^2)	
					$h*(10)$	$h_p(10,0°)$
^{252}Cf	2.645	2.13	2.4×10^{15}	~5%	385	400
D$_2$O moderated ^{252}Cf	2.645	0.55	2.1×10^{15}	18%	105	110
			($s^{-1} \cdot Bq^{-1}$)			
^{241}Am-Be	432.2	4.16	1.6×10^{-5}	< 5%[c]	391	411
^{241}Am-B	432.2	2.72	6.6×10^{-5}	< 20%[c]	408	426

Adapted with permission from International Organization for Standardization (ISO), Geneva.

[a] For unmoderated ^{252}Cf sources, the emission rate is quoted in terms of the mass of californium contained in the source. For ^{241}Am based (α,n) sources, the emission rate is related to the ^{241}Am activity.

[b] Values quoted are from Ref. [7.4]. For a more detailed discussion of the photon component (see Section 14).

[c] Value applies to a source enclosed in a lead shield of approximately 1 mm thickness.

sources. This issue is discussed further in Section 14, where the concept of simulated workplace fields is discussed.

Small radionuclide sources may be handled using long tongs, provided these handling operations are relatively brief and well rehearsed. A 37 GBq (1 Ci) ^{241}Am-Be produces a personal dose equivalent of approximately 29 μSv·h^{-1} at 1 m, and 1 μg of ^{252}Cf roughly the same. The ^{241}Am-Be sources are physically larger, making them generally easier to handle using long tongs. For higher emission rate sources, some remotely operated mechanical means of moving them from the source store to the position where they are going to be used is advisable, and mechanical or pneumatic transfer systems are commonly used.

FIG. 7.5. A manganese sulphate bath. For this model, sources are positioned on the end of a rod and are inserted into the bath from the top. A long counter, to the right in the picture, measures neutron leakage from the surface of the bath. (Courtesy of National Physical Laboratory.)

All radionuclide neutron sources also emit gamma rays, and approximate values are given in Table 7.1 for the gamma ray doses from the ISO recommended sources. Some further details are given in Section 14.

Radionuclide neutron source capsules provide one of the simplest means of producing neutron fields for a range of applications and are manufactured to very stringent quality requirements [7.16]. Despite their relative stability, it should not be forgotten that they are dynamic systems. For example, the neutron producing material inside the capsule is continuously changing because of radioactive decay; helium buildup will be occurring inside the capsule because of alpha particle emission; and the properties of the capsule itself may be changing because of radiation damage, weathering, corrosion, and stresses and strains if in a harsh working environment. To ensure the integrity of the source, many countries require regular, although not necessarily frequent, checking, for example leak testing [7.17]. Sources also usually have a recommended working life. These are proposed by the manufacturers on the basis of such factors as the toxicity of the nuclides used, total initial activity, source construction, half-life of the nuclide, typical application environments, operational experience, etc. In the case of long lived radionuclides, the recommended working life can be considerably shorter

than the half-life. Safeguarding the whereabouts and security of sources is also increasingly becoming an issue for users [7.18].

7.3. ACCELERATOR PRODUCED NEUTRONS

Accelerator produced neutrons can be divided into two groups. Either the neutrons are produced deliberately for research or calibration (e.g. at spallation neutron sources or calibration laboratories), or they are a by-product and as such may well be unwanted (e.g. around medical accelerators used for therapy). In all cases, they can constitute a radiological hazard.

7.3.1. Low energy charged particle accelerators

Various types of accelerators, including Cockcroft–Walton devices, Van de Graaff accelerators and cyclotrons, are used for research both in nuclear physics and other fields of physics where the charged particle beams are used as analytical probes. Some charged particle beams (e.g. deuterons) are more likely to produce neutrons than other beams, and neutron radiological protection may be an issue. One example of an application of this type of accelerator, which has a direct relevance to calibration of neutron dosimeters and survey instruments, is their use to produce quasi-monoenergetic neutrons by bombarding thin layers of target materials [7.19]. Further details about this aspect will be given in Section 14.

7.3.2. Accelerator based white neutron sources and spallation sources

Accelerator based pulsed white-spectrum neutron sources [7.3] are employed for high resolution measurements of microscopic neutron cross-sections used for reactor design and for nuclear physics research. These sources produce short bursts of neutrons that cover the energy range from thermal to several tens of MeV, and by utilizing time of flight techniques, measurements can be made for any energy within the range. The particles accelerated can be electrons, which are slowed down in a high Z target producing bremsstrahlung, which in turn creates neutrons by photonuclear reactions, or charged particles. In both cases, for bombarding energies above approximately 20 MeV, a compound nucleus is formed, and neutrons with an evaporation spectrum are emitted [7.20].

For bombarding energies above approximately 100 MeV, the spallation process becomes increasingly important, where the bombarding particle interacts not with the nucleus as a whole but with individual nucleons in the target nucleus, triggering an intranuclear cascade. Very high neutron yields can be achieved, and by using moderators around the neutron producing target at different

temperatures, neutron beams with different low energy spectral distributions can be created (thermal neutrons and cold neutrons). Spallation neutron sources are becoming an increasingly important tool for studies of condensed matter by neutron scattering techniques.

7.3.3. Unwanted neutron production at accelerators

Neutrons are sometimes produced as unwanted by-products at accelerators, and the fact that they are a penetrating radiation (and can also scatter down mazes) may make them a radiological hazard and an additional shielding problem. Examples are high energy accelerators used for nuclear physics research, medical accelerators used for therapy, where the patient receives a whole body neutron dose if the photon energy is sufficiently high, and light ion therapy facilities. The measurement of these neutrons can pose significant problems because of, for example, the pulsed nature of the radiation field or the presence of intense photon components.

Neutrons created around accelerators are often produced by photonuclear excitation processes, with the excited nucleus decaying by particle and gamma ray emission [7.21]. Below approximately 30 MeV, the giant dipole resonance (GDR) is the dominant excitation mechanism. At higher energies, up to approximately 150 MeV, where the wavelength of the photon decreases, the phenomenological model of photoabsorption on a neutron–proton (quasi-deuteron), which has a large dipole moment, becomes important. Figure 7.6 provides an illustration of
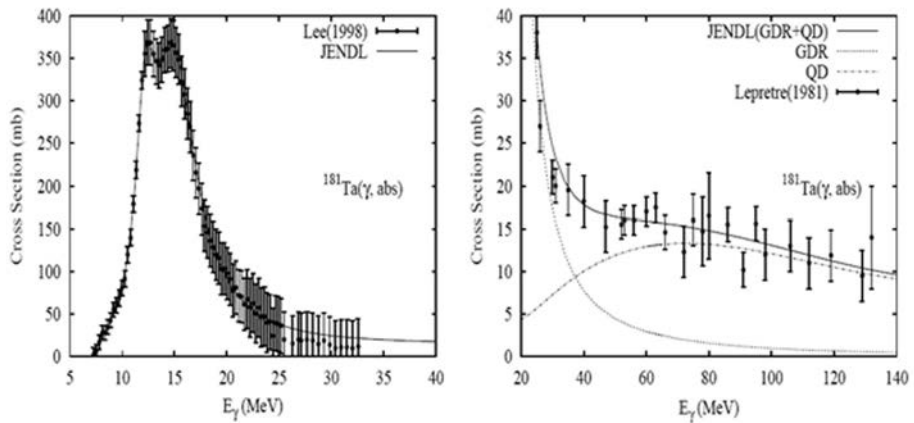

FIG. 7.6. Illustrative example of the nuclear photoabsorption cross-section. Left: the giant dipole resonance (GDR) component; right: the quasi-deuteron (QD) component, the GDR tail and their sum [7.21].

the cross-sections for the different photoabsorption mechanisms. Evaluations of photoneutron cross-sections for most elements have been compiled [7.21, 7.22].

7.4. NUCLEAR REACTORS

In a nuclear reactor, the energy is produced by a nuclear fission chain reaction, and an enormous number of fission neutrons are released in the core. Because of the moderation required to maintain the chain reaction, the spectrum outside the core (except in the cases of some very special research reactors) consists generally of low energy neutrons, and this is an important factor when considering radiation protection issues. The physics of nuclear reactors is a huge topic in its own right and cannot therefore be covered here. This subsection confines itself to a very brief description of the basic neutron production mechanisms and to the spectral characteristics that are relevant to radiation protection dosimetry.

7.4.1. Prompt fission

The energy distribution of neutrons produced in the fission process has been measured for all the common fissile elements. Several expressions have been proposed for the shape of the neutron spectrum, including the Maxwellian (see Eq. (7.1)), often used to describe the ^{252}Cf spectrum. For this equation, the value of T for ^{235}U, the most important fissile material in most reactors, is 1.29 MeV [7.23]. Two important parameters of the fission process are the average number of neutrons per fission, $\bar{v}$, and the mean energy of all the neutrons emitted from a single fission event, E_n^f. These are shown in Table 7.2 for the most important fissile elements for fission with thermal neutrons.

7.4.2. Delayed neutrons

The emission of some of the neutrons accompanying fission is delayed by times ranging from less than a second to a minute or so. They are the result of the beta decay of short lived fission product nuclei, which produce a daughter nucleus in an excited state so high in energy that neutron emission is possible. Examples of these fission products are ^{87}Br, ^{89}Br and ^{137}I, with half-lives of 55, 4.5 and 22 s, respectively. Neutrons of this type are termed 'delayed neutrons'. Their energies are lower than from prompt fission, typically 0.5 MeV or lower, and they constitute less than 1% of the total number of neutrons emitted. However, because of their time structure, they play an important role in reactor control.

TABLE 7.2. FISSION PARAMETERS FOR SEVERAL FISSILE
NUCLEI [7.24]

Nucleus	$\bar{v}$	E_n^f
^{233}U	2.48	4.90
^{235}U	2.42	4.79
^{239}Pu	2.87	5.90
^{241}Pu	2.93	5.99

The term 'delayed neutrons' is also used to cover other mechanisms of neutron emission. The ^{17}O(n,p)^{17}N, reaction, which can occur in the cooling systems of reactors (H_2O or CO_2), produces ^{17}N, which decays (half-life 4 s) by beta emission to an excited state of ^{17}O, which in turn decays by prompt neutron emission to ^{16}O. Neutron energies may be 0.4, 1.2 or 1.8 MeV. In systems where the coolant emerges rapidly from the biological shield, this can be a radiological hazard.

Another mechanism that can produce delayed neutrons in reactors is (γ,n) reactions on beryllium or deuterium, the latter reaction being particularly relevant in heavy water moderated reactors. Thresholds for photoneutron reactions in beryllium and deuterium are 1.67 and 2.23 MeV, respectively.

7.4.3.   Power reactors

Power reactors are one of the most important sources of neutron fields, and as such, they need to be monitored, and dose equivalent estimates need to be made. In view of the poor performance of many survey instruments and personal dosimeters, particularly at low neutron energies, one of the most important items of information for reliable monitoring is the neutron spectrum in any reactor environment where personnel are likely to be exposed. Over recent years, much effort has gone into characterizing spectra around reactors. It is a huge task because the spectra vary in different locations around reactors. Measurements have been performed both within the containment of water cooled reactors and outside the containment of a range of reactor types. Compilations of these data can be found in two IAEA publications [7.25, 7.26]. In all cases, the spectra tend to be highly moderated, with large numbers of thermal and epithermal neutrons

and very few neutrons above 1 MeV. Figure 7.7 shows two typical reactor spectra and illustrates the predominantly low energies encountered.

7.4.4. Research reactors

There are a very large number of research reactors of various types worldwide. Some idea of the number and variety can be found in the IAEA Research Reactor Database [7.27]. Research reactors are used for a wide variety of different purposes, including materials and fuel testing, isotope production, neutron scattering, radiography, activation analysis, geochronology, neutron capture therapy, training and teaching. They can provide a source of thermal neutrons for calibrating radiation protection devices. They can also provide filtered beams of quasi-monoenergetic neutrons to act as calibration fields at low energies [7.28], although unfortunately few such facilities are now available.

Some specially configured research reactors can provide intense fission fields, or fission fields moderated by only a small amount of material, and these are important sources for testing criticality accident dosimeters [7.29].
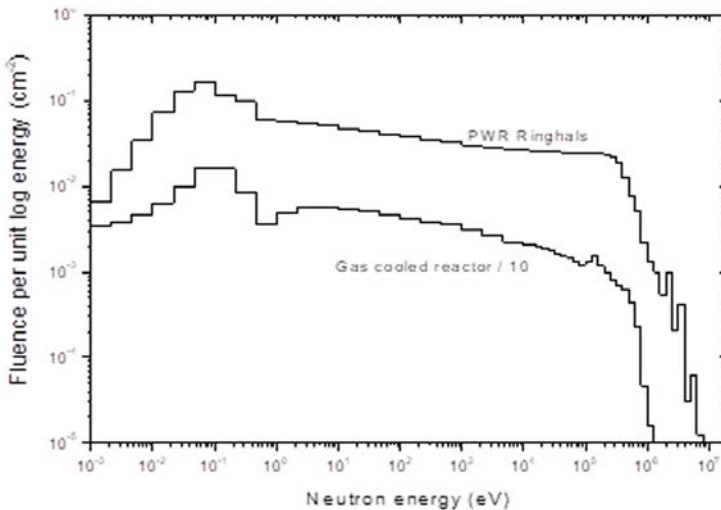
FIG. 7.7. Typical reactor spectra for a pressurized water reactor (PWR) inside the containment, and outside the containment of a gas cooled reactor. The spectra have been normalized to unit total fluence, with the gas cooled reactor data divided by 10 for the plot.

7.5. NUCLEAR FUEL FABRICATION, PROCESSING AND TRANSPORT

Neutron production in new and spent nuclear fuel is possible from fission, both spontaneous and induced, and from (α,n) reactions caused by alpha particle emitters in the material. The neutron production mechanisms are thus the same as those outlined earlier, and nuclear fuel as a source of neutrons is included separately only because the neutron spectra in which individuals are exposed tend to differ from those of other groups.

Spent nuclear fuel is usually encountered in shielded containers or flasks, and the neutron spectra around these items (see Fig. 7.8) are different to those around radionuclide sources in that they are much softer [7.31, 7.32]. The spectra are generally different to those encountered around reactors in being somewhat harder. Dose rates close to fuel flasks can be high, particularly if they contain high burnup fuel, and as a source of neutrons they are unusual since they represent a potential hazard not only to workers in the nuclear field, but also to the public when fuel flasks are transported to and from reactors.
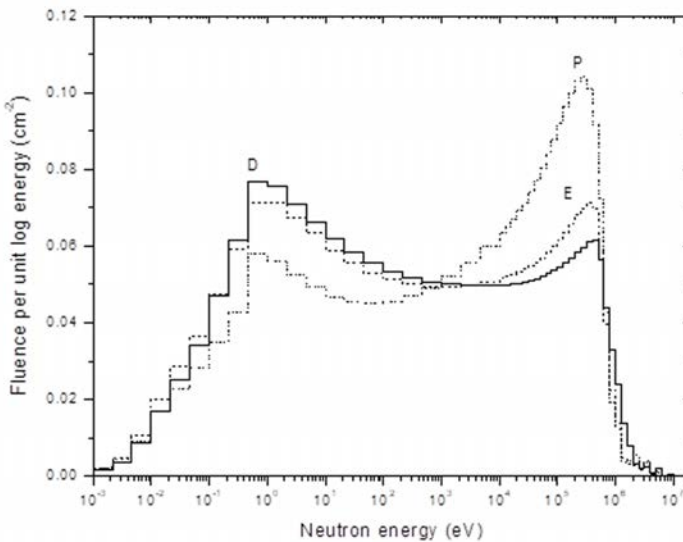
FIG. 7.8. Neutron spectra at three locations, D, E and P, in the environment of a transport cask with spent fuel elements at the Central Interim Storage Facility for Spent Nuclear Fuel (CLAB) in Oskarshamn, Sweden. (Reproduced from Ref. [7.30] with permission from Oxford University Press.)

During fuel production, workers may be exposed to fission and (α,n) spectra with very little moderation between them and the fuel, but the dose rates from unirradiated fuel are usually low [7.33].

7.6. COSMIC RAYS

One of the most important neutron fields that need to be considered in terms of the radiation protection of individuals is that at aircraft flight altitudes. This field is created by high energy cosmic ray particles, mainly protons, originating predominantly from outside the solar system, entering the upper atmosphere. There, they collide with the atomic nuclei of the air and create cascades of secondary radiation, including neutrons. The intensity would be considerably larger than it actually is but for the effects of the Earth's magnetic field and the solar wind, which deflect the cosmic ray particles and reduce the intensity. Cosmic radiation effective dose rates increase with altitude, up to a maximum at approximately 20 km (66 000 ft), and with increasing latitude, reaching a constant level at approximately 50°. The effective dose rate at an altitude of 8 km (26 000 ft) in temperate latitudes is typically up to 3 µSv·h^{-1}, but near the equator is only between about 1 and 1.5 µSv·h^{-1}. At an altitude of 12 km (39 000 ft), the values are greater by approximately a factor of two. At commercial jet aircraft flight altitudes, roughly half the dose equivalent received by individuals is from neutrons.

Much effort has gone into calculating the neutron spectrum using transport codes and estimates of the cosmic ray spectrum impinging on the upper atmosphere [7.34, 7.35]. Spectrometry measurements have also been performed [7.36, 7.37]. There is reasonable agreement on the overall shape of the spectrum, with two major neutron peaks, one at a few MeV and one at a few hundred MeV (see Fig. 7.9), and the mechanisms for producing these peaks are reasonably well understood.

The intensity of the radiation field seen on board aircraft varies not only with altitude and latitude (more precisely, location in the geomagnetic field), but also with the time in the Sun's activity cycle; however, the spectrum of the neutron component does not change significantly with these parameters. This is an important fact, since it means that instruments, if they can be calibrated in an appropriate field, can be relied upon to give reasonable estimates of dose equivalent. There is one instrument, the tissue equivalent proportional counter (TEPC), that, from theoretical considerations, is expected to perform well for flight altitude neutron spectra. A concerted effort to acquire measured dose equivalent data and to compare them with calculations has demonstrated good agreement [7.38, 7.39], and as a result, dosimetry for air crew and frequent fliers
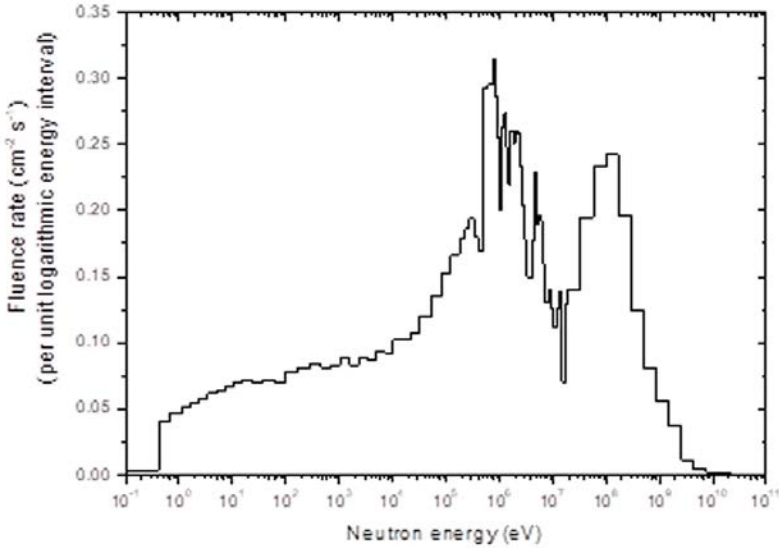
FIG. 7.9. *Neutron spectral fluence rate at an atmospheric depth of 246 g·cm⁻² (approximately 10.6 km, or just under 35 000 ft) for the month of May 1995 and a cut-off rigidity of 4 GV [7.34]. (Cut-off rigidity,* r, *is a measure of the penetration of a cosmic ray particle through the Earth's magnetic field and is defined as* r = p/q, *where* p *is the momentum of the particle and* q *is its charge.)*

is on a reasonably sound footing, with one possible exception — its reliability can be affected by particularly violent solar activity.

The effects on aircraft crew and passengers of exposure to radiation from violent events on the Sun are very complex and can result in both increases in dose rates, caused by energetic particles from the Sun arriving at the Earth, or decreases in dose rates, resulting from the effect of increased solar wind and increases in the associated magnetic field [7.39].

Increases result from solar particle events (SPEs) produced by sudden releases of energy in the solar atmosphere (solar flares) and by coronal mass ejections. These SPEs result in an increased fluence of high energy particles arriving at the Earth from the Sun. The spectra of these events are variable, but in general they are softer than for galactic cosmic rays, and only a small fraction of SPEs cause an increase in aviation altitude doses (roughly one a year). The onset of such dose increases is rapid, usually occurring over minutes, and can last for periods between hours and several days. Information about these events can be obtained from a number of sources: visual observations of the Sun, data from satellites and data from the network of ground level neutron monitors geometrically dispersed around the Earth. To date, it has not been possible to

predict from visual observations of the Sun which events will give rise to significant increases [7.40, 7.41].

Decreases in the dose rate tend to be associated with sunspot numbers, and for this reason, the average flight level doses tend to be lower at times of maximum solar activity. These so-called 'Forbush decreases' may occur several times a year and can last for several days.

In general, the overall effect of solar activity on doses for aircrew and passengers is small [7.39–7.41]; however, the possibility of an event producing dose rates of several $mSv \cdot h^{-1}$, as occurred in February 1956 [7.42], means that research continues into this problem.

7.7. SPECTRA

It is clear from the spectral distributions plotted in this section that neutron sources produce a wide range of different spectra. Not only do the primary sources of neutrons have different spectra, but the effects of varying amounts of shielding around sources also mean that spectra in workplaces where neutron dose equivalent values need to be measured are even more diverse. Some idea of the range of different spectra can be obtained from published compilations of spectra [7.25, 7.26, 7.43]. Since the instrumentation presently available to measure neutron dose equivalent cannot be relied upon to give the correct value for the full range of neutron energies of interest, it is important to have information on workplace neutron spectra. The fact that workplace spectra differ markedly from those of most calibration facilities has been the motivation for laboratories developing fields that simulate those found around workplaces. These are discussed in more detail in Section 14.

REFERENCES TO CHAPTER 7

[7.1] MARION, J.B., FOWLER, J.L., Fast Neutron Physics Part I: Techniques, Interscience Publishers, New York (1960).
[7.2] BECKURTS, K.H., WIRTZ, K., Neutron Physics, Springer-Verlag, New York (1964).
[7.3] CIERJACKS, S. (Ed.), Neutron Sources for Basic Physics and Applications, An OECD/NEA Report, Vol. 2 of Neutron Physics and Nuclear Data in Science and Technology, Pergamon Press, Oxford and New York (1983).
[7.4] INTERNATIONAL ORGANIZATION FOR STANDARDIZATION, Reference neutron radiations — Part 1: Characteristics and methods of production, International Standard 8529-1, ISO, Geneva (2001).

[7.5]   ROBERTS, N.J., JONES, L.N., Investigation of the implications of [250]Cf and [248]Cm in [252]Cf neutron sources, NPL Report DQL RN 005, National Physical Laboratory, Teddington, UK (2004).

[7.6]   LORCH, E.A., Neutron spectrum of [241]Am-B, [241]Am-Be, [241]Am-F, [242]Cm-Be, [238]Pu-^{13}C and [252]Cf isotopic neutron sources, Int. J. Appl. Radiat. Isot. **24** (1973) 585–591.

[7.7]   OWEN, J.G., WEAVER, D.R., WALKER, J., "Neutron spectra from Am/F and Am/Li (α,n) sources", Proc. Conf. Nuclear Data for Science and Technology, Antwerp, 6–10 Sep. 1982, D. Reidel, Dordrecht (1983) 492–494.

[7.8]   TAGZIRIA, H., ROBERTS, N.J., THOMAS, D.J., Measurement of the Am-Li radionuclide source spectrum, Nucl. Instrum. Methods Phys. Res. A **510** (2003) 346–356.

[7.9]   SCHWARTZ, R.B., EISENHAUER, C.M., The Design and Construction of a D_2O-Moderated [252]Cf Source for Calibrating Neutron Personal Dosimeters Used at Nuclear Power Reactors, NUREG/CR-1204, US Nuclear Regulatory Commission, Rockville, MD (1980).

[7.10] JETZKE, S., KLUGE, H., HOLLNAGEL, R., SIEBERT, B.R.L., Extended use of D_2O-moderated [252]Cf source for the calibration of neutron dosemeters, Radiat. Prot. Dosim. **44** (1992) 131–134.

[7.11] ING, H., CROSS, W.G., Spectral and dosimetric characteristics of D_2O moderated [252]Cf calibration facilities, Health Phys. **46** (1984) 97–106.

[7.12] GUALDRINI, G., BEDOGNI, R., MONTEVENTI, F., Developing a thermal neutron irradiation system for the calibration of personal dosemeters in terms of $H_p(10)$, Radiat. Prot. Dosim. **110** (2004) 43–48.

[7.13] LACOSTE, V., GRESSIER, V., MULLER, H., LEBRETON, L., Characterisation of the IRSN graphite moderated americium-beryllium neutron field, Radiat. Prot. Dosim. **110** (2004) 135–139.

[7.14] RYVES, T.B., PAUL, E.B., The construction and calibration of a standard thermal neutron flux facility at the National Physical Laboratory, J. Nucl. Energy **22** (1968) 759–775.

[7.15] AXTON, E.J., CROSS, P., ROBERTSON, J.C., Calibration of the NPL standard Ra-Be photoneutron sources by an improved manganese sulphate bath technique, J. Nucl. Energy Parts A/B **19** (1965) 409–422.

[7.16] INTERNATIONAL ORGANIZATION FOR STANDARDIZATION, Radiation protection — Sealed radioactive sources — General requirements and classification, International Standard 2919, ISO, Geneva (2012).

[7.17] INTERNATIONAL ORGANIZATION FOR STANDARDIZATION, Radiation protection — Sealed radioactive sources — Leak test methods, International Standard 9978, ISO, Geneva (2020).

[7.18] INTERNATIONAL ATOMIC ENERGY AGENCY, Code of Conduct on the Safety and Security of Radioactive Sources, IAEA/CODEOC/2004, IAEA, Vienna (2004).

[7.19] SCHUHMACHER, H., Neutron calibration facilities, Radiat. Prot. Dosim. **110** (2004) 33–42.

[7.20] SATCHLER, G.R., Introduction to Nuclear Reactions, Macmillan, London and Basingstoke (1980).

[7.21] INTERNATIONAL ATOMIC ENERGY AGENCY, Handbook of Photonuclear Data for Applications: Cross Sections and Spectra, IAEA-TECDOC Series 1178 IAEA, Vienna (2000),
https://www.iaea.org/publications/6043/handbook-on-photonuclear-data-for-applications-cross-sections-and-spectra

[7.22] DIETRICH, S.S., BERMAN, B.L., Atlas of photoneutron cross sections obtained with monoenergetic photons, At. Data Nucl. Data Tables **38** (1988) 199–338.

[7.23] INTERNATIONAL ATOMIC ENERGY AGENCY, Neutron Fluence Measurements, Technical Reports Series No. 107, IAEA, Vienna (1970).

[7.24] MICHAUDON, A., "Basic physics of the fission process", Nuclear Fission and Neutron-Induced Fission Cross-Sections, Neutron Physics and Nuclear Data in Science and Technology, Vol. 1, Pergamon Press, Oxford (1981) Ch. 2.

[7.25] INTERNATIONAL ATOMIC ENERGY AGENCY, Compendium of Neutron Spectra and Detector Responses for Radiation Protection Purposes, Technical Reports Series No. 318, IAEA, Vienna (1990).

[7.26] INTERNATIONAL ATOMIC ENERGY AGENCY, Compendium of Neutron Spectra and Detector Responses for Radiation Protection Purposes, Supplement to Technical Reports Series No. 318, Technical Report Series No. 403, IAEA, Vienna (2001).

[7.27] INTERNATIONAL ATOMIC ENERGY AGENCY, Research Reactor Database, https://nucleus.iaea.org/RRDB/RR/ReactorSearch.aspx

[7.28] MILL, A.J., A proposed technique for producing high-purity monoenergetic neutron beams between 100 eV and 2.5 keV for nuclear research, Nucl. Sci. Eng. **85** (1983) 127–132.

[7.29] ASSELINEAU, B., et al., Reference dosimetry measurements for the international intercomparison of criticality accident dosimetry SILENE June 2002, Radiat. Prot. Dosim. **110** (2004) 459–464.

[7.30] LINDBORG, L., et al., Determination of neutron and photon dose equivalent at workplaces in Sweden, a joint SSI-EURADOS comparison exercise, Radiat. Prot. Dosim. **61** (1995) 89–100.

[7.31] POSNY, F., CHARTIER, J.L., BUXEROLLE, M., Neutron spectrometry systems for radiation protection: measurements at work places and in calibration fields, Radiat. Prot. Dosim. **44** (1992) 239–242.

[7.32] RIMPLER, A., Bonner sphere neutron spectrometry at spent fuel casks, Nucl. Instrum. Methods Phys. Res. A **476** (2002) 468–473.

[7.33] ROBERTS, N.J., THOMAS, D.J., VISSER, T.P.P., Improved Bonner sphere neutron spectrometry measurements for the nuclear industry, Radiat. Phys. Chem. **140** (2017) 319–321.

[7.34] HEINRICH, W., ROESLER, S., SCHRAUBE, H., Physics of cosmic radiation fields, Radiat. Prot. Dosim. **86** (1999) 253–258.

[7.35] CLEM, J.M., DE ANGELIS, G., GOLDHAGEN P., WILSON, J.W., New calculations of the atmospheric cosmic radiation field — results for neutron spectra, Radiat. Prot. Dosim. **110** (2004) 423–428.

[7.36] GOLDHAGEN, P., CLEM, J.M., WILSON, J.W., The energy spectrum of cosmic-ray induced neutrons measured on an airplane over a wide range of altitude and latitude, Radiat. Prot. Dosim. **110 (**2004) 387–392.

[7.37] WIEGEL, B., ALEVRA, A.V., MATZKE, M., SCHREWE, U.J., WITTSTOCK, J., Spectrometry using the PTB neutron multisphere spectrometer (NEMUS) at flight altitudes and at ground level, Nucl. Instrum. Methods Phys. Res. A **476** (2002) 52–57.

[7.38] LINDBORG, L., et al., Cosmic radiation exposure of aircraft crew: compilation of measured and calculated data, Radiat. Prot. Dosim. **110** (2004) 417–422.

[7.39] LINDBORG, L., et al., Radiation Protection 140, Cosmic Radiation Exposure of Aircraft Crew Compilation of Measured and Calculated Data, Final Report of EURADOS WG5 to the Group of Experts established under Article 31 of the Euratom treaty, European Commission, Luxembourg (2004).

[7.40] LANTOS, P., FULLER N., History of the solar particle event radiation doses on-board aeroplanes using a semi-empirical model and Concorde measurements, Radiat. Prot. Dosim. **104** (2003) 199–210.

[7.41] LANTOS, P., FULLER, N., BOTTOLLIER-DEPOIS, J-F., Methods for estimating radiation doses received by commercial aircrew, Aviat., Space Environ. Med. **74** (2003) 746–752.

[7.42] ARMSTRONG, T.W., ALSMILLER, R.G., BARISH, J., Calculation of the radiation hazard at supersonic aircraft altitudes produced by an energetic solar flare, Nucl. Sci. Eng. **37** (1969) 337–342.

[7.43] INTERNATIONAL ATOMIC ENERGY AGENCY, Compendium of Neutron Spectra in Criticality Accident Dosimetry, Technical Report Series No. 180, IAEA, Vienna (1978).

8. BASIC NEUTRON DETECTION PRINCIPLES

8.1. NEUTRON DETECTION BASICS

Because neutrons have no charge, they cannot be detected directly, and their presence needs to be inferred via the detection of secondary charged particles produced either by neutron induced nuclear reactions or by neutron scattering. These secondary charged particles can be detected in a variety of ways and in a variety of different devices [8.1]. These include scintillators, solid state devices, etched track devices, or gas counters operating as ion chambers, proportional counters or Geiger–Müller counters.

The scattering of a neutron from an atomic nucleus produces a recoiling charged nucleus. For high Z atoms, the recoil energy is a small fraction of the neutron energy, but for light nuclei, a substantial fraction of the energy of the neutron can be transferred to the recoil. Neutron–proton (n–p) scattering provides the basis for a number of neutron detecting devices where the recoiling proton is detected. These devices tend only to detect fast neutrons, since only in a fast neutron scatter event is enough energy transferred to the recoil. This approach does have one advantage over some other detection mechanisms in that a measure of the neutron energy can be derived from the recoil particle spectrum. This is not straightforward, since the recoil energy depends on the scattering angle, but energy information can in many cases be extracted, and several types of fast neutron spectrometers are based on n–p scattering.

Neutrons can initiate a whole series of nuclear reactions (see Section 4), including (n,p), (n,d), (n,t), (n,α) or (n,fission) that produce charged ions, all of which can be used as a means to detect neutrons. A number of reactions have, however, become basic to neutron detection because of properties such as:

(a) A high cross-section to give reasonable detection efficiency;
(b) The exoergic nature of the reaction, which ensures the charged particles have sufficient energy to be detected easily;
(c) The ability to incorporate the target nuclide into a suitable sensor, such as a proportional counter.

Three reactions, all involving low Z nuclei, are used extensively to detect neutrons. They are:

(i) $^3\text{He}(n,p)\text{T}$;
(ii) $^6\text{Li}(n,\alpha)\text{T}$;
(iii) $^{10}\text{B}(n,\alpha)^7\text{Li}$.

All three reactions are used primarily to detect thermal neutrons. This is because their cross-sections have an approximately $1/v$ dependence at low energies, where v is the neutron velocity, which means the cross-sections are high for thermal neutrons (see Fig. 8.1). They also have high Q values (see Table 8.1). If detectors based on these reactions are placed inside or close to good moderating material, they can be used to detect fast neutrons that are moderated prior to being detected. This is the principle of albedo dosimeters and many survey instruments.

TABLE 8.1. PROPERTIES OF THREE IMPORTANT REACTIONS USED FOR NEUTRON DETECTION [8.2]

Reaction	Thermal neutron cross-section [8.3] (2200 m·s^{-1})	Q value
^{3}He(n,p)T	5333 b	764 keV
^{6}Li(n,α)T	940 b	4.78 MeV
^{10}B(n,α)^{7}Li	3837 b	2.31 or 2.79 MeV

Reproduced with permission from ICRU.
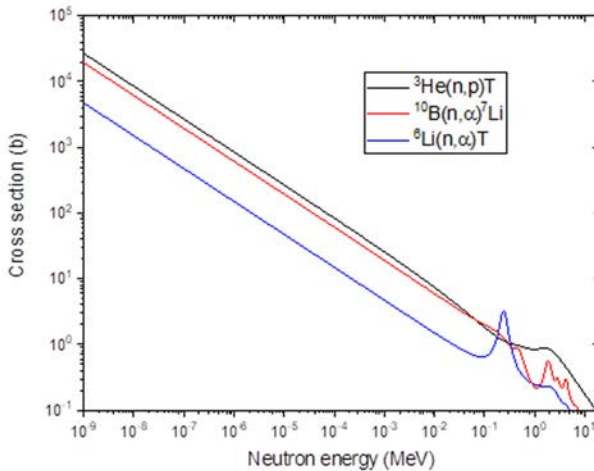
FIG. 8.1. Cross-sections [8.4] for the three important neutron detecting reactions ^{3}He(n,p)T, ^{6}Li(n,α)T and ^{10}B(n,α)^{7}Li, showing the classic 1/v dependence of the cross-section at low energies, where v *is the neutron velocity.*

The different reactions have different advantages and disadvantages. For example, the ^{6}Li(n,α)T reaction exhibits the highest energy release, that is, it has the highest reaction Q value but the lowest cross-section. The low cross-section can, however, be countered by the high number density of the lithium nuclei that can be achieved in some materials. The detection efficiency of devices incorporating these materials depends, in fact, on the product of the cross-section and the number density of the relevant isotopes.

Another reaction that is commonly used for detecting neutrons is nuclear fission. Neutrons are captured by fissile nuclei, forming a compound nucleus that splits into two energetic fragments and one or more neutrons. The high energy of the fission products makes them relatively easy to detect, either in gaseous counters, where the fissile material is often included as a thin layer within an ion chamber operated in pulsed or current mode, or using etched track material.

The fission cross-sections for different fissionable isotopes can have very different energy dependencies, as illustrated in Fig. 8.2. Thus, ^{235}U is usually used in thermal neutron detectors because of its very high thermal cross-section, whereas ^{238}U, ^{237}Np and ^{232}Th can be used as fast neutron detectors because their cross-sections in the region above 1 MeV are much higher than the values at lower energies.
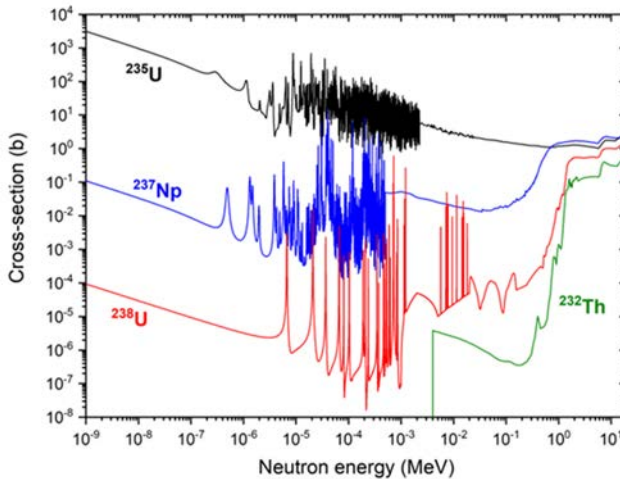
FIG. 8.2. Fission cross-sections [8.4] for the isotopes ^{235}U, ^{238}U, ^{237}Np and ^{232}Th.

8.2. DETECTORS

The basic principles underlying several neutron detecting devices are briefly outlined here without providing extensive details. These can be found elsewhere (e.g. Refs [8.1] and [8.2]).

8.2.1. Gaseous detectors

Both ^{3}He and ^{10}B, in the form of BF_3, are gases and are easily incorporated into gaseous detectors, which can be either ion chambers or proportional counters. Since the ^{3}He and ^{10}B cross-sections are well known, the detection efficiency of gaseous counters containing these materials can be calculated reasonably well if the gas pressure and the sensitive volume are known accurately. Proportional counters made of tissue equivalent material and containing a tissue equivalent gas (known as TEPCs) can provide direct information on dose deposition in tissue-like material. Some materials are incorporated into gaseous detectors in the form of thin layers of boron or fissile material on the inside surface of the detector. The gas filling is then any suitable counting gas with minimal direct response to neutrons.

Gaseous detectors for fast neutrons include proton recoil counters filled with hydrogen or methane and ^{4}He recoil counters. The ^{3}He(n,p)T reaction can also be used for the energy region from approximately 50 keV to 1.5 MeV. This type of detector is usually used for neutron spectrometry [8.5].

Gaseous detectors are not in general directional; in other words, they have no strong dependence on the direction of neutrons and thus are more appropriate for measuring ambient dose equivalent than personal dose equivalent. Small ^{3}He or BF_3 detectors are commonly used at the centre of moderator based survey instruments.

8.2.2. Scintillators

As with gaseous detectors, scintillators can be used to detect thermal neutrons or fast neutrons. To detect thermal neutrons, they usually contain an element such as ^{6}Li. Fast neutrons are usually detected predominantly via n–p scattering, although nuclear reactions can also occur in scintillator materials, adding to the events seen. A scintillator that is used frequently for detecting thermal neutrons is a lithium iodide phosphor of the alkali halide type, activated with europium and enriched in ^{6}Li [8.1]. Scintillators that detect fast neutrons are used mainly for spectrometry [8.6].

Scintillating material can take several forms, including a plastic, a crystalline material such as stilbene, a glass, and even glass fibres or a liquid.

One of the most commonly used liquid scintillators has long been known under the trade name NE213, although the present trade name is BC501A. It has good n–γ discrimination properties and is used extensively for spectrometry in the 1 MeV to 20 MeV, or higher, region [8.6].

Scintillators are not in general directional, and so, as with gaseous detectors, they are more appropriate for measuring ambient dose equivalent than personal dose equivalent.

8.2.3. Solid state devices

In most cases where solid state devices are used in neutron detectors, the solid state device is there simply to detect charged particles, and they can either be from recoils or from one of the three commonly used reactions described earlier (i.e. ^{3}He(n,p)T, ^{6}Li(n,α)T or ^{10}B(n,α)^{7}Li). The material that produces the charged particles is usually in the form of a thin layer over the sensitive volume of the solid state device. This gives the detector a response that has a dependence on the direction of the neutrons. Such detectors are thus options for measuring $H_p(10)$, which has a directional dependence. Increasingly, electronic personal dosimeters based on solid state devices with appropriate converter layers are coming on the market [8.7].

Solid state charged particle detectors are used to detect recoil protons in proton recoil telescopes. These instruments can be used both for fluence measurements and for spectrometry [8.1].

8.2.4. Etched track devices

Charged particles travelling through matter cause damage to the structure. In certain materials, referred to as etched track materials, this damage can be made visible by an etching process that preferentially attacks the damaged area. The damage tracks appear as pits on the surface. This type of material has long been used to detect heavy charged particles, such as alpha particles and fission fragments. Such etched track materials can be made into neutron detectors by incorporating a layer in which (n,α) or (n,f) reactions occur. A significant step forward in the use of etched track material was made with the introduction of PADC. This is sensitive to energetic protons and can thus detect neutrons either by including a hydrogenous 'radiator' layer or from its own hydrogen content. This material, often referred to by its trade name, CR39, has increasingly been used as the sensitive element in passive fast neutron dosimeters. The threshold for neutron detection depends on the etching process but is in the region of 50 to 100 keV. By including a converter layer, such as a material containing ^{6}Li, the plastic can also be made sensitive to thermal neutrons, and an albedo dosimeter

can thus be fabricated. In this way, it is possible to have a dosimeter that detects both fast and slow neutrons.

8.2.5. Thermoluminescent detectors

When energy from ionizing radiation is absorbed in a TL material, some of that energy causes electrons to become trapped at defects in the crystalline structure [8.8]. On heating the material, the electrons escape the traps and return to lower energy states with the release of visible light. The light is proportional to the energy absorbed. TL material is very commonly used in photon and electron dosimetry. For neutron dosimetry, the TL material is usually chosen to contain ^{6}Li or ^{10}B, giving it a good sensitivity to thermal neutrons. Personal dosimeters based on this approach are thus albedo devices that detect neutrons indirectly; incident fast neutrons are moderated and thermalized in the body and then backscattered to the thermal neutron sensitive detector (see also Section 11.1.2). Since the TL material is also sensitive to photons, some means of correcting for the photon signal must be used. A common approach is to have paired detectors, one sensitive to neutrons and one not. A subtraction technique gives the neutron signal. An example would be the use of TL dosimeters (TLDs) containing ^{6}Li paired with TLDs containing ^{7}Li.

8.2.6. Optically stimulated luminescent detectors

Optically stimulated luminescent (OSL) detectors are passive integrating dosimeters based on electron and hole trapping during irradiation (storage). The readout is performed by stimulating the detector with visible or near infrared light and measuring the luminescence resulting from the recombination of released electrons with holes trapped on luminescent centres [8.9]. In a short illumination, the amount of luminescence is proportional to the absorbed dose and intensity of stimulation light. The physics of the processes in these detectors is very similar to that in TLDs, but instead of heating the detector, optical stimulation of trapped electrons is utilized. The most widely used OSL detector material is Al_2O_3:C, but other materials like SrS:Sm,Eu are used in specific applications. To make Al_2O_3:C powder sensitive to neutrons, it is coated with material containing ^{6}Li, such as LiF or Li_2CO_3 [8.10]. These detectors are thus most sensitive to thermal and epithermal neutrons and are used in albedo devices. For subtraction of the gamma induced signal, neutron OSL detectors are used in combination with standard OSL detectors insensitive to neutrons.

8.2.7.   Fluorescent nuclear track detectors

Fluorescent nuclear track detectors (FNTDs) are a new type of luminescent detector for neutron dosimetry that combines the advantages of solid state track detectors and optical measurements, avoiding the need for long chemical etching. FNTD technology for neutron dosimetry is based on the imaging and counting of fluorescent tracks produced by recoil protons or ^{6}Li nuclear reaction products. The tracks are induced in fluorescent aluminium oxide single crystals (Al_2O_3:C,Mg) and imaged using readout apparatus based on confocal laser scanning fluorescence microscopy [8.11]. Small 4 mm × 8 mm × 0.5 mm single crystals are covered with three converters made of polyethylene, lithium fluoride and polytetrafluorethylene to discriminate signals induced by fast neutrons, moderated neutrons and gamma photons, respectively.

Although this new technique is still under development and is not in general use at the time of writing, it has been demonstrated that FNTDs can measure both neutrons and photons over a wide range of doses (0.1 mSv to 10 Sv) and energies using two different data and image processing techniques. For low doses of neutrons, track counting mode is used, whereas for doses of neutrons and gamma above 50 mSv, when neutron induced tracks and delta electrons from photons start to overlap, image processing techniques give the best results and allow neutron and gamma signals to be discriminated.

8.2.8.   Superheated emulsion detectors

Superheated emulsion neutron detectors, often called superheated drop detectors or bubble detectors, are suspensions of metastable superheated liquid drops, suspended in a viscous elastic medium, which nucleate into bubbles if charged particles deposit sufficient energy inside the drop. Figure 8.3 shows an unirradiated detector (top) and one that has been exposed to neutrons (bottom). These devices are largely insensitive to photons, but are sensitive to fast neutrons. They can also be made sensitive to thermal neutrons. Neutrons can be registered by counting bubbles optically or acoustically, or by measuring the increased volume of the medium supporting the bubbles. These detectors have been used both as personal dosimeters and as area survey devices, particularly in environments where there is a high and possibly pulsed photon component, and are discussed in Sections 10 and 11.

FIG. 8.3. Two bubble detectors: the bottom one shows a large number of bubbles following irradiation, and the top one is unirradiated. (Courtesy of National Physical Laboratory (NPL).)

REFERENCES TO CHAPTER 8

[8.1] MARION, J.B., FOWLER, J.L., Fast Neutron Physics, Part 1: Techniques, Interscience Publishers, New York (1960).

[8.2] INTERNATIONAL COMMISSION ON RADIATION UNITS AND MEASUREMENTS, Determination of Operational Dose Equivalent Quantities for Neutrons, Report 66, ICRU, Bethesda, MD (2001).

[8.3] MUGHABGHAB, S.F., DIVADEENAM, M., HOLDEN, N.E., Neutron Cross Sections Vol. 1, Neutron Resonance Parameters and Thermal Cross Sections, Academic Press, New York (1981).

[8.4] KOREA ATOMIC ENERGY RESEARCH INSTITUTE, Table of Nuclides, KAERI, Taejon, South Korea, https://atom.kaeri.re.kr/.

[8.5] TAGZIRIA, H., HANSEN, W., Neutron spectrometry in mixed fields: Proportional counter spectrometers, Radiat. Prot. Dosim. **107** (2003) 73–93, https://atom.kaeri.re.kr/

[8.6] BROOKS, F., KLEIN, H., Neutron spectrometry — historical review and present status, Nucl. Instrum. Methods Phys. Res. A **476** (2002) 1–11.

[8.7] LUSZIK-BHADRA, M., Electronic personal dosemeters: the solution to problems of individual monitoring in mixed neutron/photon fields? Radiat. Prot. Dosim. **110** (2004) 747–752.

[8.8] BECKER, K., Solid State Dosimetry, CRC Press, Cleveland, OH (1973).

[8.9] AKSELROD, M.S., McKEEVER, S.W.S., A radiation dosimetry method using pulsed optically stimulated luminescence, Radiat. Prot. Dosim. **81** (1999) 167–176.

[8.10] YUKIHARA, E.G., MITTANI, J.C., VANHAVERE, F., AKSELROD, M.S., Development of new optically stimulated neutron dosimeters, Rad. Meas. **43** (2008) 309–314.

[8.11] AKSELROD, G.M., AKSELROD, M.S., BENTON, E.R., YASUDA, N., A novel Al_2O_3 fluorescent nuclear track detector for heavy charged particles and neutrons, Nucl. Instrum. Methods Phys. Res. B **247** (2006) 296–306.

9. CHARACTERIZATION OF NEUTRON FIELDS

9.1. INTRODUCTION

Spectrometry has increasingly become an important tool in radiation protection dosimetry for neutrons. The main reason for this is that the survey instruments and personal dosimeters presently available for measuring the operational quantities do not give the correct results over the required range of energies, and in the case of personal dosimeters, they also do not have the correct angle dependence for their response. In the absence of devices with the required dose equivalent response characteristics, the reliability of all measurements with presently available area and personal dosimeters is questionable, and this is one of the fundamental problems for neutron protection level dosimetry. The importance of spectrometry is that it gives an insight into the extent of this problem.

In the context of radiation protection, neutron spectrometry measurements are performed to obtain information about the spectra in workplaces. This information can be used in several ways. First, it can be used to determine the best devices to use to measure the operational quantities in a particular workplace by comparing the neutron energy distribution with the response functions of the available devices. Second, the spectra can be used to determine correction factors for the devices chosen. The use of location specific correction factors can greatly improve dose equivalent estimates. Third, in areas where it is important to know the dose equivalent rates accurately, such as where doses are near statutory limits, a spectrum measurement can provide the best estimate of the dose equivalent by folding the measured spectrum with the relevant fluence to dose equivalent conversion coefficients.

When spectrometry measurements are performed for the reasons outlined above, it is obviously important that they cover the full range of energies over which the neutrons contribute non-negligible amounts to the total dose equivalent. A spectrometry system that can do this is thus invaluable. In addition to the operational range of a spectrometer, a characteristic that may also be important is the resolution. If the intention is to derive the dose equivalent from the measured spectrum, it can be concluded from a plot of the fluence to dose equivalent conversion coefficients for the operational quantities as a function of energy that resolution is not very important in the energy region from thermal to approximately 10 keV. The conversion coefficients are reasonably constant over this region, and it is thus not particularly important to have good resolution. However, between 10 keV and 1 MeV the conversion coefficients change rapidly with energy, and good resolution over this range is a definite advantage, since the derived total dose equivalent is sensitive to exactly where the spectrometry

system assigns the fluence in this region. From roughly 1 MeV to 10 MeV, the conversion coefficients are again reasonably constant. Above this energy the conversion coefficients become more uncertain and the spectrometry more difficult. If spectrometry is used to determine the response a device will have in a particular workplace field, the energy range over which the resolution is important may be different. In the case of a device, such as some personal dosimeters, where the response exhibits a threshold-like behaviour, that is, where the response drops to a negligible value over some of the energy range of interest, the resolution of the spectral data in the region of the threshold is critical.

The importance of neutron spectrometry to protection dosimetry has increasingly been realized, as evidenced by a workshop on this topic [9.1] and the publication of a special spectrometry handbook [9.2]. Papers on neutron spectrometers can be found in many journals; the workshop proceedings and the handbook referenced above provide an excellent starting point for locating these, and the reader who needs more information on the various spectrometers described briefly here is directed to these two publications.

9.2. REPRESENTATIONS OF NEUTRON SPECTRA

The **neutron fluence**, Φ, is the quotient of dN by da, where dN is the number of neutrons incident on a sphere of cross-sectional area da, i.e.

$$\Phi = \frac{dN}{da} \tag{9.1}$$

The differential energy distribution of the neutron fluence, Φ_E, usually referred to as the fluence spectrum, is given by

$$\Phi_E = \frac{d\Phi}{dE} \tag{9.2}$$

where $d\Phi$ is the increment of neutron fluence in the energy interval between E and $E + dE$ (see also Section 2.1). A complete representation of the neutron field at a point also involves the dependence on the solid angle, Ω, defining the direction of incidence on that point, and is written as $\Phi_{E,\Omega}(E,\Omega)$, where the subscripts characterize the variables on which the fluence depends, and the symbols in brackets are the values of these variables. Information on the angle dependence is difficult to derive, whereas a number of instruments are available that can measure the energy spectrum so that considerably more information is available for Φ_E than for $\Phi_{E,\Omega}$.

Measured neutron spectra are usually represented as histograms, and these can be presented in various forms [9.3], the two most common being the fluence per unit energy and the fluence per unit logarithmic energy interval. The latter is often referred to as the fluence per unit lethargy. Spectra are also occasionally plotted as group fluence, where each bin represents the total fluence between two energies. If the groups are chosen to have equal widths on a linear scale, the shape of the spectrum, although not necessarily the normalization, will be the same as for the fluence per unit energy. Similarly, if the groups are of equal width on a logarithmic scale, the shape will be the same as for the fluence per unit lethargy. However, if the groups are chosen with different widths, then the spectrum may appear to show structure that is not genuine but is simply a result of the different group widths.

Fast neutron spectra, such as those measured using proton recoil devices or scintillators in the keV and MeV energy region, are usually represented as fluence per unit energy. This is the best representation for displaying the features of the spectrum in this energy region. Each bin of the histogram represents the integral, ϕ_i, of the differential fluence over an energy interval, ΔE, between E_i and E_{i+1} thus:

$$\phi_i = \int_{E_i}^{E_{i+1}} \Phi_E(E)\, \mathrm{d}E \qquad\qquad (9.3)$$

and the quantity plotted, and usually also the quantity tabulated, is $\phi_i/\Delta E = \phi_i/(E_{i+1} - E_i)$.

For a spectrum measured over a very wide range of neutron energies, for example from thermal to 20 MeV or higher, a fluence per unit energy representation tends to hide the important details of the spectrum [9.4]. This is because a neutron spectrum with a substantial number of thermal neutrons will have a very large number of neutrons per unit energy interval at the lowest energy. A better representation, in terms of revealing the important features of the spectrum, is a plot of the fluence per unit logarithmic energy interval, plotted with a logarithmic representation of the energy axis. The spectrum is again usually represented as a histogram, but with bin counts $\phi_i/\left[\ln(E_{i+1}) - \ln(E_i)\right] = \phi_i/\ln(E_{i+1}/E_i)$. This representation is often described as a lethargy spectrum. The quantity lethargy, u, is defined as the natural logarithm of the ratio of a reference energy to the neutron energy; that is, $u = \ln(E_0/E)$, where E_0 is the reference energy, commonly taken as 10 MeV. When calculating the fluence per unit lethargy, the reference energy cancels out and $\phi_i/\Delta u = -\phi_i/\ln(E_{i+1}/E_i)$. Since $\mathrm{d}(\ln(E)) = \mathrm{d}E/E$, it follows that

$$\frac{d\Phi}{du} = \frac{d\Phi}{d(\ln(E_0/E))} = -E\frac{d\Phi}{dE} = -E \cdot \Phi_E(E) \tag{9.4}$$

This is the reason why, for many spectra plotted as fluence per unit lethargy, the y axis is annotated as $E \cdot d\Phi/dE$ or $E \cdot \Phi_E(E)$. The negative sign in Eq. (9.4) takes account of the fact that u increases as E decreases. In fact, most spectral plots described as fluence per unit lethargy are actually of $\phi_i/\Delta u$ against $\ln(E_i)$ rather than against u.

9.3. INTEGRAL SPECTROMETERS

There are several types of spectrometry system based on what can best be described as 'integral detectors'. In these systems, devices that respond differently to different parts of the neutron spectrum are irradiated, usually sequentially, and the spectrum unfolded from the measured responses. These measured responses are the integral of the device response function with the neutron spectrum, and if the response functions differ sufficiently, each device provides information about a particular part of the spectrum. Examples of this type of spectrometry system include multispheres (Bonner spheres), activation foils (an approach to spectrometry often called reactor dosimetry because its main application is in nuclear reactors) and the use of superheated drop (bubble) detectors with different thresholds.

All spectrometry systems of this type are described mathematically in the same way, and they share the same main difficulty; that is, the rather small amount of information that is usually available from which to unfold the neutron spectrum.

For a set of integral detectors, each detector in the set provides a single number, M_i, as shown below:

$$M_i = \int_0^{E_{max}} r_i(E) \cdot \Phi_E(E) dE \tag{9.5}$$

where

$r_i(E)$ is the response function for the ith detector;
$\Phi_E(E)$ is the neutron spectral fluence as a function of energy E.

Provided the response functions are sufficiently different, each detector provides information about a region of the spectrum, and, from the set of M_i values, information can be unfolded about $\Phi_E(E)$. Neutron spectra are

commonly expressed as histograms, and Eq. (9.5) is usually approximated by Eq. (9.6), which for *m* detectors represents a set of *m* equations:

$$M_i = \sum_{j=1}^{n} r_{ij} \cdot \Phi_j \qquad (9.6)$$

where

Φ_j is the fluence averaged over a bin extending from energy E_j to E_{j+1};

r_{ij} is the response function averaged over this energy interval, that is, the indication that would be induced in detector *i* by unit fluence in the energy interval E_j to E_{j+1}.

Probably the most significant problem with this technique is that few integral detector sets have a large number of detectors with radically different response functions, and so *m* is inevitably smaller than the number of bins, *n*, into which the spectrum needs to be divided to obtain the required energy resolution to determine dose information. If *m* is smaller than *n*, this means that the problem is underdetermined mathematically. Various unfolding techniques, based on iterative approaches or the adjustment of an a priori spectrum, have been applied to this problem and have been extensively studied [9.5, 9.6] and compared [9.7] over the years. The problem is common to all spectrometry systems of this type.

9.3.1. Multisphere spectrometers

The multisphere spectrometry system, commonly described as a Bonner sphere set after the originator [9.8], has a number of advantages and disadvantages. These are discussed and illustrated in Refs [9.9] and [9.10], where the operation of these devices is covered in detail and an extensive list of references is provided. The overriding positive feature is the fact that the Bonner sphere system covers the full energy range of interest in neutron radiation protection, that is, it can be used over the range from thermal to 20 MeV and even higher if certain modifications are made to the conventional sphere set. If properly designed, the spheres also have a near isotropic response, which means the direction dependence of the field is unimportant. The main disadvantages are poor energy resolution and an element of uncertainty in the spectrum unfolding.

A Bonner sphere set (see Fig. 9.1) consists of a number of different diameter spherical polyethylene moderators designed so that a neutron sensor can be located at the centre of each sphere. This sensor is primarily sensitive to thermal neutrons. The spheres moderate neutrons incident on them, and the sensor provides a measure of the number of thermal neutrons at the centre. For the

FIG. 9.1. *Three Bonner spheres from a set that utilizes a spherical SP9 ³He proportional counter as the central sensor, shown with their associated electronics. (Courtesy of National Physical Laboratory.)*

smaller spheres, low energy neutrons have a high probability of reaching the centre and being detected, whereas higher energy neutrons tend not to be sufficiently moderated to be detected. Conversely, for large spheres, low energy neutrons are absorbed before reaching the centre, whereas the high energy neutrons penetrate to the centre and are moderated sufficiently to have a high probability of being detected. Each sphere thus has a different response function (see Fig. 9.2), and from the information provided by the measured responses for all the spheres of the set, an estimate of the spectrum can be unfolded.

Historically, the spheres have been built with diameters that are exact inch values, or half-inch for the smaller spheres of the set. Diameters can vary from 2 inches (5.08 cm) or less, if the central sensor is small, up to 12 inches (30.48 cm) or even 15 inches (38.1 cm), with the total number of spheres being typically approximately ten. Except in places where the neutron field is known to be symmetric about some point or axis, the spheres have to be irradiated sequentially. This results in most measurements being rather lengthy, although this is mitigated to some extent by the fact that Bonner spheres tend to have high sensitivity by the standards of most radiation protection instruments. There is also a need to ensure that the field intensity and spectrum remain constant over the period of the measurements or that corrections can be made for any changes in intensity. This can be achieved by the use of an independent monitor, or ideally two monitors with different sensitivities to different energy regions of the field. If
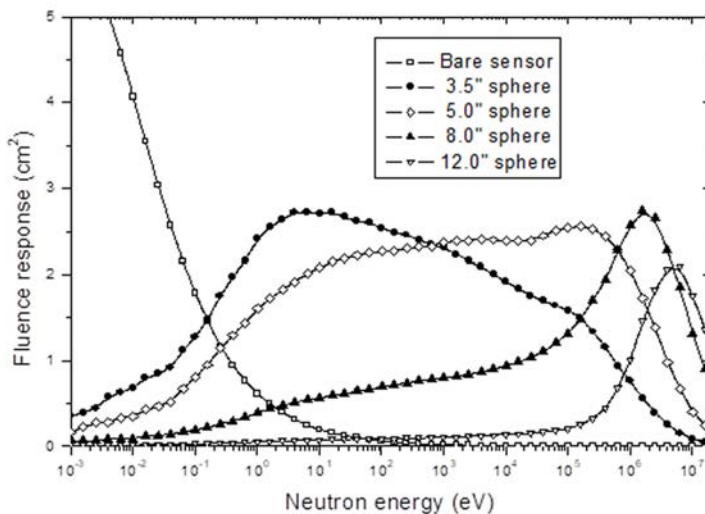
FIG. 9.2. Response functions for four spheres from a Bonner sphere set and the response function of the bare central sensor, which was a spherical ^{3}He proportional counter. (Courtesy of National Physical Laboratory.)

two such monitors are available, and they indicate that the spectrum has changed, there is little that can be done other than to limit the data used to those taken during a period when the spectrum did not change significantly. Nevertheless, the two monitor approach is useful in that it does give clear indications when the measurements need to be treated with caution.

The early Bonner sphere sets used a LiI(Eu) scintillator as the central sensor, and some extensive measurement campaigns have been reported for this combination [9.11, 9.12]. Detailed response function calculations have been performed, so well characterized sets can be produced. However, this scintillator has a significant gamma ray sensitivity, which can cause problems and usually necessitates a subtraction of gamma events from the pulse height spectrum recorded for the sensor. A step forward in the use of Bonner spheres came with the introduction of ^{3}He proportional counter detectors [9.13–9.20]. These are insensitive to gamma rays, except in very intense photon fields where gamma ray induced events pile up, and they have a good thermal neutron sensitivity. They can be obtained with spherical or right cylindrical geometry, so the isotropic response of the spheres is largely maintained (except for the presence of a thin stem to provide the electrical connection), and these sensors are the devices of choice for most Bonner sphere systems at present. For this reason, a great deal of work has gone into characterizing their response functions via both measurements and

calculations. Another obvious active sensor is the BF_3 filled proportional counter, and this device has also been employed [9.21].

One problem with active sensors is that difficulties with dead time can arise if they are operated in pulsed fields, around accelerators for example. Other sensors can be used in these environments, for example, activation foils such as indium or gold. These have an even lower gamma sensitivity, allowing them to be used in intense photon fields provided the photon energy is not so high that excessive numbers of (γ,n) neutrons are produced in the polyethylene moderators. The neutron sensitivity tends, however, to be lower than for active devices, so they are difficult to use in low intensity fields. In principle, any thermal neutron detecting material can be employed; for example, thermoluminescent dosimeters (TLDs) have also been used. The TLD material must, of course, be neutron sensitive, for example by being enriched in ^6Li or ^{10}B (e.g. TLD-600), and careful compensation for the photon sensitivity with a neutron insensitive TLD (e.g. TLD-700) is needed.

Conventional Bonner sphere sets have of the order of ten spheres, and from the measured responses for the spheres (i.e. approximately ten numbers), a spectrum covering perhaps ten decades of energy needs to be unfolded. The spectrum is usually represented as a histogram with more than ten bins, and the unfolding problem is thus mathematically underdetermined. Various approaches to overcoming this problem, including the use of any a priori information available and the requirement for a smooth final spectrum with no negative fluences, provide some help, and investigations of new unfolding techniques continue to be made. However, the final spectrum is usually not unique. Despite the unfolding problems and the poor energy resolution, a Bonner sphere measurement usually provides sufficient spectral information to make a reasonable estimate of ambient dose equivalent and to provide valuable information about the probable misreading of survey instruments. A comparison exercise for Bonner sphere measurements [9.22] indicated that, with no a priori information, ambient dose equivalent can be estimated to an accuracy of approximately 15%. With reliable a priori information a better estimate of the spectrum can be made, and the accuracy of the ambient dose equivalent derived should be better than this.

Probably because of their wide energy range, Bonner spheres have been used for more workplace field measurements than any other type of spectrometer; at least, there are more references in the literature to measurements with these devices [9.23–9.25]. The literature on spectral measurements is, however, likely to be incomplete with cases where, for commercial or security reasons, the spectral data have never been released because of sensitivity concerning dose levels.

A weakness of a conventional Bonner sphere set is that the sphere response functions above approximately 10 MeV tend to be small and similar in shape. Unfolding spectra with neutrons above 10 MeV thus proves particularly difficult.

To overcome this problem, moderator spheres with shells of some heavy metal material, for example lead or tungsten, have been introduced. High energy neutrons produce secondary neutrons by (n,*x*n) reactions in this material, and these lower energy neutrons are more readily detected. In this way, the response to high energy neutrons is significantly enhanced [9.26–9.29]. These extended Bonner sphere sets have found applications for measurements around high energy accelerators and also at aircraft flight altitudes for measurements of the neutron component of the cosmic ray field in these regions. The principle of using a heavy metal insert has also been applied in survey instruments for use in environments where there are high energy neutrons (see Section 10).

Various approaches have been proposed to address the problem of the time taken to make sequential measurements. The spherical shape makes it difficult to just add larger and larger shells. One approach has been to use right cylinders, which can be nested one inside the other, although this means the response is no longer quite as isotropic as for a sphere [9.30]. Another approach is to have a series of thermal neutron sensors within a sphere [9.31] or along the axis of a cylinder [9.32]. The use of a cylinder means the device's response function has a directional dependence, although this fact can be used if the direction of the neutrons is known.

9.3.2.   Activation detectors

Sets of activation detectors, usually in the form of thin foils, but also sometimes wires or pellets, are used for determining neutron spectra in environments where the neutron fluence is sufficiently high that easily measured levels of activity are obtained. The basis of the technique is that a number of materials with different cross-sections are irradiated, together if this is practical, and the induced activities are measured. Ideally, the cross-sections for the reactions should have different thresholds so that each gives information about a particular region of the energy spectrum. The spectrum then needs to be unfolded (cf. Section 9.7).

One example of activation detector spectrometry is the determination of reactor spectra in environments where radiation damage to reactor structural materials is an issue. This technique, often called 'reactor dosimetry', is an extensive topic area where considerable efforts have gone into determining the cross-sections for the reactions used [9.33] as well as their uncertainties, including correlation effects. This can be important if a number of cross-sections have been measured relative to a common standard. The relevance of activation detector spectrometry to routine radiation protection is very limited because of the high fluences required, but some of the efforts to develop improved spectrum unfolding codes have had input into the codes used for Bonner sphere unfolding.

Activation detector spectrometry is also used in fusion blanket measurements, in characterizing fields used for accident dosimetry comparisons and in determining spectra around accelerators producing high fluence rates, such as neutron generators producing 14 MeV deuterium on tritium (D+T) fields. The one application with a direct relevance to the protection of the individual is in nuclear accident or criticality dosimetry. This topic is covered in detail in Section 12.

9.3.3. Superheated drop (bubble) spectrometers

A novel type of integral detector spectrometer has been introduced over recent years based on the use of superheated emulsion detectors with different thresholds. The term superheated emulsions is used here to describe both superheated drop detectors and bubble damage detectors. Spectrometers based on both types of detectors have been used experimentally, and both work on the same basic principle. By varying either the composition of the detector material or the temperature, or a combination of both, detectors with different energy thresholds can be derived. Each detector gives information on the neutrons in the energy range where its response is non-zero, and the difference between the measured responses of two devices gives information on the energy region covered by one detector but not by the other. The bubbles can be counted either optically or acoustically, taking advantage of the pressure pulse emitted when drops vaporize. Figure 9.3 shows the fluence responses for a set of detectors designed to cover a relatively wide energy range.

Superheated emulsion spectrometers have a limited energy range as a result of the limited range of threshold energies available, and as with any integral detector, the resolution is generally poor. There is an added problem of getting adequate statistics for the unfolding process. Usually several detectors of the same type are provided to increase the number of bubbles counted, but even so, repeat measurements are likely to be necessary. Nevertheless, they have certain attractive features. They are small, are relatively easy to use and can have a high sensitivity. They also have the significant advantage of being insensitive to photons. A review article [9.34] is available outlining the advantages, problems and possibilities of spectrometry on the basis of this new technology.
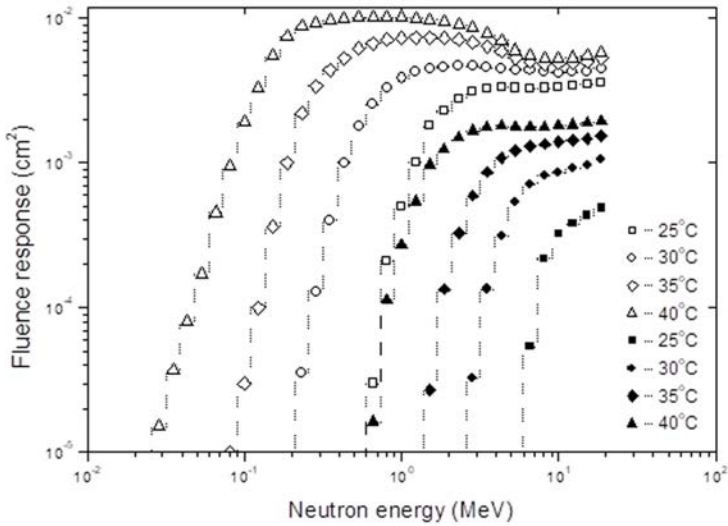
FIG. 9.3. Fluence response functions for a spectrometry system based on a set of superheated emulsion detectors with different thresholds. (Reproduced from Ref. [9.34] with permission from Oxford University Press.)

9.4. GASEOUS DETECTORS

9.4.1. Proton recoil counters

Proportional counters filled with hydrogen, in which the elastic scatter of fast neutrons produces recoil protons whose energy can easily be measured via the ionization they produce, have long been used for measurements in neutron laboratories. Because values for the (n,p) scattering cross-section are known accurately as a function of energy up to approximately 20 MeV, their response functions can be calculated absolutely. These devices have two basic applications. First, they can be used to provide an absolute measure of monoenergetic neutron fluences. These types of fields are important for instrument calibration and type testing (see Section 14). Second, the proton recoil counter can also be used as a spectrometer, providing high resolution over an energy region from approximately 50 keV to 1.5 MeV. The energy range can be extended to higher energies by replacing the hydrogen gas with methane or ^{4}He, but the advantage of this approach is questionable in view of the fact that scintillator detectors are a better option above about 1.5 MeV. The importance of good resolution in the 10 keV to 1 MeV region, where fluence to dose equivalent conversion coefficients for the operational quantities change rapidly with energy, was noted earlier, and

these devices cover a good fraction of this energy range. The use of these proton recoil counters as high resolution spectrometers is well described in Ref. [9.35].

Counters for field use are usually spherical (see Fig. 9.4), giving them a reasonably isotropic response, except for the effects of the electrical connections. The dynamic range of an individual counter is not large, and to cover the energy range from 50 keV to 1.5 MeV, three counters are usually employed with different gas pressures. A common combination is 100 kPa, 300 kPa and 1000 kPa. The lower energy limit of 50 keV is the result of overlap between neutron and gamma pulses at lower energies. To extend the measurements to lower energies would require n/γ discrimination. This is possible in principle, but difficult [9.36]. The differences in pulse shape between recoil protons produced by scattered neutrons and the electrons produced by gamma rays occur in the rise time of the pulse (cf. the case of scintillators where it occurs in the decay of the pulse). The difference occurs because electron tracks are in general longer than those of protons depositing the same energy, and charge collection for the electron tracks is therefore in general slower. The situation is complicated by tracks that run parallel to the anode where all ionization occurs at the same distance from the anode.

Typical energy resolution, $\Delta E/E$, for spherical proton recoil counters is 2–6%. For commonly used detector sizes, the efficiency is rather low. The minimum dose equivalent rate required to make a measurement is very much spectrum dependent but is of the order of 0.5 mSv·h^{-1}. Energy calibration can be achieved either by including a trace of ^{3}He gas in the counter to provide a peak at 764 keV caused by the capture of thermal neutrons, or by incorporating a small trace of an alpha particle emitting material on the anode wire. Corrections for these events then have to be made during analysis.

Although the fact that the instrument response is based on the well known (n,p) scattering reaction, calculation of the response functions should always be checked against measurements, ideally with monoenergetic
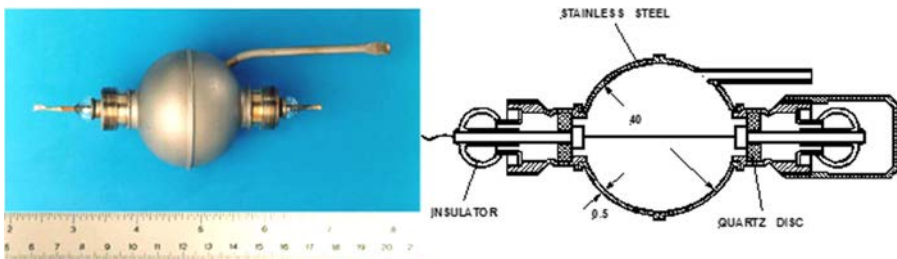
FIG. 9.4. A proton recoil proportional counter of the SP2 type. (Reproduced from Ref. [9.35] with permission from Oxford University Press.)

neutrons. This ensures that all the relevant effects are allowed for correctly in the calculations, for example, wall effects and the counter resolution. The measurement can also provide information on the exact gas pressure. The good agreement that can be achieved between measurement and calculations is illustrated in Fig. 9.5. This figure highlights the fact that, because the neutron can scatter at any angle from 0º to 180º, the pulse height spectrum, even for monoenergetic neutron bombardment, includes proton recoil energies from the full neutron energy down to zero. Unfolding of the neutron spectrum is thus essential.

To perform the spectrum unfolding, a matrix of response function data for the relevant energy range needs to be available. Unlike Bonner sphere unfolding, the problem is not mathematically underdetermined, so is in principle relatively straightforward. Complications arise because the spectra from measurements with the three counters have to be combined, and allowances for the effects of neutrons above the range for a particular counter have to be made. If there are neutrons in the spectrum that are above the range for the counter with the highest pressure, allowance must be made for these using data obtained in some other way, such as by using a scintillator.

Although a few field measurements with hydrogen recoil counters have been reported [9.37], the number is not large. Their use in the laboratory is much more extensive, and they have been used in comparison exercises [9.22, 9.38].
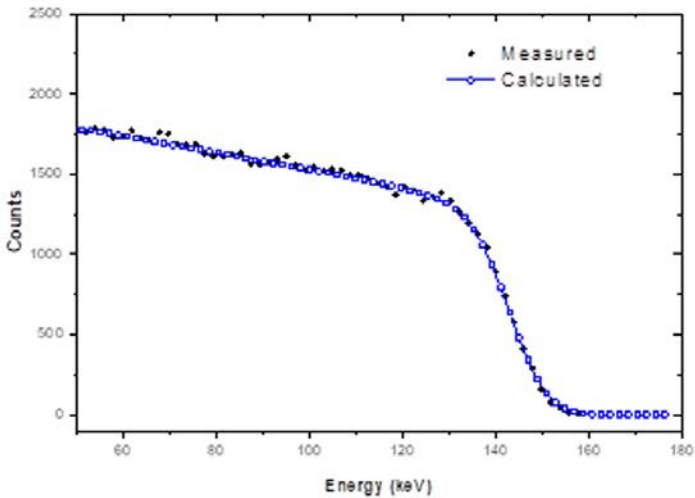
FIG. 9.5. *Measured response of a 100 kPa SP2 counter to 144 keV monoenergetic neutrons compared with calculations. (Courtesy of National Physical Laboratory.)*

This type of detector is often used as one of the component devices in a combined spectrometry instrument (see Section 9.6).

9.4.2. Helium-3 based spectrometers

The energy region from approximately 50 keV to 1.5 MeV can also be covered by instruments utilizing the ^{3}He(n,p)T reaction [9.39]. In these devices, the neutron energy is superimposed onto the 764 keV from the exothermic reaction, helping to ensure that neutron induced events are well separated from photon induced events. The instrument may be a proportional counter or a gridded ionization chamber [9.40]. The pulse height distribution for such a device bombarded with monoenergetic neutrons is shown in Fig. 9.6. The fact that the distribution has a peak at the neutron energy makes the spectrum unfolding simpler. Although instruments of this type have found applications for laboratory spectrometry, their use in field spectrometry involves one fundamental difficulty. The ^{3}He(n,p)T reaction cross-section increases rapidly as the neutron energy decreases (a $1/v$ dependence at low energies where v is the neutron velocity). A cadmium cover can be employed to exclude thermal neutrons; however, the number of intermediate neutrons in most workplace fields is such that a very
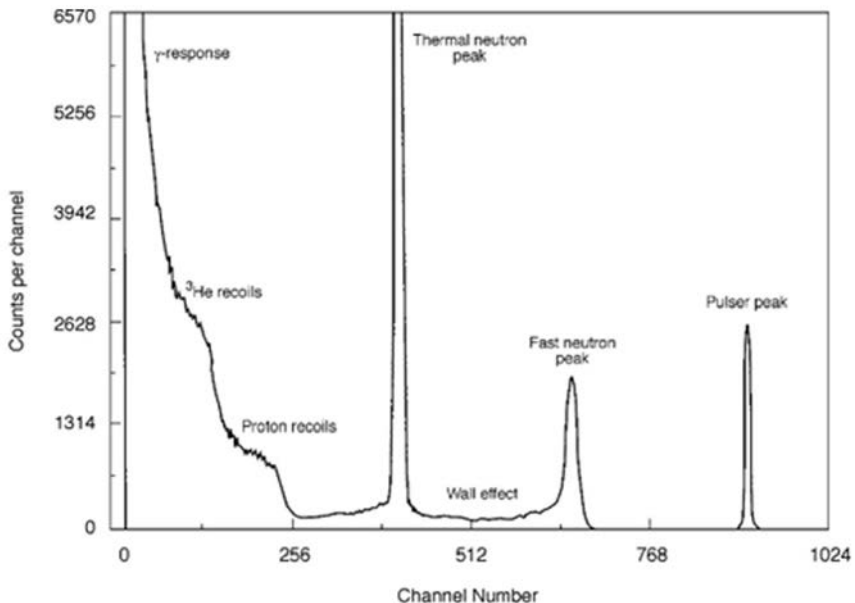
FIG. 9.6. The pulse height spectrum for a gridded ionization chamber exposed to a monoenergetic neutron field. (Courtesy of National Physical Laboratory.)

large number of ^{3}He(n,p)T reactions occur with low energy neutrons. The effect of this is that 764 keV pulses are produced in such numbers that they pile up, obliterating the data of interest in the region above 764 keV.

9.5. SCINTILLATOR SPECTROMETERS

In the neutron energy region above about 1 MeV, reliable, high resolution, spectrometric data can be determined using scintillation spectrometers [9.41–9.44]. In these devices, the main mechanism for neutron detection is (n,p) scattering, as is the case for the proton recoil counters described in Section 9.4.1. However, scintillators contain other elements, most notably carbon, and the effects of neutron scattering and reactions in these elements must be taken into account when calculating response functions. Most of the cross-sections are well known up to about 20 MeV, so the response functions can be reliably calculated. Because of the higher atom density in a scintillator compared with that in the gas of a gaseous detector, the efficiency is generally much higher.

The mechanism for detecting the energy deposition events is different to that for gaseous detectors. Energetic charged particles produced by the neutrons excite the atoms of the scintillator, which decay by emitting prompt fluorescence. This light is directed, usually via a light guide, to the photocathode of a photomultiplier tube (see Fig. 9.7). The size of the scintillator can be chosen to suit the efficiency and energy range requirements. Since all neutron fields have some level of accompanying photon radiation, n/γ discrimination is important.

Various types of scintillator materials have been used for neutron spectrometry, including plastic, anthracene, stilbene and liquid scintillators.
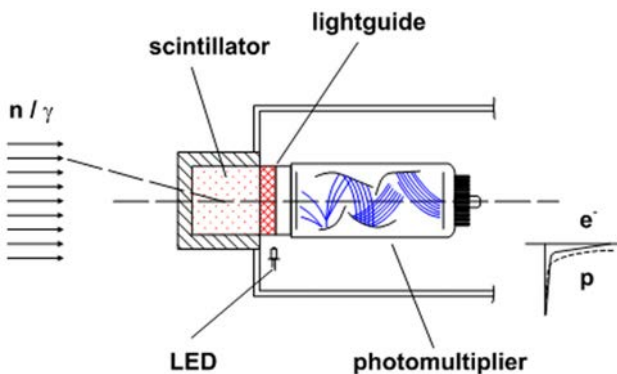
FIG. 9.7. Scintillator detector assembly consisting of an NE213 liquid scintillator, Plexiglas light guide, LED for gain stabilization and photomultiplier.

Plastics have advantages in being inexpensive and available in various shapes and sizes, but do not normally exhibit pulse shape discrimination capability, although some research has developed materials where n/γ discrimination is possible [9.45]. Anthracene and stilbene are expensive, and their crystals exhibit directional variation of the light output. Liquid scintillators are the most commonly used scintillator spectrometers in situations where n/γ discrimination is needed. It cannot usually be achieved by setting the energy threshold, since electrons released by photon interactions in the scintillator have a higher light output than corresponding energy protons. Discrimination is achieved by pulse shape analysis, using the fact that the fluorescence signals produced by electrons and heavy ions have different fall times because they tend to excite levels with different de-excitation lifetimes. One of the most commonly used liquid scintillators is one that long went under the name NE213 but has been rebranded as BC501A.

The pulse height distribution seen in a scintillator (see Fig. 9.8) has many of the characteristics of a proton recoil counter, that is, the distribution for a monoenergetic neutron has the shape of a ledge. Much of what was said in Section 9.4.1 about analysis also applies to scintillators. Obviously, it is important for the response matrix to be known accurately, and this can be derived from a combination of calculations and measurements [9.44]. One item of information that must be determined is the light output function for the detector. This is required because the light emission does not increase linearly with either electron or proton energy, or for alpha particles released in (n,α) reactions.

FIG. 9.8. *Response functions calculated for an NE213 scintillation detector and neutrons in the energy range 0.5 MeV to 20 MeV (normalized to unit neutron fluence). (Reproduced from Ref. [9.44] with permission from Oxford University Press.)*

Liquid scintillators are often important components in combined spectrometry systems, which try to take advantage of the properties of a range of spectrometric devices.

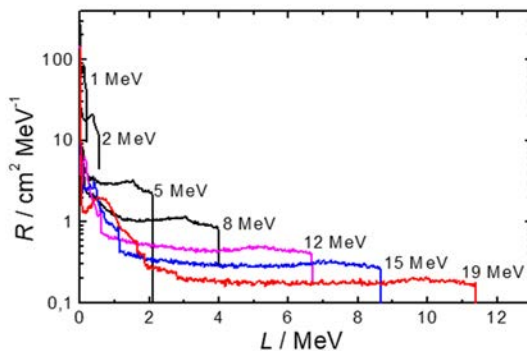Over recent years, the inorganic scintillator Cs_2LiYCl_6:Ce (CLYC) has been investigated as a neutron detector. The presence of lithium gives it a thermal sensitivity, and the chlorine (with six times as many atoms as lithium) gives it a sensitivity to fast neutrons via the $^{35}Cl(n,p)^{35}S$ reaction and also the $^{35}Cl(n,\alpha)^{32}P$ [9.46]. The material exhibits pulse shape n,γ discrimination capabilities, and for neutron energies below those that populate excited states in ^{35}S, the energy deposited in the material by the $^{35}Cl(n,p)^{35}S$ reaction is directly related to the neutron energy. This is unlike normal scintillators, in which the energy deposited is predominantly by scattering events and depends on the scattering angle.

9.6. COMBINED INSTRUMENTS

An ideal spectrum measurement would involve the use of scintillators and proton recoil counters, or a ^{3}He spectrometer, to derive the spectrum with high resolution above about 50 keV, and the use of a Bonner sphere system to determine the spectrum outside this region and to some extent also validate the high resolution data. Any other available instruments could also be used. The data from the individual spectrometers would need to be unfolded and a spectrum incorporating all the information produced [9.47]. A combined unfolding program that could analyse all the raw data simultaneously and provide a spectrum with uncertainties reflecting all the input data would be an ideal, but not presently available, option. However, the performance of a number of sets of measurements is time consuming, expensive, requires specialist knowledge, and in some instances, such as where time at the measurement site is limited, can be quite impractical. For these reasons, attempts have been made to put together commercial spectrometers to simplify and speed up the process. Two such combined spectrometry instruments have been produced: the rotating spectrometer (ROSPEC) [9.48] and the transportable neutron spectrometer (TNS) [9.49].

9.6.1. The ROSPEC

Although there can be slight variants on the actual sensors in the ROSPEC, it is based primarily on spherical hydrogen filled proportional counters to cover the 50 keV to 1.5 MeV region and a large volume counter filled with argon-methane to cover the higher energy region. The energy region below 50 keV may be

FIG. 9.9. The ROSPEC neutron spectrometer. (Picture supplied by Bubble Technology Industries.)

covered by two ^{3}He proportional counters, one covered with a layer of borated material to exclude thermal neutrons and hence provide information on the intermediate energy region. These counters are arranged on a rotating carousel to avoid the counters shielding each other in beam type fields (see Fig. 9.9). An associated laptop computer provides for rapid analysis of the spectrum and determination of dose equivalent quantities.

9.6.2. The TNS

The TNS (Transportable Neutron Spectrometer), developed in the 1980s at AEA Technology Winfrith [9.50] for the UK Ministry of Defence, has similarities to the ROSPEC but also some differences. It uses spherical proton recoil counters, with diameters of 40 mm, and hydrogen fill pressures of 100, 300 and 1000 kPa, to cover the energy range from 50 keV to 1.4 MeV. A small NE213 scintillator, with a volume of approximately 3.7 cm^3 and with pulse shape discrimination to reject gamma ray induced events, is used to obtain the spectrum in the energy region above 1.4 MeV. For the energy region below 50 keV, information is derived from two cylindrical BF$_3$ proportional counters,

one covered by a cadmium sleeve to give information on the intermediate energy neutrons, and one bare to derive the thermal neutron fluence.

Only a very small number of TNSs have been produced, but these have been used extensively to derive location specific correction factors for survey instruments and, more particularly, for personal dosimeters. The response functions, the electronics and the unfolding code used with the TNS date from the 1980s, and the system is becoming outdated. Attempts are being made to update the device by improving the electronics, possibly using digital signal processing [9.51], obtaining better response function data and investigating modern unfolding codes.

9.7. SPECTRUM UNFOLDING

Many authors have described the problems of spectrum unfolding and the approaches used to solve the mathematical equations linking the measured quantity to the spectrum. Excellent summaries can be found in papers by Matzke [9.5, 9.6].

The basic equation to be solved in neutron spectrometry is that given earlier for integral spectrometry systems, i.e.

$$M_i = \int_0^{E_{max}} r_i(E) \cdot \Phi_E(E) \mathrm{d}E \quad i = 1, \ldots, m \tag{9.7}$$

where

$r_i(E)$ is the response function;
$\Phi_E(E)$ is the neutron spectral fluence as a function of energy E.

For an integral spectrometry system, M_i is the response of an individual integrating detector, a Bonner sphere, for example, or an activation foil, and $r_i(E)$ is the response function of the ith detector. This is often called the few channel problem.

For devices such as proton recoil counters or scintillators that provide a pulse height spectrum, M_i is the reading in channel i and $r_i(E)$ is the response function that relates the counts in channel i to the spectrum $\Phi_E(E)$. This is often termed the multichannel problem.

Mathematically, Eq. (9.7) is a Fredholm type integral equation of the first kind, which has no unique solution, since a finite number of discrete measurements cannot define a continuous function $\Phi_E(E)$. To solve the unfolding problem the spectrum is conventionally represented as a vector Φ with n elements ϕ_i; in other

words, the spectrum is represented as a histogram with n bins. The equation to be solved then becomes the matrix equation:

$$M = R \times \Phi \qquad (9.8)$$

where

M is the vector of measured data M_i $i = 1, \ldots., m$;

R is the $n \times m$ rectangular fluence response matrix with elements r_{ij} linking Φ to M.

Equation (9.8) is an idealized representation of the problem. In reality, uncertainties need to be taken into consideration. The elements ϕ_i of the vector Φ have uncertainties and, ideally, the unfolding process will determine these. The matrix elements r_{ij} will also have uncertainties, although these are usually poorly known, and many unfolding codes ignore these. The measured quantities, M_i, will have uncertainties and these are usually available from the experiment. The measured values M_0 are related to the true values M by

$$M_0 = M + \varepsilon \qquad (9.9)$$

where

ε is the uncertainty vector reflecting fluctuations caused by statistical and systematic uncertainties.

Knowing the uncertainty matrix, S_{M0}, (covariance matrix with covariance terms included if known) an equation defining a χ^2 can be set up.

$$\chi^2 = (M_0 - R \cdot \Phi)^{\mathrm{T}} \cdot S_{M0}^{-1} \cdot (M_0 - R \cdot \Phi) \qquad (9.10)$$

In principle, this expression can be minimized, provided S_{M0} is non-singular, the solution for Φ being obtained from the so-called normal equation:

$$R^{\mathrm{T}} S_{M0}^{-1} M_0 = R^{\mathrm{T}} S_{M0}^{-1} R \Phi = \mathbf{B} \Phi \qquad (9.11)$$

which has a unique solution for Φ if the rank of the matrix B is maximum, that is, if it equals the number of fluence groups n.

Thus, if $n \leq m$ a solution for Φ can be derived, although there may still be some ambiguity in the solution [9.5]. If $n > m$, there is not a unique mathematical solution, and some additional information must be used. Even using additional information, the solution is in some cases derived by a trial and error approach of varying the elements of Φ in order to minimize χ^2.

One item of additional information that is used is a priori data about the spectrum, obtained, for example, from a calculation, measurements with other devices, some knowledge of the source of neutrons and degree of moderation, or at worst, a simple guess.

Codes that use a priori spectrum estimates include the group STAY'SL [9.52], LEPRICON [9.53], LSL [9.54], and the DIFBAS and DIFMAZ codes from the HEPRO [9.55] package. These were developed for reactor dosimetry unfolding where covariance data for the cross-sections are increasingly becoming available but have also been successfully used for Bonner sphere unfolding.

If a priori information is used as anything more than a starting point for the unfolding, it should be included with uncertainty estimates. If uncertainties in the response matrix elements are available, they can also be included in the analysis. The complete form of Eq. (9.10) is then

$$
\begin{aligned}
\chi^2 = {}&(\boldsymbol{M}_0 - \boldsymbol{M})^{\mathrm{T}} \cdot \mathbf{S}_{\mathrm{M0}}^{-1} \cdot (\boldsymbol{M}_0 - \boldsymbol{M}) \\
&+ (\mathbf{R}_0 - \mathbf{R})^{\mathrm{T}} \cdot \mathbf{S}_{\mathrm{R0}}^{-1} \cdot (\mathbf{R}_0 - \mathbf{R}) \\
&+ (\Phi_0 - \Phi)^{\mathrm{T}} \cdot \mathbf{S}_{\Phi0}^{-1} \cdot (\Phi_0 - \Phi)
\end{aligned}
\tag{9.12}
$$

where

$\boldsymbol{R}_0$ is the available estimate of the true response matrix $\boldsymbol{R}$,
Φ_0 is the a priori estimate of the true spectrum Φ,
$\boldsymbol{S}_{\mathbf{R0}}$ is the variance-covariance matrix for the response matrix $\mathbf{R}_0$,
$\boldsymbol{S}_{\Phi0}$ is the variance-covariance matrix for the a priori spectrum Φ_0.

STAY'SL, LEPRICON and LSL all include the second term on the right hand side in Eq. (9.12), meaning that extensive response function uncertainty data are needed.

Another group of unfolding codes can be defined as those that use the fact that the spectral fluence cannot be negative. Codes in this group include SAND-II [9.56], GRAVEL [9.55], LSL-M2 [9.54], LOUHI [9.57], BUNKI [9.58] and RADAK [9.59]. They perform a least squares adjustment with the constraint on non-negative fluence. Schmittroth [9.60] achieved this constraint with his FERRET code by using a log-normal distribution of the variables.

One of the solutions to the unfolding problem is one based on the maximum entropy principle. The MAXED code [9.61, 9.62] permits the use of a priori information, requires the solution spectrum elements to be non-negative and provides uncertainty information for the solution. It can be used for few- and multichannel problems and is now part of the HEPRO package.

Neural networks should provide another valid approach to neutron spectrum unfolding, and work in this area [9.63] has demonstrated the potential of this approach.

The complexity of spectrum unfolding means that there are many potential pitfalls for the inexperienced user of the various codes available for this task. Unfolding results from proton recoil counters and scintillators, where the problem is not underdetermined, should be independent of the code used; nevertheless, codes should not be used as 'black boxes'. Their results should be examined to see if they are reasonable in view of what is known about the source of neutrons and the moderating and shielding material present. This is even more important for the underdetermined problem where, if possible, more than one code should be used and their results compared.

9.8. COMPILATIONS OF NEUTRON SPECTRA

As already noted, one of the important uses of neutron spectral data is in predicting survey instrument and personal dosimeter responses in particular environments. In many cases, spectral data are not available for specific sites where dose equivalent measurements need to be made. Some useful guidelines can, however, be derived by considering spectral data for similar environments. Several compilations of such data have been made available specifically for this purpose. One early example is the IAEA Technical Report entitled Compendium of Neutron Spectra in Criticality Accident Dosimetry [9.64]; however, this contains a range of spectra that can be of more general use. For example, in addition to measured spectra from critical assemblies, it contains a series of leakage spectra that were calculated using a source of fission neutrons or moderated fission neutrons and their transmission through different assemblies of shielding materials. In addition, some spectrum averaged quantities of dosimetric interest and some average cross-sections are given for a number of common detectors in use for criticality.

The more recent IAEA Technical Report entitled Compendium of Neutron Spectra and Detector Responses for Radiation Protection Purposes [9.23] provides both spectral data and detector response information for a wide range of different spectra, and this publication has been updated with supplemental data [9.24]. This latter publication includes a large body of data that were gathered

for use with a computer program SPKTBIB [9.65], which allows users access to a library of neutron spectra with the option of calculating various properties such as dose equivalents, detector responses, etc.

The Compendium of Neutron Spectra and Detector Responses for Radiation Protection Purposes [9.23] contains a large number of measured and calculated spectra that are relevant for radiation protection purposes. They include spectra of calibration fields, as well as operational spectra obtained at power reactors, medical accelerators, fusion reactors and experimental accelerators. In its supplement [9.24] a series of new spectra have been added, among them spectra found at high energy accelerators and in cosmic radiation fields (these are important for exposure of aircrew) and new data on simulated workplace fields.

In addition, both compendia [9.23, 9.24] give, for each spectrum, a number of spectrum weighted dose quantities and spectrum averaged fluence responses of instruments.

Spectrum averaged fluence to dose conversion coefficients are given in Ref. [9.24] for the quantities E_{AP}, $H^*(10)$, $H_p(10)$ and also the older quantities, effective dose equivalent, H_E, and maximum dose equivalent, H_{MADE}. This allows the user to estimate the following:

(a) If the operational quantity that is used is a conservative estimate of the protection quantity for this field;
(b) If new spectrum averaged operational quantities deviate from older ones in this special field, and if instruments that were designed to measure the old quantity can still be used without significant changes.

Averaged fluence responses are given in Ref. [9.23] for a series of commonly used dosimeters (i.e. etched track dosimeters, TL albedo dosimeters, nuclear emulsion dosimeters and moderator based survey instruments) and in Ref. [9.24] for Bonner spheres with moderator radii up to 18 inches (45.72 cm) as well as data on new devices (i.e. superheated emulsion dosimeters and electronic dosimeters with silicon diodes). These data can be used to:

(a) See if the instrument selected by the user for radiation protection purposes gives responses that do not vary excessively over a range of possible spectra that need to be considered;
(b) Compare unfolding results of new spectrometers with those of existing ones;
(c) Use combinations of detectors in order to create new dosimeters with a better overall response in various fields.

As all data are available electronically, the full set of spectra can be used to fold responses of newly developed dosimeters to evaluate their spectrum

averaged fluence response and in turn, with appropriate conversion coefficients, their dose equivalent response.

Some caution is needed, however, if the responses of personal dosimeters are considered. The spectrum averaged values for the dose equivalent quantities, and also for detector responses, are only computed for neutrons incident normally to the person, phantom or dosimeter. For more complex directional incidence, the dose quantities and detector responses become dependent on the directional distribution of the radiation field considered (see Section 13.8).

In addition, with the introduction of the new ICRP recommendation [9.66], a change of the radiation protection quantity E_{AP} — using new w_R values and tissue weighting factors — needs to be considered.

9.9. LINEAR ENERGY TRANSFER SPECTROMETRY

The protection quantity effective dose and the operational quantities ambient and personal dose equivalent are all products of dose and a weighting function, which provides a measure of the quality of the radiation that has deposited that dose. The quality of the radiation is derived from the linear energy transfer (LET), so the characterization of a radiation field in terms of the LET of the energy deposition events provides an alternative to determining the energy spectrum as a means of characterizing the field for dosimetric purposes. If an instrument could be designed that measured accurately the dose deposition as a function of LET, this could provide a direct measure of the operational quantities, provided it had the required angle dependence for its response. The quantity LET is very closely related to the stopping power, so the requirement is for a device that measures both energy deposition and the rate at which energy is deposited per unit track length for the particles depositing the energy.

Unfortunately, LET cannot be measured directly, but there is another quantity that can be measured, and that is the lineal energy, y. An instrument has been devised that is designed to measure both absorbed dose deposition and its dependence on lineal energy. This is the so-called tissue equivalent proportional counter, or TEPC [9.67].

As the name suggests, a TEPC is a proportional counter made of tissue equivalent materials, so the energy deposition events that occur when the device is irradiated are very similar to those that would occur in human tissue. The instrument uses a low pressure gas with an atomic composition similar to that of muscle tissue as the fill gas in a proportional counter made of a conducting tissue equivalent plastic. A commonly used material for making the counter is A-150 plastic. The elements comprising A-150, as percentages by weight, are 10.1% H, 77.6% C, 3.5% N, 5.2% O and 1.7% F; by comparison, the elements

comprising ICRU tissue are 10.2% H, 12.3% C, 3.5% N and 72.9% O, with small amounts ($\leq$ 0.5%) of Na, Mg, P, S, K and Ca. Compared with ICRU tissue, the A-150 plastic has more carbon and less oxygen; a necessary difference in order to make a conducting solid material. Tissue equivalent gas fillings are usually based on either methane (with a composition of 10.2% H, 45.6% C, 3.5% N and 40.7% O) or propane (with a composition of 10.3% H, 56.9% C, 3.5% N and 29.3% O) [9.68]. It can be seen that, for the gas, the percentage of carbon is much reduced compared with the plastic, whereas the oxygen percentage is much higher and the match with tissue is better. Since the majority of energy deposition events for neutrons are due to collisions with hydrogen nuclei, the poor match for carbon and oxygen between A-150 plastic and tissue is not a serious drawback. Microdosimetric counters are also sometimes made with other wall materials to derive information about specific energy deposition events (e.g. carbon chambers) to investigate carbon kerma. Most counters are spherical, thus providing a near isotropic response, except for minor anisotropies introduced by the housing, the connections to the anode wire, etc.

The similarity of gas and wall composition means that a TEPC satisfies the Bragg–Gray criterion of cavity ionization theory and allows the absorbed dose to be measured precisely. The gas density is scaled by the ratio of the diameter of a typical biological cell (approximately 1–2 μm at normal tissue density) to the diameter of the counter. The gas density to achieve this simulation is of the order of 10^{-4} g·cm^{-3} [9.67]. Energy deposition events in the counter gas are then assumed to be similar to the same events in small volumes of biological tissue, hence the name *microdosimetry* [9.68] for this approach to determining radiation effects. It is an approach that has its origin in the work of Rossi [9.69], and particular designs of TEPCs are still known as Rossi counters. One of the underlying reasons for this approach is that volumes of a few μm are considered important sites in terms of relating energy deposition in tissue to adverse effects such as cancer induction.

A TEPC measures the absorbed dose as a function of the quantity lineal energy, y, which is (see Section 2) the quotient of ε by l, where ε is the energy imparted to the matter in a volume of interest, the gas of the TEPC in this case, by an energy deposition event, and l is the mean chord length in that volume (i.e. $y = \varepsilon/l$). When the volume is a sphere, the mean chord length is 2/3 the diameter. The SI unit of y is J·m^{-1}, but it is more usually expressed in terms of keV·μm^{-1}.

A cross-sectional diagram of a TEPC is shown in Fig. 9.10. This particular example is a spherical counter with an inner diameter of approximately 25.4 mm, but cylindrical counters have also been constructed. The central helical electrode surrounds a single anode wire, and the two are held at different electrical potentials. The electric field between the helix and the central wire forms the
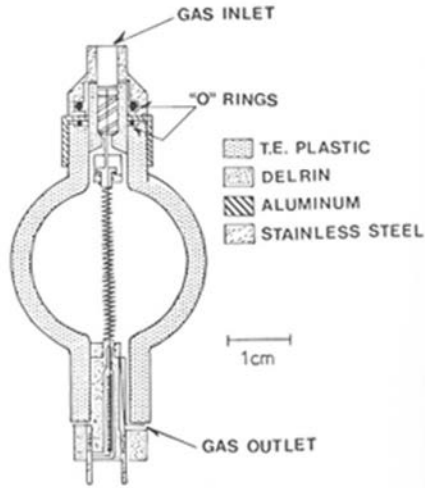
FIG. 9.10. Cross-section of TEPC showing the central helical electrode surrounding a single wire anode. The materials of construction include insulators such as Delrin and supports of aluminium and stainless steel. (Reproduced from Ref. [9.68] with permission from ICRU.)

proportional counting region. The instrument shown in Fig. 9.10 is a laboratory instrument. Those produced commercially often tend to be simpler in design, without the wire helix. From straightforward geometrical considerations it can be seen that the number of events seen in the proportional counter will increase with counter size; in fact, the efficiency increases as the square of the diameter.

The tissue equivalent gas may either be flowed through the TEPC at low pressure, as is the case with the counter pictured in Fig. 9.10, or the counter may be sealed for long term operation. Flow-through counters are laboratory devices. Counters capable of being sealed are usually used in commercially available TEPC based survey instruments.

When neutrons are incident on the TEPC, many of the reactions that are described in Section 4 occur. Elastic scattering gives rise to secondary protons, and inelastic scattering may produce alpha particles (helium nuclei) or heavier ions. Gamma rays that are incident on the TEPC, or produced by neutron interactions, may result in the production of secondary electrons that will also be detected by the TEPC.

The neutron interactions occur both in the wall of the TEPC and in the tissue equivalent gas filling. Secondary particles from interactions in the gas obviously deposit energy in the gas, the amount depending on the interaction and whether or not the secondary particle or particles strike the wall before losing all their energy. Interactions in the wall can produce secondary charged particles with

enough energy to enter the gas volume and deposit energy there. In fact, because of the relative densities of the wall and the gas, the majority of events that deposit energy in the gas originate in the wall. Depending on their energy, these particles either pass through the counter or come to a stop within the counter cavity. The particle tracks pass through the counter at various angles; therefore, a distribution of energy deposits is produced even for secondary particles of the same energy.

Figure 9.11 shows calculations of the differential fluence, or slowing down, spectra of charged particles generated by two energies of neutrons: 1 and 14 MeV. As the energy increases, nuclear reactions begin to occur, and charged particles such as alphas and deuterons become more important. In each case, the plotted spectra are normalized for a fluence of 1 cm^{-2} [9.67].

The energy deposits from charged particles are detected by the proportional counting region in the TEPC. The secondary electrons collected by the anode will result in a pulse that can be amplified, shaped and acquired by a multichannel analyser. The distribution of TEPC events can be plotted in a way that is useful for determining the nature of the incident neutron field. This is almost invariably accompanied by some percentage of gamma rays.

The range of event sizes is large; therefore, the range of lineal energy may cover six decades. An important feature of a TEPC is that the charged particles can deposit only a specific maximum energy in the counter because, as they slow
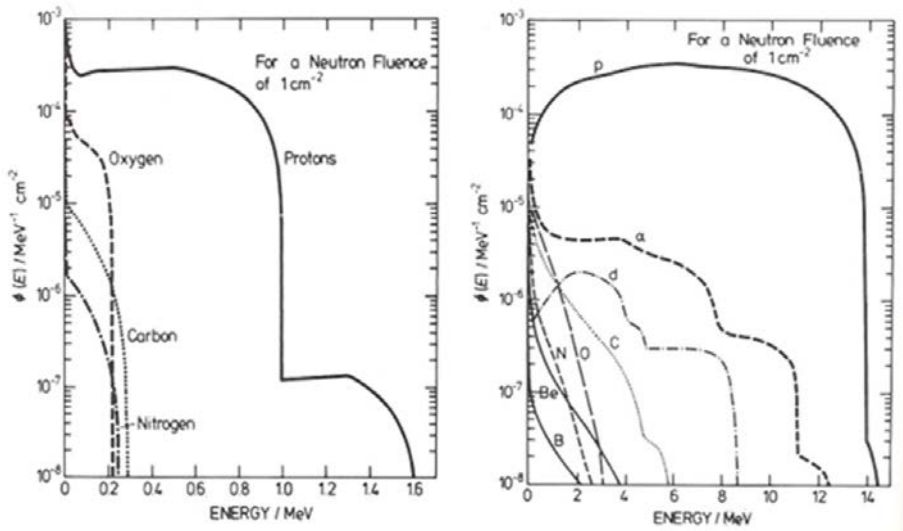
FIG. 9.11. Differential fluence (slowing down) spectra for neutrons with two different energies. The left panel shows a spectrum for 1 MeV neutrons and the right panel shows a spectrum for 14 MeV neutrons, in ICRU tissue. (Reproduced from Ref. [9.68] with permission from ICRU.)
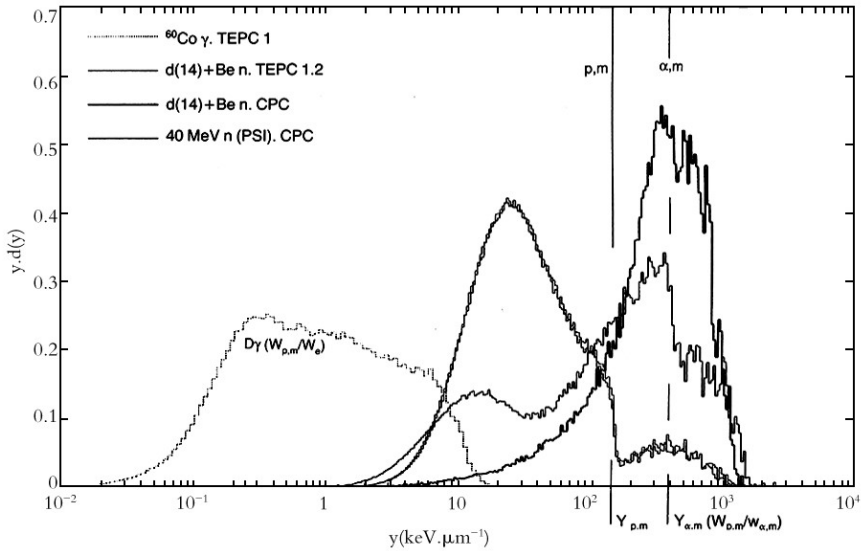
FIG. 9.12. Composite plot of TEPC event size distributions produced by ^{60}Co gamma rays, a broad neutron spectrum from 14 MeV deuterons on a Be target and two spectra taken with a graphite walled proportional counter showing events primarily caused by alpha particles. (Reproduced from Ref. [9.70] with permission from Oxford University Press.)

down, their stopping power goes through a maximum value. The largest energy deposit that can be left by a proton in a 1 μm^{-1} equivalent diameter sphere is approximately 100 keV. Since the cavity is usually a sphere, where the mean chord length is 2/3 the diameter, the maximum y value for a proton in a TEPC is approximately 150 keV·μm^{-1}. Above this value of y there are very few proton events. This can be seen in Fig. 9.12 at the point indicated as p,m. There is another point, α,m, that corresponds to the maximum energy deposit by an alpha particle. However, the drop off is not so clearly defined because of range straggling. Electrons produced by gamma ray interactions also exhibit a stopping power maximum, and thus the curve caused by ^{60}Co gamma rays shows a drop off at approximately 10 keV·μm^{-1}.

The plot in Fig. 9.12 shows the product of lineal energy, y, with the dose probability density $d(y)$, versus the lineal energy y, where $d(y) = dD(y)/dy$, the derivative of the fraction of absorbed dose delivered with lineal energy less than or equal to y. The area under the curve is proportional to the absorbed dose [9.68].

In practice, the spectrum is obtained from the measured multichannel analyser pulse height spectrum of the number of events with lineal energy between y_i and y_{i+1} by plotting the data on a logarithmic lineal energy scale with

bins of equal width on this scale. The counts in each bin need to be multiplied by the mean lineal energy of that bin, once to get the dose in that bin, and then again to obtain $y \cdot d(y)$.

This approach allows the features of the lineal energy spectrum to be seen; in other words, events resulting from recoil electrons, protons, alpha particles and heavy ions can be identified. This, in turn, enables absorbed doses, quality factors and dose equivalents to be determined for lightly ionizing and densely ionizing particles, as well as the total field. It also prevents the very large number of low y value events from dominating the plot. To derive a plot of the distribution of dose equivalent in lineal energy, the $d(y)$ values need to be multiplied by $Q(L)$. Assuming that y is an acceptable approximation to L, the required $Q(L)$ values can be calculated, and plots can be obtained of $y \cdot h(y)$ against y.

It is useful to divide the types of energy deposition events that occur in the gas of a TEPC into four types: (a) *insiders*, where the charged particle is created within the gas and stops in the gas; (b) *starters*, where the charged particle originates in the gas but leaves the gas volume before depositing all its energy; (c) *stoppers*, which are particles that originate in the wall and stop in the gas; and (d) *crossers*, which originate in the wall and cross the gas volume. In order to measure lineal energy, a TEPC should 'sample' a charged particle's track to determine the rate of energy deposition. As the neutron energy decreases, a greater number of insiders and stoppers occur, and the instruments cease to give an accurate measure of absorbed dose or dose equivalent, underestimating both these quantities.

Figure 9.13 shows a comparison of the $H^*(10)$ response function of a 127 mm TEPC with that for a Berthold LB6411 neutron dose rate monitor, which is a typical moderator based survey instrument. The under-response of the TEPC at intermediate energies is evident. The improvement of the response at thermal energies is the result of capture reactions (e.g. $^{14}N(n,p)^{14}C$), which produce higher energy charged particles. Because they tend to work well at high neutron energies, where there are fewer insiders and stoppers, TEPCs have increasingly found use in determining dose equivalent resulting from cosmic radiation to which aircrew and astronauts may be exposed [9.71].

9.10. DIRECTION DEPENDENCE OF THE NEUTRON FIELD

Because personal dose equivalent and effective dose both depend on the direction of the radiation field, any attempt to derive these quantities from a fluence measurement requires information about the direction of the fluence as well as the energy spectrum. This involves not just knowledge of how the fluence varies with direction, but also of how the spectrum varies with direction.
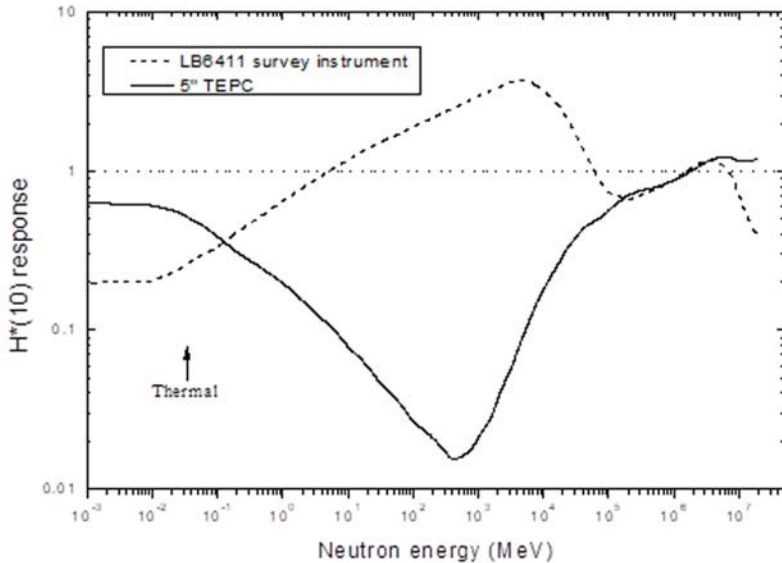
FIG. 9.13. Comparison of the response of a 5 inch (127 mm) TEPC [9.72] with that of a conventional moderator based survey instrument.

Whereas a measurement of the direction-integrated fluence spectrum in a mixed radiation field at a workplace is difficult, the task of deriving both direction and energy differential information for neutrons is an almost prohibitively complex task. Nevertheless, techniques for making these measurements have been explored [9.73].

The fact that superheated emulsion spectrometry systems (see Section 9.3.3) are small has been utilized in a device where these detectors are placed on the surface of a 30 cm diameter spherical moderator [9.74]. The presence of the sphere means that the response of each superheated emulsion detector depends on the direction of the radiation as well as the energy distribution. Information can be accumulated by using one point on the surface of the sphere and rotating the sphere, or by having the superheated emulsion spectrometry systems at various points on the surface. The task of unfolding this information is mathematically very challenging, but the equations can be solved. However, there remain problems with the quality of the superheated emulsion devices as spectrometers, with the need for reliable response function data (energy and angle dependent) and with statistics.

Another approach that has been reported in the literature uses the same basic idea of small detectors with spectrometric capabilities positioned on the surface of a moderating sphere [9.75]. In this device, six detector capsules are
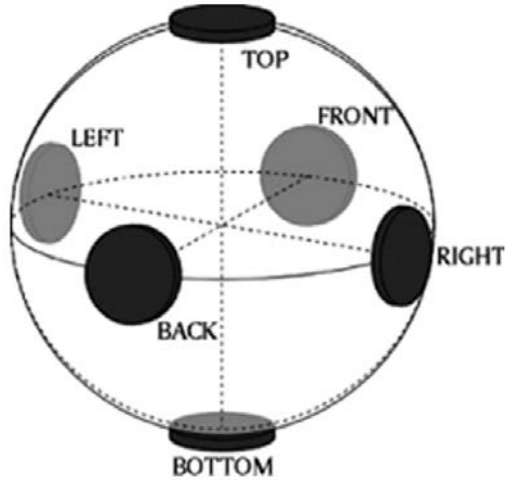
FIG. 9.14. Schematic diagram of the layout of detectors for a directional spectrometer. (Reproduced from Ref. [9.75] with permission from Elsevier.)

mounted at equidistant points on the surface of a 30 cm diameter polyethylene sphere (see Fig. 9.14). (In practice, not all capsules may be available, in which case measurements need to be performed with the sphere rotated to different orientations.) The detector capsules consist of four silicon detectors, each having a different combination of converter and shielding layers made from polyethylene, ^{6}LiF and borated plastic. Neutrons are detected via (n,p) scattering in hydrogenous converters and via capture of thermal neutrons in the ^{6}Li. These thermal neutrons may be incident on the sphere or produced by moderation within the sphere. Thermal neutron absorbing boronated plastic is used to separate incident and albedo thermal neutrons. Each detector thus has a different sensitivity to neutrons, and energy information is gathered in 16 channels. Measurements have been performed with this device, and the results are encouraging [9.75], although further work is still needed to characterize the response and further investigate the device's performance.

Information on the directional dependence of the field can also be derived by placing personal dosimeters at various positions around a phantom object, which can be a sphere, a cylinder, a slab or a cube, and which can be made from a selection of hydrogenous materials such as polyethylene, wax or water. This approach certainly provides information about the directional characteristics of the field, but it is difficult to derive truly quantitative results. A field where the spectrum varies little with direction helps in deriving the directional data, but the

analysis can only usually be performed in terms of a unidirectional component, an isotropic component or a component with rotational symmetry.

REFERENCES TO CHAPTER 9

[9.1] KLEIN, H., THOMAS, D.J., MENZEL, H.G., CURZIO, G., D'ERRICO, F. (Eds), Proc. Int. Workshop on Neutron Field Spectrometry in Science, Technology and Radiation Protection, Pisa, Italy, 4–8 Jun. 2000, Nucl. Instrum. Methods Phys. Res. A **476** (2001).

[9.2] THOMAS, D.J., KLEIN, H. (Eds), Neutron and photon spectrometry techniques for radiation protection, Radiat. Prot. Dosim. **107** (2003) 1–3.

[9.3] BARTLETT, D.T., CHARTIER, J.-L., MATZKE, M., RIMPLER, A., THOMAS, D.J., Concepts and quantities in spectrometry and radiation protection, Radiat. Prot. Dosim. **107** (2003) 23–35.

[9.4] ROHRIG, N., Plotting neutron fluence spectra, Health Phys. **45** (1983) 817–818.

[9.5] MATZKE, M., Unfolding procedures, Radiat. Prot. Dosim. **107** (2003) 155–174.

[9.6] MATZKE, M., Propagation of uncertainties in unfolding procedures, Nucl. Instrum. Methods Phys. Res. A **476** (2002) 230–241.

[9.7] ALEVRA, A.V., et al., Unfolding Bonner-Sphere Data: A European Intercomparison of Computer Codes, Laboratory Report PTB-7.22-90-1, Physikalisch-Technische Bundesanstalt, Braunschweig, Germany (1990).

[9.8] BRAMBLETT, R.L., EWING, R.I., BONNER, T.W., A new type of neutron spectrometer, Nucl. Instrum. Methods **9** (1960) 1.

[9.9] THOMAS, D.J., ALEVRA, A.V., Bonner sphere spectrometry — a critical review, Nucl. Instrum. Methods Phys. Res. A **476** (2001) 12–20.

[9.10] ALEVRA, A.V., THOMAS, D.J., Neutron spectrometry in mixed fields: multisphere spectrometers, Radiat. Prot. Dosim. **107** (2003) 37–72.

[9.11] ENDRES, G.W.R., et al., Neutron Dosimetry at Commercial Nuclear Plants Final Report of Subtask A: Reactor Containment Measurements, Report PNL-3585 NUREG/CR-1769, Pacific Northwest Laboratory, Richland, WA (1981).

[9.12] SANNA, R.S., HAJNAL, F., McLAUGHLIN, J.E., RYAN, R.M., Spectrometric Measurements within the Containment of 8 PWRs — a Data Compilation, Report EML-376, DOE Environmental Measurements Laboratory, New York (1980).

[9.13] CAIZERGUES, R., POULOT, G., Calcul de la Réponse des Sphères de Bonner pour les Détecteurs à Li, He et Mn, Rapport CEA-R-4400, CEN-Saclay, Gif-sur-Yvette, France (1972).

[9.14] BRICKA, M., DOLIAS, M., LAMBÉRIEUX, J., CAIZERGUES, J., "La reponse des detecteurs sous moderateur spherique aux neutrons monocinetiques", Proc. Symp. Neutron Monitoring for Radiation Protection Purposes, Vienna, 11–15 Dec. 1972, IAEA, Vienna (1973) 279–295.

[9.15] MOURGUES, M., "La mesure des neutrons par compteur a helium-3 sous moderateur spherique", Proc. Second Symp. on Neutron Dosimetry in Biology and Medicine, Neuherberg/München, 30 Sep.–4 Oct. 1974, EUR-5273, Vol. 2, European Commission, Luxembourg (1975) 907–931.

[9.16] ZABOROWSKI, H.L., "Dosimétrie et spectrometrie neutroniques avec les spheres de Bonner; etablissement d'une matrice log-normale de reference", Note CEA-N-2241 (Nov. 1981) and Proc. Fourth Symp. on Neutron Dosimetry, Neuherberg/München, 1–5 Jun. 1981, EUR-7448 En, Vol. 1, European Commission, Luxembourg (1981) 575–587.

[9.17] THOMAS, P.M., HARRISON, K.G., SCOTT, M.C., A multisphere neutron spectrometer using a central ^{3}He detector, Nucl. Instrum. Methods Phys. Res. A **224** (1984) 225–232.

[9.18] ALEVRA, A.V., COSACK, M., HUNT, J.B., THOMAS, D.J., SCHRAUBE, H., Experimental determination of the response of four Bonner sphere sets to monoenergetic neutrons, Radiat. Prot. Dosim. **23** (1988) 249–252.

[9.19] ALEVRA, A.V., COSACK, M., HUNT, J.B., THOMAS, D.J., SCHRAUBE, H., Experimental determination of the response of four Bonner sphere sets to monoenergetic neutrons (II), Radiat. Prot. Dosim. **40** (1992) 91–102.

[9.20] THOMAS, D.J., ALEVRA, A.V., HUNT, J.B., SCHRAUBE, H., Experimental determination of the response of four Bonner sphere sets to thermal neutrons, Radiat. Prot. Dosim. **54** (1994) 25–31.

[9.21] HARVEY, W.F., HAJNAL, F., Multisphere Neutron Spectrometry Measurements at the Los Alamos National Laboratory Plutonium Facility, Los Alamos Report LA-UR-92-3873 (Dec. 1992) and LA-12538-MS (Jun. 1993); Radiat. Prot. Dosim. **50** (1993) 13–30.

[9.22] THOMAS, D.J., et al., Results of a large scale neutron spectrometry and dosimetry comparison exercise at the Cadarache moderator assembly, Radiat. Prot. Dosim. **70** (1997) 313–322.

[9.23] INTERNATIONAL ATOMIC ENERGY AGENCY, Compendium of Neutron Spectra and Detector Responses for Radiation Protection Purposes, Technical Reports Series No. 318, IAEA, Vienna (1990).

[9.24] INTERNATIONAL ATOMIC ENERGY AGENCY, Compendium of Neutron Spectra and Detector Responses for Radiation Protection Purposes, Supplement to Technical Reports Series No. 318, Technical Reports Series No. 403, IAEA, Vienna (2001).

[9.25] RIMPLER, A., Applications, Radiat. Prot. Dosim. **107** (2003) 189–201.

[9.26] WIEGEL, B., ALEVRA, A.V., NEMUS — the PTB neutron multisphere spectrometer: Bonner spheres and more, Nucl. Instrum. Methods Phys. Res. A **476 (**2002) 36–41.

[9.27] KIM, B.H, CHANG, Y., LEE, H.S., CHO, G., Measurement of the neutron fluence and dose spectra using an extended Bonner sphere and a tissue-equivalent proportional counter, Radiat. Prot. Dosim. **110** (2004) 717–723

[9.28] CHEMINET, A., et al., "Characterization of the IRSN neutron multisphere spectrometer (HERMEIS) at European standard calibration fields", Second Int. Workshop on Fast Neutron Detectors and Applications, 6–11 Nov. 2011, Ein Gedi, Israel, IOP Publishing, Bristol (2012).

[9.29] AGOSTEO, S., et al., Characterization of extended range Bonner sphere spectrometers in the CERF high-energy broad neutron field at CERN, Nucl. Instrum. Methods Phys. Res. A **691** (2012) 56–68.

[9.30] DUBEAU, J., HAKMANA WITHARANA, S.S., ATANACKOVIC, J., YONKEU, A., ARCHAMBAULT, J.P., A neutron spectrometer using nested moderators, Radiat. Prot. Dosim. **150** (2012) 217–22.

[9.31] BEDOGNI, R., et al., First test of SP^2: A novel active neutron spectrometer condensing the functionality of Bonner spheres in a single moderator, Nucl. Instrum. Methods Phys. Res. A **767**, (2014) 159–162.

[9.32] GÓMEZ-ROS, J.M., et al., CYSP: A new cylindrical directional neutron spectrometer conceptual design, Rad. Meas. **82** (2015) 47–51.

[9.33] INTERNATIONAL ATOMIC ENERGY AGENCY, International Reactor Dosimetry File: IRDF-2002,
https://www-nds.iaea.org/irdf2002/index.htmlx

[9.34] D'ERRICO, F., MATZKE, M., Neutron spectrometry in mixed fields: superheated drop (bubble) detectors, Radiat. Prot. Dosim. **107** (2003) 111–124.

[9.35] TAGZIRIA, H., HANSEN, W., Neutron spectrometry in mixed fields: proportional counter spectrometers, Radiat. Prot. Dosim. **107** (2003) 73–93.

[9.36] HAWKES, N.P., ROBERTS, N.J., Digital dual-parameter data acquisition for SP2 hydrogen-filled proportional counters, Radiat. Prot. Dosim. **161** (2014) 253–256.

[9.37] DELAFIELD, H.J., PERKS, C.A., Neutron spectrometry and dosimetry measurements made at nuclear power stations with derived dosemeter responses, Radiat. Prot. Dosim. **44** (1992) 227–232.

[9.38] GRESSIER, V., et al., Characterisation of the IRSN CANEL/T400 facility producing realistic neutron fields for calibration and test purposes, Radiat. Prot. Dosim. **110** (2004) 523–527.

[9.39] KNOLL, G.F., Radiation Detection and Measurement, 3rd edn, John Wiley & Sons, New York (2000).

[9.40] EVANS A.E., BRANDENBERGER, J.D., High resolution fast neutron spectrometry without time-of-flight, IEEE Trans. Nucl. Sci. **NS26** (1979) 1484–1486.

[9.41] BIRKS, J.B., The Theory and Practice of Scintillation Counting, Pergamon Press, Oxford (1964).

[9.42] HARVEY, J.A., HILL, N.W., Scintillation detectors for neutron physics research, Nucl. Instrum. Methods **162** (1979) 507–529.

[9.43] BROOKS, F., KLEIN, H., Neutron spectrometry — historical review and present status, Nucl. Instrum. Methods Phys. Res. A **476** (2002) 1–11.

[9.44] KLEIN, H., Neutron spectrometry in mixed fields: NE213/BC501a liquid scintillation spectrometers, Radiat. Prot. Dosim. **107** (2003) 95–109.

[9.45] ZAITSEVA, N., et al., Plastic scintillators with efficient neutron/gamma pulse shape discrimination, Nucl. Instrum. Methods Phys. Res. A **668** (2012) 88–93.

[9.46] GIAZ, A., et al., The CLYC-6 and CLYC-7 response to γ-rays, fast and thermal neutrons, Nucl. Instrum. Methods Phys. Res. A **810** (2016) 132–139.

[9.47] TAGZIRIA, H., ROBERTS, N.J., THOMAS, D.J., Measurement of the [241]Am-Li radionuclide source spectrum, Nucl. Instrum. Methods Phys. Res. A **510** (2003) 346–356.

[9.48] ING, H., et al., ROSPEC — a simple reliable high resolution neutron spectrometer, Radiat. Prot. Dosim. **70** (1997) 273–278.

[9.49] WILLIAMS, A.M., SPYROU, N.M., BRUSHWOOD, J.M., BEELEY, P.A., Considerations in the design of an improved transportable neutron spectrometer, Nucl. Instrum. Methods Phys. Res. A **476** (2001) 149–154.

[9.50] ARMISHAW, M.J., BUTLER, J., CARTER, M.D., CURL, I.J., McCRACKEN, UKAEA Report AEEW-M-2365 RPD/MJA/1187, UK Atomic Energy Authority, Abingdon (1986).

[9.51] WEAVER, J.A., JOYCE, M.J., PEYTON, A.J., ROSKELL, J., Recent improvements to a transportable neutron spectrometer (TNS), Nucl. Instrum. Methods Phys. Res. A **476** (2002) 143–148.

[9.52] PEREY, F.G., Least-Squares Dosimetry Unfolding: The Program STAY'SL, Report ORNL/TM-6062, Oak Ridge National Laboratory, Oak Ridge, TN (1978).

[9.53] MAERKER, R.E., BROADHEAD, B.L., WAGSHAL, J.J., Theory of a new unfolding procedure in pressurized water reactor pressure vessel dosimetry and development of an associated benchmark data base, Nucl. Sci. Eng. **91** (1986) 137–170.

[9.54] STALLMANN, F.W., LSL-M2: A Computer Program for Least-Squares Logarithmic Adjustment of Neutron Spectra, Report NUREG/CR-4349, ORNL/TM-9933, Oak Ridge National Laboratory, Oak Ridge, TN (1986).

[9.55] MATZKE, M., Unfolding of Pulse Height Spectra: the HEPRO Program System, Report PTB-N-19, Physikalisch-Technische Bundesanstalt, Braunschweig, Germany (1994).

[9.56] McELROY, W.N., BERG, S., CROCKETT, T., HAWKINS, R.G., A computer-automated iterative method for neutron flux spectra determination by foil activation, Report AFWL-TR-67-41, US Air Force Weapons Laboratory, Kirtland, NM (1967).

[9.57] ROUTTI, J.T., SANDBERG, J.V., General purpose unfolding program LOUHI78 with linear and non-linear regulations, Comput. Phys. Commun. **21** (1980) 119–144.

[9.58] LOWRY, K.A., JOHNSON, T.L., Modification to Iterative Recursion Unfolding Algorithms and Computer Codes to Find More Appropriate Neutron Spectra, NRL Report 5340, Naval Research Laboratory, Washington, DC (1984).

[9.59] McCRACKEN, A.K., GRIMSTONE, M.J., "Experimental data processing program", paper presented at First ASTM-EURATOM Symp. on Reactor Dosimetry, Petten, 1975.

[9.60] SCHMITTROTH, F., A method for data evaluation with lognormal distributions, Nucl. Sci. Eng. **72** (1979) 19–34.

[9.61] REGINATTO, M., GOLDHAGEN, P., MAXED, a Computer Code for the Deconvolution of Multisphere Neutron Spectrometer Data Using the Maximum Entropy Method, Report EML-595, Environmental Measurements Laboratory, New York (1998).

[9.62] REGINATTO, M., GOLDHAGEN, P., NEUMANN, S., Spectrum unfolding, sensitivity analysis and propagation of uncertainties with the maximum entropy deconvolution code MAXED, Nucl. Instrum. Methods Phys. Res. A **476** (2002) 242–246.

[9.63] BRAGA, C.C., DIAS, M., Application of neural networks for unfolding neutron spectra measured by means of Bonner spheres, Nucl. Instrum. Methods Phys. Res. A **476** (2002) 252–255.

[9.64] INTERNATIONAL ATOMIC ENERGY AGENCY, Compendium of Neutron Spectra in Criticality Accident Dosimetry, Technical Reports Series No. 180, IAEA, Vienna (1978).

[9.65] NAISMITH, O.F., SIEBERT, B.R.L., A database of neutron spectra, instrument response functions and dosimetric conversion functions for radiation protection applications, Radiat. Prot. Dosim. **70** (1997) 241–246.

[9.66] INTERNATIONAL COMMISION ON RADIOLOGICAL PROTECTION, ICRP Publication 103, Elsevier, Amsterdam (2007).

[9.67] SCHMITZ, T., WAKER, A.J., KLIAUGA, P., ZOETELIEF, H. (Eds), Design, construction and use of tissue equivalent proportional counters, Radiat. Prot. Dosim. **61** 4 (1995).

[9.68] INTERNATIONAL COMMISSION ON RADIATION UNITS AND MEASUREMENTS, Microdosimetry, Report 36, ICRU, Bethesda, MD (1983).

[9.69] ROSSI, H.H., Specification of radiation quality, Radiat. Res. **10** (1959) 522–531.

[9.70] PIHET, P., GERDUNG, S., GRILLMAIER, R.E., KUNZ, A., MENZEL, H.G., Critical assessment of calibration techniques for low pressure proportional counters used in radiation dosimetry, Radiat. Prot. Dosim. **44** (1992) 115–120.

[9.71] LINDBORG, L., et al., Radiation Protection 140, Cosmic Radiation Exposure of Aircraft Crew, Compilation of Measured and Calculated Data, Final Report of EURADOS WG5 to the Group of Experts Established under Article 31 of the Euratom Treaty, European Commission, Luxembourg (2004).

[9.72] WAKER, A.J., private communication.

[9.73] D'ERRICO, F., BARTLETT, D.T., AMBROSI, P., BURGESS, P., Determination of direction and energy distributions, Radiat. Prot. Dosim. **107** (2003) 133–153.

[9.74] D'ERRICO, F., MATZKE, M., SIEBERT, B.R.L., Energy and angle-differential fluence measurements with superheated drop detectors, Nucl. Instrum. Methods Phys. Res. A **476** (2002) 277–290.

[9.75] LUSZIK-BHADRA, M., D'ERRICO, F., HECKER, O., MATZKE, M., A wide-range directional neutron spectrometer, Nucl. Instrum. Methods Phys. Res. A **476** (2002) 291–297.

10. NEUTRON SURVEY AND INSTALLED INSTRUMENTS

10.1. INTRODUCTION

Two types of instruments are used for area monitoring, namely portable or installed devices.

Portable (battery powered) survey meters are used in the workplace to measure the neutron dose equivalent rates in selected areas.[1] The data obtained are used to delineate those areas in which personal dosimeters should be worn or in which access limits need to be specified. Often, the results of these measurements are posted in the form of a map indicating the levels measured in specific locations. Survey instruments are active devices that provide an immediate indication of the intensity of a neutron field and so may be fitted with an alarm to warn workers of hazardous levels of neutron radiation. Some active instruments have made use of semiconductor neutron detectors, but these sensors are most often used in electronic personnel dosimeters.

Installed instruments are designed to provide a continuous indication of neutron dose equivalent rate and to alarm when a pre-set level has been reached or exceeded. These instruments are normally powered by mains voltage, since they are expected to provide a continuous indication and they will not be moved from their location. Such instruments usually have the possibility of remote readout.

The most common detector assembly used in both portable and installed neutron monitors is the moderator type, using a hydrogenous material such as polyethylene surrounding a thermal neutron detector. The widespread use of this type of survey meter is due to its relatively high sensitivity to neutrons over a wide range of energies and low sensitivity to photons, but the use of a moderator results in a device that is relatively large and heavy. This may not be a serious shortcoming in an installed monitor, but it is a consideration for its use as a portable survey meter.

Other types of detectors have been used for both portable survey and installed instruments. These include TEPCs, scintillation detectors and active superheated emulsion detectors. Recombination ionization chambers have also been used to measure the total dose equivalent rate in mixed neutron–photon radiation fields, usually in high energy neutron environments.

---

[1] Survey instruments are referred to by several different names, such as area survey instrument, area monitor, or just monitor. They are also sometimes called rem meters, rem balls or rem counters, reflecting the units in which the quantity dose equivalent was measured before the SI unit, the sievert, was introduced.

As neutron dose equivalent rates may be determined from the fluence spectrum and the fluence to dose equivalent conversion coefficients, it is also possible to use a spectrometric measuring device. Some neutron spectrometers are commercially available, and the Bonner sphere spectrometry technique can also be used for this purpose. This type of measurement is usually a 'one-off' because of the time it takes.

Since survey instruments are normally used for area or environmental monitoring, they are usually calibrated in terms of the quantity ambient dose equivalent. However, none has a truly appropriate response function for this quantity over the full energy range of interest in radiation protection. Knowledge of the dose equivalent response provides information on the energy ranges where an instrument performs well and those where it performs badly. If information is available on the neutron spectrum in which a device is to be used, its performance, that is, the likely degree of under- or over-reading, can be predicted. In the absence of detailed spectral information, even some rough data on the energy distribution, such as a breakdown of the numbers of fast, intermediate and slow neutrons, can give a useful indication of the likely performance of the survey instrument, and techniques to obtain these rough spectral indices have been developed.

10.2. MODERATOR BASED NEUTRON SURVEY INSTRUMENTS

Survey instruments are constructed so that the shape of their fluence response as a function of energy approximates that of the fluence to ambient dose equivalent conversion coefficient, and therefore they will give an indication approximately proportional to $H*(10)$. Instruments are typically constructed with a central thermal neutron sensor surrounded by a hydrogenous moderator (generally polyethylene), whose thickness is chosen to optimize the dose equivalent response as a function of energy. A thermal neutron absorbing material is included in a layer, sometimes a perforated layer, within the polyethylene, not far from the central thermal neutron sensor. This preferentially absorbs some of the thermal neutrons, and the result is a more dose equivalent response function than can be obtained with just a polyethylene moderator [10.1].

The forerunner of survey instruments of this type was the so-called Andersson–Braun (A–B) design [10.2], where a cylindrical BF_3 proportional counter is enclosed in a cylinder of polyethylene roughly 47 cm long by 20 cm diameter. A perforated sleeve of boron plastic is included within the polyethylene, at a distance of approximately 16 mm from the outside of the proportional counter tube, to act as a partial thermal neutron absorber. The design has been modified over time to improve the dose equivalent response by altering the position of the sensor and the sleeve design [10.3]. Several A–B type instruments, with

marginally different designs, have become available commercially over the years, and they continue to be used extensively. Instruments of this type include the Neutron Monitor NM2, the NRC AN/PDR-70 (SNOOPY) neutron survey meter and the Studsvik/Alnor Neutron Dose Rate Meter 2202 D, two of which are shown in Fig. 10.1. The Studsvik/Alnor instrument has a shorter cylinder than the original design and rounded edges at one end of the cylinder in order to make the response more isotropic.

In the 1960s, Leake produced a spherical version of the moderator based instrument, first with a LiI(Eu) crystal [10.4] as the central sensor, and then with a spherical ^{3}He proportional counter [10.5], which has a much lower photon sensitivity than the LiI(Eu) crystal. The diameter chosen for the polyethylene sphere was 20.8 cm, which gives a lighter instrument than the classic A–B design. However, the reduced mass of polyethylene has a consequence in that the Leake device has a higher over-read for dose equivalent in the intermediate energy region. This is illustrated in Fig. 10.2, which shows the ambient dose equivalent responses of three commonly used survey instruments, including the Leake device. The data have been calculated using Monte Carlo neutron transport, and these results agreed well with the available measured data [10.6]. The Leake counter has a near flat dose equivalent response in the important region around 1 to 2 MeV, whereas the other two have a dip in the region around 0.4 MeV, which

FIG. 10.1. Several commonly used area survey instruments: from the left, a Leake type monitor, a Studsvik/Alnor 2202 D, an NM2 monitor and a Berthold LB6411. (Courtesy of National Physical Laboratory.)
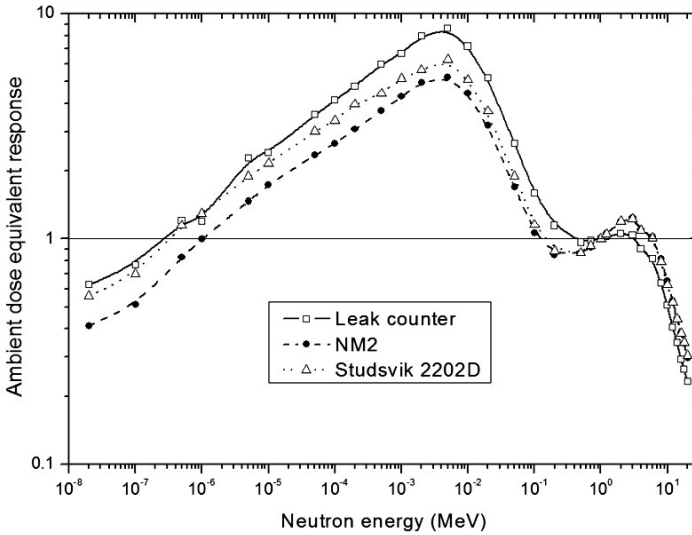
FIG. 10.2. Ambient dose equivalent response functions for three area survey instruments. The responses have been normalized to unity at 1 MeV, that is, to have the correct response at 1 MeV. All measurements are for neutron incidence from the reference direction, which is the side of the sphere opposite the electronics for the Leake detector and through the side of the cylinder for the NM2 and Studsvik 2202 D. Data from Ref. [10.6].

means they can under-read in fields with a large fraction of the dose equivalent in this region. In order to allow for the high response in the intermediate energy region, the calibration of the Leake counter in some variants of this instrument is set so that it under-reads the ambient dose equivalent for a ^{252}Cf source by approximately 15% [10.6]. Recent variants on the Leake design have produced instruments with higher sensitivity [10.7].

Other survey instruments with spherical moderators include the Thermo Electron Corporation ASP-2e/NRD Neutron Survey Meter, the Eberline PNR-4 and the Ludlum Model 12-4 Neutron Counter, which are all based on 22.9 cm moderating spheres. With the extra mass of polyethylene compared with the Leake device, their response functions would tend to be more like those of the Studsvik 2201 D and the NM2.

Interesting variants of these instruments are made in Japan [10.8]. The TPS-451C is similar to the Studsvik 2202 D, except that the thermal sensor is a ^{3}He tube, and the NSN1 has similarities to the Leake counter, being based on a spherical moderator of the same outer diameter, except that the central ^{3}He sensor has a larger diameter and the gas pressure is higher. This increases the neutron sensitivity, but the presence of the larger diameter sensor means that

the polyethylene thickness is reduced, and the over-reading in the intermediate energy region is greater. In France, the CRAMAL 31 (now the CANBERRA PNM-200), which uses a 25 mm diameter by 25 mm long cylindrical ^{3}He tube at the centre of a 20 cm diameter polyethylene sphere, is extensively used.

With the rather poor match of the response of neutron survey instruments to the required dose equivalent quantity, it is perhaps surprising that they are as commonly used as they are. However, in most workplace fields the fact that the majority of the dose equivalent occurs in the energy region where their response is reasonably good, and the fact that there can be some degree of cancellation between over-reading and under-reading in different energy regions, means that their indications are usually within 50% of the correct answer, often better, and that significant over-reading, by amounts of the order of a factor of two, tends to occur only for very soft fields [10.6]. The quantity that these instruments are intended to measure has changed over the years. However, the fact that the changes have not been particularly radical [10.9], combined with the fact that the goodness of the fit of the instrument response functions to the dose equivalent curve as a function of energy, did not change dramatically when the quantity changed [10.10], means that they continue to be widely used.

Considering that the A–B and Leake instruments were first made before the widespread availability of neutron transport calculations, the original designers did a reasonable job of finding the optimal design for a moderator based dose equivalent meter. Attempts to design improved moderator based instruments using modern Monte Carlo radiation transport codes such as MCNP have met with limited success [10.11]. Although some slight enhancement in the dose equivalent response curve may be obtained, no really drastic improvement is possible. The Berthold LB 6411 instrument [10.12] was designed using the MCNP code. It has a spherical 25 cm diameter moderator and a higher sensitivity ^{3}He counter than the original Leake device, but the response function shape is similar to that for the NM2 with some underestimation of the dose equivalent in the region just below 1 MeV (see Fig. 10.3).

Spherical instruments have the advantage of a more isotropic response, which is one of the requirements for an instrument designed to measure ambient dose equivalent. An investigation of the angle dependence of response of several spherical and cylindrical instruments can be found in Ref. [10.6], along with a discussion of the effects of the presence or absence of an individual holding the instrument.

A conventional moderator based survey instrument has only one item of information from which to derive the dose equivalent, namely the counts from the central thermal sensor, and relies entirely on the device having a response function that matches the dose equivalent conversion coefficient curve. One attempt to improve on this situation is the Dineutron device [10.13] (currently
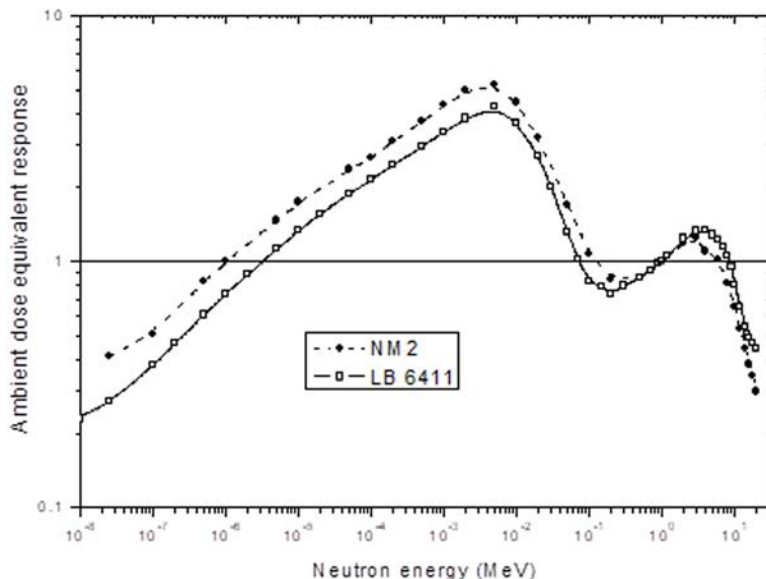
FIG. 10.3. Comparison of the ambient dose equivalent response functions of the NM2 and the LB 6411 survey instrument. As in Fig. 10.2, the curves have been normalized to unity at 1 MeV. Data from Ref. [10.6].

sold by Canberra), which has two polyethylene moderating spheres, each with a ^{3}He central sensor, thus providing two pieces of information. From these, the instrument derives values for dose, dose equivalent and a quality factor. The spheres are smaller than in conventional moderator based instruments, being 6.4 and 10.7 cm in diameter, and the overall weight is thus only approximately 3.5 kg for a Dineutron, compared with 6 kg for a Leake counter or 10.5 kg for the Studsvik 2202 D. Neither of the small spheres has a response function matching the fluence to dose equivalent conversion coefficient curve, and the instrument indications are computed from the individual sphere counts and their ratio. The Dineutron was designed primarily for measurements around pressurized water reactors. Because the ratio of counts in the two spheres is not unique to one field, and different fields can produce the same ratio, the instrument's performance can be variable [10.14, 10.15] and is rather dependent on the field in which it is calibrated. In particular, the use of a D_2O moderated ^{252}Cf source for calibration is not recommended [10.14].

As can be seen from Figs 10.2 and 10.3, the response of moderator based survey instruments falls off abruptly above 10 MeV, leading to a drastic underestimation of the ambient dose equivalent, and this underestimation

increases with increasing neutron energy. At reactor fields this does not represent a problem, but outside the shielding at high energy hadron accelerators, used, for example, in elementary particle research or proton therapy, the neutron energies extend to much higher than 10 MeV, and the dose equivalent is often dominated by the neutron component. The poor high energy response is thus a serious problem if these devices are used in these environments. High energy neutrons are also an important component in the cosmic ray exposure of aircraft personnel at flight altitudes.

A very significant increase in the high energy response of moderator based instruments can be obtained by incorporating heavy metal components into the moderator. By inserting a lead layer, 1 cm thick, outside the thermal neutron attenuating layer of a conventional A–B type instrument, Birattari et al. [10.16] were able to develop an instrument with a much extended range (see Fig. 10.4). High energy neutrons interacting with the lead produce evaporation or spallation neutrons via inelastic scattering reactions, and these are subsequently moderated by the polyethylene. No significant effect is produced on neutrons with energy below approximately 10 MeV, so the response in this region is not significantly
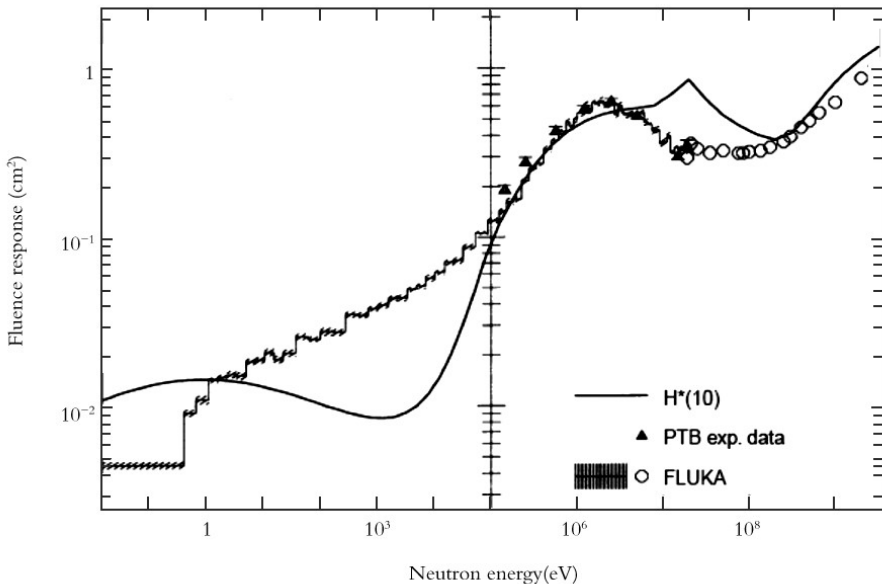
FIG. 10.4. *Absolute neutron fluence response (counts per unit fluence) of the spherical rem counter LINUS as measured at the Physikalisch-Technische Bundesanstalt (PTB) and as calculated with the Monte Carlo radiation transport code FLUKA. (Reproduced from Ref. [10.16] with permission from Oxford University Press.)*

altered. Cylindrical and spherical versions of this instrument are now available, with good characterization data, and they go by the name LINUS.

An alternative design to the LINUS, based on the same basic idea, is the Wide Energy Neutron Detection Instrument, WENDI [10.17]. Here, the material used to produce evaporation or spallation neutrons is tungsten, which may either be incorporated into the polyethylene or used as a powder in a layer close to the central sensor. The tungsten also has an effect on modifying the intermediate energy response by resonance absorption.

Because the central sensors used in moderator based devices are thermal neutron sensors, which take advantage of the large signals available from BF_3 or ^3He counters, they exhibit very low photon sensitivity. The presence of photons only tends to present problems when the intensity is so high that events pile up and exceed the discriminator set in the counter to separate neutron and photon induced events. The dose rate at which this occurs depends on the photon energy.

The performance of a moderator based neutron survey instrument in a pulsed field depends on the pulse width, the repetition rate of the radiation field and the slowing down time of the neutrons in the moderator, a parameter that depends on the neutron energy. If measurements are performed within a room where scattered neutrons reach the monitor, these may well arrive after the beam pulse. Readings can thus be difficult to interpret. During a pulse, the neutron fluence may be very high, and dead time in the central detector means that events are missed. If the moderation time is long compared with the pulse width, events can still be registered outside the pulse. Further complications may be introduced by photon pile up if there are significant numbers of photons in the burst, and finally the instrument may be sensitive to electromagnetic radiation associated with the pulses.

A paper by Dinter and Tesch [10.18] provides an approach to interpreting instrument readings using knowledge of dead times and slowing down times in moderators. It provides data for Leake and A–B detectors and also for plain moderating spheres of diameters 30 and 45 cm. Some further results have been reported by Liu [10.19]. It would, however, be useful to improve the range of available data to include different energies and more instruments. Systematic investigations of the extent of the problems have been undertaken [10.20] and approaches to overcoming them proposed [10.21], including the use of activation [10.22].

The fact that moderator based survey instruments using a single thermal neutron sensor at the centre cannot provide an ideal dose equivalent response has led some researchers to investigate the possibilities of improving the response by using additional thermal neutron sensors at different depths. In particular, the use of silicon diode detectors, made sensitive to thermal neutrons by a layer of some lithium containing compound, has been investigated [10.23, 10.24]. The diodes

are placed at various positions within the sphere and thus have different response functions to the central sensor. The diodes can be at a single depth [10.23] or a range of depths [10.24] and provide additional information that can be combined with that from the central sensor to provide a more dose equivalent response. To date, these devices have only been produced as prototypes, and no commercial version is available. Because the diodes are not at the centre, their responses depend on the direction of the incident neutrons. This can be seen as a serious drawback, since it goes against the basic requirement for a device measuring ambient dose equivalent, namely that it should have an isotropic response. Conversely, it does offer the possibility of deriving directional information about the field and thus obtaining a better estimate of effective dose. The complexity of analysing the signals to provide this information has to date meant that this option has not been realized.

10.3. TEPCs

The TEPC [10.25] is designed to measure the distribution of absorbed dose as a function of lineal energy. With this information, different types of radiation can be identified and separated, and absorbed dose can be converted to dose equivalent. Since the counter is built from a material that is roughly tissue equivalent, such as A-150 tissue equivalent plastic (design composition, per cent by weight, H 10.1, N 3.5, O 5.5, C 77.6, Ca 1.8, F 1.7; cf. ICRU tissue, H 10.2, N 3.5, O 72.9, C 12.3, Ca 0.007), the absorbed dose measured is close to that for human tissue. In principle, the instrument thus appears to have features that make it an ideal survey instrument. However, as described in Section 9, the device has drawbacks that mean that, although it is an excellent instrument for neutrons at certain energies — specifically high energies — it does not perform well at all energies. There are three battery powered instruments commercially available: the HANDI, the REM500 and the Hawk.

The earliest of these was the HANDI [10.26], which is shown in Fig. 10.5. This instrument is based on a spherical, 59 mm diameter, A-150 tissue equivalent plastic walled counter [10.27]. The electronics provides a lineal energy spectrum of limited resolution (16 channels of equal width on a logarithmic scale) [10.28], but the device provides dose and dose equivalent information suitable for radiation protection. The small size of the counter means the sensitivity is rather low.

The REM500 and the Hawk, shown in Fig. 10.6, are both produced by Far West Technology and are both based on spherical A-150 tissue equivalent plastic counters. The REM500 [10.29, 10.30] is a lightweight instrument (weighing approximately 2.3 kg) that provides absorbed dose and dose equivalent information on a digital display. A lineal energy spectrum can be downloaded to

FIG. 10.5. The HANDI TEPC, produced by the University of Saarland. (Photo kindly provided by H. Schuhmacher, PTB.)

FIG. 10.6. Two commercially available instruments based on TEPCs: the Hawk on the left and the REM500 on the right. (Courtesy of National Physical Laboratory.)

a computer for more detailed analysis. It is based on a 57 mm diameter counter, and as such suffers somewhat from a rather low sensitivity. A non-standard dependence of Q on LET (actually on lineal energy y) is used to try to overcome the poor low energy response of the device. The Hawk [10.31, 10.32] was designed specifically for cosmic ray dose measurements and over recent years has contributed significantly to knowledge of cosmic ray doses at aircraft flight altitudes. It has a 5 inch (12.7 cm) diameter counter, thus making it significantly more sensitive than the REM500. Spectral data are written to a flash memory card, from which they can be downloaded to a computer. The Hawk can provide both photon and neutron data, whereas the REM500 is restricted to neutrons.

10.4. RECOMBINATION IONIZATION CHAMBERS

When an energetic ionizing particle travels through the gas of an ionization chamber, ion pairs are formed in a column along the track. The electric field in the chamber causes these ion pairs to separate and to drift towards the positive and negative electrodes. However, if positive ions collide with free electrons, or with negative ions created by electron attachment, recombination can occur with the loss of ion pairs.

Recombination is usually split into initial (or columnar) recombination, a result of the high ion density along the track and volume recombination, which occurs after the ions have left the vicinity of the track. Volume recombination tends to be important only at high irradiation rates. Conversely, initial recombination, which dominates at high gas pressure, can occur at any irradiation rate; its magnitude depends on the electric field strength and on the ionization density. The ionization density is closely related to LET, from which Q values are derived, and hence a measurement of initial recombination holds out the prospect of deriving quality factor data to go along with the absorbed dose information available from an ionization chamber. In this way, dose equivalent information can be derived from recombination ionization chambers. Such devices have been used for some years in radiation protection [10.33]; however, a work on improvements via advanced methods of analysing the data has been introduced [10.34].

Recombination chambers are high pressure tissue-equivalent ionization chambers, designed and operated in such way that ion collection efficiency in the chamber is governed by the initial recombination of ions. The output signal of the chamber is the ion current (or collected charge) as a function of collecting voltage. One of the best known chambers of this type is the REM-2 [10.35], shown in Fig. 10.7. It has 25 parallel-plate tissue-equivalent electrodes with a spacing of 7 mm. The chamber is filled to 1 MPa with a mixture of methane and

5% nitrogen. It weighs 6.5 kg and has an effective wall thickness equivalent to approximately 18 mm of tissue. In Fig. 10.8 an example is given of the saturation curves that can be measured with this device. Data on the Q value are obtained from measurements of the ion current at different collecting voltages. In principle, the more voltages measured, the greater the amount of data that can be extracted.

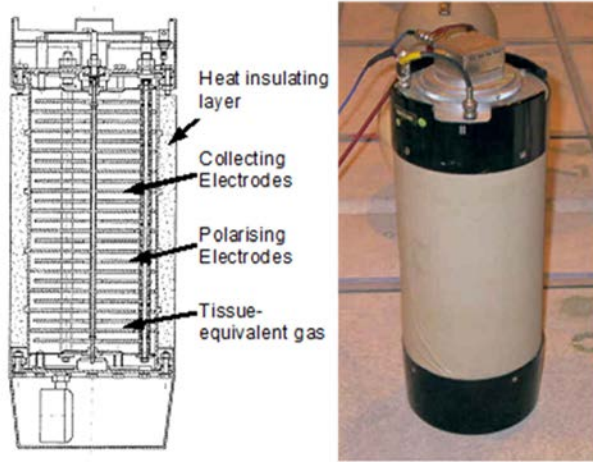*FIG. 10.7. Cross-sectional view of the REM-2 recombination chamber [10.34] and a photograph of the instrument. (Photo kindly supplied by Sabine Myer, Paul Scherrer Institute, Switzerland.)*
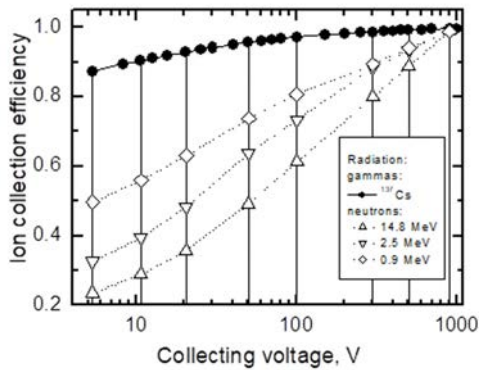

FIG. 10.8. Ion collection efficiency in a REM-2 recombination chamber versus collecting voltage for ^{137}Cs gamma rays and neutrons of three different energies. (Reproduced from Ref. [10.38] with permission from Oxford University Press.)

Prior to the introduction, in ICRP 60 [10.36], of a form for the quality factor as a function of LET, which has a peak at 100 keV·µm^{-1} and which decreases above this LET value, the relationship between Q and LET (see, for example, ICRP 26 [10.37]) involved Q being constant up to 3.5 keV·µm^{-1} and increasing monotonically with LET up to a value of 175 keV·µm^{-1}, after which Q was constant. For a relationship of this type, it was possible to define a quantity called the recombination index of radiation quality, Q_4. This could be derived from measurements, in the unknown field and in a reference gamma radiation field, of the ion collection efficiency at just two voltages. Experiments have shown [10.38] that Q_4 is a good approximation to the Q value of ICRP 26 and can be used to estimate a value of dose equivalent as defined using this Q value. However, the form of the Q to LET relationship of ICRP 60 requires a more complex analysis involving information on ion collection efficiency at a greater number of voltages. This analysis can, nevertheless, be performed and values for $H^*(10)$ ICRP 60 derived. In fact, coarse histogram data can be derived of the dose distribution as a function of LET [10.34].

Although, at present, there is no commercially available recombination chamber, this type of instrument is finding an increasing range of applications, for example around medical accelerators [10.39], for boron neutron capture therapy (BNCT) dosimetry [10.40] and in pulsed high energy fields [10.41]. Investigation of the possible approaches to maximizing the information available from such devices continues [10.42].

10.5. SUPERHEATED EMULSION DETECTORS

Superheated drop detectors [10.43] or bubble (damage) detectors [10.44], commonly referred to simply as 'bubble detectors', are often used as personal dosimeters because of their ability to give an immediate visual display of the dose equivalent (see Section 11; for a review of their properties, see Ref. [10.45]). However, in some respects they have characteristics more akin to those required of a survey instrument. Their response is reasonably isotropic, and they can be calibrated in terms of $H^*(10)$. Also, they have a high sensitivity and are largely insensitive to gamma rays. In contrast to moderator based devices, they are small and light and could thus be used in confined spaces.

Bubble detectors are not high accuracy devices. For more than 100 bubbles (10% statistics) it becomes difficult to establish the true number of bubbles, since some get hidden behind others. There is thus a dynamic range problem, and detectors with different sensitivities, that is, different numbers of bubbles per unit dose equivalent, need to be used. Each bubble detector needs to be calibrated separately, since the quoted sensitivity is not exact. They are temperature

sensitive, although allowance for this effect can be made by either applying a temperature correction or using a temperature compensated variety. Lastly, they have a finite lifetime. Nevertheless, they do provide an immediate rough indication of the neutron dose equivalent. Their lack of gamma sensitivity has resulted in their use to determine neutron contamination around medical electron accelerators [10.46, 10.47].

10.6. SCINTILLATION DETECTORS

Various scintillator based devices have become commercially available, including the N-Probe, the Proton Recoil Scintillator — Los Alamos (PRESCILA) and the JANUS. These derive dose equivalent information either directly or via a measurement of the neutron spectrum. Such devices are invariably lighter than moderator based survey instruments and may also provide photon dose equivalent information. Their eventual acceptance as serious rivals to moderator based instruments will probably depend on how they compare in terms of having a truly dose equivalent response over those energy regions where the dose equivalent is highest.

The N-Probe from Bubble Technology Industries uses two separate detectors to provide spectral information over the neutron energy range from thermal to 20 MeV. An NE213 type liquid scintillator is used from 800 keV to 20 MeV, and a ^{3}He proportional counter is used to cover the energy region thermal to 800 keV. Gamma ray signals are rejected using sophisticated pulse shape discrimination circuitry. Pulse height distributions from both detectors are shown during data collection. These distributions are merged and processed automatically to yield the actual neutron spectrum from which dose equivalent values can be derived. In principle, this is an instrument with many desirable features, since it is small and light (4.1 kg) and provides invaluable information on the neutron spectrum; however, there is at present a dearth of information in the open literature to confirm and document its actual performance.

The PRESCILA [10.48] was developed at Los Alamos and is marketed as the model 2363 by Ludlum Measurements, Inc. It uses two types of scintillator, one sensitive to fast neutrons and the other a thermal scintillator element. Together they provide a wide energy response from thermal to well beyond 20 MeV. The fast neutron scintillator consists of a blended mixture of ZnS(Ag) powder as the phosphor and an epoxy glue, the latter providing a hydrogenous matrix within which recoil protons are created. These recoils deposit sufficient energy in individual phosphor grains, compared with the amount a secondary electron can deposit, that gamma ray induced events can be eliminated by simple pulse height discrimination. Thermal and epithermal neutrons are detected using a scintillator

consisting of a mixture of ^{6}LiF and ZnS(Ag) powder. A fairly substantial Lucite light guide, used to direct light from the fast scintillators to the photomultiplier tube, and a borated polyethylene frame provide moderation for the thermal scintillator. Data can be read off a display or downloaded to a computer.

According to the developers, the dose equivalent response function of the PRESCILA has similarities (see Fig. 10.9) to those of moderator based survey instruments; in particular, there is a significant (greater than a factor of ten) over-response in the intermediate energy region. There is also a prominent under-response centred on a neutron energy of approximately 500 keV. The device has a reasonably isotropic angle dependence of response. Overall, the dose equivalent response is not as good as that of a moderator based device in the region below 10 MeV, although the cancellation effects of under- and over-response in actual workplace fields make it very difficult to predict which type of instrument would give the best response in a particular environment. The main advantages of the device are its low weight and the improved response in
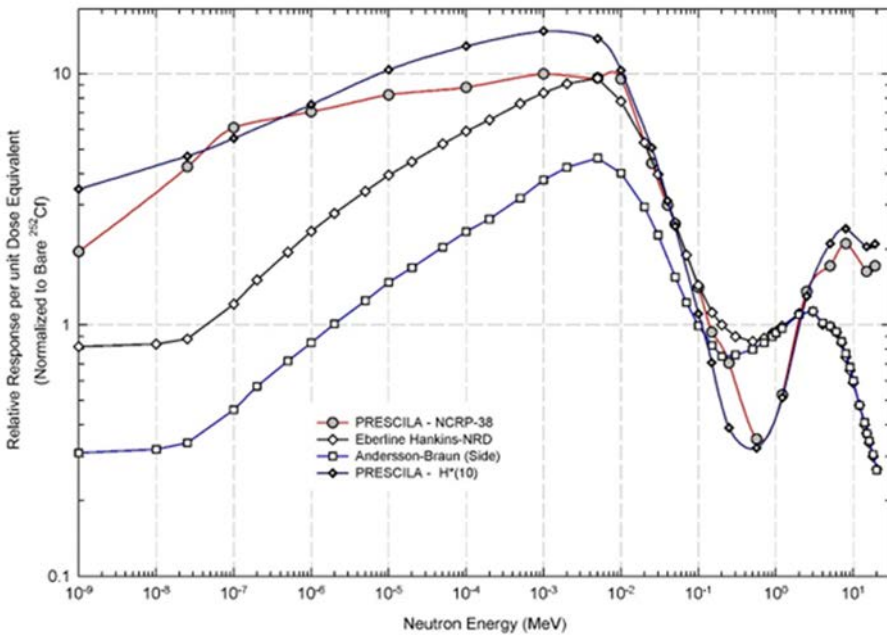

FIG. 10.9. *Comparison of the dose equivalent response of the PRESCILA with those of two moderator based instruments [10.48]. Data for the PRESCILA are given for conversion coefficients from NCRP-38 [10.49] and for ambient dose equivalent H*(10). (Reproduced from Ref. [10.48] with permission from Lippincott Williams & Wilkins.)*

the region above 10 MeV as compared with normal moderator based devices without heavy metal annuli.

The JANUS RMD-2014 neutron and gamma survey meter from Imaging & Sensing Technology (IST) is a scintillator based device incorporating two matched cerium activated glass scintillators, one containing enriched ^{7}Li and the other enriched ^{6}Li. The ^{7}Li scintillator provides information on the gamma ray field, and information on the neutron field is derived from the difference between the signals in the ^{6}Li scintillator and those in the ^{7}Li scintillator. A small amount of polyethylene around the scintillator provides some neutron moderation. With a weight of approximately 0.5 kg, the device is extremely light for a survey instrument; however, to date there is no information in the literature on its response function.

10.7. COMBINED INSTRUMENTS

None of the instruments discussed in this section have an ideal dose equivalent response. However, some of the instruments have very different ambient dose equivalent response functions. The use of two or more instruments can thus provide some indication of the type of spectrum for the field in which the measurements are being made and possibly a better estimate of the dose equivalent. Additional information can be obtained from devices that are not intended to have dose equivalent responses, such as bare thermal detectors or thermal detectors in small moderating spheres, that is, devices that are very sensitive to low and intermediate neutrons.

One example that falls into this category is the Dineutron instrument (see Section 10.2). Other examples are combinations of devices used to characterize workplace fields in order to calibrate albedo personal dosimeters. Amongst these can be included the 3 inch to 9 inch ratio (9/3) method of Hankins [10.50], the 'single sphere technique' of Piesch and Burgkhart [10.51, 10.52] and the approach of Harvey and Hart [10.53], which uses two silicon detectors, each with a thin layer of ^{6}LiF, one within a small polyethylene sphere. These are described in more detail in Section 14.2.10.

The fact that a moderator based survey instrument over-reads in the intermediate energy region but a TEPC based device under-reads in this energy region suggests the possibility of deriving an improved dose equivalent estimate from an appropriate combination of the indications from the two devices. An approach based on the use of a Leake counter and a HANDI TEPC has been proposed [10.54], and the idea has been taken further with an investigation of the use of a Leake counter and a Hawk TEPC [10.55].

10.8. INSTALLED INSTRUMENTS

Installed radiation instruments are usually gamma monitors or contamination monitors, but in areas where neutrons represent a hazard, neutron monitors may also be installed. An International Electrotechnical Commission (IEC) standard is available covering the requirements for these devices [10.56]. They are often similar in concept to survey instruments [10.8], but are wall mounted and will include an audible and/or visual alarm. Usually they include a remote readout, often to a central location, and the readings are often stored to provide a historical record of dose equivalent rates.

In areas around high energy accelerators where there are pulsed mixed radiation fields, including neutrons and possibly exotic particles, installed monitors are often ion chambers such as that shown in Fig. 10.10. These have the advantage of operating satisfactorily in pulsed fields, but have the disadvantage that it is not possible to differentiate among the various radiation types creating the ionization within a particular chamber. A dual ion chamber approach may then be used, with one chamber sensitive to photons and neutrons and the other chamber largely insensitive to neutrons.
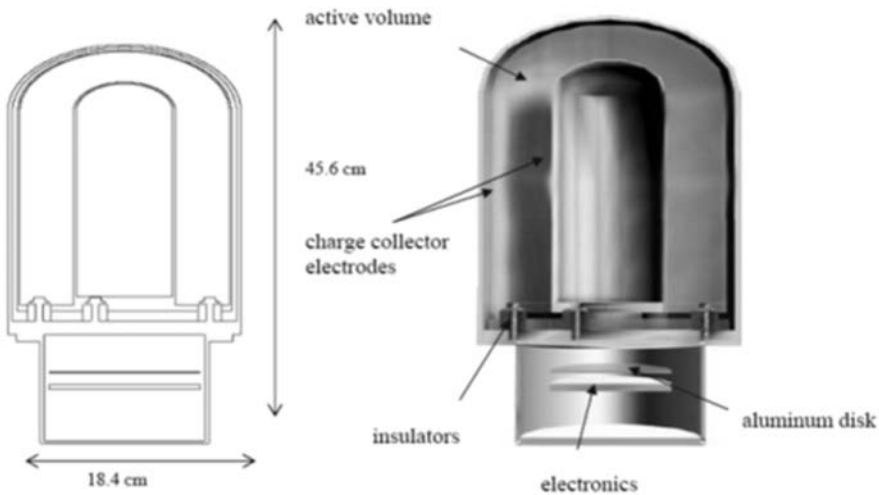

FIG. 10.10. Schematic diagram of the IG5 ion chamber often used as an installed monitor around high energy accelerators. (Reproduced from Ref. [10.57] with permission from Oxford University Press.)

10.9. CHOICE OF INSTRUMENT

When choosing a survey instrument or an installed device, careful consideration should be given to the performance requirements dictated by the characteristics of the field in which it will be used. The matters to consider include the energy spectrum of the workplace neutron field, whether the neutron source is pulsed, whether there is an intense accompanying photon field, whether weight is a serious issue and the overall accuracy requirement. An IEC standard [10.58] is available that defines type tests for instruments designed to measure ambient dose equivalent. In addition to radiological requirements, this considers requirements for the indication (reading); effects of influence quantities; electrical characteristics; electromagnetic compatibility; mechanical, safety and environmental characteristics, and finally the documentation.

REFERENCES TO CHAPTER 10

[10.1] COSACK, M., LESIECKI, H., Dose equivalent survey meters, Radiat. Prot. Dosim. **10**, (1985) 111–119.

[10.2] ANDERSSON, I.Ö., BRAUN, J., A neutron rem counter with uniform sensitivity from 0.025 eV to 10 MeV, Neutron Dosimetry: Proc. Symp. on Neutron Detection, Dosimetry and Standardization, Vol. 2, Harwell, 10–14 Dec. 1962, IAEA, Vienna (1963) 87–95.

[10.3] HANKINS, D.E., A modified A-B remmeter with improved directional dependence and thermal neutron sensitivity, Health Phys. **34** (1978) 249–254.

[10.4] LEAKE, J.W., A spherical dose equivalent neutron detector, Nucl. Instrum. Methods **45** (1966) 151–156.

[10.5] LEAKE, J.W., An improved spherical dose equivalent neutron detector, Nucl. Instrum. Methods **63** (1968) 329–332.

[10.6] TANNER, R.J., et al., Practical Implications of Neutron Survey Instrument Performance, Report HPA-RPD-016, Health Protection Agency, Chilton, UK (2006).

[10.7] LEAKE, J.W., CLEMENTS, J., CROYDON, W.F., LOWE, T., MASON, R.S., Improvements to the Leake neutron detector III: Increased sensitivity and compliance with ANSI and IEC standards, Nucl. Instrum. Methods Phys. Res. A **783** (2015) 80–84.

[10.8] SAEGUSA, J., et al., Evaluation of energy responses for neutron dose-equivalent meters made in Japan, Nucl. Instrum. Methods Phys. Res. A **516** (2004) 193–202.

[10.9] McDONALD, J.C., SCHWARTZ, R.B., THOMAS, R.H., Neutron dose equivalent conversion coefficients have changed in the last forty years… haven't they? Radiat. Prot. Dosim. **78** (1998) 147–149.

[10.10] LEAKE, J.W., The effect of ICRP (74) on the response of neutron monitors, Nucl. Instrum. Methods Phys. Res. A **421** (1999) 365–367.

[10.11] TAN, M., CHEN, C.M., WEN, Y.Q., WANG, Z., The energy response of a spherical neutron dose equivalent counter, Nucl. Instrum. Methods Phys. Res. A **339** (1994) 573–579.

[10.12] BURGKHART, B., FIEG, G., KLETT, A., PLEWNIA, A., SIEBERT, B.R.L., The neutron fluence and H*(10) response of the new LB 6411 REM counter, Radiat. Prot. Dosim. **70** (1997) 361–364.

[10.13] MORGUES, M., CAROSSI, J.C., PORTAL, G., "A light REM-counter of advanced technology", Proc. Fifth Symp. on Neutron Dosimetry, Munich/Neuherberg 17–21 Sep. 1984, EUR 9762, Commission of the European Communities, Luxembourg (1985).

[10.14] AROUA, A., et al., Study of the response of two neutron monitors in different neutron fields, Radiat. Prot. Dosim. **44** (1992) 183–187.

[10.15] RIMPLER, A., Dose equivalent response of neutron survey meters for several neutron fields, Radiat. Prot. Dosim. **44** (1992) 189–192.

[10.16] BIRATTARI, C., et al., The extended range neutron rem counter LINUS: overview and latest developments, Radiat. Prot. Dosim. **76** (1998) 135–148.

[10.17] OLSHER, R.H., et al., WENDI: an improved neutron rem meter, Health Phys. **79** (2000) 170–181.

[10.18] DINTER, H., TESCH, K., Moderated REM meters in pulsed neutron fields, Nucl. Instrum. Methods **136** (1976) 389–392.

[10.19] LIU, J.C., et al., Neutron detection time distributions of multisphere LiI detectors and AB REM meter at 20 MeV electron linac, Radiat. Prot. Dosim. **71** (1997) 252–259.

[10.20] CARESANA, M., et al., Intercomparison of radiation protection instrumentation in a pulsed, neutron field, Nucl. Instrum. Methods Phys. Res. A **737** (2014) 203–213.

[10.21] LEAKE, J.W., LOWE, T., MASON, R.S., WHITE, G., A new method of measuring a large pulsed neutron fluence or dose exploiting the die-away of thermalized neutrons in a polyethylene moderator, Nucl. Instrum. Methods Phys. Res. A **613** (2010) 112–118.

[10.22] LUSZIK-BHADRA, M., HOHMANN, E., OTTO, TH., A new neutron monitor with silver activation, Radiat. Meas. **45** (2010) 1258–1262.

[10.23] BARTLETT, D.T., TANNER, R.J., JONES, D.G., A new design of neutron dose equivalent survey instrument, Radiat. Prot. Dosim. **74** (1997) 267–271.

[10.24] BRUSHWOOD, J.M., GOW, J.P.D., BEELEY, P.A., SPYROU, N.M., Development and testing of an active area neutron dosemeter, Radiat. Prot. Dosim. **110** (2004) 263–266.

[10.25] SCHMITZ, T., WAKER, A.J., KLIAUGA, P., ZOETELIEF, H. (Eds), Design, construction and use of tissue equivalent proportional counters, Radiat. Prot. Dosim. **61** 4 (1995).

[10.26] KUNZ, A., et al., The Homburg area neutron dosemeter HANDI: characteristics and optimisation of the operational instrument, Radiat. Prot. Dosim. **44** (1992) 213–218.

[10.27] KUNZ, A., MENZEL, H.G., AREND, E., SCHUHMACHER, H., GRILLMAIER, R.E., Practical experience with a prototype TEPC area monitor, Radiat. Prot. Dosim. **29** (1989) 99–104.

[10.28] KUNZ, A., PIHET, P., AREND, E., MENZEL, H.G., An easy-to-operate portable pulse-height analysis system for area monitoring with TEPC in radiation protection, Nucl. Instrum. Methods Phys. Res. A **299** (1990) 696–701.

[10.29] THOMAS, D.J., TAYLOR, G.C., "Response function measurements for the REM 500: a microdosimetric counter based area survey instrument", paper presented at Int. Conf. on Radiation Dosimetry and Safety, 31 Mar.–2 Apr. 1997, Taipei, Taiwan.

[10.30] AROUA, A., BUCHILLIER, T., GRECESCU, M., HÖFERT, M., Neutron measurements around high energy lead ion beam at CERN, Radiat. Prot. Dosim. **70** (1997) 437–440.

[10.31] LEWIS, B.J., et al., Aircrew exposure from cosmic radiation on commercial airline routes, Radiat. Prot. Dosim. **93** (2001) 293–314.

[10.32] TAYLOR, G.C., et al., The evaluation and use of a portable TEPC system for measuring in-flight exposure to cosmic radiation, Radiat. Prot. Dosim. **99** (2002) 435–438.

[10.33] ZIELCZYNSKI, M., Use of columnar recombination for determination of relative biological efficiency of radiation, Nukleonika **7** (1962) 176–182 (in Russian).

[10.34] GOLNIK, N., Review of recent achievements of recombination methods, Radiat. Prot. Dosim. **70** (1997) 211–214.

[10.35] ZIELCZYNSKI, M., GOLNIK, N., RUSINOWSKI, Z.A., Computer controlled ambient dose equivalent meter based on a recombination chamber, Nucl. Instrum. Methods Phys. Res. A **370** (1996) 563–567.

[10.36] INTERNATIONAL COMMISSION ON RADIOLOGICAL PROTECTION, ICRP Publication 60, Pergamon Press, Oxford and New York (1991).

[10.37] INTERNATIONAL COMMISSION ON RADIOLOGICAL PROTECTION, ICRP Publication 26, Pergamon Press, Oxford and New York (1977).

[10.38] GOLNIK, N., BREDE, H.J., GULDBAKKE, S., H*(10) response of the REM-2 recombination chamber in monoenergetic neutron fields, Radiat. Prot. Dosim. **74** (1997) 139–144.

[10.39] GOLNIK, N., KAMIŃSKI, P., ZIELCZYNSKI, M., A measuring system with a recombination chamber for neutron dosimetry around medical accelerators, Radiat. Prot. Dosim. **110** (2004) 273–276

[10.40] TULIK, P., GOLNIK, N., ZIELCZYNSKI, M., Recombination chambers filled with different gases — studies of possible application for BNCT beam dosimetry, Radiat. Prot. Dosim. **110** (2004) 669–673.

[10.41] MAYER, S., GOLNIK, N., KYLLÖNEN, J.E., MENZEL, H.G., OTTO, T., Dose equivalent measurements in a strongly pulsed high-energy radiation field, Radiat. Prot. Dosim. **110** (2004) 759–763.

[10.42] ZIELCZYNSKI, M., A new approach to the dosimetry of mixed radiation using a recombination chamber, Radiat. Prot. Dosim. **110** (2004) 267–271.

[10.43] APFEL, R.E., The superheated drop detector, Nucl. Instrum. Methods **162** (1979) 603–608.

[10.44] ING, H., BIRNBOIM, H.C., A bubble-damage polymer detector for neutrons, Nucl. Tracks Radiat. Meas. **8** (1984) 285–288.

[10.45] D'ERRICO, F., Radiation dosimetry and spectrometry with superheated emulsions, Nucl. Instrum. Methods B **184** (2001) 229–254.

[10.46] BOURGOIS, L., DELACROIX, D., OSTROWSKY, A., Use of bubble detectors to measure neutron contamination of a medical accelerator photon beam, Radiat. Prot. Dosim. **74** (1997) 239–246.

[10.47] DAS, M., SAWAMURA, T., KITAICHI, M., SAWAMURA, S., Application of superheated emulsion in neutron spectrometry at 45 MeV electron LINAC, Nucl. Instrum. Methods Phys. Res. A **517** (2004) 34–41.

[10.48] OLSHER, R.H., et al., PRESCILA: A new, lightweight neutron rem meter, Health Phys. **86** (2004) 603–612.

[10.49] NATIONAL COUNCIL ON RADIATION PROTECTION AND MEASUREMENT, Report No. 038 — Protection Against Neutron Radiation, NCRP, Bethesda, MD (1971).

[10.50] HANKINS, D.E., "The effect of energy dependence on the evaluation of albedo neutron dosimeters", Proc. Ninth Midyear Topical Symp. on Operational Health Physics, Denver, USDOE, Washington, DC (1976) 861–868.

[10.51] PIESCH, E., BURGKHARDT, B., "Measurement of neutron field quantities using the single sphere albedo technique," Proc. Fifth Symp. on Neutron Dosimetry, Munich/Neuherberg, 17–21 Sep. 1984, EUR 9762, Commission of the European Communities, Luxembourg (1985) 403–414.

[10.52] PIESCH, E., BURGKHARDT, B., COMPER, W., The single sphere albedo system — a useful technique in neutron dosimetry, Radiat. Prot. Dosim. **10** (1985) 147–157.

[10.53] HARVEY, J.R., HART, C.D., A neutron survey instrument which gives information on the low energy neutron spectrum and can be used for albedo dosemeter calibration, Radiat. Prot. Dosim. **23** (1988) 277–280.

[10.54] NAISMITH, O.F., SIEBERT, B.R.L., THOMAS, D.J., Response of neutron dosemeters in radiation protection environments: an investigation of techniques to improve estimates of dose equivalent, Radiat. Prot. Dosim. **70** (1997) 255–260.

[10.55] TAYLOR, G.C., THOMAS, D.J., "Improved measurements of neutron dose equivalent rates using a dual instrument technique", Proc. 14th Symp. on Microdosimetry, Venice, Sep. 2005, Radiat. Prot. Dosim. **122** (2006) 393–395.

[10.56] INTERNATIONAL ELECTROTECHNICAL COMMISSION, Radiation protection instrumentation — Installed dose equivalent rate meters, warning assemblies and monitors for neutron radiation of energy from thermal to 15 MeV, International Standard IEC 61322, IEC, Geneva (1994).

[10.57] THEIS, C., FORKEL-WIRTH, D., PERRIN, D., ROESLER, S., VINCKE, H., Characterisation of ionisation chambers for a mixed radiation field and investigation of their suitability as radiation monitors for the LHC, Radiat. Prot. Dosim. **116** (2005) 170–174.

[10.58] INTERNATIONAL ELECTROTECHNICAL COMMISSION, Radiation protection instrumentation — Neutron ambient dose equivalent (rate) meters, International Standard IEC 61005, edn 3.0, IEC, Geneva (2014).

11. PERSONAL NEUTRON DOSIMETERS

11.1. NEUTRON DOSIMETER TYPES

Personal neutron dosimeters can be worn as an adjunct to the more common photon dosimeter or photon–beta dosimeter, but some designs of personal dosimeters combine the functions of photon, beta and neutron dosimeters into a single unit [11.1]. The detection methods used for personal neutron dosimetry are varied, and each has its advantages and disadvantages. The following subsections describe the characteristics of the most commonly employed personal neutron dosimeters. Many types of neutron dosimeters have been, and continue to be, under development; however, this section will focus primarily on those dosimeters that are commercially available and widely used. The required characteristics of these devices are covered in two IEC standards [11.2, 11.3]. Some advances will be included to show the possible directions of future work.

It is important to define the requirements for a personal neutron dosimeter before deciding on the specific design to be used. For instance, consideration should be given as to the characteristics of the neutron fields expected to be encountered. The relative fractions of neutron and gamma ray doses present will influence the dosimeter choice, along with the energy and angle distribution of the neutron fluence. The choice of dosimeter will also be influenced by the need to either obtain an immediate indication from the dosimeter, for example, where neutron dose rates are high, or to read it out at the end of a time period that may vary from days to months [11.4]. Practical considerations such as size, weight, susceptibility to environmental conditions including temperature and humidity, the method of wearing the dosimeter in the proper orientation and cost will all need to be evaluated for a particular application. Specific details on the operational principles and applications of each neutron dosimeter type are provided in the following subsections.

Among the most commonly used passive neutron dosimeter types are etched track dosimeters and TLD albedo dosimeters. These may be worn for extended periods of time, ranging from several weeks to as much as one year. At the end of the prescribed time period, they are processed and their readings are analysed to determine the personal dose equivalent. Commercial processing of these dosimeters is available. Etched track detectors have an inherent insensitivity to photons, so they are useful in workplace situations where there might be a large photon component in the mixed neutron–photon field. The photon component of the mixed field may be measured using another dosimeter with a high sensitivity to photons and low sensitivity to neutrons.

FIG. 11.1. A commercially available etched track dosimeter containing both a hydrogenous and a boron loaded converter layer. These can be seen inside the dosimeter case on the right. The etched track plastic material is on the left. (Courtesy of Chiyoda Technol.)

11.2. ETCHED TRACK DOSIMETERS

When neutrons interact with insulating materials, such as the plastic film shown in Fig. 11.1, the secondary charged particles that are produced, such as protons and alpha particles, will cause damage in the material, and that damage can provide an indication of dose equivalent. In addition to charged particles produced within the plastic, particles from a conversion layer are often used, for example, a hydrogenous layer in contact with the plastic. Protons from (n,p) reactions with hydrogen can then enter the plastic. The damage sites in the plastic are treated chemically or electrochemically, and visible pits or tracks are formed that can be counted and related to the dose equivalent to which the dosimeter has been exposed. Since there is a LET dependent threshold for production of visible tracks, the fluence response as a function of energy for these detectors exhibits a threshold that is dependent upon the track detector material, as well as the methods used for processing and readout.

This lower energy region of the fluence response can be improved by the use of certain converter layers, such as boron loaded Teflon, over an area of the plastic film. When low energy neutrons interact with the material, alpha particles are produced by the ^{10}B(n,α)^{7}Li interaction and damage tracks are produced. A similar effect can be obtained using a lithium loaded material producing charged particles via the ^{6}Li(n,α)T reaction.

As neutron energy increases into the region above a few MeV, secondary charged proton energies increase, and these particles deposit their energy deeper in the detector. The tracks formed by these higher energy charged particles are less visible at the surface of the detector, so the fluence response decreases at higher neutron energies. An example of the personal dose equivalent, $H_p(10)$, response of two etched track dosimeters is shown in Fig. 11.2.

The material most often used in etched track dosimeters is PADC, which is commercially available under the trade name of CR-39. This plastic is sensitive to energetic protons and can detect fast neutrons either from a hydrogenous radiator or from its own hydrogen content (see also Section 8.2.4). Chemical and electrochemical etching of PADC dosimeters dissolves material within the charged particle damage track, thus making it more visible [11.5]. Tracks can be counted using optical systems, some of which have been automated for use by dosimetry services. Etched track dosimeters are also commercially available, as are services to read out the dosimeters. It should be noted that electrochemically etched dosimeters have a lower fast neutron threshold than chemically etched dosimeters, but the threshold is also strongly dependent on the readout method [11.4].
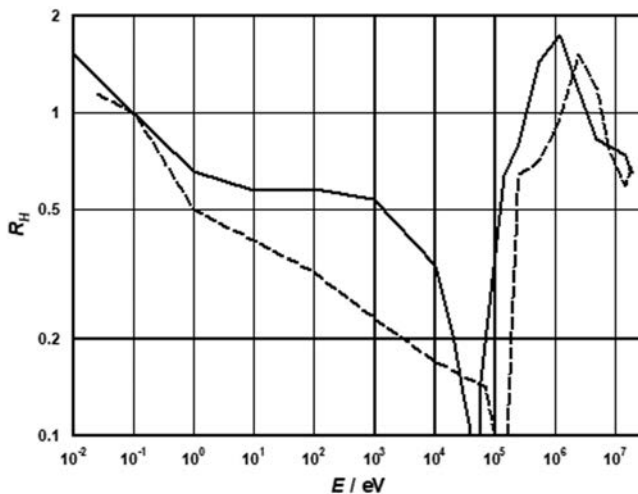
FIG. 11.2. The personal dose equivalent response, R_H, as a function of energy is shown for two etched track dosimetry systems using converters. One has been chemically etched (dashed line), the other electrochemically etched (solid line). Both have converter layers to extend the response to low energies. The curves are normalized to 1 mSv^{-1} for neutrons from a ^{241}Am-Be source. (Reproduced from Ref. [11.4] with permission from ICRU.)

11.3. THERMOLUMINESCENT ALBEDO DOSIMETERS

Thermoluminescent albedo dosimeters are sensitive to both photons and neutrons, and thus require an additional dosimeter element that will preferentially detect photons in a mixed field. In workplaces in the nuclear industry, where low energy neutrons often predominate, these dosimeters can have a somewhat lower dose equivalent detection limit than etched track dosimeters.

TLDs have been used to measure photon dose equivalent for many years [11.6–11.8]. The thermoluminescence mechanism involves the ionization of electrons as a result of the energy deposited by the incident radiation, which then become trapped in metastable states. Heating the material to a few hundred degrees Celsius results in the recombination of electrons and holes, leading to the emission of light that is proportional to the dose deposited by the ionizing radiation. Thermoluminescence can occur in an inorganic material, such as LiF into which parts per million quantities of impurities have been incorporated. Mg and Ti impurities in small concentrations produce defects in the LiF crystal lattice structure, which can act as luminescence centres or trapping sites, via the creation of energy levels in the forbidden band between the valence and conduction bands. When ionizing radiation imparts energy to valence band electrons and excites them into the conduction band, some of the electrons will become trapped at the impurity centres. Heating of the material can then provide enough energy to release the electrons from traps, whereupon they can recombine with holes in the valence band. This results in the emission of light, whose intensity is measured using a photomultiplier tube. The trapping sites in LiF:Mg,Ti (this notation indicates that Mg and Ti are added as impurities or dopants) can retain trapped electrons for quite some time (i.e. months or longer). When these TLDs are read out by heating, a quantity of light is emitted that is proportional to the accumulated dose deposited over the entire time period. Thus, the amount of energy stored as trapped electrons in the dosimeter material will be proportional to a worker's personal dose equivalent, which can be measured after a period of one week, one month or one year. During extended time periods there is a loss of signal caused by leaking of electrons from traps, but this 'fading' can be measured and accounted for in the determination of personal dose equivalent.

TLD materials containing ^{6}Li or ^{10}B are more sensitive to thermal neutrons than photons because of the large low energy neutron cross-sections of the ^{6}Li(n,α)T and ^{10}B(n,α)^{7}Li reactions. Materials such as ^{6}LiF:Mg,Ti and ^{6}LiF:Mg,Cu,P, $Li_2B_4O_7$:Mn and $^6Li_2{}^{10}B_4O_7$:Mn are all effective low energy neutron thermoluminescent detectors. Many other solid state materials with varying dopants have been used as TLDs [11.6–11.8], but only a few combinations serve as useful neutron detectors.

Since neutron fields are nearly always accompanied by some fraction of photons, it is necessary to evaluate the contributions from both types of radiation, and this can be accomplished by using additional TLDs that are more sensitive to photons than neutrons. A TL material such as LiF can be enriched in the isotope ^{7}Li, thus lowering its sensitivity to neutrons and making it a more efficient photon detector in a mixed neutron–photon field. When the same material is enriched in ^{6}Li, it becomes an effective low energy neutron detector. Thus, the use of the two materials, ^{7}LiF:Mg,Ti and ^{6}LiF:Mg,Ti, makes it possible to measure the separate contributions of photons and neutrons in a mixed field.

TLD albedo neutron dosimeters rely on the principle of using one detector for albedo neutrons reflected from the body of a worker, while another detector in the dosimeter is used to measure the slow neutrons in the field [11.9]. Since the detectors are mounted in a dosimeter that is worn on the body of a worker, the dosimeter will be exposed to slow neutrons from a source in the workplace as well as albedo neutrons reflected from the body. The differentiation between slow neutrons from the source and albedo neutrons, which are also slow, is carried out using cadmium or boron loaded plastic filters to absorb low energy neutrons (see Section 3). The indication from the incident source neutrons is obtained from the readings of two neutron sensitive detectors, such as ^{6}LiF:Mg,Ti, one of which is behind a slow neutron absorbing material and receives albedo neutrons, while the other has an absorber behind it facing the body and thus records incident slow neutrons. The ratio of the indications of the two neutron sensitive detectors can also be used as a correction factor to account for different neutron spectra in different workplace locations. A schematic diagram of an albedo neutron dosimeter [11.1] is shown in Fig. 11.3, which shows the TLD detectors and various filters. The difference in the indications of TLDs 2 and 3 indicates the thermal neutron contribution. Detector 4 gives an indication of the thermal plus fast neutron contribution. Detector 1 indicates primarily the photon dose equivalent that is used to compute the neutron personal dose equivalent.

The lower dose equivalent detection limit for an albedo dosimeter using LiF:Mg,Ti is in the range of 20–100 µSv. The higher values are associated with higher energy neutron fields [11.9]. The response increases linearly with increasing dose equivalent, to doses well above normal protection levels. The angle dependence of the dose equivalent response of a TLD albedo neutron dosimeter to unmoderated and moderated ^{252}Cf fission neutrons agrees quite well with that expected for $H_p(10)$, up to an angle of 90° [11.10].

TLDs offer a number of advantages for personal dosimetry, including simplicity, low cost, ease of automated reading, durability, linearity of response over a wide range and a low detection limit. Automated readers for TLDs are available, and commercial services can also process these dosimeters. Their main shortcomings are a strong energy dependence and high photon sensitivity.
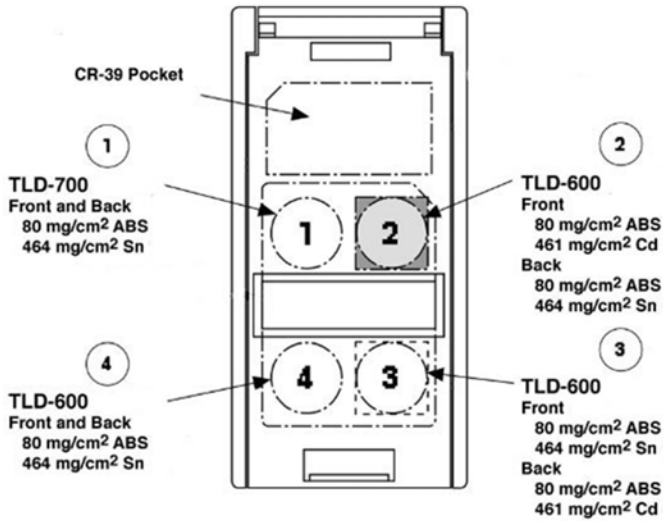
FIG. 11.3. Multipurpose neutron–photon dosimeter where elements 2 and 3 have cadmium filters approximately 0.53 mm thick in front (facing the neutron source) and back (facing the wearer), respectively. TLD-700 and TLD-600 refer to ^{7}LiF:Mn,Ti and ^{6}LiF:Mn,Ti, respectively. ABS (acrylonitrile-butadiene-styrene) plastic and Sn filters are used to place the detectors at the required depths and also to filter certain photon energies [11.1]. (Courtesy of the Pacific Northwest National Laboratory, operated by Battelle for the US Department of Energy.)

TLDs are relatively insensitive to environmental influence quantities, such as temperature, pressure and electromagnetic fields. They must, however, be protected from contamination by materials such as dirt or oils from fingerprints that could interfere with light emission during heating to approximately 300°C. Some TLDs are also sensitive to visible or ultraviolet light. The personal dose equivalent response is shown in Fig. 11.4 as a function of neutron energy for a typical TLD albedo neutron dosimeter.

Because of the strong energy dependence of the albedo dosimeter's response, as seen in Fig. 11.4 by the drop off in response above about 100 keV, a single calibration factor cannot be used in different neutron fields with widely varying spectra. Instead, location specific calibration factors can be established based on a characterization of the neutron energy spectrum at each location (see Section 14), or a simulated workplace calibration field can be used [11.11]. If a dosimeter is used in locations with similar neutron spectra, it is necessary to keep a record of the location(s) in which the dosimeter was used and to apply appropriate calibration factors to the reading (see Sections 5 and 14). It should also be kept in mind that a cadmium filter may produce secondary gamma rays
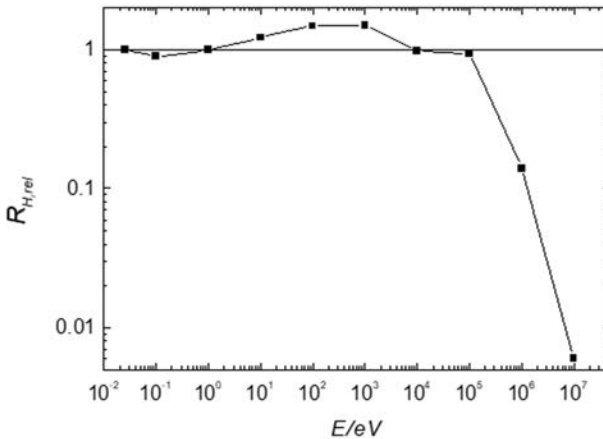
FIG. 11.4. An example of personal dose equivalent response as a function of neutron energy for a TLD albedo dosimeter is shown for a dosimeter-to-body gap of 2 cm. Fluence to personal dose equivalent conversion coefficients from ICRP 74/ICRU Report 57 [11.12] are used. (Reproduced from Ref. [11.4] with permission from ICRU.)

resulting from neutron interactions. These 558 keV gamma rays may be detected by the TL material, and it will be necessary to account for their contribution to the signal produced by the albedo dosimeter.

Since TLD albedo dosimeters are sensitive to albedo neutrons reflected from the body, it is necessary to keep them close to the body surface. These dosimeters should not be worn on a necklace that permits a distance larger than 1–2 cm to be interposed between the body surface and the rear face of the dosimeter [11.13].

Another type of neutron dosimeter making use of physical principles similar to TLDs is based on the use of phosphate glass in which luminescence centres can be created by neutron irradiation [11.14]. This type of dosimeter is not widely used, but improvements in production may make it viable in some applications.

11.4. COMBINED ETCHED TRACK AND TL DOSIMETERS

The advantages of etched track dosimeters in the higher energy region and of albedo dosimeters in the low energy region have indicated the advantages of a dosimeter based on both approaches. Etched track dosimeters with both a 'fast' converter, a hydrogenous layer, and a 'slow' converter, a layer containing lithium
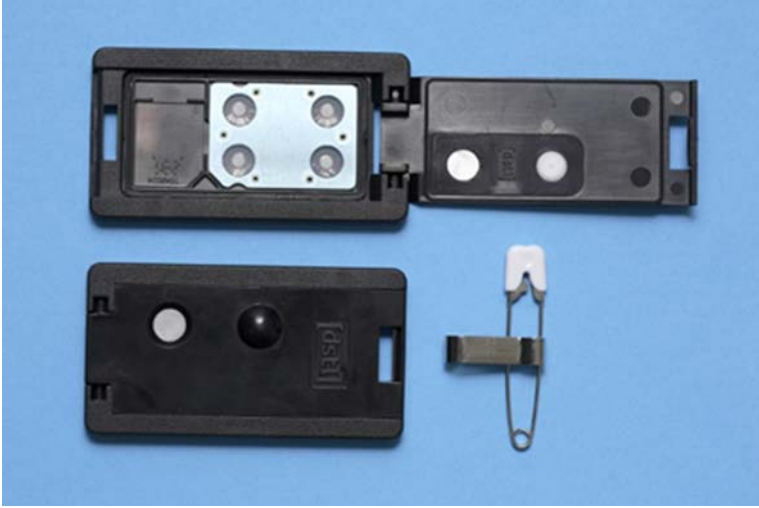
FIG. 11.5. An example of a combined etched track and TLD. The etched track material is to the left in the upper picture and the TLD elements are to the right of it. (© Crown copyright (2011), Dstl. This material is licensed under the terms of the Open Government Licence.)

or boron, go some way to combining these two features. Another approach is to include both etched track and TLD elements in the same dosimeter. Figure 11.5 shows such a dosimeter, and Fig. 11.4 illustrates the various elements schematically.

11.5. SUPERHEATED EMULSION DOSIMETERS

Neutron bubble detectors are also known as superheated emulsion dosimeters or superheated drop detectors. When irradiated by neutrons, visible bubbles are formed, so this type of dosimeter can be read out optically either by a person counting the bubbles or by the use of an automated optical system that performs the counting. The bubbles can also be detected acoustically. These dosimeters are sensitive, with a relatively low dose equivalent detection limit, and they do not respond to photons at the dose rates encountered in radiation protection [11.15, 11.16]. The materials used to produce the bubbles have neutron energy thresholds that can be altered by changing their temperature and pressure. In this way, the detectors can serve as simple spectrometers and indicate an approximate neutron fluence spectrum [11.17]. They are commercially available but are somewhat more expensive than either etched track or TLD
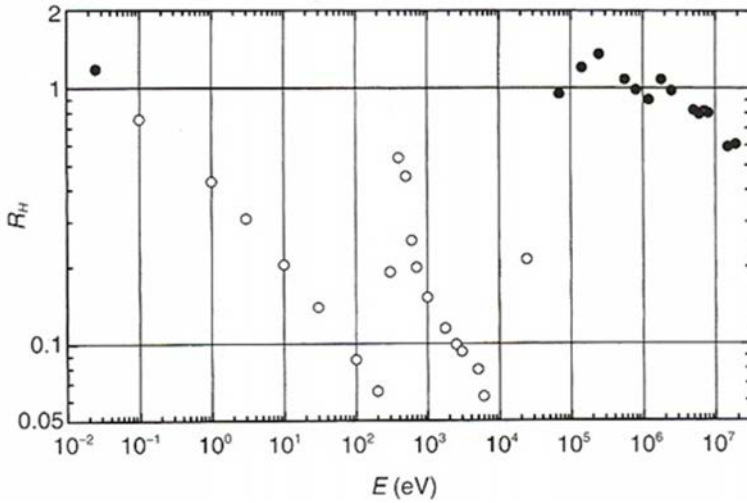
FIG. 11.6. Ambient dose equivalent response as a function of neutron energy for a superheated emulsion detector. The open circles are calculated values and the closed circles are measured values. The response is normalized to one for a ^{241}Am-Be neutron source. (Reproduced from Ref. [11.16] with permission from Oxford University Press.)

albedo dosimeters. Superheated emulsion dosimeters are also susceptible to environmental conditions such as temperature and vibration.

Superheated emulsion detectors make use of halocarbon and hydrocarbon droplets that are overexpanded (superheated) and suspended in a polymeric material or aqueous gel. The dosimeter material is superheated at room temperature, and the charged particles resulting from neutron interactions produce bubbles in the dosimeter. The bubbles persist after irradiation and can be detected and counted using a number of methods, including direct counting by observation or by automated optical and acoustical techniques. The acoustical method detects the sound made when neutron interactions form the bubbles [11.16].

Figure 11.6 shows the energy response of a superheated emulsion detector [11.16]. Most emulsion compositions are relatively insensitive to low LET radiations such as photons and electrons. The range of doses is dependent on the number of bubbles that can be counted. When the bubble density reaches the maximum value, it may no longer be possible to discriminate individual bubbles.

11.6. NUCLEAR EMULSION DOSIMETERS

Nuclear emulsion dosimeters have long been used for personal neutron monitoring, but it is becoming more difficult to obtain the film stock for these dosimeters. Nuclear emulsion dosimeters are susceptible to environmental conditions such as extremes of temperature and humidity. They have a relatively high neutron energy threshold, and their processing and analysis are fairly labour intensive [11.18, 11.19]. Nonetheless, nuclear emulsion dosimeters continue to be used in some laboratories that have extensive experience in their use.

Photographic film may be used as a neutron dosimeter, since neutron interactions with the film emulsion will result in the production of secondary charged particles that cause the silver halide in the emulsion to form an image after development. Since the emulsion contains nitrogen, secondary protons will be produced by the ^{14}N(n,p)^{14}C reaction, along with elastically scattered protons from hydrogen atoms. High energy neutrons above approximately 20 MeV will produce spallation reactions resulting in the formation of multiple tracks from a single event, known as 'stars'. Analysis of the tracks left by protons can be performed to determine the distribution of neutron energies, and the dose equivalent can also be evaluated. After development, nuclear emulsions can be
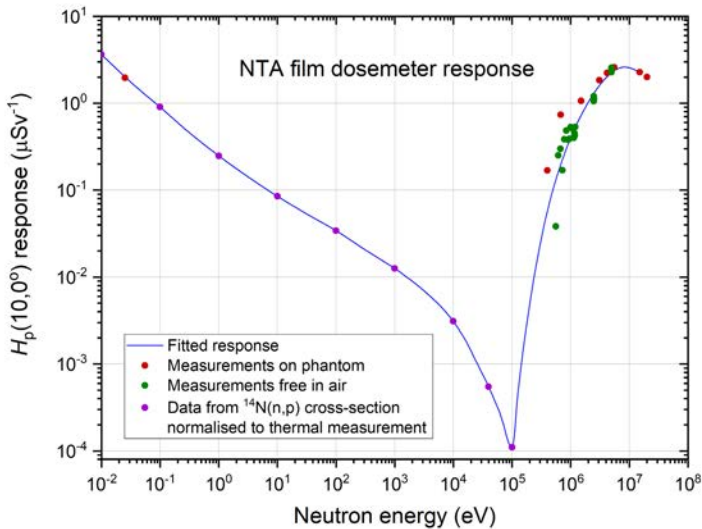

FIG. 11.7. The personal dose equivalent response, R_H, of an NTA film dosimeter for frontal irradiation is shown as a function of the energy, E, of incident neutrons, normalized to unity for Am-Be neutrons [11.18]. (Data from Ref. [11.19], plot courtesy of National Physical Laboratory.)

analysed using an optical densitometer to measure the transmission at particular wavelengths or by direct counting of tracks under magnification. Since the evaluation of proton tracks is a skill acquired after some experience, this type of dosimeter may not be suitable for all applications. The particular film emulsion used most often is referred to as Nuclear Type A, which had been commercially available but may no longer be obtainable.

Figure 11.7 shows the personal dose equivalent response of a nuclear emulsion dosimeter. The response to slow and thermal neutrons is relatively high, then drops with increasing energy, and the fast neutron threshold for detection is at approximately 0.5 MeV. The lower limit of detection is a few hundred μSv. It has often been found necessary to take special care to enclose nuclear emulsions in packaging that will minimize the effects of humidity. Ambient temperature can also affect the performance of nuclear emulsion dosimeters.

11.7. ELECTRONIC DOSIMETERS

Electronic personal dosimeters using semiconductor detectors have certain advantages over the passive dosimeters described above. These active devices provide an immediate indication of personal dose equivalent and dose equivalent rate. Electronic dosimeters can provide audible and visual alarms at preset levels. Circuitry within the device can store a record of personal dose equivalent as a function of time, and in some models the indication of the device can be broadcast to a central station for analysis and storage of data. The disadvantages of these devices are primarily their cost and relatively large size in comparison with the passive neutron dosimeters described above; but they can be useful to monitor and control specific activities, and for this application they may be quite effective.

Electronic neutron dosimeters make use of semiconductor detectors that can measure the deposition of energy from neutron induced charged particles. These semiconductor detectors generally do not contain hydrogen, so their intrinsic response to low energy neutrons is limited, but similar techniques to those used in passive dosimeters, such as the placement of ^{6}Li or ^{10}B films in contact with a detector in order to increase sensitivity to low energy neutrons, can be used to make an albedo type dosimeter. Hydrogenous converter layers can also be used in conjunction with semiconductor detectors, thus increasing their response to neutrons above 100 keV to 1 MeV. A characteristic of electronic dosimeters that can limit their energy response is the electronic noise that may accompany small amplitude pulses produced by low energy neutrons. This noise must be filtered out, and in the process the response to low energy neutrons may be reduced. Interference from photon induced pulses must also be considered;

therefore the processing of pulses produced by the detector must include a method to separate out the contribution of photons to the neutron personal dose equivalent. For example, one commercially available device with an electronic threshold at approximately 1 MeV to cut off photon induced signals showed a strong energy dependence of its dose equivalent response at intermediate energies (over-response in the range of 2 keV to 100 keV) [11.20]. Two-diode devices can be used to subtract the photon component with paired detectors, only one of which has a hydrogenous converter layer [11.21]. With solid state detectors such as p−n junctions, this approach may allow the detection threshold for fast neutrons via recoil protons to be reduced to approximately 200 keV using just an electronic threshold. Photon discrimination is also possible, in principle, with pulse shape analysis, but this approach requires specially designed electronics [11.22]. Figure 11.8 shows several electronic neutron dosimeters, and a review of their performance characteristics is given in Ref. [11.23].

Figure 11.9 shows the ratio of measured personal dose equivalent, $H_{p,m}(10)$, to the conventionally true value of personal dose equivalent, $H_{p,c}(10)$, as a function of neutron energy for some of the electronic dosimeters shown in Fig. 11.8.

In addition to the electronic personal neutron dosimeters mentioned above, there is a detector that relies on a somewhat different principle of operation

FIG. 11.8. Examples of electronic neutron dosimeters. 1: RADOS DIS-N; 2: FUJI Electric NRNO; 3: Siemens EPD-N and EPD-N2; 4: GSF; 5: SAPHYDOSE-N; 6: University of Munich AMIRA; 7: PTB DOS-2002; 8: ALOKA PDM-313. (Reproduced from Ref. [11.23] with permission from Oxford University Press.)
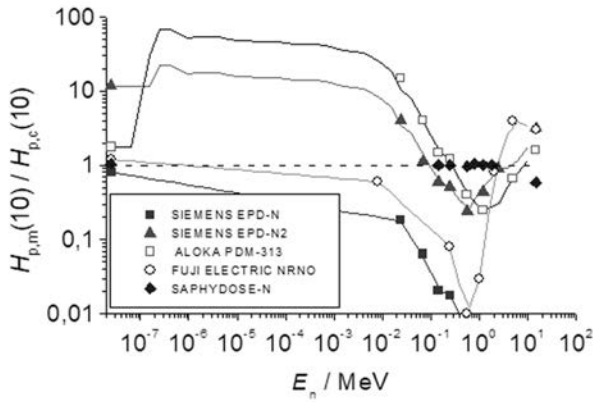
FIG. 11.9. Neutron personal dose equivalent response for normally incident neutrons as a function of neutron energy for commercially available dosimeters. (Reproduced from Ref. [11.23] with permission from Oxford University Press.)
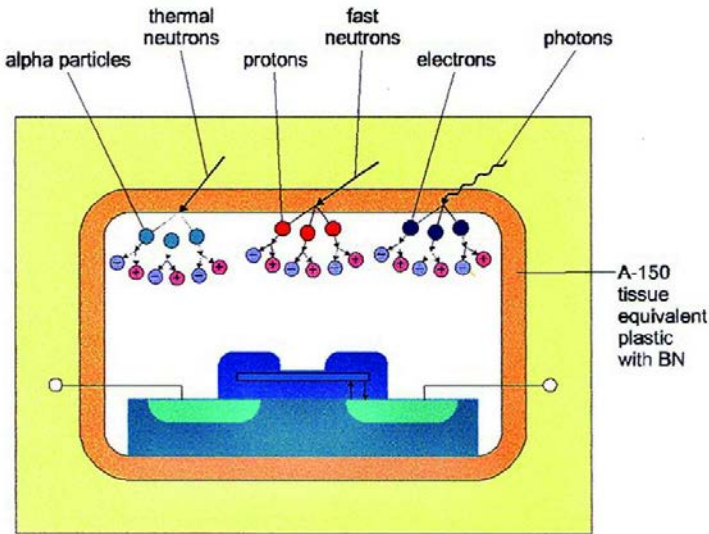
FIG. 11.10. Schematic view of DIS dosimeter showing secondary charged particles generated by neutron interactions in the A-150 plastic wall of the device. Particles are detected by the solid state detector at the base of the dosimeter. (Reproduced from Ref. [11.25] with permission from Oxford University Press.)

than the use of semiconductors. This device is the direct ion storage (DIS) dosimeter [11.24]. It consists of a small ionization chamber with an electronic circuit (an electrically erasable programmable read only memory, known as EEPROM) that detects and stores the charge deposited by neutron induced secondary particles, as shown in Fig. 11.10. The A-150 plastic chamber wall has an elemental composition similar to ICRU tissue. A commercial reader is available to display and record the indications from the dosimeters. The neutron dose is calculated by taking the difference in indications between a neutron/photon device that uses an ionization chamber with wall materials made of A-150 plastics, or polyethylene containing mixtures of boron nitride or $LiNO_3$, and a similar photon sensitive device that uses an ionization chamber with wall materials made of Teflon and/or graphite. The neutron energy response of the device is shown in Fig. 11.11.

The miniaturization of electronics, and the ability to now generate reasonably high bias voltages from batteries, has led to options for new sensors to be incorporated into active personal dosimeters, such as small high pressure ^{3}He tubes. The availability of silicon photomultipliers opens up the possibility of using small volume scintillators, such as CLYC. Both these options offer potentially higher sensitivity.
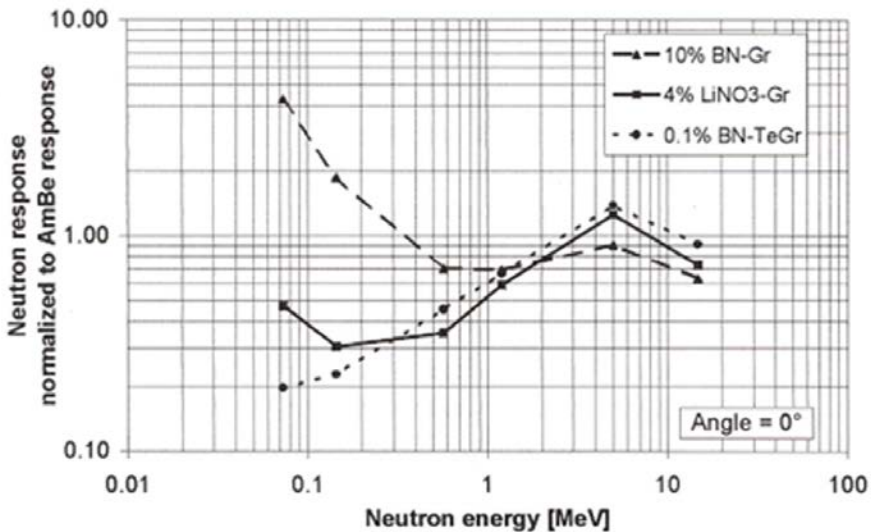
FIG. 11.11. Response of DIS dosimeter normalized to the response obtained when exposed to Am-Be neutrons. (Reproduced from Ref. [11.25] with permission from Oxford University Press.)

11.8. DOSIMETERS FOR SPECIALIZED APPLICATIONS

High energy neutrons can be found in the vicinity of large particle accelerators used for nuclear physics research and near accelerators used for medical applications. Commercial aircraft can also encounter high energy neutrons produced by galactic cosmic rays [11.26]. These neutrons can range in energy from thermal to many GeV (see Section 7). The operational quantities, $H^*(10)$ and $H_p(10)$, are used for monitoring in high energy neutron fields, but in the particular case where, in aircraft, the dose equivalent rate does not significantly vary, the ambient dose equivalent rate, $\dot{H}^*(10)$, may be sufficient for monitoring. Alternatively, the effective dose for aircrew can be calculated using an approved computer code [11.27].

Both TLDs and etched track dosimeters have been used to monitor high energy neutron dose equivalents [11.28–11.32]. The characteristic shapes and sizes of etched tracks can be identified as resulting from various densely ionizing high energy particles and spallation events in the PADC plastic detector. The dose equivalent responses of several types of etched track detectors are shown in Fig. 11.12 [11.33]. Because of the lack of available neutron beams, the responses for energies higher than 200 MeV have been determined with proton beams.
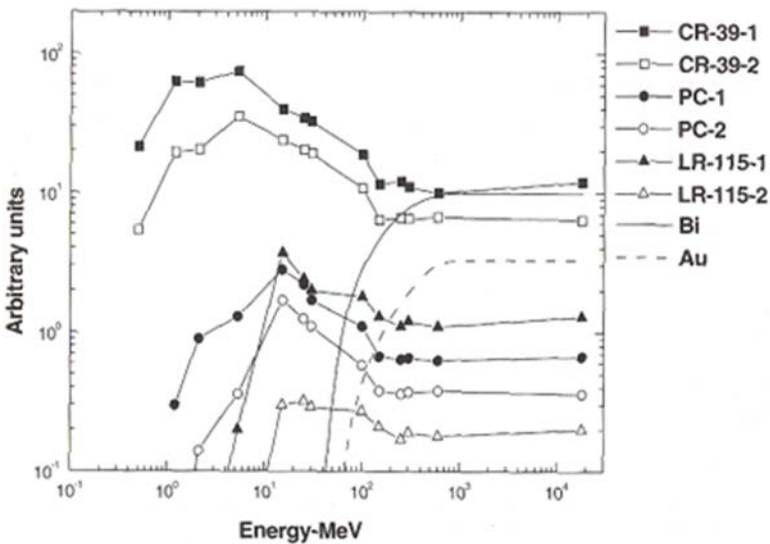
FIG. 11.12. *Comparison of dose equivalent responses of a number of etched track detectors for high energy neutrons. PC stands for polycarbonate, LR-115 is cellulose nitrate, and Bi and Au represent detectors based on the (n,fission) reaction in these elements. (Reproduced from Ref. [11.33] with permission from Oxford University Press.)*

Superheated nuclear emulsion dosimeters have also been used to measure high energy neutrons when the dosimeter is placed in a lead cylinder of up to 3 cm in thickness [11.34]. The lead enclosure generated additional neutrons through (n,xn) reactions (where x is an integer, 2, 3, 4, …) initiated by the incident high energy neutrons. The fluence response as a function of neutron energy for this dosimeter was evaluated using quasi-monoenergetic neutron beams produced at a research cyclotron and is shown in Fig. 11.13.

These high energy neutron dosimeters have been developed for specific purposes by researchers and are not generally available commercially. However, some commercial dosimetry services provide specialized neutron dosimeters for particular high energy neutron applications.
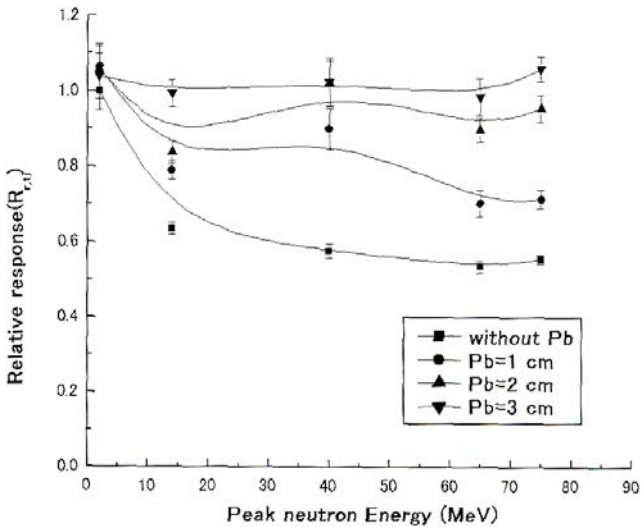
FIG. 11.13. Response relative to the ambient dose equivalent for superheated emulsion detectors surrounded with varying thicknesses of lead. (Reproduced from Ref. [11.34] with permission from Oxford University Press.)

REFERENCES TO CHAPTER 11

[11.1]   RATHBONE, B.A, HUNEYCUTT, S.E., JOHNSON, M.L., Hanford External Dosimetry Technical Basis Manual, PNL-MA-842, Pacific Northwest National Laboratory, Richland, WA (2011).

[11.2]   INTERNATIONAL ELECTROTECHNICAL COMMISSION, Radiation protection instrumentation — Passive integrating dosimetry systems for environmental and personal monitoring Part 1: General characteristics and performance requirements, International Standard IEC 62387-1, IEC, Geneva (1994).

[11.3]   INTERNATIONAL ELECTROTECHNICAL COMMISSION, Radiation protection instrumentation — Measurement of personal dose equivalents $H\mathrm{p}(10)$ and $H\mathrm{p}(0,07)$ for X, gamma, neutron and beta radiations — Direct reading personal dose equivalent meters, International Standard IEC 61526, IEC, Geneva (2013).

[11.4]   INTERNATIONAL COMMISSION ON RADIATION UNITS AND MEASUREMENTS, Determination of Operational Dose Equivalent Quantities for Neutrons, Report 66, ICRU, Bethesda, MD (2001).

[11.5]   GRIFFITH, R.V., TOMMASINO, L., "Etch track detectors in radiation dosimetry", The Dosimetry of Ionizing Radiation, Vol. 3 (KASE, K.R., BJARNGARD, B.E., ATTIX, F.H., Eds), Academic Press, New York (1990) Ch. 4.

[11.6]   FOWLER, J.F., ATTIX, F.H., "Solid state integrating dosimeters", Radiation Dosimetry, Vol. 2, Academic Press, New York (1966) 241–290.

[11.7]   CAMERON, J.R., SUNTHARALINGHAM, N., KENNEY, G.N., Thermoluminescent Dosimetry, University of Wisconsin Press, Madison, WI (1968).

[11.8]   HOROWITZ, Y., YOSSIAN, D., Computerised glow curve deconvolution: application to thermoluminescence dosimetry, Radiat. Prot. Dosim. **60** (1995) 1–114.

[11.9]   PIESCH, E., BURGKHARDT, B., Albedo dosimetry system for routine personnel monitoring, Radiat. Prot. Dosim. **23** (1988) 117–120.

[11.10]   TANNER, J.E., McDONALD, J.C., STEWART, R.D., WERNLI, C., Dose equivalent response of personal neutron dosemeters as a function of angle, Radiat. Prot. Dosim. **70** (1997) 165–168.

[11.11]   CHARTIER, J.-L., JANSKY, B., KLUGE, H., SCHRAUBE, H., WIEGEL, B., Recent developments in the specification and achievement of realistic neutron calibration fields, Radiat. Prot. Dosim. 70 (1997) 305–312.

[11.12]   INTERNATIONAL COMMISSION ON RADIOLOGICAL PROTECTION, Conversion Coefficients for Use in Radiological Protection Against External Radiation, ICRP Publication 74, Pergamon Press, Oxford and New York (1995); ICRU, Conversion Coefficients for Use in Radiological Protection Against External Radiation, ICRU Report 57, International Commission on Radiation Units and Measurements, Bethesda, MD (1998).

[11.13]   PIESCH, E., BURGKHARDT, B., VENKATARAMAN, G., Study of the phantom distance effect of albedo neutron dosemeters, Radiat. Prot. Dosim. **3** (1982) 39–45.

[11.14]   BURGKHARDT, B., UGI, S., VILGIS, M., PIESCH, E., Experience with phosphate glass dosemeters in personal and area monitoring, Radiat. Prot. Dosim. **66 (**1996) 83–88.

[11.15]   ING, H., BIRNBOIM, H.C., A bubble-damage polymer detector for fast neutrons, Nucl. Tracks Radiat. Meas. **8** (1984) 285–288.

[11.16]   D'ERRICO, F., BOS, A.J.J., Passive detectors for neutron personal dosimetry: state of the art, Radiat. Prot. Dosim. **110** (2004) 194–200.

[11.17]   D'ERRICO, F., Radiation dosimetry and spectrometry with superheated emulsions, Nucl. Instrum. Methods **184** (2001) 229–254.

[11.18]   DREW, D.W., THOMAS, D.J., Measurements of the Response Functions of PADC Track-Etch and NTA Film Personal Neutron Dosemeters Over the Energy Range from 100 keV to 5 MeV, NPL Report CIRM 11, National Physical Laboratory, Teddington, UK (1998).

[11.19]   TANNER, R.J., et al., Effect of the Energy Dependence of Response of Neutron Personal Dosemeters Routinely Used in the UK on the Accuracy of Dose Estimation, NRPB-W25, National Radiological Protection Board, Chilton, UK (2001).

[11.20]   ALBERTS, W.G., DIETZ, E., GULDBAKKE, S., KLUGE, H., Response of an electronic neutron dosemeter, Radiat. Prot. Dosim. **53** (1994) 207–210.

[11.21]   BARELUND, B., et al., Principles of an electronic dosemeter using a PIPS detector, Radiat. Prot. Dosim. **44** (1992) 363–366.

[11.22]   BORDY, J.-M., et al., Single diode detector for individual neutron dosimetry using pulse shape analysis, Radiat. Prot. Dosim. **70 (**1997) 73–78.

[11.23]   LUSZIK-BHADRA, M., Electronic personal dosemeters: the solution to problems of individual monitoring in mixed neutron/photon fields? Radiat. Prot. Dosim. **110** (2004) 747–752.

[11.24]   FIECHTNER, A., BOSCHUNG, M., WERNLI, C., Present status of the personal neutron dosemeter based on direct ion storage, Radiat. Prot. Dosim. **110** (2004) 213–217.

[11.25]   FIECHTNER, A., WERNLI, C., KAHILAINEN, J., A prototype personal neutron dosemeter based on an ion chamber and direct ion storage, Radiat. Prot. Dosim. **96** (2001) 269–272.

[11.26]   HEINRICH, W., ROESLER, S., SCHRAUBE, H., Physics of cosmic radiation fields, Radiat. Prot. Dosim. **86** (1999) 253–258.

[11.27]   SCHRAUBE, H., HEINRICH, W., LEUTHOLD, G., MARES, V., ROESLER, S., EPCARD, European program package for the calculation of aviation route doses, GSF-Bericht 08/02, Neuherberg (2002), available at https://www.helmholtz-muenchen.de/en/epcard-neu/index.html

[11.28]   HORWACIK, T., BILSKI, P., OLKO, P., SPURNY, F., TUREK, K., Investigations of doses on board commercial passenger aircraft using CR-39 and thermoluminescent detectors, Radiat. Prot. Dosim. **110** (2004) 377–380.

[11.29]   BARTLETT, D.T., HAGER, L.G., TANNER, R.J., The use of passive personal neutron dosemeters to determine the neutron dose equivalent component of radiation fields in spacecraft, Radiat. Prot. Dosim. **110 (**2004) 405–409.

[11.30]   HÖFERT, M., BARTLETT, D.T., PIESCH, E., Personnel neutron monitoring around high energy accelerators, Radiat. Prot. Dosim. **20** (1987) 103–108.

[11.31]   SPURNÝ, F., Dosimetry of neutrons and high energy particles with nuclear track detectors, Radiat. Meas. **25** (1995) 429–436.

[11.32]   SPURNÝ, F., TUREK, K., Track-etched detectors for the dosimetry of the radiation of cosmic origin, Radiat. Prot. Dosim. **109** (2004) 375–381.

[11.33]   TOMMASINO, L., Advanced passive detectors for neutron dosimetry and spectrometry, Radiat. Prot. Dosim. **110** (2004) 183–186.

[11.34]   DAS, M., et al., Superheated emulsions as high-energy neutron dosemeters, Radiat. Prot. Dosim. **110 (**2004) 325–331.

12. NUCLEAR ACCIDENT DOSIMETRY

12.1. INTRODUCTION

In nuclear facilities where fissionable material is present and there is a potential for a criticality accident, special dosimeter types must be provided. A nuclear criticality accident may result from fissile material being placed in a geometry or physical position where a chain reaction can occur. The position or location of the fissile material resulting in a criticality could include its proximity to hydrogenous material such as water. Hydrogenous materials can reflect and moderate fast neutrons, thereby increasing the population of slow neutrons that can contribute to the chain reaction.

Since the neutron fluence spectrum produced in a criticality accident will likely differ from the ambient spectra in the facility [12.1], the accident dosimeter should have a capability for providing a simple, few channel, neutron fluence spectrum. The neutron spectrum resulting from a criticality depends upon the geometry of the material, the composition of surrounding materials such as water, and the composition and geometry of walls that might reflect neutrons. Since nuclear accident doses may amount to several gray, the dynamic range of these dosimeters must be larger than for the types of dosimeters normally used in routine power plant operation. At accident levels, protection quantities such as dose equivalent should not be used [12.2] because the protection quantities take into account the stochastic biological effects at low doses. At high doses above a few tenths of a gray, deterministic effects such as cell killing occur, and the radiation weighting factors used for low doses are not appropriate. Absorbed doses to tissue should be determined, and a value of the relative biological effectiveness should be evaluated for the specific neutron fluence spectrum. The relative biological effectiveness is the ratio of the dose of 250 kVp X rays to produce a particular biological effect (usually cell killing) to the dose of neutrons to produce the same effect. Nuclear accident dosimeters must also be able to measure large absorbed doses of gamma rays in the presence of the aforementioned large doses of neutrons. Because of the serious effects of a criticality incident, it is necessary that nuclear accident dosimeters be read out quickly, usually within 24 hours, so that appropriate medical decisions can be made.

12.2. INSTALLED AND PERSONAL NUCLEAR ACCIDENT DOSIMETERS

Nuclear accident dosimeters are of two general types: those that are worn on the body and those that are installed at fixed locations in the facility. Installed accident dosimeters should be capable of determining neutron absorbed dose with an accuracy of about ±25% from 0.1 Gy to approximately 100 Gy [12.3] and should be able to provide an approximate, few channel, neutron spectrum. These dosimeters should also be capable of measuring fission gamma ray doses from 0.1 Gy to approximately 100 Gy in the presence of neutron radiation with an accuracy of approximately ±25%. Installed nuclear accident dosimeters need to be mounted with a minimal amount of shielding between the potential sources of a criticality and the dosimeter so that the neutron fluence spectrum is not altered by the presence of the shielding and the installed dosimeter will then be exposed to approximately the same fluence spectrum as would an exposed worker. The neutron background radiation at the point of the installed dosimeter should be relatively low so that the reading taken during an emergency is not confounded by a large intrinsic background reading. Personal neutron accident dosimeters should likewise be capable of measuring absorbed dose from 0.1 Gy to approximately 10 Gy with an accuracy of about ±25% [12.3].

Personal neutron accident dosimeters may include several detector materials with different neutron activation cross-sections that are sufficiently well known for a simple fluence spectrum to be determined. Activation foils are commonly used for this purpose. The specific detectors are chosen because their cross-sections are large and exhibit several thresholds in the energy region where neutrons are expected. This region is from thermal to approximately 20 MeV. The neutron interactions in the foils should also produce radionuclides that decay with convenient half-lives, usually of the order of hours, rather than seconds or years. Thus, gamma rays emitted can be conveniently counted using standard NaI or high purity germanium detector systems. The counting of gamma rays is the most convenient method of readout, although some materials will undergo reactions producing beta particles that can be counted with gas flow proportional counters or scintillation detectors. Neutron activation foils composed of indium, copper or gold, and pellets of cadmium-covered sulphur, may be used to estimate the neutron fluence in the energy range expected in criticality accidents. Some properties of these detectors are listed in Table 12.1. The cross-sections for these materials exhibit energy thresholds, as is shown in Fig. 12.1 [12.4], and thus permit the determination of a simple energy spectrum.

Fixed nuclear accident dosimeters are usually passive devices containing activation foils, TLDs and etched track dosimeters. Active criticality alarms have also been designed and used in nuclear facilities. They may incorporate high range ionization chamber detectors and have usually been developed by the

facilities themselves. An example of a fixed passive accident dosimeter is shown in Fig. 12.2 [12.7].

Another type of installed nuclear accident dosimeter is shown in Fig. 12.3. The activation foils used to provide a few channel fluence spectrum evaluation are identified. The foils are enclosed in a 0.8 mm thick Cd box to allow the measurement of all but thermal neutrons. Foils fixed to the outside of the Cd box are used to evaluate the thermal neutron fluence [12.8].
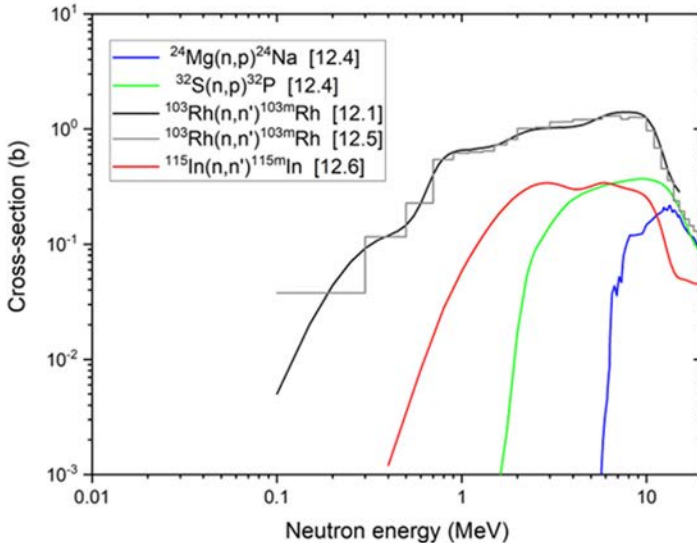
FIG. 12.1. *Cross-sections for neutron induced reactions in several activation foil materials. The energy range over which these cross-sections extend is comparable to the energy range expected in a nuclear criticality accident. Data were derived from Refs [12.1], [12.4], [12.5] and [12.6]. Note that the data from Ref. [12.5] are given as evaluated group cross-sections. (Courtesy of National Physical Laboratory.)*

TABLE 12.1. PROPERTIES OF NEUTRON DETECTORS IN CRITICALITY ACCIDENTS

Neutron energy region	Detector materials	Interactions
Thermal	Cu; In, Au	$^{63}Cu(n,\gamma)^{64}Cu$; $^{115}In(n,\gamma)^{116m}In$; $^{197}Au(n,\gamma)^{198}Au$
Epithermal	Au; Cu	Resonance capture: ^{197}Au; ^{63}Cu
Fast	Rh, In, S, Mg	(n, n′) and (n,p) reactions: ^{103}R, ^{115}In, ^{32}S, ^{24}Mg
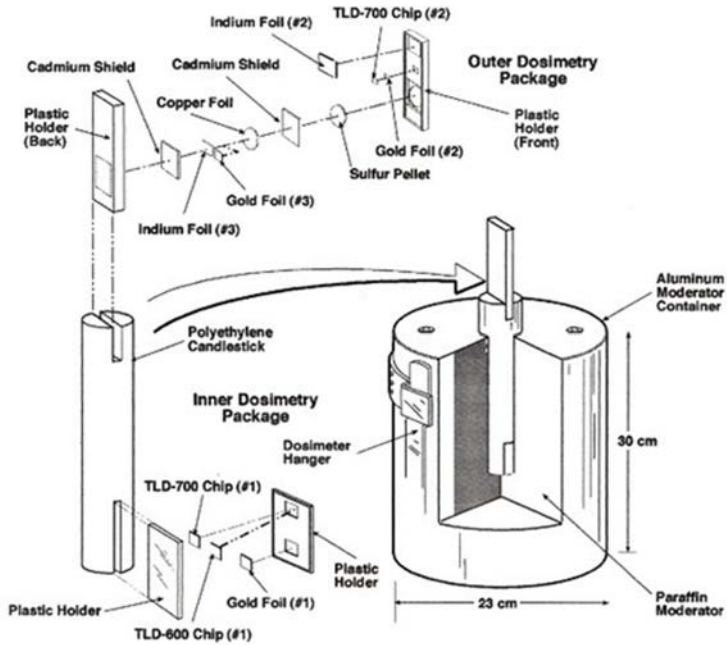
FIG. 12.2. Cutaway view of an installed neutron accident dosimeter containing TLDs for measuring neutron and photon doses. Activation foils and pellets of various materials comprise a simple, few channel spectrometer. Detectors are placed free in air at the top of the dosimeter and within a hydrogenous moderator (paraffin) in order to estimate the effect of moderation of the neutron fluence spectrum within the body [12.7]. (Courtesy of the Pacific Northwest National Laboratory, operated by Battelle for the US Department of Energy.)
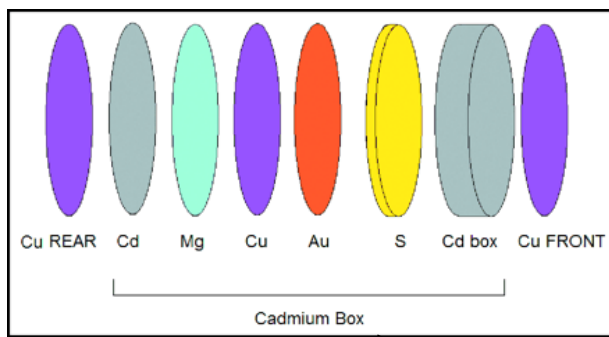
FIG. 12.3. This diagram shows the activation foils contained in the ENEA Radiation Protection Institute's area accident dosimeter enclosed in a cadmium box. (Reproduced from Ref. [12.8] with permission from Oxford University Press.)
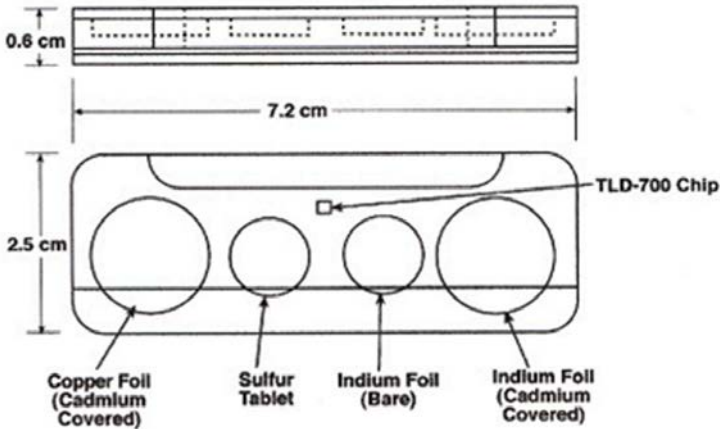
FIG. 12.4. This diagram shows a cross-section and top view of a personal neutron accident dosimeter that may be worn by workers in a nuclear facility. It contains some of the same elements that are used in the installed area monitor, shown in Fig. 12.2 [12.7]. (Courtesy of the Pacific Northwest National Laboratory, operated by Battelle for the US Department of Energy.)

A personal nuclear accident dosimeter is similar in many respects to an installed nuclear accident dosimeter. TLDs and activation foils and pellets, and possibly etched track detectors, are included to provide information similar to that provided by the installed dosimeter. An example of a personal nuclear accident dosimeter is shown in Fig. 12.4.

12.3. SUPPLEMENTAL DOSIMETRY APPROACHES

Supplemental methods of dosimetry may also be used in the event of a criticality accident. These include methods for identifying individuals who have received significant neutron doses based on measurements of ^{24}Na activity induced in the human body. The activity is produced by activation of naturally occurring ^{23}Na by thermal neutron capture. Measurements can be made by placing a photon detector such as a Geiger–Müller probe against the abdomen or armpit of the exposed individual [12.9]. As mentioned earlier, the reaction ^{32}S(n,p)^{32}P has been used in dosimeter detectors. This reaction also occurs in the sulphur contained in human hair and can be used to estimate criticality doses. Analysis of ^{32}P from various parts of the body can also provide information as to the orientation of the incident radiation.

Analysis of the blood of an exposed worker may also be performed to provide information determined from the induced activity of elements in the

blood. Comparison of ^{32}P and blood sodium activation can provide a measure of spectral hardness. Additional neutron interactions that can occur in the exposed individual include capture of thermal neutrons by ^{37}Cl producing ^{38}Cl, which decays with a 37 min half-life and emits 2.17 MeV gammas (47% abundance) and 1.64 MeV gammas (38% abundance). Immediately following exposure, approximately 50% of the blood activity will be from ^{38}Cl that can be counted using a NaI detector [12.10]. Analysis of chromosome aberrations can also provide an estimate of the absorbed dose delivered [12.11].

In the absence of personal nuclear accident dosimeters, metal objects carried by employees can provide estimates of exposure to neutron radiation from analysis of the activation produced. Objects can be counted using gamma spectroscopic equipment, and an assessment of neutron exposure can then be made.

12.4. TOKAIMURA CRITICALITY ACCIDENT

Criticality accidents are thankfully rare; however, their consequences can be serious. This subsection outlines the events that occurred in a recent criticality accident, explains how doses were calculated and describes the outcomes.

On 30 September 1999, a criticality accident occurred at a uranium processing plant operated by the JCO Company in Tokaimura, Japan. The action of pouring a large amount of enriched uranium solution (18.8% ^{235}U by mass) into a precipitation tank led to a chain reaction, which continued for approximately 20 h. External doses in the environment have been estimated by using measurements and calculations [12.12].

The reaction burst was indicated by a gamma ray monitor (an argon-filled ionization chamber) at the JCO facility and by two neutron monitors (moderator type with ^{3}He proportional counters) located approximately 1.7 km and 2.0 km from the JCO site at the Japan Atomic Energy Research Institute (JAERI). Measurements with portable rem counters and ionization chambers started 7 h later at closer distances (approximately 40 m to 750 m). These measurements gave an almost time independent ratio of neutron to photon dose equivalent of 9:1. It indicated that the gamma dose rate was mainly due to prompt and secondary gamma rays, and the contribution from fission products was relatively small.

The measured data were used, together with transport calculations, to determine values for $H^*(10)$ and E. Calculated values of $H^*(10)$ photon dose equivalent at a distance of 300 m were compared with those of TLDs and agreed within approximately 30%. From the calculations, it was concluded that the dose to people who stayed outside a 350 m zone was less than 1 mSv [12.12].

The doses of overexposed workers were estimated by measurement of the specific activity of ^{24}Na in blood [12.13] using methods based on

documents of the IAEA and Oak Ridge National Laboratory. The estimated doses for the three most highly exposed individuals were 5.4 Gy from neutrons and 13 Gy from photons (patient A); 2.9 Gy from neutrons and 4.5 to 6.9 Gy from photons (patient B); and 0.81 Gy from neutrons and 1.3 to 2.0 Gy from photons (patient C). Unfortunately, patients A and B subsequently died; A 12 weeks and B 7 months after the accident.

REFERENCES TO CHAPTER 12

[12.1]   INTERNATIONAL ATOMIC ENERGY AGENCY, Compendium of Neutron Spectra in Criticality Accident Dosimetry, Technical Reports Series No. 180, IAEA, Vienna (1978).

[12.2]   INTERNATIONAL COMMISSION ON RADIOLOGICAL PROTECTION, ICRP Publication 60, Pergamon Press, Oxford and New York (1991).

[12.3]   INTERNATIONAL ATOMIC ENERGY AGENCY, Dosimetry for Criticality Accidents — A Manual, Technical Reports Series No. 211, STI/DOC/10/211, IAEA, Vienna (1982).

[12.4]   KOREA ATOMIC ENERGY RESEARCH INSTITUTE, Cross section plotter, http://atom.kaeri.re.kr/

[12.5]   PAVLIK A., MIAH, M.M.H., STROHMAIER, B., VONACH. H., Update of the evaluation of the cross section of the neutron dosimetry reaction ^{103}Rh(n,n′)^{103m}Rh, IAEA, INDC(AUS)-015, 1995.

[12.6]   CAI, DUNJIU, Evaluation of the cross-sections for dosimetry reactions, IAEA, INDC(CPR)-024, 1991.

[12.7]   RATHBONE, B.A., Hanford Dosimetry Manual, PNL Report, PNL-MA-842, Pacific Northwest National Laboratory, Richland, WA (2005).

[12.8]   GUALDRINI, G., BEDOGNI, R., FANTUZZI, E., MARIOTTI, F., The ENEA criticality accident dosimetry system: a contribution to the 2002 International Intercomparison at the Silene Reactor, Radiat. Prot. Dosim. **110** (2004) 465–469.

[12.9]   TAKAHASHI, F., ENDO, A., YAMAGUCHI, Y., Dose assessment from activated sodium within a body in criticality accidents, Radiat. Prot. Dosim. **106** (2003) 197–206.

[12.10]   HANKINS, D.E., Dosimetry of criticality accidents using activations of the blood and hair, Health Phys. **38** (1980) 529–541.

[12.11]   LINDHOLM, C., SALOMAA, S., Dose assessment of past accidental or chronic exposure using FISH chromosome painting, Radiat. Prot. Dosim. **88** (2000) 21–25.

[12.12]   ENDO, A., YAMAGUCHI, Y., SAKAMOTO, M., TSUDA, S., External doses in the environment from the Tokaimura criticality accident, Radiat. Prot. Dosim. **93** (2001) 207–214.

[12.13]   ISHIGURE, N., ENDO, A., YAMAGUCHI, Y., KAWACHI, K., Calculation of the absorbed dose for the overexposed patients at the JCO criticality accident in Tokai-mura, J. Radiat. Res. **42** Suppl. (2001) 137–148.

13. CHOOSING AN OPERATIONAL SYSTEM

13.1. INTRODUCTION

The choice of dosimeters and survey meters for use as part of a neutron monitoring system depends on a number of factors. Among these factors are the size, number and types of neutron sources, the shielding provided, the energy distributions of the neutron fields, the activities of the workers and the need to monitor dose equivalents to which members of the general public may be exposed. This section will provide guidance as to which devices or systems are appropriate for a number of commonly encountered workplace locations with sources of neutrons.

The complexity and extent of devices and procedures for monitoring neutron exposures should be commensurate with the size of the facility in which the work is performed. A small university laboratory with a single neutron source may require that only one or two workers be monitored and that a single area be subject to surveying. However, a nuclear power plant or fuel fabrication facility may require an extensive set of personal neutron monitors, survey meters, nuclear accident dosimeters and perimeter survey devices to confirm that the level of radiation at the power plant's boundary does not exceed the limit for the general public.

Neutron sources are nearly always shielded using moderating materials that reduce their energy to the point where most of the neutrons have been thermalized. Nevertheless, there are some activities that involve work with neutron sources that are minimally shielded. These activities may take place in a source fabrication facility or a reactor fuel reprocessing plant. No single personal dosimeter will be appropriate for all situations. In fact, it can be said that there is no 'perfect' dosimeter or survey meter. Several devices discussed in earlier sections can be used in a variety of situations, and others are best used only for one or two specific neutron fields.

13.2. PERSONAL DOSIMETERS

Nuclear reactors and their immediate vicinities include a number of areas where neutron monitoring is required to be conducted. Work areas near the reactor containment, or for situations when maintenance is needed within the containment, generally require the use of more than one personal dosimeter type, since there is at present no single dosimeter that has the capability to cover the range of neutron energies encountered. A combination of TLD albedo and etched

track dosimeters is often used because the TLD albedo system performs well at lower neutron energies, whereas the etched track system responds well to higher energy neutrons. Both of these personal dosimeter types are small, lightweight and relatively inexpensive. Commercial equipment is available to perform the readout of TLD dosimeters. Processing systems for etched track dosimeters are also available. Some modern dosimeters may even contain both TLD and etched track sensors.

Neutron dosimeters based on the use of NTA emulsion have been used; however, since the film has been delisted by its manufacturer, Kodak, this method of dosimetry cannot be recommended.

Both TLD albedo and etched track dosimeters can be used in smaller institutions, such as university research laboratories or medical centres. They can also be found in a wide variety of facilities, including high energy accelerators. Their main advantages for use in smaller facilities are that they are compact and relatively inexpensive, respond well to a wide variety of neutron fields and do not require any specialist training for use if the dosimeters are read out by a commercial supplier that can also provide records of worker dose equivalents.

Superheated drop (bubble) dosimeters have desirable characteristics in that they are also relatively small and lightweight. They can provide an immediate visual indication of the presence of neutrons; however, an accurate value for dose equivalent will require readout and analysis in a dosimetry laboratory by a trained dosimetrist. Superheated drop dosimeters are available commercially, but they have not yet been universally adopted for use in many facilities. These dosimeters are more appropriate for use in specialized applications such as those described in Section 12.

Electronic personal neutron dosimeters also have certain advantages for use in specific situations. These devices are not generally useful for monitoring large numbers of workers because they are too expensive and a bit too large as compared with TLD albedo or etched track dosimeters, but electronic dosimeters have a number of advantages that make them particularly suitable for monitoring non-routine work, such as maintenance, or for monitoring occasional entries into radiation areas. In some installations, electronic dosimeters are used as a form of 'turnstile' control, where the worker's electronic dosimeter serves as an admission ticket. Electronic dosimeters generally have the capability to store accumulated personal dose equivalent, so this quantity can be electronically queried, and if it exceeds a specified amount the worker may be refused access to the area. Another useful aspect of the electronic dosimeter for use in access control is the fact that such instruments will alarm at preset levels of dose equivalent or dose equivalent rate. Certain designs have the capability to broadcast their indications to a central control station, and this feature is useful for hazardous applications where work needs to be carefully controlled. Electronic personal neutron dosimeters

are recommended for use in workplaces where immediate readout, alarming at preset levels of dose equivalent and perhaps the broadcast of results to a central station are required. This would normally be in a large nuclear power plant or government nuclear facility.

13.3. SURVEY INSTRUMENTS

Survey instruments are used to perform measurements of the ambient dose equivalent, or ambient dose equivalent rate, in radiation areas. Usually, such measurements are carried out before workers enter these areas, but surveys may also be performed after work has begun in order to ensure that the required dose equivalent rates are not exceeded. Because the determination of ambient dose equivalent rates in a workplace consists of performing a series of measurements at various points in the workplace, survey instruments are usually handheld devices that should be reasonably lightweight and simple to operate.

Section 10 described several types of survey instruments, and the instrument most commonly employed is the device that makes use of a hydrogenous moderator surrounding a ^{3}He, ^{10}B or ^{6}Li based detector having a high sensitivity to low energy neutrons. These instruments have a relatively uniform response to neutrons over a wide range of energies. Their response is such that ambient dose equivalent rates at the low range of those normally encountered in the workplace can be measured.

Survey meters having large hydrogenous moderators can be battery powered and are therefore portable. However, the presence of several kilograms of a moderator such as polyethylene makes the instruments somewhat clumsy to use for long periods of time. In practice, this drawback has not proven to be serious, and this type of instrument is in widespread use. Smaller, more lightweight instruments are available and are useful in certain situations, but the conventional moderator based instrument is probably the best choice for most neutron monitoring applications.

13.4. INSTALLED AREA MONITORS

Instruments designed for use as installed monitors usually make use of the same operating principle as portable survey meters, namely the incorporation of a hydrogenous moderator surrounding a low energy neutron detector. Since these instruments are mounted on a wall or other part of a facility, such as a roof beam or pillar, it is possible and in fact desirable to operate the instruments with mains

power. Monitors of this type are normally connected to an auditory and a visual alarm and may also be connected to a central monitoring station.

In addition to moderator based instruments, large volume, and in some cases pressurized, ionization chambers have also been used successfully to monitor ambient dose equivalent rates as fixed installed monitors. Area monitoring ionization chambers have more restrictive requirements than moderator based instruments, but their advantage is that they are somewhat less expensive and simpler to operate. Ionization chambers used to monitor neutron fields should be constructed of a tissue equivalent plastic, as described in Section 10. Since ionization chambers measure absorbed dose or kerma rate, a conversion coefficient must be applied in the electronic circuitry to enable the devices to display the ambient dose equivalent rate. As mentioned in Section 14, calibration of dose equivalent measuring devices must be carried out carefully. Differences in response between the neutron reference calibration source and the workplace neutron source must be taken into account. In addition, since the ionization chamber measures both neutron and gamma ray doses equally well, the contribution to the total dose from gamma rays must be subtracted. Fortunately, the characteristics of the neutron and gamma ray fields at the position of the installed monitor can be determined, and appropriate corrections can be made to the indications of the ionization chamber to yield ambient dose equivalent rate.

13.5. ACCIDENT DOSIMETERS

Accident dosimeters may be used as personal dosimeters for those workers performing tasks in a nuclear facility where there is a possibility of a criticality accident. Accident dosimeters may also be installed as fixed area monitors. Both applications may be needed in a facility. Staff members who need to work in an area that could experience a criticality incident need to be issued accident dosimeters. These specialized dosimeters are normally worn in addition to neutron or multipurpose neutron–beta–gamma dosimeters.

Installed accident dosimeters may also be needed even when workers are not present in a nuclear facility. They will function as area alarm meters, and if a criticality accident takes place, whether or not workers are present in the immediate vicinity, they can provide an alarm to evacuate any personnel from the facility. As is the case for installed ionization chamber based area monitors, the characteristics of the neutron and gamma ray fields produced by a criticality incident will normally be known beforehand, and so the response of the monitor can be calibrated to alarm at a correct level of radiation intensity. In the case of a criticality accident, the device may be calibrated to measure absorbed dose or tissue kerma rates, which are more appropriate quantities for measurement during

an accident. Personal dose equivalent and ambient dose equivalent are used for protection levels of ionizing radiation intensity, but at levels above approximately 1 Sv, absorbed dose or tissue kerma should be measured.

13.6. SUMMARY OF DOSIMETER OPTIONS

Table 13.1 provides a brief summary of areas where neutron dosimetry is required and devices that could be used to obtain the required information.

TABLE 13.1. SUGGESTED DOSE EQUIVALENT MEASURING DEVICES FOR SOME NEUTRON EXPOSURE LOCATIONS

Neutron field type	Personal dosimeters	Area survey meters	Accident dosimeter[a]
Nuclear reactor	TLD/ETD/SSD/ SDD[b]	Moderator based	Criticality locket
Fuel processing plant	TLD/ETD/SSD/ SDD	Moderator based	Criticality locket
Waste storage facility	TLD/ETD/SSD/ SDD	Moderator based	May be needed
Medical facility	TLD/ETD/SSD/ SDD	Moderator based	Not normally needed
High energy accelerator	ETD/SSD/SDD	Extended range moderator type	Not normally needed
Cosmic (aircrew and space)	ETD/SSD/SDD	TEPC or extended range moderator based	Not normally needed

[a] Accident dosimeters may not be commercially available and may need to be fabricated for specific applications. See Section 12.

[b] TLD — thermoluminescent dosimeter (albedo); ETD — etched track dosimeter; SSD — solid state device (active personal dosimeter); SDD — superheated drop detector (bubble detector).

13.7. INVESTIGATION OF DEVICE PERFORMANCE

When the most appropriate measuring device for a particular job has been selected, using the guidelines presented above, there may still be a need to verify that the chosen device provides a dose equivalent estimate that is within the acceptance criteria specified for the particular measurements that it is intended to perform. In cases where no instrument meets the required accuracy criteria, field specific correction factors may need to be determined and used to improve the dose equivalent estimates. One way of deriving these correction factors is by using a selection of dose equivalent measuring instruments to help characterize the field (see Section 10).

However, to verify that any device's indications are acceptable in terms of accuracy, or to determine accurate correction factors, the most thorough approach (usually only warranted in areas where doses approach statutory limits) involves predicting the indication of the device using information on the energy and direction dependence of the neutron field and the energy and angle dependence of the response of the device; that is, the full device response function. If all this information is available, the dose equivalent at a selected point in the field can be derived from the field information. The predicted indication of a device with its reference point placed at the selected point can be derived from folding its fluence response function with the directional distribution of the spectral fluence. A comparison of the predicted indication and the calculated dose equivalent gives information on the expected accuracy of the device. The folding process is detailed in Eq. (13.1):

$$R = \iint_{\Omega\,E} R_{\Omega,E}(\mathbf{\Omega},E) \cdot \Phi_{\Omega,E}(\mathbf{\Omega},E) \; d\mathbf{\Omega} \; dE \tag{13.1}$$

where

R is the response of the device in the field of interest (in dose equivalent if the device provides a dose equivalent indication);

$R_{\Omega,E}(\mathbf{\Omega},E)$ is the device's response to neutrons of energy E incident at the reference point of the device from a solid angle defined by the vector $\mathbf{\Omega}$;

$\Phi_{\Omega,E}(\mathbf{\Omega},E)$ is the directional distribution of the fluence defined in terms of energy E and solid angle defined by $\mathbf{\Omega}$.

For area survey instruments, which are intended to measure ambient dose equivalent, the process is simpler, since the quantity has been designed to remove the angular dependence of the field. The appropriate equation is then:

$$R = \int_E R_E(E) \cdot \Phi_E(E) \ dE \tag{13.2}$$

The ambient dose equivalent, $H^*(10)$, at the reference point can be calculated with Eq. (13.3):

$$H^*(10) = \int_E h_\Phi^*(E) \cdot \Phi(E) dE \tag{13.3}$$

where

$h_\Phi^*(E)$ is the fluence to ambient dose equivalent conversion coefficient, as described in Section 6.

A comparison of R and $H^*(10)$ gives an indication of the expected accuracy of the instrument, and their ratio can be used as a correction factor.

To calculate the personal dose equivalent, the directional characteristics of the field must be considered, as must the position and orientation of the individual. In the calculation, the individual is replaced by a phantom, since the only fluence to personal dose equivalent conversion coefficients available are for dosimeters on a phantom. For uniform irradiation conditions — in a broad, parallel neutron beam, or in a field that can be treated as comprising a number of such beams, incident from the front half space of the phantom — an estimate of the personal dose equivalent can be determined using the energy and direction distributions of the neutron fluence and the fluence to dose equivalent conversion coefficients given as a function of energy and angle of incidence in Section 6. These were calculated for a plane parallel beam incident on a calibration slab phantom and are the only conversion coefficient data currently available. A further requirement for these calculations is that the presence of the phantom has a negligible influence on the incident neutron fluence at the point of test. Under these conditions:

$$H_{\text{p,slab}} = \int_\alpha \int_E h_{\text{p,slab}}(\alpha, E) \cdot \Phi_{\Omega, E}(\alpha, E) \ d\alpha \ dE \tag{13.4}$$

where

α is the angle between the normal to the phantom at the position of the dosimeter and the direction of the incident radiation;

$h_{p,slab}(\alpha, E)$ is the fluence to personal dose equivalent conversion coefficient, as described in Section 6;

$\Phi_{\Omega,E}(\alpha, E)$ is the fluence incident on the dosimeter at angle α.

Information about the energy spectrum of workplace fields can be obtained from measurements and from calculations (see Section 9). However, information about the direction dependence of the field is rarely available. Calculation can provide this information, but there are only few examples of this [13.1]. The measurement approach is particularly complex. Instruments to determine the angle dependence of the fluence, or of the dose equivalent, have been investigated [13.2], but there is only evidence of one successful application, and that is within the EVIDOS project (see Section 13.8). Available spectral data are sometimes used to verify personal dosimeter indications, but the approach tends to be either to assume normal incidence on the dosimeter, thus providing, in most cases, an estimate of the maximum possible value of personal dose equivalent, or to make broad simplifying assumptions about the direction dependence [13.3], for instance, that the fast neutron component is incident normally on the dosimeter but the low energy scattered component is isotropic.

For area survey instruments, the fact that direction information is not needed means that there are many more examples of predictions for instrument indications from spectral measurements. An early example [13.4] showed that the Leake counter (at least in its guise as the Harwell Instruments 0949 monitor) is unlikely to over-respond by more than a factor of two in real workplace fields, despite the fact that the ambient dose equivalent response function is considerably too high in parts of the intermediate energy region. This is because the instrument reads roughly correctly at energies around 1 MeV, where much of the dose equivalent occurs in most fields. For similar moderator based instruments with greater thicknesses of polyethylene, there is a tendency for the device to under-read in the region from 100 keV to 1 MeV, and this can result in the instruments under-reading in workplace fields, despite the response function being in general too high in the intermediate energy region below about 100 keV.

There now exists a reasonably large body of data about survey instrument responses in known neutron spectra [13.3, 13.5–13.8], indicating that there can be significant under- and over-reading. However, the fact that the instrument response is sometimes too high and sometimes too low, when viewed over the full range of energies of interest, means that there is often a tendency for under- and

FIG. 13.1. Predicted H*(10) response of the 0949 version of the Leake area survey instrument for irradiation from the reference direction, designated as 0°, and for isotropic incidence (ISO) [13.9].

over-reading to cancel, giving results that may not be as bad as might be expected from the rather poor ambient dose equivalent responses of these devices.

Figures 13.1 and 13.2 show examples of predictions for the $H^*(10)$ response of two area survey instruments, the 0949 variant of the Leake counter and the Studsvik 2202 D in a variety of neutron fields including workplace fields and calibration fields [13.9]. For both instruments, the predictions are presented for a field incident from the reference direction and for an isotropic field, namely one with equal intensity from all angles. For the spherical Leake instrument, the reference direction is from the opposite side to the electronics, and for the basically cylindrical Studsvik instrument it is through the side of the moderating cylinder.

The figures reveal information about both the fields and the instrument performance. The responses are plotted against the spectrum averaged fluence to $H^*(10)$ conversion coefficient for the fields, and from the spread of these values it
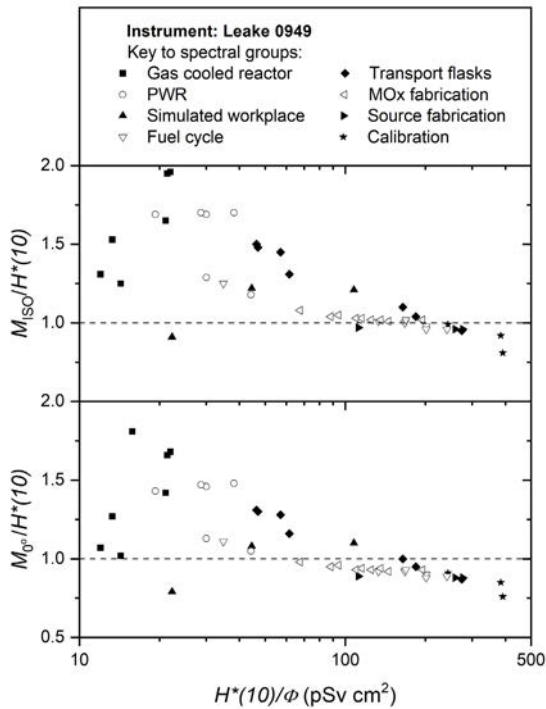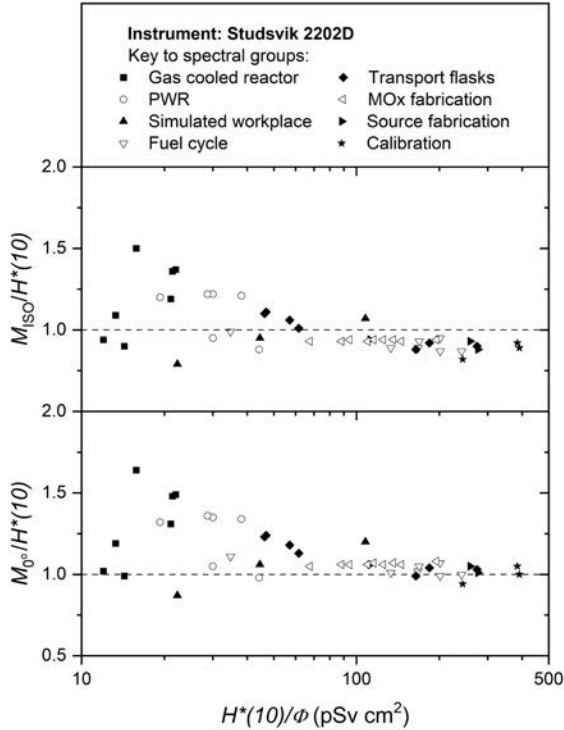
FIG. 13.2. Predicted H*(10) response of the Studsvik 2202 D area survey instrument for irradiation from the reference direction, designated as 0°, and for isotropic incidence (ISO) [13.9].

can be seen that there is no one field that is characteristic of a particular area; the vicinity of a gas cooled reactor or around a transport container for used nuclear fuel, for example. For both instruments, the over-response in the intermediate energy region results, in general, in over-reading for soft fields (i.e. for smaller values of $H^*(10)/\Phi$). In an attempt to counter this tendency, the usual setting of the Leake instrument [13.10] results in under-reading for the hard neutron spectra provided by [241]Am-Be and [252]Cf calibration sources. The difference between the responses for incidence along the reference direction and for an isotropic field give an idea of the effect of the electronic unit attached to the instrument, and in the case of the Studsvik instrument, the fact that the moderator is not spherical.

In situations where end users want information on the accuracy of the response of particular instruments in their workplace fields but have no access to spectrometric data for their field, some useful information can be obtained by using a spectrum measured in a similar environment at a different establishment. A significant number of spectral measurements have now been

performed [13.11], and useful compilations of these data can be found in two IAEA publications [13.12, 13.13].

A related technique for deriving information about instrument performance in particular workplace fields is by making measurements in one of the simulated workplace fields that can be found in some laboratories [13.14]. Some validation information for the performance of particular devices in particular types of fields can be obtained by choosing a simulated workplace field with appropriate characteristics. Care should, however, be exercised in interpreting the results of such measurements. In particular, this applies to situations where the response of a device is zero over part of the energy range, the overlap between the non-zero region of the response function and the spectra of the simulated and of the actual workplace fields is small, and the spectra differ in this small overlap region [13.15].

13.8. RESULTS OF THE EVIDOS PROJECT

The evaluation of individual dosimetry in mixed neutron and photon radiation fields (EVIDOS) project, funded by the European Commission within its 5th Framework Programme, was one of the largest projects in the first decade of the 2000s in the field of dosimetry and spectrometry of mixed neutron–photon workplace fields at nuclear facilities [13.16]. It was a cooperation of partners from seven institutions and seven countries within Europe. Table 13.2 gives an overview of the facilities and workplaces visited during the measurement campaigns.

TABLE 13.2. FACILITIES VISITED AND WORKPLACE FIELDS INVESTIGATED DURING THE EVIDOS PROJECT [13.17]

Measurement period	Facility and location	Radiation fields
C0: 10 Oct.– 26 Nov. 2002	Simulated workplace fields, IRSN, Cadarache, France	IRSN CANEL IRSN SIGMA
C1: 1–3 Apr. 2003	Nuclear power plant, Krümmel, Germany	BWR Krümmel T — top BWR Krümmel SAR — control rod room Cask NTL M — centre of long side Cask NTL S — side

TABLE 13.2. FACILITIES VISITED AND WORKPLACE FIELDS
INVESTIGATED DURING THE EVIDOS PROJECT [13.17] (cont.)

Measurement period	Facility and location	Radiation fields
C2: 18–22 Jun. 2003	Fuel processing plant, Belgonucléaire, Dessel, Belgium and Research reactor VENUS, SCK CEN, Mol, Belgium	Belgonucléaire 1 — bare MOX fuel rods Belgonucléaire 2 A — unshielded rack Belgonucléaire 2B — shielded rack Belgonucléaire 3 — storage room SCK CEN VENUS C — control room SCK CEN VENUS F — side shielding wall
C3: 8–12 Nov. 2004	Nuclear power plant, Ringhals, Väröbacka, Sweden	PWR Ringhals A — inside containment PWR Ringhals L — entrance lock Cask TN D — centre of long side Cask TN N — centre of end plate
C4: 23–25 May 2005	Nuclear facility[a]	Nuclear facility 1 — door Nuclear facility 2 — corridor Nuclear facility 3 — inside room

Reproduced from Ref. [13.17] with permission from Oxford University Press. BWR: boiling water reactor; IRSN: Institut de Radioprotection et de Sûreté Nucléaire; MOX: mixed oxide fuel; PWR: pressurized water reactor; SCK CEN: Belgian Nuclear Research Centre.

[a] For security reasons, details of this facility and of its radiation fields may not be disclosed in this report.

In order to evaluate the indications of radiation protection instruments (survey instruments, passive personal dosimeters and new active electronic dosimeters), the reference values for radiation protection quantities have been determined by spectrometry as a function of the energy and direction of the incident neutrons. For this purpose, measurements have been performed using a well characterized Bonner sphere spectrometer and a new directional spectrometer.

A directional spectrometer with silicon diodes mounted in six detector capsules on the surface of a 30 cm diameter polyethylene sphere (see Fig. 13.3) was used during all campaigns.

Each detector capsule contained four silicon detectors, which were covered by different hydrogenous and ^{6}Li containing layers and absorbers (see Fig. 13.4). This allowed a rough spectrum to be deduced in terms of contributions from thermal, epithermal, intermediate and fast neutrons.

FIG. 13.3. Directional spectrometer as used within the EVIDOS project. (Reproduced from Ref. [13.17] with permission from Oxford University Press.)
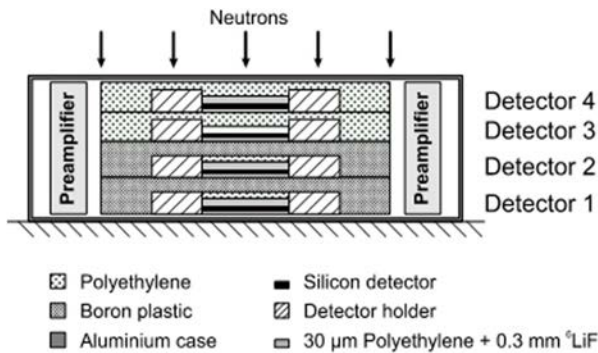
FIG. 13.4. Schematic diagram of the detector capsule. (Reproduced from Ref. [13.17] with permission from Oxford University Press.)

In addition, the scattering, absorption and moderation within the sphere gives additional information on the energy of neutrons, but chiefly serves to give information on their directional distribution. Neutrons with energies less than a few MeV — which usually contribute to dose at nuclear facilities such as those investigated during the project — are only detected in the capsules that face their incident direction, while neutrons coming from other directions are absorbed by the sphere.

The response function of this new spectrometer — the pulse height spectra of all 24 diodes — was fully characterized in terms of the energy and direction

of incoming neutrons by measurements in quasi-monoenergetic fields and, in the epithermal and intermediate energy region, by means of the Monte Carlo code MCNP [13.17].

The analysis of the data provided by the directional spectrometer during the measurement campaigns was performed using different unfolding codes, with and without prior information. The results were neutron energy spectra for a series of 14 to 20 incident directions. Since the response functions of the directional spectrometer overlapped in such a way that, in general, the directional distribution was not independent of the energy distribution, the best solution obtained was from unfolding using the MAXED code [13.18] when prior information about the energy distribution was available from the Bonner sphere spectrometer. The resulting spectra were in turn folded with appropriate conversion coefficients in order to get the quantities $H^*(10)$, $H_p(10)$ and E.

Figures 13.5 to 13.7 show some results for dose equivalent quantities as they were obtained using this spectrometry (taken from Ref. [13.19]).

Figure 13.5 shows relative contributions to $H^*(10)$ from 14 directions: FRONT (which was assigned as the main dose direction), BACK, RIGHT, LEFT, UP and DOWN (defined as seen by a person looking towards the FRONT direction) and eight directions in between, abbreviated by the first letter of the surrounding directions. It can be clearly stated that the dose distribution in the field at position 2 A at Belgonucléaire (MOX fuel in a steel box) is strongly
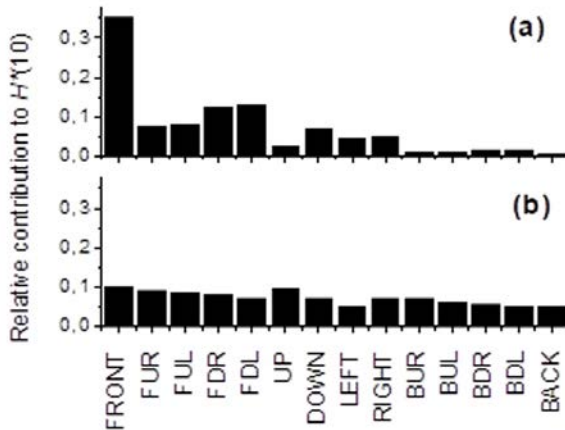
FIG. 13.5. Relative contribution from 14 directional intervals to the ambient dose equivalent H*(10) for position 2 A at Belgonucléaire (a) and position A at the Ringhals nuclear power plant (b). (Reproduced from Ref. [13.19] with permission from Oxford University Press.)

forward directed, whereas it is almost isotropic at position A at the Ringhals nuclear power plant (pressurized water reactor, inside containment).

Figures 13.6 and 13.7 show the ratios $H_p(10)/H^*(10)$ and $E/H^*(10)$ as obtained in the simulated workplace fields SIGMA [13.20] and CANEL [13.21] and in the real workplace fields as given in Table 13.2 for different orientations of a phantom or a person. In all cases, the values of $H_p(10)$ and E were smaller than those of $H^*(10)$, indicating that $H^*(10)$ can be used as a conservative estimate of personal dose equivalent and effective dose. In most cases, the 'FRONT' values were the highest values among the different directions, with the exception of a position at the research reactor (VENUS F) and at the Krümmel nuclear power plant (boiling water reactor SAR), where the main dose came from slightly above and did not coincide with the assigned FRONT direction. The lowest values of $H_p(10)$ — up to a factor of 5 smaller than $H^*(10)$ — for the FRONT direction were found at reactors, and also in the case of more strongly shielded positions at fuel storage processing (see Fig. 13.6). In these cases, values from different directions are also similar and indicate a more isotropic distribution of neutrons. Figure 13.7 shows that effective dose is generally only 30% to 50% of $H^*(10)$.

A comparison of the values shown in Figs 13.6 and 13.7 shows that the personal dose equivalent is in most cases a conservative estimate of the effective dose for the FRONT direction — with the exception of some cases at reactors, where it was found to be slightly non-conservative. However, the introduction of new w_R values as recommended by the ICRP (see Fig. 5.8) has an especially

FIG. 13.6. *Ratio of personal dose equivalent* $H_p(10)$ *and ambient dose equivalent* $H^*(10)$ *as determined in all workplace fields investigated for different orientation of the phantom. (Reproduced from Ref. [13.19] with permission from Oxford University Press.)*

high influence for the fields at reactors. Using these new w_R values (but without consideration of changed tissue weighting factors) would result in values of effective dose almost a factor of two lower than the values shown here at power reactor positions [13.19]. Hence, it can be stated that estimation of effective dose is conservative in all cases for the FRONT direction for the investigated workplaces. However, the effective dose can be underestimated strongly if the dosimeter is not worn towards the main dose direction, especially in fields with stronger directional dose distributions (compare 'BACK' values in Figs 13.6 and 13.7).

13.8.1. Neutron survey instrument results

Five different neutron survey instruments were used at almost all of the measurement locations: four commercially available moderator type instruments (Studsvik 2202 D, Berthold LB 6411, Harwell N91 (a version of the Leake instrument) and Thermo Electron WENDI-2) and a prototype based on TEPC (SSI Sievert instrument). The area monitors slightly under-read in hard fields, but the values were mainly between 0.5 and 1.5. This means that the effective dose is never underestimated by these instruments (see Fig. 13.6).

Larger differences for measured values, as compared with the reference values of $H_p(10)$, were found for personal dosimeters (see Fig. 13.8 and

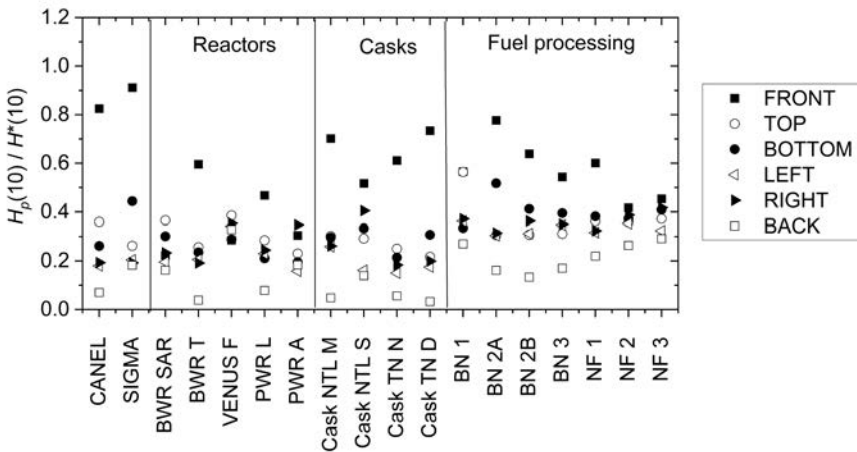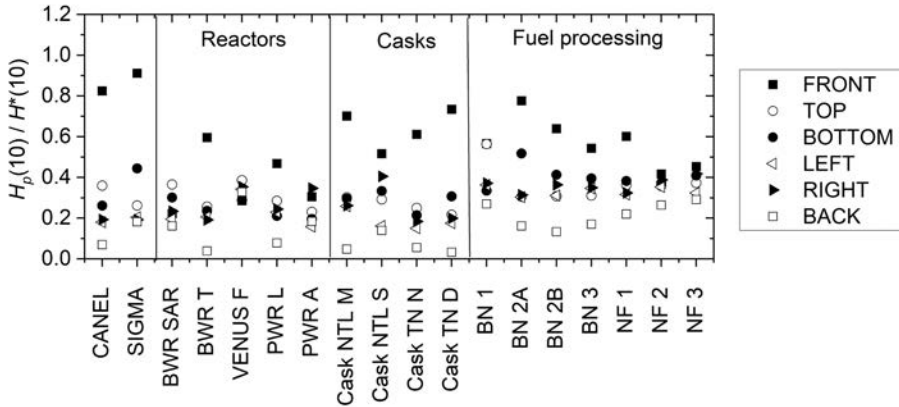*FIG. 13.7. Ratio of effective dose E and ambient dose equivalent* H*(10) *as determined in all workplace fields investigated for different orientation of the person. (Reproduced from Ref. [13.19] with permission from Oxford University Press.)*

Ref. [13.22]). The results are summarized below. More information on the dosimeters used and related references can be found in Refs [13.17] and [13.23].

13.8.2. Etched track detector results

Nuclear track detectors from the National Radiological Protection Board (NRPB) and Paul Scherrer Institute (PSI) were also used. The evaluation of the NRPB PADC is based on a combination of chemical and electrochemical etching, and the evaluation of PSI is based on chemical etching. Both dosimeter types delivered under- and over-responses with an overall spread that was approximately a factor of three to four.

13.8.3. Thermoluminescent albedo dosimeter results

As TLDs usually require field specific correction factors that depend on the dosimeter itself and on the characteristics of the fields, only the local devices as used in the facilities visited were used. The TLD albedo dosimeters at Krümmel were evaluated by means of location specific calibration factors. For the measurements at the cask, these were a factor of two higher than inside the reactor. The large uncertainties at the cask (see Fig. 13.8) result from short irradiations of only approximately 2 h. The measurements tend toward over-response in most cases, with an overall spread that is approximately a factor of four.

The dosimeters at Ringhals are usually used with field specific correction factors. Three different over-response factors, depending on where the person has been working, are used. These factors have been determined using knowledge from earlier spectrometric investigations of the workplaces at Ringhals. Although the dosimeter uses no albedo shielding and chiefly detects thermal and epithermal neutrons, the spread of the measured responses (roughly a factor of three) is acceptable, and the mean response close to unity. The results of the campaign will be used to improve the field dependent correction factors.

13.8.4. Superheated emulsion dosimeter results

The commercially available bubble dosimeters for fast neutrons (BTI PND) were used, in some cases in combination with dosimeters for thermal neutrons (BTI BDT), by the Belgian Nuclear Research Centre (SCK CEN). In addition, the HpSLAB, an instrument that uses a superheated drop detector at 10 mm depth in a slab phantom and provides a direct indication of bubbles by counting signals acoustically, was used. The response varied by a factor of roughly two for the HpSLAB and a factor of roughly three for the SCK CEN

PND+BDT, indicating in both cases a tendency to overestimate the reference values (see Fig. 13.8).

13.8.5. Electronic dosimeter results

The electronic personal dosimeters used were those few devices that have been commercially available over the past few years (Thermo Electron EPD-N, Aloka PDM-313), dosimeters from the first industrial prototype series (Thermo Electron EPD-N2, Saphydose-n) and laboratory prototypes that were sufficiently advanced in design to be lightweight battery operated devices (PTB DOS-2002, DMC2000GN, DIS-N). The values measured with the Aloka PDM-313, Thermo Electron EPD-N2, Saphydose-n and DOS-2002 showed variations in response as compared with the reference values by one order of magnitude and more, with a tendency to over-responding, especially in the reactor fields (see full symbols in Fig. 13.8). In these fields, a large number of low energy neutrons (< 100 keV) contribute to the fluence, and these produce a high reading since dosimeters usually over-respond in this energy region (see Fig. 11.8). The DMC2000GN only became available in the last two measuring campaigns. Its results were close to those of the PTB DOS-2002, from which it had been developed. In all
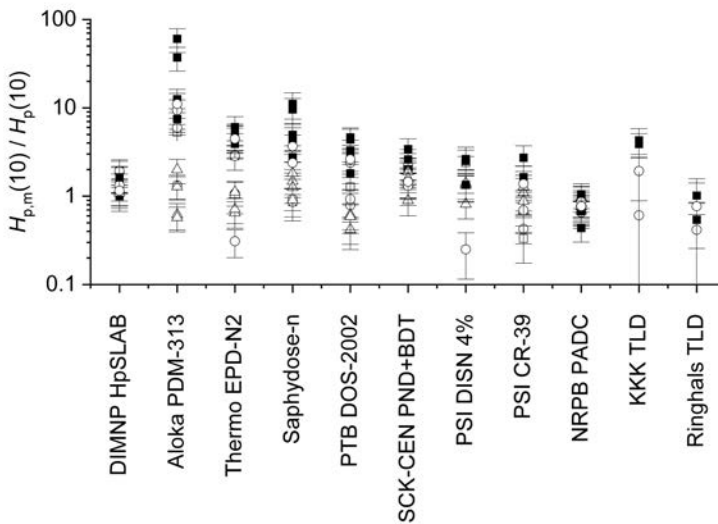

FIG. 13.8. Response of different personal dosimeters in the simulated workplace field CANEL (□), the reactor fields (■), the fields at transport casks (○) and the fields at the fuel facility Belgonucléaire (Δ). (Reproduced from Ref. [11.23] with permission from Oxford University Press.)

cases, field dependent correction factors were needed in order to get reliable dose indications (cf. the approach adopted for TLD albedo dosimeters).

A special problem arose when using the DIS-N prototype dosimeter based on direct ion storage. Although its neutron response is comparable to, or even better than, those of other electronic dosimeters (see Fig. 11.10), the subtraction of a photon reading resulted, for several fields with a high photon dose equivalent contribution, in negative results that were displayed as zero readings. The reason for this is that the chambers used for neutron and photon detection (with wall material made of polyethylene +4% $LiNO_3$) and those used for photon detection (with wall material made of Teflon containing 60% graphite) did not show exactly the same photon response as a function of energy and angle.

It has been shown [13.23] that the response of locally used personal dosimeters can be improved with the help of a reference directional spectrometer or a reference personal dosimeter, such as a superheated drop detector embedded to approximately 10 mm depth in a polymethyl methacrylate (PMMA) phantom (see DIMNP HpSLAB in Fig. 13.8), after a slight adjustment of the mean response of this instrument and the additional use of indications provided by area monitors.

REFERENCES TO CHAPTER 13

[13.1]   TANNER, R.J., et al., Effect of the Energy Dependence of Response of Neutron Personal Dosemeters Routinely Used in the UK on the Accuracy of Dose Estimation, NRPB-W25, National Radiological Protection Board, Chilton, UK (2001).

[13.2]   D'ERRICO, F., BARTLETT, D.T., AMBROSI, P., BURGESS, P., Determination of direction and energy distributions, Radiat. Prot. Dosim. **107** (2003) 133–153.

[13.3]   BARTLETT, D.T., BRITCHER, A.R., BARDELL, A.G., THOMAS, D.J., HUDSON I.F., Neutron spectra, radiological quantities and instrument and dosemeter responses at a magnox reactor and a fuel reprocessing installation, Radiat. Prot. Dosim. **44** (1992) 233–238.

[13.4]   HARRISON, K.G., The response of a spherical neutron survey meter, Nucl. Instrum. Methods **166** (1979) 197–201.

[13.5]   THOMAS, D.J., WAKER, A.J., HUNT, J.B., BARDELL, A.G., MORE, B.R., An inter-comparison of neutron field dosimetry systems, Radiat. Prot. Dosim. **44** (1992) 219–222.

[13.6]   DELAFIED, H.J., PERKS, C.A., Neutron spectrometry and dosimetry measurements made at nuclear power stations with derived dosemeter responses, Radiat. Prot. Dosim. **44** (1992) 227–232.

[13.7]   LINDBORG, L., et al., Determination of neutron and photon dose equivalent at workplaces in nuclear facilities in Sweden, Radiat. Prot. Dosim. **61** (1995) 89–100.

[13.8]   BARTLETT, D.T., HAGER, L.G., TANNER, R.J., HALEY, R.M., COOPER, A.J., Comparison of neutron dose quantities and instrument and dosemeter readings in a MOX fabrication plant, Nucl. Instrum. Methods Phys. Res. A **476** (2001) 446–451.

[13.9]   TANNER, R.J., et al., Practical Implications of Neutron Survey Instrument Performance, HPA-RPD-016, Health Protection Agency, Chilton, UK (2006).

[13.10]   LEAKE, J.W., The effect of ICRP (74) on the response of neutron monitors, Nucl. Instrum. Methods Phys. Res. A **421** (1999) 365–367.

[13.11]   RIMPLER, A., Applications, Radiat. Prot. Dosim. **107** (2003) 184–204.

[13.12]   INTERNATIONAL ATOMIC ENERGY AGENCY, Compendium of Neutron Spectra and Detector Responses for Radiation Protection Purposes, Technical Reports Series No. 318, IAEA, Vienna (1990).

[13.13]   INTERNATIONAL ATOMIC ENERGY AGENCY, Compendium of Neutron Spectra and Detector Responses for Radiation Protection Purposes, Supplement to Technical Reports Series No. 318, Technical Reports Series No. 403, IAEA, Vienna (2001).

[13.14]   INTERNATIONAL ORGANIZATION FOR STANDARDIZATION, Reference neutron radiations: Characteristics and methods of production of simulated workplace neutron fields, International Standard 12789-1, ISO, Geneva (2008).

[13.15]   THOMAS, D.J., HORWOOD, N., TAYLOR, G.C., Neutron Dosemeter Responses in Workplace Fields and the Implications of using Realistic Neutron Calibration Fields, NPL Report CIRM 27, National Physical Laboratory, Teddington, UK (1999).

[13.16]   SCHUHMACHER, H., et al., Evaluation of Individual Dosimetry in Mixed Neutron and Photon Radiation Fields, Report PTB-N49, Physikalisch-Technische Bundesanstalt, Braunschweig, Germany (2006).

[13.17]   LUSZIK-BHADRA, M., REGINATTO, M., LACOSTE, V., Measurement of energy and direction distribution of neutron and photon fluences in workplace fields, Radiat. Prot. Dosim. **110** (2004) 237–241.

[13.18]   REGINATTO, M., LUSZIK-BHADRA, M., D'ERRICO, F., An unfolding method for directional spectrometers, Radiat. Prot. Dosim. **110 (**2004) 539–543.

[13.19]   LUSZIK-BHADRA, M., et al., Characterisation of mixed neutron-photon workplace fields at nuclear facilities by spectrometry (energy and direction) within the EVIDOS project, Radiat. Prot. Dosim. **124** (2007) 219–229.

[13.20]   LACOSTE, V., GRESSIER, V., MULLER, H., LEBRETON, L., Characterisation of the IRSN graphite moderated americium-beryllium neutron field, Radiat. Prot. Dosim. **110 (**2004) 135–139.

[13.21]   LACOSTE, V., GRESSIER, V.*,* Monte Carlo simulation of the IRSN CANEL/T400 realistic mixed neutron/photon radiation field. Radiat. Prot. Dosim. **110 (**2004) 123–127.

[13.22]   LUSZIK-BHADRA, M., et al., Summary of personal neutron dosemeter results obtained within the EVIDOS project, Radiat. Prot. Dosim. **125** (2007) 293–299.

[13.23]   LINDBORG, L., et al., Application of workplace correction factors to dosemeter results for the assessment of personal doses at nuclear facilities, Radiat. Prot. Dosim. **124** (2007) 213–218.

14. CALIBRATION AND TYPE TESTING

14.1. INTRODUCTION

Before they are used, both area survey instruments and personal dosimeters should undergo a thorough radiological *type test* to determine their radiological characteristics. The goal of the test is to ensure these devices have suitable energy and angle response functions for the fields in which they will be used. The devices should also undergo periodic laboratory calibrations or checks to confirm that their performance remains stable. The frequency and types of routine calibrations performed will depend on national requirements but would typically be at intervals of approximately one year. Calibrations are generally performed at national or regional standards laboratories or at labs that have been accredited by a national accreditation body. In addition to type tests and formal calibrations, other categories of test are performed at various times, as follows:

(a) *Special calibrations*. These have to be performed, for example, if the device is operated under abnormal circumstances, or if the routine calibration or type testing provides insufficient information.
(b) *Routine calibration/test*. A routine test will be of a confirmatory nature, being performed either to check the calibration carried out by the manufacturer or to check whether the calibration factor is sufficiently stable during the continued long term use of a device. Stability checks do not necessarily have to be performed as absolute measurements but may be relative to an acceptance test result to provide evidence that the device is still functioning correctly. Such tests may be performed, for example, with a simple test jig, for which results were obtained at the time of the acceptance test.
(c) *Acceptance tests or tests before first use*. These are contractual tests carried out on all instruments of a particular type before they are put into service for the first time. These tests are intended to demonstrate that every instrument in a consignment conforms to its specification and is suitable for the intended purpose. Such tests should provide a check of any faults or potential faults. They can be undertaken by the manufacturer, the user or an independent laboratory.

The split into different types of tests and calibrations outlined above is not a universally accepted hierarchy, but it is a reasonable outline of the types of measurements performed in most countries. Further details of the various approaches to the examination, testing and calibration of radiation protection devices can be found in several references (e.g. Refs [14.1–14.3]).

The goal of *calibration* is to determine, under *standard test conditions*, the relationship between values indicated by a device — in the present case, a personal dosimeter or survey meter — and the *conventionally true values* of the quantity to be measured. The *calibration factor*, N, is the factor by which the indication of the device is multiplied to obtain the value of the quantity to be measured. It is given by

$$N = G / M \tag{14.1}$$

where M is the indication in a calibration field under controlled standard test conditions, and the conventionally true value of the quantity is G. Devices may be calibrated in terms of various quantities, and so the quantity should always be specified; for example, a fluence calibration (where $G = \Phi$) or a dose equivalent calibration (where $G = H$).

The primary reference quantity for the calibration of devices used for neutron protection is neutron fluence, either at a specific energy (monoenergetic fluences) or with a well defined neutron spectrum (radionuclide source fields, thermal fields and simulated workplace fields). Fluence is the primary quantity because the required dose equivalent quantities are derived from the fluence using internationally agreed fluence to dose equivalent conversion coefficients. However, to determine the appropriate conversion coefficient, the spectrum of the radiation field must be known. Although in the context of radiation protection the calibration quantity of interest to the end user will almost invariably be dose equivalent, it is recommended that the fluence is also quoted on all calibration certificates, since this enables the user to make allowances for any changes that occur in the dose quantities with time.

As outlined above, the concept of a calibration, that is, a measurement of the *response* of a device in a neutron field of known fluence and spectrum, and with known angle of incidence on the device, appears straightforward. However, there are a number of issues. A calibration factor is a unique property of a device and therefore should not depend upon the calibration facility used or the experimental techniques employed. Ensuring this can be problematic. The main difficulties are in providing a standard field where the fluence and spectrum are known to the required accuracy. One of the most significant problems is correcting for unwanted components, such as scattered neutrons in radionuclide source fields and in monoenergetic fields, or higher energy neutrons in thermal calibration facilities, and much of the work of characterizing calibration facilities involves this aspect. The problems in making these corrections have been dealt with extensively in the literature. A complete discussion of the recommended procedures is given in ISO Standard 8529-2 [14.4].

A *type test* usually involves a number of response measurements in well characterized fields. The underlying techniques involved in both calibrations and type tests are thus the same, but the requirements for accuracy, the range of measurements and the reasons for performing the measurements are different. Type test requirements have been covered by international standards [14.5] and papers in the literature [14.6].

Some calibration laboratories and end users refer to the concept of an instrument being 'within calibration'. This essentially means that a tolerance range is defined for a device, for instance ± 30%, and the device is said to be within calibration if its response is within ± 30% of the true value. This is NOT the concept of a calibration as defined in international standards [14.7], but it is a concept that is employed by some calibration labs and end users. The end user needs to be very clear about the actions such a calibration laboratory undertakes for a device outside the allowed tolerance. Options are to fail it or adjust it to be within tolerance.

Reference conditions for *influence quantities*, for example temperature, humidity, pressure, etc., are defined for radiological calibrations [14.8], and all measurements should be performed under *standard test conditions*. These define a range of acceptable values for influence quantities centred around the reference condition.

Two other measurements sometimes come under the heading of calibration. First, tests for the linearity of a device's indication as a function of the dose equivalent rate. This may include an overload test to ensure the device continues to indicate overload when the dose equivalent rate is above the maximum and returns to the correct value after overload. Second, testing of gamma rejection. This test should be undertaken by applying a photon field, for example from a ^{60}Co or ^{137}Cs source, at the same time as the instrument is exposed to neutrons.

14.2. CALIBRATION FIELDS AND CALIBRATION FUNDAMENTALS

Reference radiations for the calibration of radiation protection measuring devices that are used in the energy region below 20 MeV are described in ISO Standard 8529-1 [14.9]. This discusses neutron reference radiations produced using reactors and accelerators and also recommends four radionuclide based neutron sources: D_2O-moderated ^{252}Cf, ^{252}Cf, ^{241}Am-B and ^{241}Am-Be. In ISO Standard 8529-2 [14.4] the approaches to characterizing the reference fields are described, and in 8529-3 [14.8] the calibration techniques are covered. Once a conventionally true value has been established for the physical quantity neutron fluence, fluence to dose equivalent conversion coefficients are used to calculate the ambient, or personal, dose equivalent. Values for the fluence to dose

equivalent conversion coefficients as a function of energy are given in ICRP 74 [14.10] and ICRU Report 57 [14.11]. For the quantity $H_p(10)$, values are also given as a function of angle of incidence.

Calibration facilities for neutron energies above 20 MeV are required for cosmic ray dosimetry in space and at aircraft flight altitudes, and for protection level dosimetry around high energy accelerators. Well characterized high energy fields are also in demand for testing the radiation hardness of semiconductor devices used in the electronic systems of aircraft and spacecraft. Few such fields are available, and their characterizations in terms of neutron spectra and fluence are often poorly known in comparison with lower energy fields. Conversion coefficient data are also less well established (see Section 6).

Other calibration fields discussed in this section are thermal fields, which can be based on either a reactor, an accelerator or radionuclide sources; white sources, which with time of flight can be used to determine response functions; and simulated workplace fields. The concepts of field calibrations and the importance of traceability are also covered.

For radionuclide source based calibration, accelerator based monoenergetic calibrations, and to some extent high energy calibrations, one of the most important corrections that has to be performed is for the effects of room and air scattered neutrons. These corrections are performed using either distance variation techniques to pick out the direct unscattered component or the shadow cone technique, where the correction is performed by measuring and subtracting the scattered component. A separate subsection (14.2.5) deals with this problem after the fields have been described (14.2.2 and 14.2.3).

14.2.1. Calibration laboratory features

Any calibration laboratory should have procedures covering its quality management system, administrative arrangements and technical operations. Guidance can be found in standard ISO/IEC 17025 [14.12].

One obvious requirement is a means of producing neutrons. For routine calibrations, this most frequently entails the use of radionuclide sources, and many secondary or routine calibration laboratories are restricted to this method. The sources are usually ^{252}Cf or ^{241}Am-Be. Radionuclide sources cannot be switched off, and appropriate means must be found to handle them. These can be 'manual', that is, the use of long tongs, if the dose rates from the sources are not too high, but may need to be completely automatic, such as the use of robotics or pneumatic transport systems, if the dose rates make manual handling hazardous.

Accelerator based monoenergetic neutrons are invaluable for type testing. They have the very useful feature that the neutron producing accelerator beam

can be switched off, or 'parked', on beam stops when setting up experiments. For accelerator based measurements, monitoring instruments are required.

In all calibrations, some means must be provided for taking readings from the devices being calibrated. If the indication is an electrical signal, cables need to be available running from the irradiation area to a shielded location. If a meter indication needs to be taken, some form of camera system is required. Webcam technology can satisfy this requirement simply and cheaply.

For radionuclide source or accelerator based calibration and type testing, the irradiation room should ideally be as large as possible to minimize room scatter. (This decreases with increasing room size.) The requirement for size can present problems of cost, since, except in special cases where an exclusion zone can be drawn around the area [14.13], the room has to have thick shield walls to reduce neutron doses to acceptable levels outside.

Some calibrations are performed at facilities that are not primarily designed as calibration laboratories. Examples include thermal calibrations being performed at research reactors whose primary purpose is research, teaching or materials investigations, and the use of reactor filtered beams or white sources. In such situations, those performing the calibrations have to make the best of the available facilities and often have to characterize the field under less than ideal conditions. Limited access is one obvious potential problem.

14.2.2. Radionuclide fields

Calibrations with radionuclide source capsules are usually performed with one or more of the ISO recommended sources mounted free in air, ideally in a low-scatter environment. Other types of sources, with different energy distributions, can be used either for type testing or when it is felt that the spectrum of another type of source is more appropriate for the field in which the device being calibrated will be used.

The approach using radionuclide sources is to determine the neutron fluence at the *point of test*, and if a dose equivalent calibration is required, to convert this fluence to dose equivalent using the appropriate fluence to dose equivalent conversion coefficient. The fluence, Φ, arriving from the source, usually quoted in cm^{-2}, is given by

$$\Phi = \frac{B\,F_\mathrm{I}\,t}{4\pi l^2} = \frac{B_\Omega\,t}{l^2} \tag{14.2}$$

where

B is the source emission rate into 4π sr (s^{-1});

F_I is a correction for anisotropy of emission from the source;

t is the irradiation time (s);

l is the distance between the centre of the source and the point of test (cm);

B_Ω is the angular source strength, i.e. the number of neutrons emitted per second into unit solid angle in the direction Ω.

Note that Eq. (14.2) takes no account of neutron scatter in the air, or the walls, floor and ceiling of a calibration room. This is discussed in Section 14.2.5.

The dose equivalent, H, is given by

$$H(10) = \Phi \, h(10) \qquad\qquad\qquad (14.3)$$

where

$H(10)$ is the dose equivalent, $H^*(10)$ or $H_p(10)$, depending on the fluence to dose equivalent conversion coefficient used;

$h(10)$ is the fluence to dose equivalent conversion coefficient used, either $h^*(10)$ or $h_p(10)$, averaged over the spectrum of the radionuclide source.

     To determine the neutron fluence, the source emission rate, B, needs to be known, and this can be measured to an accuracy of 1 or 2%. The technique most commonly employed for this is a manganese bath measurement. The anisotropy of the emission from the source also needs to be known [14.14], and this is best measured using a flat response counter to avoid any problems with small changes of the spectrum with direction of emission. The correction factor, F_I, is the ratio of the emission rate in the direction towards the device being calibrated compared with the average emission rate into 4π sr. For physically large sources, the anisotropy can be quite pronounced, as illustrated in Fig. 14.1. With these two items of information, the fluence arriving directly from the source at any angle relative to the axis of the source, and any distance from the source, can be calculated using the inverse square law. Most radionuclide neutron sources are cylindrical. Emission is assumed to be isotropic about the axis of the cylinder, and the preferred direction for calibration is perpendicular to this axis.

     One advantage of using the ISO recommended radionuclide sources is that reasonably good information is available about their spectra (see Section 7), and spectrum averaged fluence to dose equivalent conversion coefficients have been calculated. These are tabulated in ISO 8529-3 and are reproduced in Table 14.1. Because source construction techniques and capsule designs differ among manufacturers, some allowance must be made for possible differences
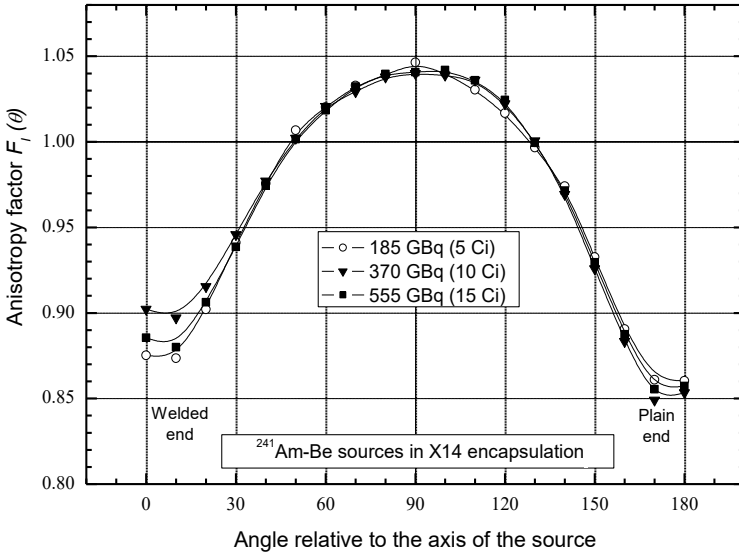
FIG. 14.1. Anisotropy factors for ^{241}Am-Be sources with three different amounts of ^{241}Am, each one in an X14 capsule. The anisotropy factor FI(θ) is the emission rate at angle θ relative to the average value [14.14]. (Courtesy of National Physical Laboratory.)

TABLE 14.1. SPECTRUM AVERAGED CONVERSION COEFFICIENTS FROM NEUTRON FLUENCE TO DOSE EQUIVALENT FOR ISO RECOMMENDED RADIONUCLIDE SOURCES

Neutron source	Fluence to dose equivalent conversion coefficient (pSv·cm^2)							
	$h*(10)$	$h_{p,\text{slab}}(10,\alpha)$						
		$\alpha = 0°$	$\alpha = 15°$	$\alpha = 30°$	$\alpha = 45°$	$\alpha = 60°$	$\alpha = 75°$	
^{252}Cf (D$_2$O moderated)	105	110	109	109	102	87.4	56.1	
^{252}Cf	385	400	397	409	389	346	230	
^{241}Am-B(α,n)	408	426	424	443	431	399	289	
^{241}Am-Be(α,n)	391	411	409	424	415	389	293	

in the spectra. The ISO recommendation [14.4] is an uncertainty component of 1% for the conversion coefficient of ^{252}Cf sources and 4% for ^{241}Am-B and ^{241}Am-Be sources.

The D$_2$O moderated ^{252}Cf source consists of a ^{252}Cf source capsule — which is usually physically rather small, typically a cylinder approximately 8 mm diameter by 10 mm long — at the centre of a 300 mm diameter sphere of D$_2$O, held within a spherical steel shell, with a 1 mm layer of cadmium on the outside to absorb thermal neutrons. (Some laboratories only include the cadmium layer over half the sphere, thus providing two different spectra from the two halves.) There is no more detailed technical specification provided for the configuration, and arrangements at different laboratories may vary in terms of source capsule size, construction of the steel sphere and tube into which the ^{252}Cf source is placed or the purity of the D$_2$O. The recommended uncertainty in the spectrum averaged fluence to dose equivalent conversion coefficients for this source [14.4] is 4%; however, a calibration laboratory concerned about the highest accuracy levels should consider calculating and/or measuring the spectrum for their particular D$_2$O moderated ^{252}Cf source configuration. From this information, fluence to dose equivalent conversion coefficients for that specific configuration can be calculated.

The D$_2$O moderated ^{252}Cf source presents one unique problem when used for calibration [14.15]. Its large size means that shadow cone measurements of scatter are difficult, and corrections may need to be made not only for the finite size of any device calibrated (geometry correction) but also the finite size of the source.

The dose equivalent rates available from radionuclide sources tend to be a little low for calibrating personal dosimeters, and so fairly long irradiations may be required to deliver significant dose equivalents to these devices. Area survey instruments tend to have higher sensitivities, and the low dose equivalent rates tend not to be a problem. A 1 μg ^{252}Cf source has a neutron emission rate of approximately 2.3×10^6 s^{-1}, and this corresponds to a dose equivalent rate (ambient or personal) of roughly 26 μSv·h^{-1} at 1 m. Calibration sources can be tens of μg, or even 1 mg or more, but handling increasingly becomes a problem for higher output sources. A 1 GBq ^{241}Am-Be source has an emission rate of about 6×10^4 s^{-1}, corresponding to a dose equivalent rate of roughly 0.7 μSv·h^{-1} at 1 m. Typical calibration sources have activities roughly in the range 30 to 600 GBq. When they were first made, americium based sources were produced with activities that were an exact, or a nearly exact, number of Ci or mCi. This convention has continued, and they still tend to be sold in this way. A 1 Ci (37 GBq) ^{241}Am-Be source has an emission rate of approximately 2.3×10^6 s^{-1}.

Throughout this section it has been assumed that the radionuclide source is a capsule that can be used in a low-scatter environment, and the whole thrust of the approach has been to perform the calibration for the free in air spectrum of the sources as given by ISO [14.9]. This is the usual approach; however, neutron sources are also available inside large shielded irradiators, which produce a collimated beam of neutrons. This approach removes some of the problems of room scatter, but introduces a whole new set of problems associated with changes in the spectrum caused by collimator scattering. These can be estimated using neutron transport codes but should be validated using a transfer instrument. If the transfer instrument is calibrated in a free in air field, then corrections need to be applied for the different response in a collimated beam. This correction is essentially the ratio of the spectrum averaged responses of the device in the two fields. These values can be obtained by folding the instrument response function with the two spectra.

14.2.3. Monoenergetic neutron fields

The ideal facility for measuring the response function of a radiation protection device, for example as part of a type test, is one that provides monoenergetic neutron fields of suitable intensity over the full energy range of interest. Such a facility can partly be realized at accelerator laboratories where neutrons are produced by nuclear reactions induced by charged particle beams [14.16]. By using thin neutron producing targets, in which the bombarding charged particles lose little energy traversing the target layer, neutron fields that are almost monoenergetic can be produced over the energy range from a few keV up to 20 MeV [14.17, 14.18]. Certain energies have been recommended by ISO [14.9] for use in this energy range (see Table 14.2).

To minimize the problems of correcting for room scatter, a large low-scatter facility, such as that shown in Fig. 14.2, is a significant advantage. The smaller the scatter correction, the less accurately it needs to be known. A 10% uncertainty in a 10% scatter correction only introduces a 1% uncertainty in a measured response.

Although there is a large region between thermal energies and a few keV where monoenergetic neutrons cannot be produced, the availability of monoenergetic fluences with energies between a few keV and 20 MeV is very important in determining device response functions, since this is a region where a large fraction of the dose equivalent occurs in most radiation protection situations.

For a radionuclide source, the emission rate, once measured, can be predicted at any subsequent time, provided the half-life is known. For accelerator produced neutrons, the fluence normally has to be measured each time the accelerator is run. Since the fluence measuring instrument and the device to be calibrated cannot both be in the same place at the same time, the procedure

TABLE 14.2. MONOENERGETIC NEUTRON ENERGIES
RECOMMENDED IN ISO 8529-1 AND THE REACTIONS USED TO
PRODUCE THEM

Neutron energy (MeV)	Reaction used
0.024	$^{45}Sc(p,n)^{45}Ti$
0.144	$^{7}Li(p,n)^{7}Be$ or $T(p,n)^{3}He$
0.250	$^{7}Li(p,n)^{7}Be$ or $T(p,n)^{3}He$
0.565	$^{7}Li(p,n)^{7}Be$ or $T(p,n)^{3}He$
1.20	$T(p,n)^{3}He$
2.50	$T(p,n)^{3}He$
2.80[a]	$D(d,n)^{3}He$
5.00	$D(d,n)^{3}He$
14.8[a]	$T(d,n)^{4}He$
19.0	$T(d,n)^{4}He$

[a] Neutron energies produced using a deuteron energy of a few hundred keV.

involves employing a standard device to measure the fluence relative to a monitor indication. The standard device is then replaced by the device to be calibrated and the monitor used to derive the fluence at the device. The monitor is a vital part of the arrangement, and it is important that it is not affected by the presence or absence of a device at the *point of test*, or if it is, that corrections can be derived for this dependence.

Several types of fluence measuring devices can be employed. Proton recoil instruments such as hydrogen filled proportional counters, scintillators and proton recoil telescopes are commonly used [14.20]. They can be considered to have some of the characteristics of a primary instrument, since they are based on the well known n–p scattering cross-section. Another instrument that has features that make it an excellent device for measuring neutron fluence is the long counter [14.16, 14.20]. It has a high efficiency and a near flat response, with neutron energy over a range from a few keV to roughly 6 MeV. However, it is

FIG. 14.2. Low scatter environment for neutron calibrations. Monoenergetic neutrons are produced at the centre of the circle seen at left in the picture at about 6 m from the nearest solid surface (the floor). (Courtesy of National Physical Laboratory.)

not an absolute device, and its efficiency needs to be determined. With modern neutron transport codes, backed up with measurements using radionuclide sources, the efficiency can be derived to an accuracy of the order of a few per cent [14.21]. One other characteristic of a long counter needs to be known, and that is the position of the effective point of measurement of the device. This parameter, normally known as the effective centre position, can be measured and also calculated by simulating an effective centre measurement [14.22].

If fluence rates are sufficiently high, foil activation can be used to provide an accurate measure of the fluence [14.23]. One reaction that produces high fluences is the $T(d,n)^4He$ reaction when the bombarding deuterons have energies in the region between 120 keV and roughly 400 keV. Neutrons with energies between 14 and 15 MeV are produced, and the fluences can be measured using iron or aluminium foils and the reactions $^{56}Fe(n,p)^{56}Mn$ and $^{27}Al(n,\alpha)^{24}Na$ respectively, although the short half-life, of approximately 2.5 h, for ^{56}Mn means that the resulting activity needs to be measured very soon after the irradiation [14.24]. The $T(d,n)^4He$ reaction is highly exothermic, and the associated particle technique can be employed to determine the fluence with relatively low uncertainty [14.25–14.27].

Calibrations with monoenergetic neutron fields involve a number of corrections, the most important usually being for scatter from the walls of the

room and in the air. For the room scattered neutron component, correction techniques very similar to those employed for radionuclide sources can be used (see Section 14.2.5). Other corrections include:

(a)   Target scatter, where neutrons scatter in the target backing or the target can. These effects are not included in the room and air scatter corrections, and allowance must be made using some other technique, such as neutron transport calculations or time of flight measurements [14.28].

(b)   Neutron production from the backing on which the thin neutron producing target layer is deposited. Efforts are usually made to find backings with minimal neutron production.

(c)   Variation of neutron energy with emission angle. This variation can be calculated from the kinematics of the neutron producing reaction.

(d)   Contaminant sources of neutrons produced by reactions of the accelerated beam with unwanted components in the target (e.g. oxygen or carbon).

Whereas the fluence from a radionuclide source varies according to the half-life, the fluence at an accelerator based facility can change dramatically with time over an irradiation, and a reliable monitor that is a measure of the neutron fluence produced by the target is essential, particularly when applying the shadow cone scatter correction technique. Typical monitors are fixed, moderator-based, detectors such as long counters, and/or the beam current on the target. Both, however, need to be treated with caution, the fixed monitor because its indication may be affected by scatter from different sized devices at the point of test, and the beam current because the beam 'spot' may move on the target and the target layer may not be completely uniform. For some reactions, such as the $^{45}Sc(p,n)^{45}Ti$ where the yield varies significantly with very small changes in the beam energy, the beam current is not a suitable monitor.

The spectrum of the neutrons, although usually described as monoenergetic, is probably better described as quasi-monoenergetic because the primary neutron peak has a finite width, and because target effects introduce unwanted neutron components. These are due, for example, to neutron scattering in the target and to unwanted neutron production from the target backing and possibly from reactions with contaminants in the target layer [14.29]. Another correction to be considered is that for field uniformity over the device or devices being calibrated. Both the neutron fluence and energy vary with angle for the reactions used to produce monoenergetic neutrons, and allowance may need to be made for this, for example, when calibrating personal dosimeters if several dosimeters are distributed over the face of a phantom placed relatively close to the neutron producing target [14.30, 14.31].

Fluence and dose equivalent rates depend on the beam currents that can be used and on the target thickness chosen. Beam currents are usually limited by target heating effects that can result in loss of target material [14.20]. Higher yields can be obtained using thicker target layers; however, the thicker the layer, the greater the energy width of the primary neutron peak.

Although monoenergetic neutron fields are ideal for measuring instrument response characteristics, there is a scarcity of locations where these fields are available. This derives mainly from the fact that they are large and expensive measurement facilities. Monoenergetic neutron measurements are usually part of a type test rather than a routine calibration, except in cases where an instrument is going to be used at fields that have a strong monoenergetic component, such as areas around a 14 MeV neutron source, where a 14 MeV calibration might be more appropriate than one with a radionuclide source.

Several monoenergetic field facilities are situated at national metrology laboratories, and the soundness of fluence and dose equivalent calibrations in such fields is validated in international 'key' comparison exercises organized by the International Committee of Weights and Measures (CIPM) [14.32], or more specifically by Section (III) of the Consultative Committee for Ionizing Radiation.

14.2.4. High energy calibration facilities

The fields recommended in ISO 8529-1 [14.9] for calibration and type testing are restricted to the energy region below 20 MeV. There is, however, a need for calibration facilities at higher energies to characterize the devices used for measurements of cosmic ray fields in space and at aircraft flight altitudes and also for measurements around high energy accelerators. A small number of facilities exist where quasi-monoenergetic fields with energies in the region between 20 and 200 MeV are available. The use of the terms 'monoenergetic' and 'quasi-monoenergetic' is somewhat arbitrary. Even the best so-called monoenergetic neutron fields at energies below 20 MeV have some contaminant, usually lower energy, neutrons produced, for example, by scattering in the neutron producing target. At higher energies, these undesirable components are greater, and the term quasi-monoenergetic tends to be used. Considerable effort is required to characterize the fields, in particular to measure the broad lower energy components [14.33]. Time of flight spectrometry is an important tool for these pulsed beams.

High energy calibration fields have been established at several cyclotrons that are primarily used for medium energy nuclear physics research. Neutrons with energies extending up to approximately 90 MeV were available at the Université Catholique de Louvain in Louvain-la-Neuve, Belgium, [14.34] and are available in Japan at JAERI [14.35]. Higher energies are available

at RIKEN [14.36] in Japan, the iThemba Laboratory for Accelerator-Based Sciences (iTL) in Cape Town, South Africa, [14.37] and at The Svedberg Laboratory, TSL, in Sweden [14.38].

14.2.5. Scatter correction techniques

Since calibrations are normally performed inside shielded rooms, there will always be a problem with neutrons being scattered from the walls, floor and ceiling of the room into the device being calibrated. Equipment located within the room can further add to this scatter, as does the air in the room. The air has two effects: scattering out neutrons from the solid angle defined by the source and device, and scattering in neutrons that would not otherwise have been incident on the device. The scattered neutrons have a different spectrum to the primary neutrons, and their number is usually unknown. Corrections must therefore be applied for their effects. Low scatter facilities with large rooms provide a significant advantage because the number of scattered neutrons that arrive at the device is minimized. Another option is a room with thin walls that allow the neutrons to escape [14.13]. This latter approach is rarely feasible, however, because of radiological protection considerations. Corrections thus have to be determined and applied, and ISO Standard 8529-2 [14.4] gives a full and detailed description of the various approaches. Only an outline is given here, simply to explain the principles of the methods.

Two basic techniques are used for determining scatter corrections. The first involves utilizing the fact that the direct, unscattered neutron fluence has a $1/l^2$ dependence on l, which is the distance between the source and the effective point of measurement of the device being calibrated. This direct component can be picked out by making measurements at a series of distances. (The effective point of measurement, or effective centre, of the device should coincide with the reference point indicated by the manufacturer but may not always do so. The effective centre is essentially that point associated with a device for which its response varies as $1/l^2$ in a scatter-free environment.) There are several variants on this approach, which will be referred to here as the *distance variation* technique. The second technique involves the use of neutron absorbing material, usually a 'shadow cone', placed between the source and the device being calibrated in order to completely attenuate all the direct neutrons from the source while interfering as little as possible with the scattered neutrons. This approach is usually called the *shadow cone* technique.

14.2.5.1. The distance variation scatter correction technique

Following the approach of ISO Standard 8529-2, the indication, $M_T(l)$, of a device in a neutron field consisting of direct neutrons from a source and scattered neutrons is written as

$$M_T(l) = \frac{k}{l^2}\left\{\frac{F_G(l)}{F_A(l)} + F_S(l) - 1\right\} \qquad (14.4)$$

where

l	is the distance between the centre of the source and the effective centre of the device;
k	is the characteristic constant for the source and device combination;
$F_G(l)$	is a geometry factor correction;
$F_A(l)$	is an air attenuation (air out-scatter) correction;
$F_S(l)$	is the correction function that describes the contribution from in-scattered neutrons.

The assumption is made in Eq. (14.4) that $M_T(l)$ has been corrected for any device non-linearity due, for example, to high rates. Using the distance variation technique, a value for k can be extracted from Eq. (14.4), and hence a value for the fluence response of the device, R_Φ. From R_Φ, the dose equivalent response, R_H, can be derived. The constant, k, is defined by

$$k = \dot{M}_C\, l^2 \qquad (14.5)$$

where $\dot{M}_C$ is the count rate of the device in the direct neutron field at distance l, i.e. after corrections have been made for all extraneous effects. The response R_Φ is defined by

$$R_\Phi = \frac{\dot{M}_C}{\varphi} = \frac{M_C}{\Phi} \qquad (14.6)$$

where φ is the fluence rate at the device, and Φ is the fluence over a time t for which the device indication was M_C. The fluence rate φ is related to the angular source emission rate, B_Ω (cf. Eq. (14.2)) by

$$\varphi = \frac{B_\Omega}{l^2} \tag{14.7}$$

and k can thus be related to R_Φ by

$$k = R_\Phi \, B_\Omega = R_\Phi \, \varphi \, l^2 \tag{14.8}$$

For a radionuclide source calibration, B_Ω can be derived from Eq. (14.2). For accelerator based measurements, B_Ω must be determined by one of the techniques outlined in subsection 14.2.3.

If the position of the effective centre is not known, then l can be written as $l = l' + r_D$, where r_D is the distance from the surface of the instrument to the effective centre and l' is the distance between the centre of the source and the surface of the instrument. The value of r_D can thus be included as an unknown variable in the measurement and fitting procedure used to derive the scatter correction. A value for r_D can be determined in this way, although the precision is usually poor because of the number of other unknown variables in Eq. (14.4). For spherical moderator based devices, such as a spherical area survey instrument or a Bonner sphere, the position of the effective centre is taken to be at the geometric centre of the sphere. For cylindrical devices irradiated from the side, the effective centre is assumed to be on the geometrical axis.

The geometry correction factor $F_G(l)$ corrects for the finite size of the device, specifically the fact that not all parts of the device are uniformly irradiated in the field of a point source. Various expressions are presented for $F_G(l)$ in the relevant ISO Standard [14.4], some being approximations of the general formula, and the complexity of the expression used depends somewhat on the size of the correction. Correction factors are presently only available for spherical devices, so it is recommended that measurements with other shaped devices are made only in regions where $F_G(l)$ is close to unity. For this, l should be greater than twice the effective diameter of the device. By convention, no geometry correction is made for dosimeter calibrations on a phantom.

The air out-scatter correction $F_A(l)$ can be calculated from the scattering cross-sections for the oxygen and nitrogen in the air. The correction is given by

$$F_A(l) = e^{(l\Sigma)} \tag{14.9}$$

where Σ is the linear attenuation coefficient obtained by averaging the total neutron cross-section for oxygen and nitrogen over the spectrum of the source. Values are presented in Ref. [14.4] for commonly used radionuclide sources.

The scatter correction factor $F_S(l)$ is derived by making measurements of $M_T(l)$ as a function of distance l and fitting the data to Eq. (14.4). This is referred to as the *generalized fit method*. It is a refinement of the earlier approach commonly called the *polynomial fit method* [14.39]. The assumption is made that $F_S(l)$ has the form

$$F_S(l) = 1 + A'l + s\,l^2 \qquad (14.10)$$

where A' and s are associated with air and room scatter, respectively. Measurements need to be made at no less than 30 distances and, unless geometry effects are negligible, the fitted parameters will include those defining the geometry correction as well as k, A' and s.

A variant on the generalized fit method is the *semi-empirical method* [14.40, 14.41]. There are strong similarities. In the semi-empirical approach, the equation linking $M_T(l)$ to R_Φ is

$$\frac{M_T(l)}{\Phi F_G(l)(1+Al)} = R_\Phi(1+S\,l^2) \qquad (14.11)$$

Here, S is the fractional room scatter contribution at unit distance and can be identified with s in the generalized fit method. The term $(1+Al)$ allows for air scatter, but here corrects for the net effect of air scatter (i.e. in-scatter minus out-scatter). The parameter A thus differs from A' in the generalized fit method. The approach is again to make measurements as a function of distance; however, the parameter A is not derived from the fit but from calculations. Values are provided in an annex to Ref. [14.4].

A second variant on the generalized fit method is the *reduced-fitting method* [14.42]. This is a simplified approach applicable when l is reasonably large ($\geq$ three times the device diameter). The assumption is made that the air scatter term is negligible compared with the room scatter term. This is the case in all but the largest low-scatter rooms at reasonably large values of l. The equation, a simplified version of Eq. (14.4), is

$$M_T(l) = \frac{k}{l^2} + S \qquad (14.12)$$

The parameters k and S, and the effective centre distance if not known, may be determined from a weighted least squares fit. Fewer data points are required than for the other two distance variation methods.

FIG. 14.3. *A shadow cone being used with neutrons from an accelerator target. (Courtesy of National Physical Laboratory.)*

14.2.5.2. *The shadow cone scatter correction technique*

The idea behind the shadow cone technique is simple and straightforward. A cone of absorbing material is placed between the source of neutrons and the device being calibrated in order to cut out all the direct neutrons in the solid angle defined by the geometry of the source–device combination. The measurement with the shadow cone provides an estimate of the response to scattered neutrons, and by subtracting this from the result of the measurement without a shadow cone, the response of the device to the direct neutrons from the source is obtained. Corrections for air out-scatter from the solid angle defined by the source–device geometry have to be applied. The equation describing the process is

$$\left[M_T(l) - M_S(l)\right] F_A(l) = \frac{k}{l^2} \tag{14.13}$$

where $M_S(l)$ is the indication of the device with a shadow cone present, and the other symbols have the same meaning as in the previous subsection. The arrangement of a shadow cone for a measurement is shown in Fig. 14.3 and schematically in Fig. 14.4.

A series of measurements, with and without a shadow cone, for a number of distances, should be performed to check that Eq. (14.13) holds for the

arrangements at a particular calibration facility. A plot of $\left[M_T(l) - M_S(l)\right]$ against $1/l^2$ should be a straight line passing through the origin. The response can be determined from the value derived for k.

The design of the shadow cone should ensure that all, or at least a sufficiently large fraction (i.e. > 99.9%) of the direct neutrons from the source are absorbed. A common design consists of 20 cm of iron followed by 30 cm of a hydrogenous material such as polyethylene or wax. The hydrogenous material is usually loaded with 5% or more of boron to absorb thermal neutrons.

It is evident from Fig. 14.4 that a given shadow cone only has the ideal shape for the cone defined by a particular source–device combination. Even so, some scattered neutrons that would have been incident on the device are absorbed by the cone, for example neutrons scattered in the air close to the source (see example in Fig. 14.4). For measurements with different source–device combinations and at different source to device distances, a range of shadow cones with different angles is required. It is essential that the cone shadows all the direct neutrons, so in any experiment, bearing in mind the difficulty of positioning a heavy cone in precisely the right place, the tendency is to slightly 'over shadow'. This is the safer option; however, an upper limit for the shadowed area of a factor of two larger than the device is suggested [14.4].

Accepting the fact that the shadow cone dimensions are rarely going to be absolutely ideal, there is nevertheless an optimum position for any cone. At very

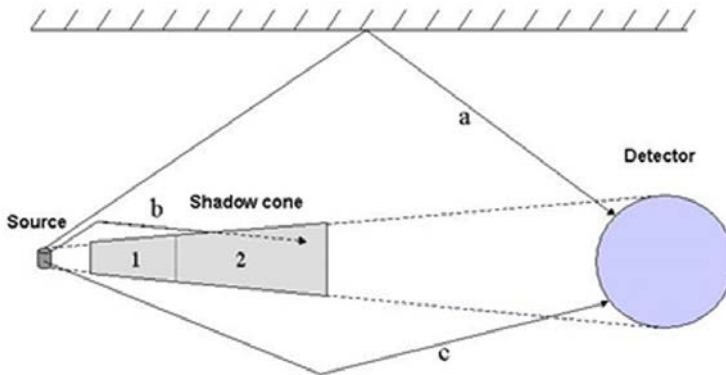*FIG. 14.4. Schematic diagram of a shadow cone ideally positioned between source and detector. Material 1 is a metal (usually iron, although copper has also been used), and material 2 is a hydrogenous material (e.g. polyethylene or wax), preferably with a boron content. Path (a) represents room scatter, path (b) air scatter with the neutron absorbed by the shadow cone and path (c) air scatter with the neutron striking the detector.*
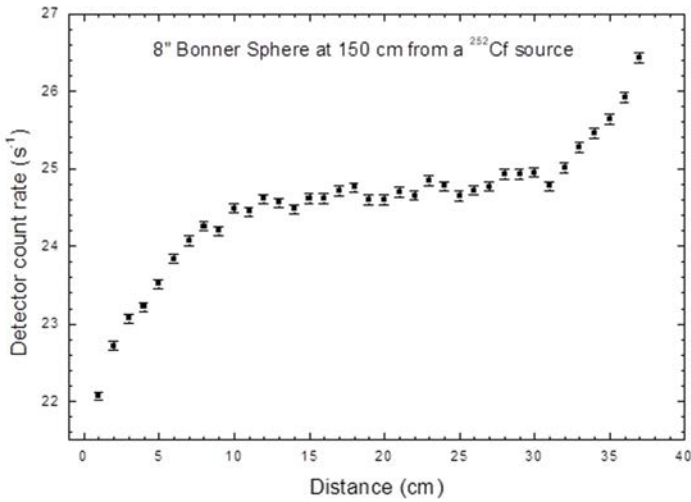
FIG. 14.5. Variation of detector count rate as a function of the distance between the source and the narrow end of the shadow cone. The optimum source to cone distance is at the mid-point of the plateau region.

small separation distances between the source and cone, the device indication will underestimate the scatter component, since the cone effectively shadows much of the hemisphere in the direction of the device. Too large a distance between source and cone will eventually result in incomplete shadowing. For many source–device–cone combinations, there is a range of source to cone separation distances that gives optimum shadowing. This range can be found experimentally (see Fig. 14.5).

14.2.5.3. Choice of scatter correction technique

The various scatter correction techniques have limitations and advantages. For example, the shadow cone technique requires a very large shadow cone for the heavy water moderated ^{252}Cf source; the generalized fit method is only applicable to spherical devices if small distances are used and geometry corrections need to be applied. The semi-empirical method requires calculated air scatter corrections for each device, and only a limited number are available; also, the technique does not work well in large rooms where air scatter dominates room scatter. For the reduced-fitting method, the user needs to confirm that none of the effects neglected (e.g. air scatter) is important. A more detailed list is provided in Ref. [14.4].

If devices of a particular type are calibrated regularly at a laboratory, the distance variation methods can be used to derive the scatter correction for one instrument of this type, and the same correction can be applied to all other instruments of the same type. Where instruments of many different types are to be calibrated, a technique such as the use of a shadow cone may be preferable for determining the scatter correction, since this only involves two measurements: one with and one without a cone. The reduced-fitting method, which requires less data to be gathered than the other two distance variation approaches, can also be used routinely.

Whichever scatter correction technique is chosen, it should be compared against at least one of the other techniques. This is the only way in which the efficacy of the approach can be confirmed.

14.2.6. Thermal neutron calibration facilities

When an instrument response function is plotted on a logarithmic energy scale, which is the normal approach in neutron radiation protection physics, it is obvious that a large proportion of the energy range of interest lies below the lower limit (a few keV) for monoenergetic neutron measurements (see Section 14.2.3). Any well specified neutron fields with low energies are thus very valuable for extending response function measurements, and one of the most useful facilities in this respect is a thermal neutron field.

Thermal reference fields can be produced using reactors, accelerators or radionuclide sources, and they all involve the slowing down of fast neutrons in a moderator. A thermal neutron fluence spectrum usually has the form of a Maxwellian distribution, characterized by a peak neutron energy given by kT, where k is Boltzmann's constant, 8.617×10^{-5} eV·K^{-1}, and T is the moderator temperature in kelvin. Because no moderator is perfect, thermal fields usually contain a $1/E$ component extending to higher energies. (Neutrons slowing down in an ideal moderator have a spectrum with a $1/E$ dependence, where E is the neutron energy, and the energy region between the original fast neutrons and the thermal distribution tends to be called the $1/E$ region.) As a result of the presence of this component, most thermal calibrations have to be performed using the cadmium difference method. This involves making a measurement with the device bare and also under a cadmium cover of about 1 mm thickness, which captures all neutrons with energies less than about 0.5 eV.

Historically, standard fluences have been measured using activation foils [14.43], and the fluence has been quoted using the Westcott convention [14.44, 14.45]. This allows a measure of the fluence to be given with small uncertainties. Although this approach is ideal for comparing thermal cross-sections in activation measurements, it is not the quantity required when

using the thermal facility to calibrate devices used to measure neutron dose equivalent. The quantity required is the 'true' fluence, and to derive this from the Westcott fluence requires spectral information.

It is a mistake to think of a thermal field as being monoenergetic. Viewed on a linear energy scale, the Maxwellian peak is of course very narrow, but when viewed on a logarithmic scale the distribution is rather wide, as illustrated in Fig. 14.6.

A thermal calibration thus provides the response over a particular neutron energy distribution, and for a comparison between a measured and calculated thermal response, the calculation should be performed for the energy distribution of the thermal field in which the measurement is performed. This may not always be known accurately but should always be taken into account when considering thermal calibrations. Ideally the thermal energy spectrum should be measured using time of flight [14.46] (see Fig. 14.6), but this is not always possible, and information on the distribution may have to be gleaned from data such as the cadmium ratio for a gold foil measurement of the fluence [14.47], which can provide an estimate of the 'effective' Maxwellian temperature based on a semi-empirical relationship [14.48]. The spectrum needs to be known not only to compare calculations and measurements, but also to derive the dose equivalent of the field from the fluence [14.47].
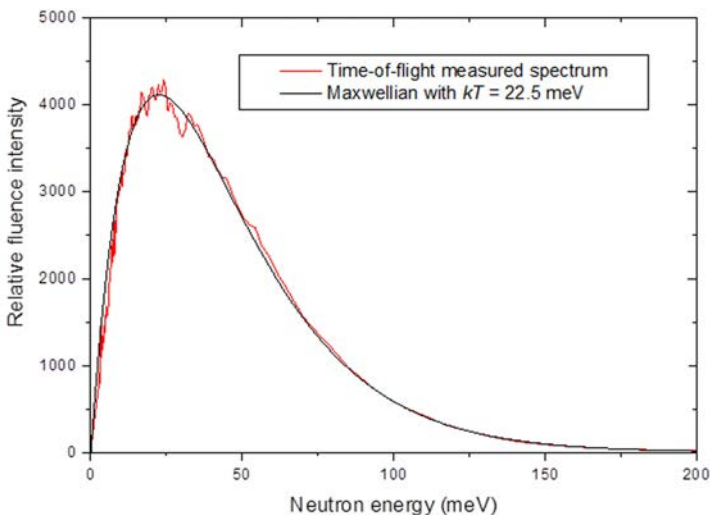

FIG. 14.6. A Maxwellian thermal distribution compared with a time of flight measurement made at a standard facility based on a research reactor. (Reproduced from Ref. [14.46] with permission from Physikalisch-Technische Bundesanstalt, Germany.)

The use of a reactor is the most obvious approach to providing thermal neutron calibration fields. Several national standards laboratories are able to offer this approach [14.46, 14.49]. Very pure thermal fields can be made available with low, or even zero, high energy neutron and photon components. One drawback, however, may be the small diameter of the beam, necessitating scanning for irradiation of most objects [14.46]. When scanning is performed, great care should be taken when performing any required dead time corrections, since the indication of the instrument can be very variable. The next most obvious approach is probably to use a radionuclide source, or a collection of radionuclide sources within a moderator, usually graphite or polyethylene. Examples of this approach are described in Refs [14.50] and [14.51]. Source based systems have the advantage that, because the arrangement is usually reasonably simple, the neutron spectrum can be calculated using modern Monte Carlo transport codes (see the two aforementioned references for details).

Thermal fields can also be produced by generating primary neutrons using an accelerator and moderating these to provide a thermal calibration field. This is, of course, the means of producing thermal neutrons for neutron scattering experiments at large spallation sources [14.52], but thermal neutron calibration facilities are not generally available at such sites. An example of this approach where a facility was designed specifically for calibration purposes is described in Ref. [14.53]. Neutrons are produced by bombarding beryllium targets inside a graphite moderating block with deuterons. Thermal fluence rates in excess of 10^7 cm^{-2}·s^{-1} can be produced in a small cavity at the centre of the moderator, which was originally intended for foil activation work. This is considerably smaller than available, for example, at an irradiation port within a reactor, but is nevertheless adequate for many thermal activation measurements. For larger devices, up to 30 cm in diameter, a thermal column beam can be extracted with fluence rates up to approximately 4×10^4 cm^{-2}·s^{-1}, adequate for calibrating survey instruments and even personal dosimeters, albeit with irradiation times of several hours. One advantage of the accelerator approach is that the fluence can be varied by altering the beam intensity; saturation tests can even be performed for some devices. There is also the advantage, in terms of radiation protection, that the neutron field can be switched off for setting up instrumentation and outside experimental run times.

14.2.7. Reactor filtered beams

The need to provide neutron calibration fields with energies that bridge the large gap between thermal and the lowest energies available using radionuclide sources or monoenergetic accelerator based fields has long been recognized. One means of providing such fields is via reactor filtered beams, whereby neutron

interference (or window) filters located in beam tubes at high flux reactors can produce a variety of energies, including 2 keV (scandium filter) [14.54], 24.5 keV (iron filter) [14.55–14.57] and 144 keV (silicon filter) [14.5]. Figure 14.7 shows the ^{56}Fe total cross-section with the pronounced dip at 24.5 keV that enables the iron filtered beam to be produced. The large number of other dips at higher energies illustrates the problems of possible higher energy contaminant components. (Because of the transmission of 24.5 keV neutrons, there are always potential problems with iron as a neutron shield.) Lower energies than those listed above are achievable in principle [14.58], and proposals have been made for an international reactor filtered neutron beam project [14.59], but without success to date. Unfortunately, however, few of these facilities are available, and some of those that were available in the past have now been closed down.

14.2.8. White sources

Accelerator based pulsed white neutron sources can produce neutrons with energies covering the range from thermal to several tens of MeV [14.61]. They are an extremely efficient source for high resolution measurements of microscopic neutron cross-sections. They can also be used to measure instrument response functions if the instrument has timing properties that allow time of flight measurements. This is not usually the case for survey instruments and personal
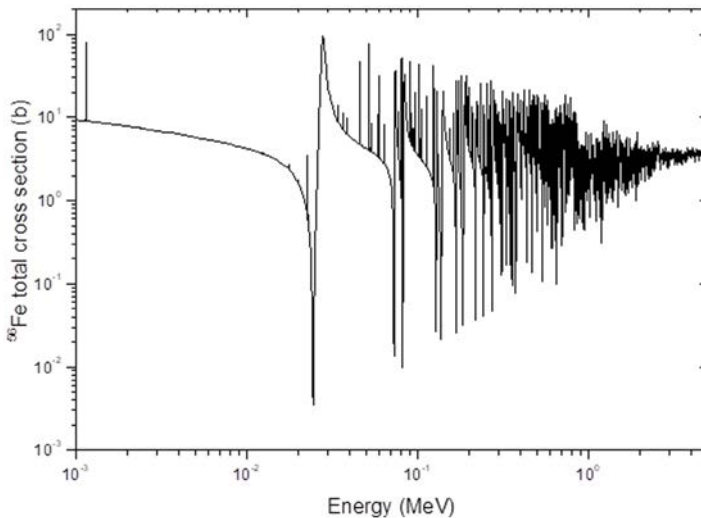

FIG. 14.7. The ^{56}Fe total cross-section, illustrating the dip at 24.5 keV that allows neutrons of this energy to be produced by iron filtered reactor beams. Data derived from Ref. [14.60].

dosimeters, but it can provide an extremely useful means of characterizing the response of devices such as neutron spectrometers [14.62].

14.2.9. Simulated workplace fields

Because of the characteristics of available neutron personal dosimeters and survey meters, namely their poor dose equivalent response, it is not possible to obtain reliable measurements in the workplace when using devices calibrated with sources specified in ISO 8529-1 if the workplace spectrum differs markedly from the calibration source spectrum. At least two possibilities exist for improving the situation. First, the neutron spectrum of the workplace field can be measured and a factor calculated to correct the response of the detector. Second, a facility can be constructed to produce a neutron field that simulates the energy spectrum found in the workplace. When this field has been properly characterized, it can be used to investigate the response of personal dosimeters and survey meters in workplace environments. This approach has been employed at a number of laboratories. Several facilities are described in ISO Standard 12789-1 [14.63], although some of these facilities may no longer be available and others have been introduced [14.64, 14.65].

A comparison of neutron spectra in nuclear power plants and in the vicinity of transport casks containing spent fuel elements with spectra for conventional calibration sources reveals that these workplace spectra are much softer than those of calibration fields. Other radiation environments may contain neutrons having much higher energies. For example, neutrons with energies greater than 10 MeV, contributing 30–50% of the ambient dose equivalent and personal dose equivalent, have been found in the vicinity of high energy particle accelerators [14.66, 14.67]. In aircraft, the high energy component may be even higher [14.68]. A calibration field has been developed at CERN, the European Organization for Nuclear Research, that simulates the neutron spectrum at aircraft flight altitudes [14.69]. This has played a major part in underpinning cosmic ray dosimetry for aircrew. Figure 14.8 compares the simulated field spectrum with the neutron spectrum it is intended to replicate.

It is clear that a range of different types of simulated fields is required. They can be based on radionuclide sources, accelerators or reactors. A variety of absorbing and scattering material is placed between the primary source and the detector to modify the initial source spectrum and to produce the required characteristics. To characterize the field, it is necessary to measure and calculate the energy spectrum and to determine the angle dependence of the neutron fluence at the reference position. This can be a significant task [14.65].

Since many workplace fields have very soft spectra, it might be supposed that any soft simulated field is likely to be a better calibration facility than the
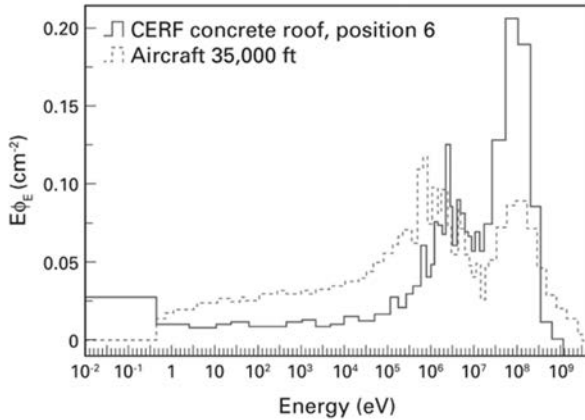
FIG. 14.8.   Comparison of the CERN–EU High-Energy Reference Field (CERF) neutron spectrum with the neutron spectrum at an altitude of 10.6 km (35 000 feet), as calculated by Heinrich et al. [14.70]. The total fluence is normalized to unity. (Reproduced from Ref. [14.69] with permission from Oxford University Press.)

rather hard fields provided by conventional radionuclide sources. The fact that survey instrument responses can both under- and over-read, and the fact that some fast neutron dosimeters have energy thresholds below which they do not respond, means that the supposition above is not always the case [14.71].

14.2.10.   Field calibrations

Because albedo dosimeters are sensitive primarily to low energy neutrons (see Section 11), their calibration in the fast neutron fields produced by conventional radionuclide sources is of limited value without information about the ratio of the dosimeter response in the calibration field and the workplace field. An alternative approach is a direct workplace field calibration, and various techniques for have been derived. These basically involve characterising the dose equivalent in the fields where the dosimeter will be used and calibrating the dosimeter, on phantom, in these environments to provide field specific calibration factors.

An example of this latter approach is the so-called single sphere technique of Piesch and Burgkhart [14.72, 14.73]. This involves mounting the albedo dosimeters at points around a 300 mm diameter polyethylene sphere that acts as a survey meter for determining the dose equivalent. When evaluating the reliability and accuracy of this approach consideration needs to be given to the response

function of the albedo dosimeter and to any knowledge of the spectral and angle properties of the field.

An approach, similar in principle, but using quite different instrumentation, has been described by Harvey and Hart [14.74]. The instrument used consists of two silicon diode detectors, each with a thin layer of ^{6}LiF. One of these detectors is positioned at the centre of a 3 inch (76.2 mm) sphere of polyethylene and gives information mainly on the intermediate energy region, whereas the other is used bare and primarily provides information on the thermal region. Information from a conventional area survey instrument can also be utilized. The absolute response functions of both detectors can be determined with reasonable accuracy, and the indications of the two devices can be combined in various proportions to mimic the response of an albedo dosimeter. The instrument can be used to assess the most appropriate dosimeters to use in a particular environment and gives information used in the interpretation of albedo dosimeter indications.

A third approach is the so-called 9/3 sphere ratio method described by Hankins [14.75, 14.76]. In this technique, the ratio of the indications of a small BF_3 probe in a 9 inch (22.86 cm) polyethylene sphere to the indications of the same probe in a 3 inch (7.62 cm) sphere of the same material is used as a measure of spectral hardness. The two spheres are not plain polyethylene. The 9 inch sphere is in fact a commercially available survey instrument that incorporates cadmium to give a better dose equivalent response (cf. Section 10), whereas the outside of the 3 inch sphere is covered in a 0.3 mm thick layer of cadmium. The response of the 3 inch sphere mimics that of an albedo detector. A graph is available that provides a relationship between the 9 inch to 3 inch ratio and the calibration factor for an albedo dosimeter [14.76]. The calibration factor increases as the ratio decreases. When plotted on a log–log graph, there is a straight line relationship between correction factor and ratio. The calibration factors vary over a wide range — two orders of magnitude for neutron fields with mean energies between 2 keV and 14 MeV.

14.2.11. Traceability

The method used to provide traceability to national standards depends on the type of reference radiation field, but traceability is usually achieved using a transfer standard. This may be, for example, a radionuclide source or an agreed-upon transfer instrument. Strictly, the calibration of the field is valid only at the time of the calibration, but it can subsequently be determined from a knowledge of the half-life and isotopic composition of the radionuclide source or knowledge of the properties of the transfer instrument.

For calibrations with neutron fields produced by radionuclide neutron sources, traceability can be established either by using a source whose angular

emission rate characteristics have been determined by a reference laboratory, or by determining the fluence rate at the point of test using an agreed-upon transfer instrument, calibrated at a reference laboratory. If the source is encapsulated according to the recommendations in ISO Standard 8529-1 [14.9], it can be assumed that the fluence to dose equivalent conversion coefficients recommended in this standard may be used.

Traceability for accelerator produced neutron beams can be provided by using a transfer instrument that has been agreed upon by the calibration and the national standards laboratories. The transfer instrument should be used in the same manner, for similar neutron fields, as when it was calibrated, and all the proper corrections should be applied.

Reactor-produced thermal or filtered neutron beams can be determined as being traceable to national standards using the general principles mentioned above. For example, the thermal neutron fluence rate may be measured by the activation of gold foils, for which the measurement is traceable to a national standard.

14.3. CALIBRATION OF PARTICULAR DEVICES

Any calibration factor is, in principle, only valid at the time of calibration. To ensure that no change occurs after the calibration measurement, it is recommended that any device sent for calibration is checked for consistency of indication, for example with a test source in a fixed jig, before dispatch and after it returns. This is not always practical, for example for single use devices such as etched track dosimeters, but some checks may still be performed, assuming that samples from a particular batch are all the same.

14.3.1. Area survey instruments

Calibrations and type test measurements for survey instruments are made easier by the fact that they are quite sensitive devices, and so measurements can be performed reasonably quickly in the types of dose rates normally available in calibration facilities. For radionuclide sources or for monoenergetic fields, corrections for room and air scattered neutrons have to be performed, for example by making measurements with shadow cones or by applying correction factors previously determined for instruments of a particular type.

Although these devices are intended to have an isotropic response, the presence of electronic units means that even in devices based on spherical moderators, this requirement is not fully met, and measurements of the angle dependence of response need to be made at least during a type test. Full

details of how survey instrument calibration should be performed are given in ISO Standard 8529 parts 1 to 3 [14.4, 14.8, 14.9].

14.3.2. Personal dosimeters

Passive personal dosimeters, that is to say, dosimeters that do not provide an immediately available estimate of the personal dose equivalent but need first to be processed, can be divided into those that detect fast neutrons and those that detect moderated slow neutrons. The latter are termed albedo dosimeters and are one of the most commonly used personal dosimeters worldwide. Different considerations apply when calibrating these two rather different types of dosimeters.

14.3.2.1. Passive fast neutron personal dosimeters

With the decline in the use of dosimeters based on nuclear track emulsions (film), the most common passive fast neutron personal dosimeters are those based on a particular etched track plastic material, often known under the trade name CR-39, and sometimes by the acronym PADC, which stands for its chemical name, polyallyl diglycol carbonate (see Section 11). Routine calibrations are usually performed using an ^{241}Am-Be or a ^{252}Cf source, with the dosimeters mounted on phantom reasonably close to the source. The phantom recommended by ISO is a 30 cm × 30 cm × 15 cm slab phantom with walls made from PMMA, 2.5 mm thick on the front, 10 mm thick on the sides and filled with water [14.8], and the recommended source to phantom distance is 75 or 50 cm. The reasons for the rather close distance are twofold. It both helps provide a reasonable dose equivalent rate to counter the rather low sensitivity of many personal dosimeters and allows scattered neutrons to be neglected. The direct neutron component from the source decreases as the distance squared, the air scatter component is roughly proportional to the inverse of the distance, and the room scatter is approximately constant near the centre of a large room. Short distances thus maximize the direct component relative to the scatter. The fact that etched track dosimeters have a threshold for detection at approximately 50 to 200 keV, allied to the fact that the scattered field is of lower energy than the direct, combined with the shielding effect of the phantom for some scattered neutrons, all help in minimizing the response to scattered neutrons, thus allowing them to be ignored during calibration. Ideally, however, the fact that they are negligible should be demonstrated by a calibration laboratory, for example via simulation calculations.

More than one dosimeter is usually mounted on the phantom face during a calibration. These should be sufficiently far apart to ensure that scattering

between dosimeters is not an issue. Corrections for the individual distances from the source to each dosimeter are easily made by measuring the distance of the dosimeters from the centre of the phantom face in addition to the distance from the source to the centre of the phantom face.

Etched track dosimeters can be made sensitive to thermal neutrons by including a material in close proximity to the plastic that produces charged particles following thermal neutron capture; ^{6}Li and ^{10}B are obvious materials, and nitrogen is another. The presence of such thermally sensitive elements can give the dosimeter some of the characteristics of an albedo dosimeter, in which case the issues inherent in calibrating albedo dosimeters need also to be considered.

14.3.2.2. *Albedo neutron dosimeters*

Personal dosimeters based on the albedo principle are used where the fluence spectrum contains primarily lower energy neutrons, such as might be encountered at a nuclear power plant. The radiation sensitive elements in an albedo dosimeter are usually TL detectors mounted in the dosimeter assembly (see Section 11). Since these dosimeters respond primarily to the low energy neutrons reflected from the body of the wearer, these dosimeters must be calibrated while mounted on a phantom. Suitable phantoms for this purpose are recommended by ISO [14.8] and consist of either a 30 cm × 30 cm × 15 cm PMMA-walled, water filled tank, or a similarly sized phantom of solid PMMA.
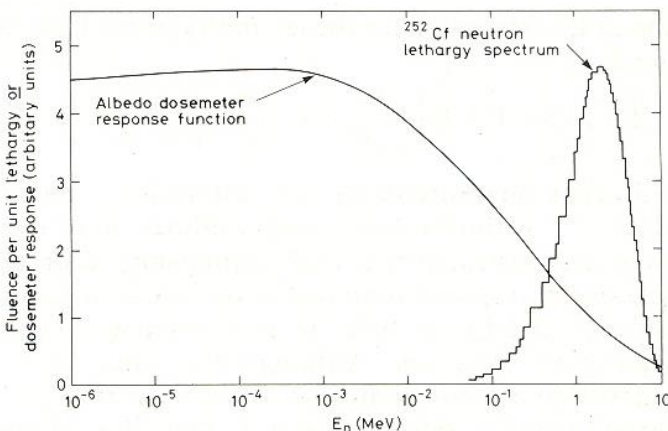

FIG. 14.9. *A typical albedo dosimeter response function plotted together with the energy spectrum of a ^{252}Cf radionuclide source. (Reproduced from Ref. [14.77] with permission from Oxford University Press.)*

Albedo dosimeters can be calibrated in standard radionuclide fields using the approaches outlined earlier in this section; however, the value of these calibrations is questionable. Figure 14.9 shows a typical albedo dosimeter response function and also the ^{252}Cf energy spectrum. It is clear that the majority of the ^{252}Cf neutrons occur in an energy region where the dosimeter response is decreasing rapidly from the near constant value below about 1 keV. If the dosimeter is to be used in an unscattered ^{252}Cf field, this approach is reasonable, but if it is to be used in an environment containing a large number of low energy neutrons, as is usually the case, the approach is not ideal. In such a situation, a field dependent correction factor would need to be applied. Alternatively, a field calibration (cf. Section 14.2.10) might well be preferable.

14.3.2.3. Active (electronic) personal dosimeters

An increasing number of active personal dosimeters are becoming commercially available. These are usually electronic dosimeters based on semiconductor devices [14.78], although other devices exist, such as the ion chamber based RADOS DIS-N [14.79], TEPC based devices and ones using either a very small ^{3}He detector or scintillator. Semiconductor based devices usually consist of one or more silicon detector with radiators of hydrogenous material and/or thermally sensitive material. A silicon detector with a hydrogenous radiator has many of the characteristics of an etched track device, and one with a thermally sensitive radiator has many of the properties of an albedo dosimeter. All the issues outlined above for passive devices need to be taken into consideration when performing calibrations. In particular, it is important to know the detection mechanism(s) of any active dosimeter in order to interpret calibration results and decide on its fitness for purpose. The greater size of active dosimeters may mean that only a few can be mounted on a phantom at one time.

14.3.3. Reference point for personal dosimeters

The normal calibration concept of defining a point of test in space, where the value of the quantity of interest is known, and arranging for the reference point of a measuring device to be at that point raises problems for the quantity personal dose equivalent. This is because it is defined as the dose equivalent at a depth d in the body but is actually measured using a personal dosimeter worn on, or near, the surface of the body. In a situation where the irradiation is with a plane parallel beam of neutrons, which is the situation assumed when calculating the fluence to dose equivalent conversion coefficients, there would be no problem, as the quantity has the same value anywhere in the beam. The problem arises because the majority of calibrations are performed with a source of neutrons that

approximates to a point source, so the fluence, and hence any dose equivalent quantity, has a $1/l^2$ dependence on the distance l from the source. The question that is raised is, then, where in the 'body plus dosimeter' combination (or 'calibration phantom plus dosimeter' combination) should the reference point be assigned?

In addition to this being a practical problem for calibrations, there is a conceptual issue. In principle, the calibration situation could be modelled to calculate the personal dose equivalent for that situation, and a point of test could be defined where the process of multiplying the fluence at that point with the internationally agreed fluence to dose equivalent conversion coefficient (calculated for a plane parallel beam) would give the correct value of $H_p(d)$ *for that situation*. This would differ for every source or neutron monoenergetic field used. Also, the calibration would be specific to the calibration situation, which would probably not match the situation at the place where the dosimeter was worn.

The reference point issue is still not fully resolved. It has generated discussion papers [14.80] and the revision of international standards [14.81]. In this situation, most calibration labs take the pragmatic approach of calculating the personal dose equivalent using the fluence at a point on the surface of the phantom behind the location where the dosimeter is mounted. (If the position of the neutron sensitive element within the dosimeter is known, the point should be behind the sensor.) The point where the fluence was determined should be stated on a calibration certificate, as it then provides the option to the supplier or user of the dosimeter of modifying the calibration result should they wish to use a different point.

14.3.4. Other devices — bubble detectors, installed monitors, spectrometers

Bubble detectors have some of the characteristics of an active device, in that they give an immediate estimate of the dose equivalent. Although their near isotropic response means they have the angle dependence required of a survey instrument, their small size and convenience means they are often used as personal dosimeters. They should be calibrated in accordance with their use, specifically, on phantom to the quantity personal dose equivalent if they are to be used as personal dosimeters, and free in air to the quantity ambient dose equivalent if they are to be used as survey devices.

By their very nature, installed monitors are difficult to calibrate once in position. They are therefore usually calibrated prior to installation. It is important that some means be provided of checking that their response does not change with time, either by routine checks with a radionuclide source, or by having a very small source as an integral part of the monitor. If the checking is done via routine measurements with an external source, the first check should be performed as

soon as possible after calibration to minimize the chance of changes between the calibration and the first check.

Spectrometers for field use are usually characterized using a combination of calculations and response measurements at different energies. The work involved is quite substantial, and some means of verifying that characteristics such as energy response (if applicable) and efficiency are checked regularly should be instigated to ensure the continued reliability of the spectrometer.

14.4. PERFORMANCE TESTING AND ACCURACY REQUIREMENTS

Performance requirements, in terms of accuracy, types of tests to be undertaken, testing frequency, etc., for both survey instruments and personal dosimeters tend to be set by the relevant national body. The particular tests undertaken in any country will depend largely on the requirements laid down by these bodies. They may include the following:

(a) Initial approval testing;
(b) Routine performance testing or calibration with bias and standard deviation requirements;
(c) Internal quality assurance testing.

In many countries, routine performance testing is required to be undertaken annually. For personal dosimeters, there is often the requirement that they are provided by dosimetry services that have to be approved by some competent body [14.82].

Technical guidance, together with a discussion of accuracy requirements for individual monitoring, may be found in a European Commission document [14.83]. Although aimed mainly at dosimetry for photons, the underlying principles also apply in the case of neutrons. Specific requirements for neutron personal dosimeters are covered in a recent ISO Standard [14.84].

One excellent means of performance testing is to participate in national or international comparison exercises. Examples of these are the exercises organized by the IAEA, the European Radiation Dosimetry Group (EURADOS) and Oak Ridge National Laboratories. The issue of harmonization of dose equivalent measurements in different countries is also increasingly being addressed [14.85], with the international comparison exercise as the main tool for the investigation [14.86].

14.5. PHOTON COMPONENTS OF NEUTRON CALIBRATION FIELDS

Because all available techniques for producing standard neutron fields also produce photons, it is impossible to realize pure neutron calibration fields. This causes problems when calibrating devices that respond to both photons and neutrons but do not discriminate between the two types of radiation, such as ionization chambers used as installed monitors. Corrections can be applied if, for example, the photon response of the device is known to be dose equivalent and the photon dose equivalent in the calibration field is known, or if the photon response function of the device is known and so is the photon spectrum of the calibration field.

Table 14.3 gives a summary of information about the photon dose equivalent in radionuclide neutron source fields.

For ^{241}Am based sources, there are two basic mechanisms whereby photons are produced: the decay of the ^{241}Am and the de-excitation of excited states produced in the product nucleus by the (α,n) reaction. For ^{241}Am-Be sources, the excited states are those of ^{12}C formed in the ^{9}Be(α,n)^{12}C reaction. The predominant gamma ray emitted in the decay of ^{241}Am has an energy of 59.54 keV, although other energy gamma rays, albeit of much lower intensity, are emitted over the range up to almost 1 MeV. The 59.54 keV gamma rays can be removed by using a relatively thin lead shield. The de-excitation of the ^{12}C nucleus gives rise to high energy gamma rays, the predominant one being at 4.438 MeV, and the intensity of this gamma ray, relative to the neutron emission rate, is approximately 0.59 [14.93, 14.94]. The intensities of the higher energy gamma rays are very much lower than for the 59.53 keV gamma ray, but they are much more difficult to remove by using absorbing layers, and allowance for their presence must be made when characterizing instruments with a photon sensitivity.

The gamma dose rate for an ^{241}Am-Be source with a 1 mm thick lead absorber has been measured [14.90–14.94] to be approximately 3.2% of the neutron dose equivalent rate and is generally accepted to be < 5% [14.9]. In the absence of the lead shield, the gamma dose rate is much higher, but it decreases as the americium content, and hence physical size, of the source increases. The gamma dose decreases from about 50% for a 37 GBq (1 Ci) source to about 20% for a 555 GBq (15 Ci) source [14.95]. For other ^{241}Am based (α,n) sources, the photon component is larger relative to the neutron dose equivalent [14.90, 14.94] because the neutron producing cross-sections are in general lower. ^{238}Pu-Be sources do not have the problem of the intense 59.53 keV gamma ray fluence, but the same higher energy gamma rays are present [14.96, 14.97]. The photon dose rates are similar to those for ^{241}Am-Be with a 1 mm lead shield [14.91, 14.92].

In the case of ^{252}Cf sources, photons are produced in the spontaneous fission process, from fission products and from alpha decay, which is the predominant

TABLE 14.3. PHOTON DOSE EQUIVALENTS IN THE FIELDS OF RADIONUCLIDE NEUTRON SOURCES[a]

Source[b]	McDonald et al.[c] (1984) [14.87]	Spurný et al. (1997) [14.88]	ISO 8529-1 (2001) [14.9]	Jósefowicz et al.[d] (2004) [14.89, 14.90]	Langner et al. (2007) [14.91]	McKay et al.[e] (2008) [14.92]
		Photon dose or dose equivalent as a percentage of the neutron dose equivalent				
^{252}Cf		$(3.8 \pm 0.5)\%$	5%	4.8%	$(4.3 \pm 0.6)\%$	$(5.9 \pm 0.2)\%$
D_2O mod. ^{252}Cf	18%	$(12 \pm 2)\%$	18%		$(14.2 \pm 2.3)\%$	$(17.6 \pm 0.8)\%$
^{241}Am-Be						$(21.4 \pm 0.8)\%$
^{241}Am-Be (Pb)		$(3.3 \pm 0.5)\%$	< 5%	3.5%	$(2.7 \pm 0.6)\%$	$(3.3 \pm 0.2)\%$
^{39}Pu-Be				3.4%		
^{241}Am-B						$(179 \pm 8)\%$
^{241}Am-B (Pb)			< 5%			
^{241}Am-F						$(480 \pm 30)\%$
^{241}Am-Li						$(2800 \pm 100)\%$

TABLE 14.3. PHOTON DOSE EQUIVALENTS IN THE FIELDS OF RADIONUCLIDE NEUTRON SOURCES[a] (cont.)

Source[b]	Photon dose or dose equivalent as a percentage of the neutron dose equivalent				
	McDonald et al.[c] (1984) [14.87]	Spurný et al. (1997) [14.88]	ISO 8529-1 (2001) [14.9]	Jósefowicz et al.[d] (2004) [14.89, 14.90]	Langner et al. (2007) [14.91]	McKay et al.[e] (2008) [14.92]
^{241}Am-Li (Pb)		$(34 \pm 5)\%$				$(32 \pm 2)\%$

a Except where indicated to the contrary, the values are for ratios of ambient dose equivalent.

b Source identifiers including (Pb) indicate that the source was enclosed within an approximately 1 mm thick lead shield.

c Quantity described as 'ratio of gamma dose to neutron dose equivalent'.

d Data are an average of results from the two references. Photon dose equivalent rates were taken to be the same as the quoted dose rates. The percentage figures were calculated for ambient neutron dose equivalent. This involved recalculating the data from Ref. [14.91], which was given in terms of the earlier quantity, maximum dose equivalent, H_{MADE}. To calculate the percentage from the data presented in Ref. [14.92], the neutron ambient dose equivalent was calculated from the quoted source emission rate.

e Data measured with various devices, but results shown are for measurements with energy compensated Geiger–Müller tubes, which were considered the most reliable and are for $H^*(10)_\gamma/H^*(10)_n$.

decay mode (97%). For the fission reaction, the majority of the photons are emitted by the excited fragments after the end of neutron evaporation. The energy spectrum of these photons exhibits an exponential decrease above 1.5 MeV extending to energies in excess of 8 MeV [14.98]. The total gamma dose rate for a radionuclide ^{252}Cf source is of the order of 5% of the neutron dose equivalent rate [14.90–14.94]; however, the actual value will depend on the age of the source, as fission products will build up with time.

For a D$_2$O moderated ^{252}Cf source, the photon dose rate is much higher because of neutron reactions in the surrounding materials. Early measurements using tissue equivalent plastic ion chambers and proportional counters, together with Geiger–Müller counters and TLDs, yielded a value of 18% for the photon dose relative to the neutron dose equivalent [14.89]. Later values [14.90, 14.93, 14.94] vary between approximately 12% and 19% but, as with the bare ^{252}Cf source, the value will depend somewhat on the age of the source.

Information on the photon spectra of several radionuclide neutron source fields can be found in Ref. [14.99].

Investigations of the photon dose components and the photon spectra in accelerator produced monoenergetic neutron fields have been undertaken using Geiger–Müller counters and time of flight [14.100].

REFERENCES TO CHAPTER 14

[14.1]   INTERNATIONAL ATOMIC ENERGY AGENCY, Guidelines on Calibration of Neutron Measuring Devices, Technical Reports Series No. 285, IAEA, Vienna (1988).

[14.2]   INTERNATIONAL ATOMIC ENERGY AGENCY, Calibration of Radiation Protection Monitoring Instruments, Safety Reports Series No. 16, IAEA, Vienna (2000).

[14.3]   SCOTT, C., BURGESS, P., WOODS, M., The Examination, Testing and Calibration of Portable Radiation Protection Instruments, Measurement Good Practice Guide No. 14, National Physical Laboratory, Teddington, UK (1999).

[14.4]   INTERNATIONAL ORGANIZATION FOR STANDARDIZATION, Reference neutron radiations — Part 2: Calibration fundamentals of radiation protection devices related to the basic quantities characterizing the radiation field, International Standard 8529-2, ISO, Geneva (2000).

[14.5]   INTERNATIONAL ELECTROTECHNICAL COMMISSION, Radiation protection instrumentation — Neutron ambient dose equivalent (rate) meters, International Standard IEC 61005, Edition 3.0, IEC, Geneva (2014).

[14.6]   BARTLETT, D.T., ALBERTS, W.G., Type testing and calibration of personal dosemeters, Radiat. Prot. Dosim. **54** (1994) 259–266.

[14.7]   ISO/IEC Guide 99:2007, International vocabulary of metrology — Basic and general concepts and associated terms (VIM), ISO, Geneva (2007).

[14.8]   INTERNATIONAL ORGANIZATION FOR STANDARDIZATION, Reference neutron radiations — Part 3: Calibration of area and personal dosimeters and determination of their response as a function of neutron energy and angle of incidence, International Standard 8529-3, ISO, Geneva (1998).

[14.9]   INTERNATIONAL ORGANIZATION FOR STANDARDIZATION, Reference neutron radiations — Part 1: Characteristics and methods of production, International Standard 8529-1, ISO, Geneva (2001).

[14.10]   INTERNATIONAL COMMISSION ON RADIOLOGICAL PROTECTION, Conversion Coefficients for Use in Radiological Protection Against External Radiation, ICRP Publication 74, Pergamon Press, Oxford and New York (1996).

[14.11]   INTERNATIONAL COMMISSION ON RADIATION UNITS AND MEASUREMENTS, Conversion Coefficients for Use in Radiological Protection Against External Radiation, Report 57, ICRU, Bethesda, MD (1998).

[14.12]   INTERNATIONAL ORGANIZATION FOR STANDARDIZATION, General requirements for the competence of testing and calibration laboratories, ISO/IEC 17025, ISO, Geneva (2017).

[14.13]   GRESSIER, V., et al., AMANDE: A new facility for monoenergetic neutron fields production between 2 keV and 20 MeV, Radiat. Prot. Dosim. 110 (2004) 49–52.

[14.14]   BARDELL, A.G., BURKE, M., HUNT, J.B., TAGZIRIA, H., THOMAS, D.J., Anisotropy of Emission from Radionuclide Neutron Sources, NPL Report CIRM 24, National Physical Laboratory, Teddington, UK (1998).

[14.15]   KLUGE, H., WEISE, K., HUNT, J.B., Calibration of neutron sensitive spherical devices with bare and D_2O moderated Cf sources in rooms of different sizes, Radiat. Prot. Dosim. 32 (1990) 233–244.

[14.16]   MARION, J.B., FOWLER, J.L., Fast Neutron Physics Part I, Monographs and Texts in Physics and Astronomy, Interscience Publishers, New York (1960).

[14.17]   NOLTE, R., THOMAS, D.J., Monoenergetic fast neutron reference fields: I. Neutron production, Metrologia 48 (2011) S263–S273.

[14.18]   NOLTE, R., THOMAS, D.J., Monoenergetic fast neutron reference fields: II. Field characterization, Metrologia 48 (2011) S274–S291.

[14.19]   SCHUHMACHER, H., Neutron calibration facilities, Radiat. Prot. Dosim. 110 (2004) 33–42.

[14.20]   HUNT, J.B., The Calibration and Use of Long Counters for the Accurate Measurement of Neutron Flux Density, NPL Report RS(EXT)5, National Physical Laboratory, Teddington, UK (1976).

[14.21]   TAGZIRIA, H., THOMAS, D.J., Calibration and Monte Carlo modelling of neutron long counters, Nucl. Instrum. Methods Phys. Res. A 452 (2000) 470–483.

[14.22]   ROBERTS, N.J., TAGZIRIA, H., THOMAS, D.J., Determination of the Effective Centres of the NPL Long Counters, NPL Report DQL RN 004, National Physical Laboratory, Teddington, UK (2004).

[14.23]   RYVES, T.B., International fluence-rate intercomparison for 144 and 565 keV neutrons, Metrologia 24 (1987) 27–37.

[14.24]   HUYNH, V.D., International comparison of flux density measurements for monoenergetic fast neutrons, Metrologia 16 (1980) 31–49.

[14.25] HERTEL, N.E., WEHRING, B.W., Absolute monitoring of DD and DT neutron fluences using the associated-particle technique, Nucl. Instrum. Methods **172** (1980) 501–506.

[14.26] GAISER, J.E., HARPER R.C., WARREN, W.H., ALFORD, W.L., Measuring the neutron yield from T(d,n)^{4}He, Nucl. Instrum. Methods **178** (1980) 249–251.

[14.27] THOMAS, D.J., LEWIS, V.E., Standardization of neutron fields produced by the H(d,n)He reaction, Nucl. Instrum. Methods **179** (1981) 397–404.

[14.28] GULDBAKKE, S., SCHLEGEL, D., "The spectral neutron fluence produced by the integration of charged particles with solid state targets ($E_n > 1$ MeV)", Proc. Int. Conf. Neutrons in Research and Industry, 9–15 Jun. 1996, Crete, Proc. SPIE 2867, SPIE, Bellingham, WA (1997) 286–289.

[14.29] BÖTTGER, R., et al., Problems associated with the production of monoenergetic neutrons, Nucl. Instrum. Methods Phys. Res. A **282** (1989) 358–367.

[14.30] HAWKES, N.P., THOMAS, D.J., TAYLOR, G.C., Corrections associated with on-phantom calibrations of neutron personal dosemeters, Radiat. Prot. Dosim. **170** (2016) 35–38

[14.31] KRÁLÍK, M., VYKYDAL, Z., Practical metrological aspects of neutron personal dosimetry, Radiat. Prot. Dosim. **170** (2016) 54–57.

[14.32] INTERNATIONAL COMMITTEE OF WEIGHTS AND MEASURES, http://www.bipm.org/en/committees/

[14.33] NOLTE, R., et al., Quasi-monoenergetic neutron reference fields in the energy range from thermal to 200 MeV, Radiat. Prot. Dosim. **110** (2002) 97–102.

[14.34] SCHUHMACHER, H., et al., Quasi-monoenergetic neutron beams with energies from 25 to 70 MeV, Nucl. Instrum. Methods Phys. Res. A **421** (1999) 454–465.

[14.35] BABA, M., et al., Characterisation of a 40–90 MeV 7-Li(p,n) neutron source at TIARA using a proton recoil telescope and a TOF method, Nucl. Instrum. Methods Phys. Res. A **428** (1999) 284–295.

[14.36] NAKAO, N., KUROSAWA, T., NAKAMURA, T., UWAMINO, Y., Development of a quasi-monoenergetic neutron field and measurements of the response function of an organic liquid scintillator for neutron energy range from 66 to 206 MeV, Nucl. Instrum. Methods Phys. Res. A **476** (2002) 176–180.

[14.37] NOLTE, R., et al., High-energy neutron reference fields for the calibration of detectors used in neutron spectrometry, Nucl. Instrum. Methods Phys. Res. A **476** (2002) 369–373.

[14.38] CONDÉ, H., et al., A facility for studies of neutron-induced reactions in the 50–200 MeV range, Nucl. Instrum. Methods Phys. Res. A **292** (1990) 121–128.

[14.39] HUNT, J.B., The calibration of neutron sensitive spherical devices, Radiat. Prot. Dosim. **8** (1984) 239–251.

[14.40] EISENHAUER, C.M., HUNT, J.B., SCHWARTZ, R.B., Calibration techniques for neutron personal dosimetry, Radiat. Prot. Dosim. **10** (1985) 43–57.

[14.41] EISENHAUER, C.M., Review of scattering corrections for calibration of neutron instruments, Radiat. Prot. Dosim. **28** (1989) 253–262.

[14.42] SCHRAUBE, H., GRÜNAUER, F., BURGER, G., "Calibration problems with neutron moderator detectors", Proc. Symp. Neutron Monitoring for Radiation Protection Purposes, IAEA STI/PUB/318, Vol. 2, IAEA, Vienna (1972) 453–464.

[14.43] AXTON, E.J., Absolute measurement of the neutron flux density in the A.E.R.E. reactor 'GLEEP', J. Nucl. Energy Parts A/B **17** (1963) 125–135.

[14.44] WESTCOTT, C.H., The specification of neutron flux and nuclear cross-sections in reactor calculations, J. Nucl. Energy **2** (1955) 59–76.

[14.45] WESTCOTT, C.H., WALKER, W.H., ALEXANDER, T.K., "Effective cross sections and cadmium ratios for the neutron spectra of thermal reactors", Proc. Second United Nations Int. Conf. on the Peaceful Uses of Atomic Energy, Vol. 16, Nuclear Data and Reactor Theory, UN, Geneva (1958).

[14.46] BÖTTGER, R., FRIEDRICH, H., JANßEN, H., The PTB thermal neutron calibration field at GeNF, PTB-Bericht Report PTB-N-47, Physikalisch-Technische Bundesanstalt, Braunschweig, Germany (2004).

[14.47] THOMAS, D.J., KOLKOWSKI, P., Thermal Fluence and Dose Equivalent Standards at NPL, NPL REPORT DQL RN008, National Physical Laboratory, Teddington, UK (2005).

[14.48] GEIGER, K.W., VAN DER ZWAN, L., Slowing Down Spectrum and Neutron Temperature in a Thermal Neutron Flux Density Standard, Metrologia **2** (1966) 1–5.

[14.49] NIST, Calibrations: Neutron Device Calibrations, https://www.nist.gov/programs-projects/calibrations-neutron-device-calibrations.

[14.50] LACOSTE, V., GRESSIER, V., MULLER, H., LEBRETON, L., Characterisation of the IRSN graphite moderated americium-beryllium neutron field, Radiat. Prot. Dosim. **110** (2004) 135–139.

[14.51] GUALDRINI, G., BEDOGNI, R., MONTEVENTI, F., Developing a thermal neutron irradiation system for the calibration of personal dosemeters in terms of $H_p(10)$, Radiat. Prot. Dosim. **110** (2004) 43–48.

[14.52] ISIS Neutron and Muon Source, https://www.isis.stfc.ac.uk

[14.53] RYVES, T.B., PAUL, E.B, The construction and calibration of a standard thermal neutron flux facility at the National Physical Laboratory, J. Nucl. Energy **22** (1968) 759–775.

[14.54] SCHRODER, I.G., SCHWARTZ, R.B., McGARRY, E.D., "The 2-keV filtered beam facility at the NBS reactor", Proc. Conf. Nuclear Cross-Sections and Technology, Washington, DC, Mar. 1975, NBS Special Publication 425, Vol. 1, National Bureau of Standards, Washington, DC (1975) 89–92.

[14.55] TSANG, F.Y., BRUGGER, R.M., A versatile neutron beam filter facility with silicon and iron filters, Nucl. Instrum. Methods **134** (1976) 441–447.

[14.56] McGARRY, E.D., SCHRODER, I.G., "A 25-keV neutron beam facility at NBS", Proc. Conf. Nuclear Cross-Sections and Technology, Washington, DC, Mar. 1975, NBS Special Publication 425, Vol. 1, National Bureau of Standards, Washington, DC (1975) 116–118.

[14.57] ALBERTS, W.G., LESIECKI, H., Neutron flux density measurements and rem counter calibration at the 24.5 keV filtered beam of the FMRB, Radiat. Prot. Dosim. **2** (1982) 241.

[14.58] MILL, A.J., A proposed technique for producing high-purity monoenergetic neutron beams between 100 eV and 2.5 keV for nuclear research, Nucl. Sci. Eng. **85** (1983) 127–132.

[14.59] HARVEY, J.R., MILL, A.J., The status of a proposed international filtered neutron beam project, Proc. Fourth Symp. on Neutron Dosimetry, Munich-Neuherberg, 1–5 Jun. 1981, EUR 7448, Vol. 1, Commission of the European Communities, Luxembourg (1981) 431–441.

[14.60] KOREA ATOMIC ENERGY RESEARCH INSTITUTE, Table of the Isotopes, KAERI, Taejon, South Korea, http://atom.kaeri.re.kr/

[14.61] CIERJACKS, S. (Ed.), Neutron Sources for Basic Physics and Applications, An OECD/NEA Report, Vol. 2 of Neutron Physics and Nuclear Data in Science and Technology, Pergamon Press, Oxford (1983).

[14.62] HILDEBRAND, A., PARK, H., KHURANA, S., NOLTE, R., SCHMIDT, D., Experimental Determination of the Response Matrix of a BC501 Scintillation Detector using a Wide Neutron Spectrum: A Status Report, PTB Report 6.42-05-1, Physikalisch-Technische Bundesanstalt, Braunschweig, Germany (2005).

[14.63] INTERNATIONAL ORGANIZATION FOR STANDARDIZATION, Reference neutron radiations — Characteristics and methods of production of simulated workplace neutron fields, International Standard 12789-1, ISO, Geneva (2008).

[14.64] TAYLOR, G.C., THOMAS, D.J., BENNETT, A., A realistic field facility to simulate reactor spectra, Radiat. Prot. Dosim. **110** (2004) 111–115.

[14.65] GRESSIER, V., et al., Characterisation of the IRSN CANEL/T400 facility producing realistic neutron fields for calibration and test purposes, Radiat. Prot. Dosim. **110** (2004) 523-527.

[14.66] McCASLIN J., et al., An intercomparison of dosimetry techniques in radiation fields at two high-energy accelerators, Health Phys. **33** (1977) 611–621.

[14.67] DINTER H., TESCH. K., Determination of neutron spectra behind lateral shielding of high energy proton accelerators, Radiat. Prot. Dosim. **42** (1992) 4–10.

[14.68] PARETZKE H.G., HEINRICH W., Radiation exposure and radiation risk in civil aircraft, Radiat. Prot. Dosim. **48** (1993) 33–40.

[14.69] MITAROFF, A., SILARI, M., The CERN-EU high-energy Reference Field (CERF) facility for dosimetry at commercial flight altitudes and in space, Radiat. Prot. Dosim. **102** (2002) 7–22.

[14.70] HEINRICH, W., ROESLER, S., SCHRAUBE, H., Physics of cosmic radiation fields, Radiat. Prot. Dosim. **86** (1999) 253–258.

[14.71] THOMAS, D.J., HORWOOD, N., TAYLOR, G.C., Neutron Dosemeter Responses in Workplace Fields and the Implications of Using Realistic Neutron Calibration Fields, NPL Report CIRM 27, National Physical Laboratory, Teddington, UK (1999).

[14.72] PIESCH, E., BURGKHARDT, B., "Measurement of neutron field quantities using the single sphere albedo technique", Proc. Fifth Symposium on Neutron Dosimetry, Munich/Neuherberg, 17–21 Sep. 1984, EUR 9762, Commission of the European Communities, Luxembourg (1985) 403–414.

[14.73] PIESCH, E., BURGKHARDT, B., COMPER, W., The single sphere albedo system — a useful technique in neutron dosimetry, Radiat. Prot. Dosim. **10** (1985) 147–157.

[14.74] HARVEY, J.R., HART, C.D., A neutron survey instrument which gives information on the low energy neutron spectrum and can be used for albedo dosemeter calibration, Radiat. Prot. Dosim. **23** (1988) 277–280.

[14.75] HANKINS, D.E., A Small, Inexpensive-Albedo Neutron Dosimeter, Report LA-5261, Los Alamos Scientific Laboratory, Los Alamos, NM (1973).

[14.76] HANKINS, D.E., "The effect of energy dependence on the evaluation of albedo neutron dosimeters", Proc. Ninth Midyear Topical Symp. on Operational Health Physics, Denver, USDOE, Washington, DC (1976) 861–868.

[14.77] EISENHAUER, C.M., HUNT, J.B., SCHWARTS, R.B., Calibration techniques for neutron personal dosimetry, Radiat. Prot. Dosim. **10** (1985) 43–57.

[14.78] LUSZIK-BHADRA, M., Electronic personal dosemeters: the solution to problems of individual monitoring in mixed neutron/photon fields?, Radiat. Prot. Dosim. **110** (2004) 747–752.

[14.79] FIECHTNER, A., WERNLI, C., KAHILAINEN, J., A prototype personal neutron dosemeter based in an ion chamber and direct ion storage, Radiat. Prot. Dosim. **96** (2001) 269–272.

[14.80] BARTLETT, D.T., Editorial: Personal dose equivalent, $H_p(d)$, and reference point for calibration, Rad. Prot. Dosim. **121** (2006) 209–210.

[14.81] INTERNATIONAL ORGANIZATION FOR STANDARDIZATION, Reference point of personal dosemeters, International Standard 29661: 2012/Amd. 1:2015 to Reference radiation fields for radiation protection — Definitions and fundamental concepts, ISO, Geneva (2015).

[14.82] INTERNATIONAL ORGANIZATION FOR STANDARDIZATION, Radiological protection — Criteria and performance limits for the periodic evaluation of dosimetry services, International Standard 14146, ISO, Geneva (2018).

[14.83] ALVES, J., et al., Technical Recommendations for Monitoring Individuals Occupationally Exposed to External Radiation, Radiation Protection No. 160, European Commission, Luxembourg (2009).

[14.84] INTERNATIONAL ORGANIZATION FOR STANDARDIZATION, Radiation protection — Passive personal neutron dosemeters — Performance and test requirements, International Standard 21909-1, ISO, Geneva (2015).

[14.85] DIETZE, G., MENZEL, M.-G., Editorial: Harmonisation and dosimetric quality assurance in individual monitoring for external radiation, Radiat. Prot. Dosim. **89 (**1–2) (2000).

[14.86] FANTUZZI, E., et al., EURADOS IC2012N: EURADOS 2012 intercomparison for whole-body neutron dosimetry, Radiat. Prot. Dosim. **161** (2014) 73–77.

[14.87] McDONALD, J.C., GRIFFITH, R.V., PLATO, P.A., MIKLOS, J.A., Measurement of gamma ray dose from a moderated ^{252}Cf source, Radiat. Prot. Dosim. **9** (1984) 113–118.

[14.88]   SPURNÝ, F., VOTOCKOVA, I., BOTTOLLIER-DEPOIS, J.-F., KURKDJIAN, J., PAUL, D., Test of instruments for neutron and gamma ray measurements at several radionuclide neutron sources, Radiat, Prot. Dosim. **70 (**1997) 353–356.

[14.89]   JÓZEFOWICZ, K., GOLNIK, N., ZIELCZYŃSKI, M., Dosimetric parameters of simple neutron + gamma fields for calibration of radiation protection instruments, Radiat. Prot. Dosim. **44** (1991) 139–142.

[14.90]   JÓZEFOWICZ, K., GOLNIK, N., ZIELCZYŃSKI, M., Standard fields of old neutron sources — parameters and traceability, Radiat. Prot. Dosim. **110** (2004) 107–110.

[14.91]   LANGNER, F., et al., Photon contributions to ambient dose equivalent H*(10) in the wide-spectrum neutron reference fields of the IRSN, Radiat, Prot. Dosim. **126** (2007) 145–150.

[14.92]   McKAY, C.J., et al., Photon Doses in NPL Standard Radionuclide Neutron Fields, NPL Report IR12, National Physical Laboratory, Teddington, UK (2009).

[14.93]   CROFT, S., The use of neutron intensity calibrated Be(α,n) sources as 4438 keV gamma-ray reference standards, Nucl. Instrum. Methods Phys. Res. A **281** (1989) 103–116.

[14.94]   MOWLAVI, A., KOOHI-FAYEGH, R., Determination of 4.438 MeV gamma-ray to neutron emission ratio from a [241]Am-Be neutron source, Appl. Radiat. Isot. **60** (2004) 959–962.

[14.95]   ROBERTS, N.J., HORWOOD, N.A., McKAY, C.J., Photon doses in NPL standard neutron fields, Radiat. Prot. Dosim. **161** (2014) 157–160.

[14.96]   MAYER, S., OTTO, T., GOLNIK, N., Determination of the photon-contribution of a [238]Pu-Be source, Nucl. Instrum. Methods Phys. Res. B **213** (2004) 214–217.

[14.97]   VEGA-CARRILLO, H.R., MANZANARES-ACUŇA, E., BECERRA-FERREIRO, A.M., CARRILLO-NUŇEZ, A., Neutron and gamma-ray spectra of [239]PuBe and [241]AmBe, Appl. Rad. Isot. **57** (2002) 167–170.

[14.98]   HOTZEL, A., et al., High-energy gamma-rays accompanying the spontaneous fission of [252]Cf, Z. Phys. A **356** (1996) 299–308.

[14.99]   ROBERTS, N.J., Photon spectra in NPL standard radionuclide neutron fields, Radiat. Prot. Dosim. **180** (2018) 62–65.

[14.100] NEUMANN, S., GULDBAKKE, S., MATZKE, M., SOSAAT, W., Photon Spectrometry in Monoenergetic Neutron Fields, Report PTB-N-41, Physikalisch-Technische Bundesanstalt Braunschweig, Germany (2001).

DEFINITIONS

The following definitions are specific to this publication and are either not provided in, or are different from, those provided in the IAEA Safety Glossary: Terminology Used in Nuclear Safety and Radiation Protection (2018 Edition).

The symbol '*' denotes a definition that differs from that provided in the IAEA Safety Glossary.

calibration*. Operation that, under specified conditions, (i) establishes a relation between the quantity values with measurement uncertainties provided by measurement standards and corresponding indications with associated measurement uncertainties; and (ii) uses this information to establish a relation for obtaining a measurement result from an indication.

calibration conditions. Conditions within the range of standard test conditions actually prevailing during the calibration measurement.

calibration factor. The multiplying factor that relates a device indication under reference exposure conditions to the quantity of interest. It is the reciprocal of the response, when the response is determined under reference conditions.

conventional true value of a quantity. The value attributed by formal agreement to a quantity for a given purpose; usually, it is the best estimate of the value.

> **Note:** The conventional value is sometimes called the assigned value, best estimate, conventional true value or reference value. A conventional value is, in general, regarded as being sufficiently close to the true value for the difference to be insignificant for the given purpose.

conversion coefficient. The ratio of the absorbed dose or dose equivalent of interest, defined for special reference irradiation conditions and usually derived by means of neutron transport calculations, to the reference neutron fluence causing it.

detector. Device or substance that indicates the presence of a phenomenon, body or substance when a threshold value of an associated quantity is exceeded.

dosimeter. A device, instrument or system that can be used to measure or evaluate any quantity that can be related to the determination of either absorbed dose

or dose equivalent. This implies that the response function is proportional to the conversion coefficient of the quantity to be measured.

indication. Quantity value provided as the output of a measuring system; sometimes called reading.

measurement result. Information about the magnitude of a quantity, obtained experimentally.

measuring system. Set of measuring instruments and other devices or substances assembled and adapted to the measurement of quantities of specified kinds within specified intervals of values.

phantom. Artefact constructed to simulate the scattering properties of the human body, or parts of the human body such as the extremities.

point of test. The point in the radiation field at which the conventional true value of a quantity to be measured is known.

quantity. Property of a phenomenon, body or substance, to which a magnitude can be assigned.

reaction Q value. For a given nuclear reaction, the difference between the sum of the kinetic and radiant energies of the particles formed and the sum of the kinetic and radiant energies of the reacting particles.

Note: For exoergic reactions, $Q > 0$; for endothermic reactions, $Q < 0$.

reference condition. Operating condition prescribed for evaluating the performance of a measuring instrument or measuring system, or for comparison of measurement results.

reference direction. The direction, in the coordinate system of the dosimeter, with respect to which the angle of radiation incidence is measured in reference fields.

reference point. The point of the device to be used in order to position the device with respect to the point of test.

response. The response of a device is the indication divided by value of the physical quantity causing it. It should be specified with reference to this

quantity, e.g. fluence response or dose equivalent response. The response is the reciprocal of the calibration factor.

response function. The response of a device as a function of an independent variable. The variable may be, for example, energy or angle of incidence of radiation on the device, resulting in an energy or an angle response function.

sensitivity. Quotient of the change in the indication of a measuring system and the corresponding change in the value of the quantity being measured.

standard. Realization of the definition of a given quantity, with the stated value and measurement uncertainty, used as a reference.

Note: Many of the terms above are adapted from JCGM 200:2012, International Vocabulary of Metrology — Basic and general concepts and associated terms (2012), available from the BIPM web site (https://www.bipm.org/en/publications/guides/vim.html), or ISO 29661, Reference radiation fields for radiation protection — Definitions and fundamental concepts 2012, available from the ISO web site (https://www.iso.org/standard/45622.html).

LIST OF ACRONYMS AND ABBREVIATIONS USED IN THE REPORT

CLYC	scintillator material Cs_2LiYCl_6:Ce
DIS	direct ion storage
IEC	International Electrotechnical Commission
ICRP	International Commission on Radiological Protection
ICRU	International Commission on Radiation Units and Measurements
IRSN	Institut de Radioprotection et de Sûreté Nucléaire
ISO	International Organization for Standardization
JAERI	Japan Atomic Energy Research Institute
KAERI	Korea Atomic Energy Research Institute
LET	linear energy transfer, sometimes called linear collision stopping power
MOX	mixed oxide fuel
NPL	National Physical Laboratory, UK
NRPB	National Radiological Protection Board (now UK Health Security Agency)
OSL	optically stimulated luminescent
PADC	polyallyl diglycol carbonate
PMMA	polymethyl methacrylate
PSI	Paul Scherrer Institute, Switzerland
PTB	Physikalisch-Technische Bundesanstalt, Germany
PWR	pressurized water reactor
RBE	Relative Biological Effectiveness
SCK CEN	Belgian Nuclear Research Centre
SPE	solar particle event
TEPC	tissue equivalent proportional counter
TL	thermoluminescent
TLD	thermoluminescent dosimeter
TNS	transportable neutron spectrometer

CONTRIBUTORS TO DRAFTING AND REVIEW

Cruz Suarez, R.	International Atomic Energy Agency
Hajek, M.	International Atomic Energy Agency
Luszik-Bhadra, M.	Physikalisch-Technische Bundesanstalt, Germany
Ma, J.	International Atomic Energy Agency
McDonald, J.C.[†]	Pacific Northwest National Laboratory, United States of America
Thomas, D.J.	National Physical Laboratory, United Kingdom

ORDERING LOCALLY

IAEA priced publications may be purchased from the sources listed below or from major local booksellers.

Orders for unpriced publications should be made directly to the IAEA. The contact details are given at the end of this list.

NORTH AMERICA

Bernan / Rowman & Littlefield
15250 NBN Way, Blue Ridge Summit, PA 17214, USA
Telephone: +1 800 462 6420 • Fax: +1 800 338 4550
Email: orders@rowman.com • Web site: www.rowman.com/bernan

REST OF WORLD

Please contact your preferred local supplier, or our lead distributor:

Eurospan Group
Gray's Inn House
127 Clerkenwell Road
London EC1R 5DB
United Kingdom

Trade orders and enquiries:
Telephone: +44 (0)176 760 4972 • Fax: +44 (0)176 760 1640
Email: eurospan@turpin-distribution.com

Individual orders:
www.eurospanbookstore.com/iaea

For further information:
Telephone: +44 (0)207 240 0856 • Fax: +44 (0)207 379 0609
Email: info@eurospangroup.com • Web site: www.eurospangroup.com

Orders for both priced and unpriced publications may be addressed directly to:
Marketing and Sales Unit
International Atomic Energy Agency
Vienna International Centre, PO Box 100, 1400 Vienna, Austria
Telephone: +43 1 2600 22529 or 22530 • Fax: +43 1 26007 22529
Email: sales.publications@iaea.org • Web site: www.iaea.org/publications

This IAEA Safety Report describes neutron monitoring procedures and equipment that may be used for radiation protection in nuclear power production, medical and industrial applications, research institutions and civil air service. It provides guidance on measuring operational quantities of neutron radiation and practical advice for safely carrying out neutron radiation protection dosimetry, including methods for establishing traceability of those measurements to national standards. This publication is intended for designers and manufacturers of radiation monitors and personal dosimeters and radiation protection professionals who develop radiation protection standards or neutron monitoring programmes.

INTERNATIONAL ATOMIC ENERGY AGENCY
VIENNA